

# THE JOURNAL OF PHYSICAL CHEMISTRY

(Registered in U. S. Patent Office)

|   |     |
|---|-----|
| Balwant Rai Puri, Lekh Raj Sharma and M. L. Lakhanpal: Freezing Point of Water Held in Porous Bodies at Different Vapor Pressures.....  | 289 |
| William D. Harkins and Richard S. Stearns: A New Adsorption Isotherm and the Distribution of Energy Sites on the Surface of Some Finely Divided Solids.....                       | 292 |
| R. Nelson Smith, Conway Pierce and Cliffe D. Joel: The Low Temperature Reaction of Water with Carbon.....   | 298 |
| Karol J. Mysels: Charge Effects in Light Scattering by Colloidal Solutions.....   | 303 |
| Paul R. Basford, William D. Harkins and Sumner B. Twiss: Effect of Temperature on the Adsorption of <i>n</i> -Decane on Iron.....   | 307 |
| G. J. Young, J. J. Chessick, F. H. Healey and A. C. Zettlemoyer: Thermodynamics of the Adsorption of Water on Graphon from Heats of Immersion and Adsorption Data.....            | 313 |
| William T. Holser: Fugacity of Water at High Temperatures and Pressures.....  | 316 |
| O. D. Bonner: A Selectivity Scale for Some Monovalent Cations on Dowex 50.....  | 318 |
| Shigehiko Kurosaki: The Dielectric Behavior of Sorbed Water on Silica Gel.....  | 320 |
| Kurt A. Kraus and Robert W. Holmberg: Hydrolytic Behavior of Metal Ions. III. Hydrolysis of Thorium(IV).....  | 325 |
| J. H. Singleton and G. D. Halsey, Jr.: The Adsorption of Argon on Xenon Layers.....   | 330 |
| Benjamin Carroll and Eli Freeman: The Behavior of Colloidal Silicate Solutions as Revealed by Adsorption Indicators.....  | 335 |
| K. Bril and P. Krumholz: The Polarographic Reduction of Copper Ethylenediamine Tetraacetate.....  | 339 |
| Harold Edelhoach and Hugh S. Taylor: The Adsorption of Gases on Calcium Fluoride.....   | 344 |
| Leo Brewer and Russell K. Edwards: The Stability of SiO Solid and Gas.....  | 351 |
| Melvin A. Cook, Rex O. Daniels, Jr., and J. Hugh Hamilton: Influence of Adsorption of Water and Quinoline on the Surface Conductivity of a Synthetic Alumina-Silica Catalyst..... | 358 |
| Sidney A. Greenberg: Calcium Silicate Hydrate. (I).....   | 362 |
| C. Howard Shomate: A Method for Evaluating and Correlating Thermodynamic Data.....  | 368 |
| Rustum Roy and M. W. Shafer: Phases Present and Phase Equilibrium in the System $\text{In}_2\text{O}_3\text{-H}_2\text{O}$ .....  | 372 |
| P. F. Whelan: The Effect of the pH of Xanthate Solutions on the Contact Angle between a Bubble of Air and an Iron Disulfide Surface not of Minimum Rugosity.....                  | 375 |
| NOTE: F. J. Baur: Crystalline Triacetin.....  | 380 |
| NOTE: S. S. Mitra and Y. P. Varshni: Three Additive Functions for the <i>n</i> -Paraffins.....  | 381 |
| NOTE: John P. Fowler and Marvin C. Tobin: The Thermal Decomposition of Cyclotrimethylenetrinitrosamine.....   | 382 |
| NOTE: Alexander Lehrman and Donald Schweitzer: The Liquidus Curve of the Binary System Cadmium Acetate-Potassium Acetate.....   | 383 |

THE JOURNAL OF PHYSICAL CHEMISTRY will appear monthly in 1954  
After January 1, 1954, Notes and Communications to the Editor  
will be accepted for publication.

# THE JOURNAL OF PHYSICAL CHEMISTRY

(Registered in U. S. Patent Office)

W. ALBERT NOYES, JR., EDITOR

ALLEN D. BLISS

ASSISTANT EDITORS

ARTHUR C. BOND

## EDITORIAL BOARD

R. P. BELL

R. E. CONNICK

S. C. LIND

E. J. BOWEN

PAUL M. DOTY

H. W. MELVILLE

G. E. BOYD

J. W. KENNEDY

W. O. MILLIGAN

MILTON BURTON

E. A. MOELWYN-HUGHES

Published monthly by the American Chemical Society at 20th and Northampton Sts., Easton, Pa.

Entered as second-class matter at the Post Office at Easton, Pennsylvania.

The *Journal of Physical Chemistry* is devoted to the publication of selected symposia in the broad field of physical chemistry and to other contributed papers.

Manuscripts originating in the British Isles, Europe and Africa should be sent to F. C. Tompkins, The Faraday Society, 6 Gray's Inn Square, London W. C. 1, England.

Manuscripts originating elsewhere should be sent to W. Albert Noyes, Jr., Department of Chemistry, University of Rochester, Rochester 3, N. Y.

Correspondence regarding accepted copy, proofs and reprints should be directed to Assistant Editor, Allen D. Bliss, Department of Chemistry, Simmons College, 300 The Fenway, Boston 15, Mass.

Business Office: American Chemical Society, 1155 Sixteenth St. N. W., Washington 6, D. C.

Advertising Office: American Chemical Society, 332 West 42nd St., New York 36, N. Y.

Articles must be submitted in duplicate, typed and double spaced. They should have at the beginning a brief Abstract, in no case exceeding 300 words. Original drawings should accompany the manuscript. Lettering at the sides of graphs (black on white or blue) may be pencilled in, and will be typeset. Figures and tables should be held to a minimum consistent with adequate presentation of information. Photographs will not be printed on glossy paper except by special arrangement. All footnotes and references to the literature should be numbered consecutively and placed on the manuscript at the proper places. Initials of authors referred to in citations should be given. Nomenclature should conform to that used in *Chemical Abstracts*, mathematical characters marked for italic, Greek letters carefully made or annotated, and subscripts and superscripts clearly shown. Articles should be written as briefly as possible consistent with clarity and should avoid historical background unnecessary for specialists.

Symposium papers should be sent in all cases to Secretaries of Divisions sponsoring the symposium, who will be responsible for their transmittal to the Editor. The Secretary of the Division by agreement with the Editor will specify a time after which symposium papers cannot be accepted. The Editor reserves the right to refuse to publish symposium articles, for valid scientific reasons. Each symposium paper may not exceed four printed pages (about sixteen double spaced typewritten pages) in length except by prior arrangement with the Editor.

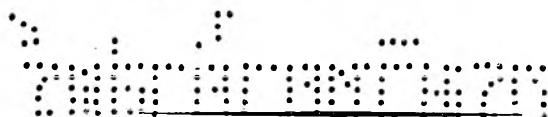
Remittances and orders for subscriptions and for single copies, notices of changes of address and new professional connections, and claims for missing numbers should be sent to the American Chemical Society, 1155 Sixteenth St., N. W., Washington 6, D. C. Changes of address for the *Journal of Physical Chemistry* must be received on or before the 30th of the preceding month.

Claims for missing numbers will not be allowed (1) if received more than sixty days from date of issue (because of delivery hazards, no claims can be honored from subscribers in Central Europe, Asia, or Pacific Islands other than Hawaii), (2) if loss was due to failure of notice of change of address to be received before the date specified in the preceding paragraph, or (3) if the reason for the claim is "missing from files."

Subscription Rates: to members of the American Chemical Society, \$8.00 for 1 year, \$15.00 for 2 years, \$22.00 for 3 years; to nonmembers, \$10.00 for 1 year, \$18.00 for 2 years, \$26.00 for 3 years. Postage free to countries in the Pan American Union; Canada, \$0.40; all other countries, \$1.20. Single copies, \$1.25; foreign postage, \$0.15; Canadian postage \$0.05.

The American Chemical Society and the Editors of the *Journal of Physical Chemistry* assume no responsibility for the statements and opinions advanced by contributors to THIS JOURNAL.

The American Chemical Society also publishes *Journal of the American Chemical Society*, *Chemical Abstracts*, *Industrial and Engineering Chemistry*, *Chemical and Engineering News*, *Analytical Chemistry*, and *Journal of Agricultural and Food Chemistry*. Rates on request.



---

---

# THE JOURNAL OF PHYSICAL CHEMISTRY

(Registered in U. S. Patent Office) (Copyright, 1954, by the American Chemical Society)

VOLUME 58

APRIL 19, 1954

NUMBER 4

---

---

## FREEZING POINT OF WATER HELD IN POROUS BODIES AT DIFFERENT VAPOR PRESSURES

BY BALWANT RAI PURI, LEKH RAJ SHARMA AND M. L. LAKHANPAL

*Department of Chemistry, Panjab University, Hoshiarpur, India*

*Received December 29, 1952*

A method for determining freezing points of capillary condensed moisture, based on dilatometric measurements, has been described. The freezing point depressions of water held in four different porous bodies at different vapor pressures, determined by this technique, have been compared with the theoretical values derived from thermodynamic considerations. The results appear to offer support to the theory of capillary condensation.

According to the capillary condensation hypothesis, vapors condense to liquids in the pores of an adsorbent because of the lowering of vapor pressure brought about by surface tension effects. The properties of the adsorbed liquids, particularly their freezing and boiling points, are expected, therefore, to be different from those associated with the same materials in bulk conditions. A number of investigations designed to determine effects of capillary condensation on freezing points of adsorbates are reported in literature. Foote and Saxton<sup>1</sup> and Jones and Gortner<sup>2</sup> deduced from dilatometric measurements that water adsorbed on silica gel behaves abnormally below its bulk freezing point. Coolidge<sup>3</sup> from the adsorption isotherms of benzene on charcoal and Milligan and Rachford<sup>4</sup> from the isotherms of water on silica gel, above and below the normal freezing points of the liquids, plotted on a relative pressure basis, concluded that the adsorbates did not undergo phase transformation even at temperatures well below their normal freezing points. Emmett and Cines<sup>5</sup> cited identical observations made by Brunauer and Emmett in the case of adsorption of acetylene on iron catalysts. Patrick and Land<sup>6</sup> and Patrick and Kemper<sup>7</sup> found evidence for fairly large freezing point depressions in the case of a number of substances adsorbed on silica gel.

Kubelka<sup>8</sup> derived an approximate equation for the melting point lowering as a function of the radius of the capillaries assuming the heat of fusion to remain constant with the temperature.

By examination of the vapor pressure-temperature curves, Batchelor and Foster<sup>9</sup> for dioxane on ferric oxide gel, and Brown and Foster<sup>10</sup> for ethylenediamine on silica gel, observed freezing point depressions of 7.3 and 6.8°, respectively. Higuti and co-workers<sup>11-13</sup> determined recently the freezing point depressions in the case of nitrobenzene, *o*-nitrophenol, benzene and carbon tetrachloride adsorbed on silica gel, by measuring either dielectric polarizations or heat capacities of the adsorbates at different temperatures. The determined values were compared with those calculated from a theoretical formula derived thermodynamically. The agreement, however, was not so good.

In the present work a dilatometric method for determining freezing point of water adsorbed on porous bodies has been described and the results obtained in the case of four different substances at different vapor pressures have been compared with the theoretical values. This method seems to be simpler than those based on the measurements of low vapor pressures or heat capacities.

- (1) H. W. Foote and B. Saxton, *J. Am. Chem. Soc.*, **39**, 1103 (1917).
- (2) I. D. Jones and R. A. Gortner, *THIS JOURNAL*, **36**, 387 (1932).
- (3) A. S. Coolidge, *J. Am. Chem. Soc.*, **46**, 596 (1924).
- (4) W. O. Milligan and H. Rachford, *ibid.*, **70**, 2922 (1948).
- (5) P. H. Emmett and M. Cines, *THIS JOURNAL*, **51**, 1261 (1947).
- (6) W. A. Patrick and W. E. Land, *ibid.*, **38**, 1201 (1934).
- (7) W. A. Patrick and W. A. Kemper, *ibid.*, **42**, 369 (1938).

- (8) P. Kubelka, *Z. Elektrochem.*, **38**, 611 (1932).
- (9) R. W. Batchelor and A. G. Foster, *Trans. Faraday Soc.*, **40**, 300 (1944).
- (10) M. J. Brown and A. G. Foster, *Nature*, **169**, 37 (1952).
- (11) I. Higuti, *Science Rep. Tôhoku Univ.*, Series 1, **33**, 174 (1949).
- (12) I. Higuti and M. Shimizu, *THIS JOURNAL*, **56**, 198 (1952).
- (13) I. Higuti and Y. Iwagami, *ibid.*, **56**, 921 (1952).

### Experimental

**Materials.**—The materials used in these investigations were: (i) silica ge., (ii) "barium aluminosilicate" gel having  $0.5\text{BaO}\cdot\text{Al}_2\text{O}_3\cdot\text{SiO}_2$  as its approximate composition, (iii) a sample of bentonite and (iv) a sample of clay loam. Both the gels were prepared fresh in the laboratory.

Twenty-five-gram portions of the gels and 50-g. portions of the sample of bentonite and clay loam were placed in vacuum desiccators maintained at  $25 (\pm 1^\circ)$  containing sulfuric acid-water mixtures corresponding to different relative vapor pressures of water. The increase in weight was determined after about a week and then daily till it became constant. This usually required ten to twelve days time and was taken to indicate the approach of equilibrium of the samples with the surrounding atmospheres.

**Apparatus and Procedure.**—The apparatus devised for determining freezing point of capillary condensed water is shown in Fig. 1. It consists of a glass vessel, A, blown from a Pyrex tubing. It is about 11 cm. long and 3 cm. wide and is fitted with a ground joint, J, J'. The inner part, J, is fused at its lower end with a glass tube, B, which passes more than half way into the vessel, A. The tube B is closed from below except for two small holes which permit the passage of the wires of a copper-eureka thermocouple cemented immediately at the end of the tube. The inner part, J, of the joint, also carries at its upper end a graduated fused-in capillary tube, t, of about 0.5-cm. bore, which opens into the vessel A, through the side of the tube B, at the point h, as shown in the figure.

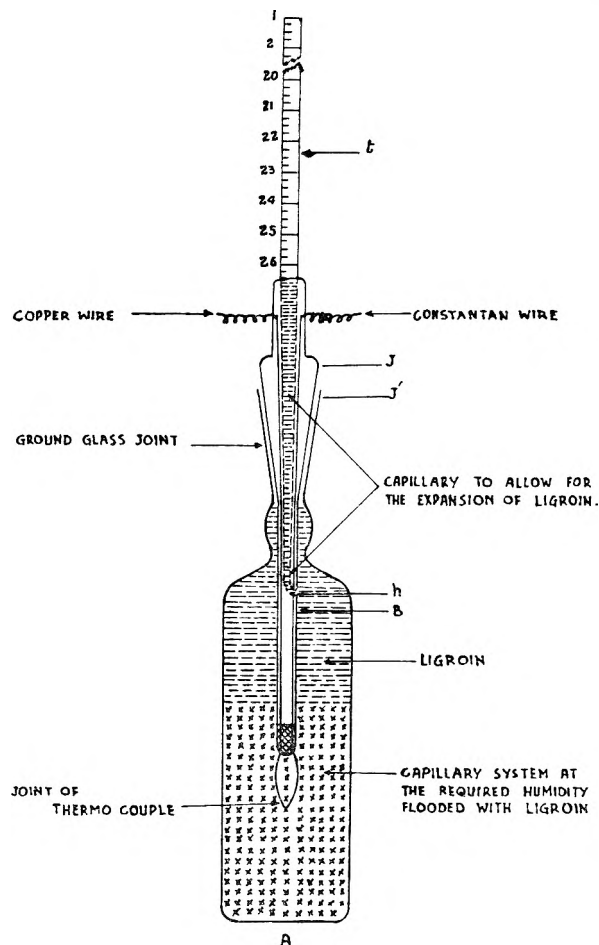


Fig. 1.—Apparatus for the determination of freezing point of capillary condensed moisture.

The sample under examination was transferred to the vessel, A, so as to fill more than half of it and ligroin was gradually poured over it till the space not occupied by the solid particles was completely filled up. The stopper, J, with its attached parts was then placed in position, as shown in the figure. The ligroin thus displaced rose into the gradu-

ated tube, t, through the capillary opening, h. This permitted air-free filling of the apparatus. More ligroin was added into the capillary tube, t, directly from above, so as to fill nearly two-thirds of it.

The entire apparatus, almost up to the level of the ligroin, was then lowered into a wide-mouth Dewar flask containing a suitable freezing mixture, capable of giving a temperature several degrees below the theoretical freezing point of water at the vapor pressure of the body under examination. For temperatures as low as  $-20^\circ$ , an ice-salt-bath was used. For lower temperatures, carbon dioxide snow mixed with alcohol was necessary.

The above flask was fitted with a stopper having two bores, one for holding the tube, t, and the other for a glass stirrer. A considerable amount of the capillary condensed moisture became frozen after an interval of about 20 minutes. This could be verified easily, particularly in the case of the two gels, from the "frosted" appearance of the samples. The temperature of the bath was then allowed to rise gradually by loosening the stopper of the flask and stirring the freezing mixture gently. The position of the ligroin meniscus in the tube, t, was noted by means of a magnifying glass after about every one degree centigrade rise of temperature.

The movement of the ligroin meniscus in the tube, t, with rise in temperature would, obviously, be given by the relative magnitudes of two opposing effects, namely, *expansion* of the ligroin and *contraction* of the capillary system caused by melting of the frozen water. The first effect, however, predominated and consequently there was a net rise in the ligroin meniscus. But as soon as fusion of the entire amount of the frozen moisture was completed, the second effect disappeared altogether and the rise of the ligroin level with subsequent increase in temperature became steeper. The positions of the ligroin meniscus taken before and after the critical stage, when plotted against the corresponding temperatures, were seen to fall on two curves with different slopes and the temperature at which the abrupt change in the slope was noticed, was taken as the temperature of maximum melting, or the temperature at which the phase transformation from solid to liquid state was just completed. Obviously, this would also correspond to the temperature at which the condensate liquid would commence to freeze, if gradually cooled. The plot of ligroin meniscus against corresponding temperatures in one of the determinations is shown in Fig. 2 to illustrate the procedure.

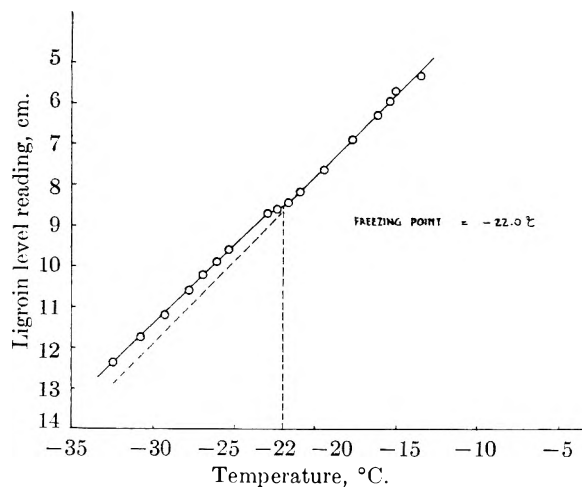


Fig. 2.—Determination of the freezing point of capillary condensed moisture in silica gel when relative vapor pressure ( $x'$ ) is 0.774.

It took nearly nine hours to complete one determination. The rate of heating was quite slow, the temperature rising by about  $1^\circ$  after every half an hour. The position of the ligroin meniscus at a particular temperature was noted after ascertaining that the temperature of the freezing mixture outside the vessel A (measured by another thermocouple) was within  $0.4^\circ$  of the inside temperature. Mean of the two temperatures was then taken.

Replicate determinations of freezing points were also made in the case of silica gel to check reproducibility of the

results. The values obtained are given in brackets in Table II. The method seems to be capable of yielding reproducible results.

**Theoretical Calculation of the Freezing Point Depression of Capillary Condensed Water.**—The lowering of vapor pressure consequent upon the condensation of liquids in capillary pores is given by the Kelvin equation

$$-\log_e p/p_0 = -\log_e x = \frac{2\gamma M}{r\rho RT} \quad (1)$$

where  $x$  is the ratio of the actual vapor pressure  $p$  and the saturation vapor pressure  $p_0$  of the condensate;  $\gamma$ ,  $M$  and  $\rho$  are its surface tension, molecular weight and density, respectively;  $r$  is the radius of the capillaries involved;  $R$  is the gas constant, and  $T$  is the absolute temperature.

The adsorbents used in the freezing point measurements were first brought into equilibrium with atmospheres of known relative humidities of water as already mentioned. But when air in the water-air interface was replaced by ligroin and the temperature of the system was lowered to its freezing point, say  $T'$ , the system may be considered to have assumed a new relative vapor pressure,  $x'$ , given by the equation

$$-\log_e x' = \frac{2\gamma' M}{r\rho RT'} \quad (2)$$

where  $\gamma'$  is the interfacial tension between ligroin and water at temperature,  $T'$ . The small change in density with temperature has been ignored.

From equation 1 and 2 we have

$$\log_e x' = \log_e x \times \frac{\gamma' T}{\gamma T'} \quad (3)$$

The validity of such a relationship has been proved by Puri and Crowther<sup>14</sup> in the case of soils.

The values of interfacial tension between ligroin and water were carefully determined at different temperatures in the range of 4.5 to 35° and are given in Table I. The values at the freezing points were obtained by extrapolation. Substituting these and other appropriate values in equation 3 the new relative vapor pressures ( $x'$ ) were calculated. These along with the original values of vapor pressures ( $x$ ) and the pore radii ( $r$ ) calculated by means of the Kelvin equation are given in Table II.

TABLE I

INTERFACIAL TENSION BETWEEN LIGROIN AND WATER AT DIFFERENT TEMPERATURES

| Temp., °C. | Interfacial tension, dynes/cm. | Temp., °C. | Interfacial tension, dynes/cm. |
|------------|--------------------------------|------------|--------------------------------|
| 32.0       | 35.15                          | 17.0       | 31.59                          |
| 31.0       | 35.00                          | 15.0       | 31.41                          |
| 22.0       | 32.83                          | 8.5        | 29.07                          |
| 20.0       | 32.60                          | 4.5        | 28.80                          |

The well known thermodynamic relationship between lowering of vapor pressure and depression of freezing point is given by the equation

$$-\log_e \frac{p}{p_0} = \frac{\Delta H \Delta T}{RT_0 T} \quad (4)$$

where  $T_0$  is the normal freezing point of the liquid at the vapor pressure  $p_0$ ,  $T$  is the freezing point at the lower vapor pressure  $p$ ,  $\Delta T$  is the depression in freezing point ( $T_0 - T$ ), and  $\Delta H$  is the molar heat of fusion of the liquid and may be assumed to remain constant for small range of  $\Delta T$ .

However for a large range of  $\Delta T$ ,  $\Delta H$  is no longer constant. The "best" values of the National Bureau of Standards<sup>15,16</sup> for the properties of water and ice give the relationship

$$-\log_e p/p_0 = 0.9686 \times 10^{-2} \Delta T - 0.56 \times 10^{-6} (\Delta T)^2 + 0.72 \times 10^{-8} (\Delta T)^3 \quad (5)$$

The values of  $\Delta T$  corresponding to different relative vapor pressures ( $x'$ ) were calculated by means of this equation.

## Results and Discussion

The freezing point depression of water held in the various adsorbents at different relative vapor pressures, as determined by the technique described in this paper, are recorded in Table II. It is seen that the values obtained at a given relative vapor pressure are about the same in the case of all the samples examined which were of different nature and were known to differ appreciably from one another in their moisture content-vapor pressure relationships. This shows that the freezing point depression of the sorbed water depends largely on the radius of the capillary pores in which it is condensed.

The theoretical values are also included in Table II in an appropriate column. The agreement between the determined and the calculated values is seen to be fairly good up to the capillary pores of radius 37.3 Å. and even in the case of the next lower size, *viz.*, 24.5 Å., it is perhaps not so bad.

Batchelor and Foster<sup>9</sup> assuming that the Kelvin equation is valid for the solid phase as well and that the vapor pressure of ice in a capillary is different from that outside, showed good agreement between the observed and the calculated values of freezing point depression of dioxane adsorbed on ferric oxide gel. They, however, confined themselves to a small range of  $\Delta T$  only and the smallest pore size examined by them was as wide as 88 Å. in radius.

The agreement obtained by us in the case of the capillary pores of radius  $\geq 24.5$  Å. appears to be better than that reported by Higuti and Iwagami<sup>13</sup> in the case of benzene and carbon tetrachloride adsorbed on silica gel although the lower range of the capillary radius examined by them was 40 Å. This may, however, be due to the difference in the nature of the adsorbates used by them.

The validity of the agreement between the determined and the calculated values is seen to decrease as we approach finer capillary sizes. The reason for this probably lies in the fact that the properties such as density and surface tension of the condensates in very fine capillary pores are not the same as in the bulk form as is tacitly assumed in the Kelvin equation. There is an indica-

(14) E. M. Crowther and A. N. Puri, *Proc. Roy. Soc. (London)*, **A-106**, 232 (1924).

(15) N. S. Osborne, H. F. Stinson and D. C. Ginnings, *Natl. Bur. Standards J. Research*, **23**, 197 (1939).

(16) N. S. Osborne, *ibid.*, **23**, 643 (1939).

TABLE II

FREEZING POINT DEPRESSIONS OF WATER HELD IN THE VARIOUS POROUS BODIES AT DIFFERENT RELATIVE VAPOR PRESSURES

| Relative vapor pressure ( $x$ ) of the system (original) | Corresponding capillary radius, Å. | Relative vapor pressure ( $x'$ ) assumed by the system f.p. | Theoretical f.p. depression ( $\Delta T$ ), °C. | Determined f.p. depression (°C.) in the case of |                            |           |           |
|--|------------------------------------|---|---|---|----------------------------|-----------|-----------|
|  |                                    |   |   | Silica gel                                      | Barium aluminosilicate gel | Bentonite | Clay loam |
| 0.975  | 413.0                              | 0.998   | 0.25  | 0.40 (0.51)                                     | ...                        | 0.55      | 0.54      |
| .860   | 69.4                               | .936  | 6.83  | 5.00 (5.40)                                     | 5.84                       | 6.30      | 5.38      |
| .756   | 37.3                               | .885  | 12.62   | 11.38 (10.98)                                   | 10.92                      | 10.77     | 10.76     |
| .653   | 24.5                               | .831  | 19.10   | 16.15 (16.00)                                   | 15.00                      | 17.30     | 15.54     |
| .557   | 17.8                               | .774  | 26.42   | 22.96 (22.00)                                   | 20.40                      | 22.80     | ...       |
| .472   | 13.9                               | .721  | 33.67   | 28.00 (28.46)                                   | 28.56                      | 28.00     | 28.14     |
| .404   | 11.5                               | .673  | 40.85   | 33.00 (32.72)                                   | 32.00                      | 32.80     | 33.00     |
| .341   | 9.7                                | .621  | 49.14   | 44.00 (42.10)                                   | ...                        | 43.68     | ...       |

tion<sup>17</sup> that even the heat of vaporization of a capillary condensate is different from that of the same liquid in bulk. The same may be true for the heat of fusion as well. In the words of Emmett<sup>18</sup>—“in dealing with capillaries that are one to ten molecular diameters in size one has little information as to the way in which density, surface tension and other properties of the adsorbed molecules may differ from those of the adsorbate in bulk.” Pierce, Wiley and Smith<sup>19</sup> have shown that the

(17) C. P. Carman, *THIS JOURNAL*, **57**, 56 (1953).

(18) P. H. Emmett, *Chem. Revs.*, **43**, 69 (1948).

(19) C. Pierce, J. W. Wiley and R. N. Smith, *THIS JOURNAL*, **53**, 669 (1949).

Kelvin equation is not applicable in the case of capillaries a few molecular diameters in width. The calculations of pore diameters by the Kelvin equation are also reported to break down for pores below 20 to 25 Å. in radius.<sup>20</sup> Keeping the above limitation in view, the results presented in this paper may be considered to offer a fair amount of support to the view that freezing point depression of a capillary condensate is governed, to a fairly large extent, by the surface tension effects as required by the theory of capillary condensation.

(20) C. Pierce and R. N. Smith, *ibid.*, **57**, 64 (1953).

## A NEW ADSORPTION ISOTHERM AND THE DISTRIBUTION OF ENERGY SITES ON THE SURFACE OF SOME FINELY DIVIDED SOLIDS<sup>1</sup>

BY WILLIAM D. HARKINS<sup>2</sup> AND

*George Herbert Jones Laboratory, University of Chicago, Chicago, Illinois*

RICHARD S. STEARNS

*Chemical and Physical Research Laboratories, Firestone Tire and Rubber Company, Akron, Ohio*

*Received February 17, 1953*

An adsorption isotherm has been derived which may be written in the form  $-RT \ln p/p^\circ = U_m - RT/n \ln (\theta/1 - \omega\theta)$ , where  $p/p^\circ$  is the relative pressure,  $\theta$  is the relative surface coverage,  $\omega$ ,  $n$  and  $U_m$  are constants. The adsorption of ethane, ethylene, nitrogen and oxygen on several finely divided solids are found to be represented by the above equation from very low surface coverage up to the completion of a monolayer. It is shown that a distribution of energy sites may be calculated from the constants of the isotherm. When this is done it is found that  $n$  is representative of the width of the essentially Gaussian distribution, and  $U_m$  is representative of the heat of adsorption at the maximum in the distribution curve. The constant  $\omega$  is shown to be representative of adsorbate-adsorbate interaction on the surface of the solid and to be dependent on the polarizability of the adsorbate and the extent and magnitude of the surface heterogeneity as represented by  $U_m$  and  $n$ .

### I. Introduction

In an effort to gain information concerning the surface characteristics of some finely divided solids from the adsorption isotherm the adsorption of ethane and ethylene on several carbon blacks and rutile was measured at very low relative pressures and consequently low surface coverage. An attempt is made to interpret the data in terms of the concept of surface heterogeneity and the distribution of energy sites as formulated by

Halsey<sup>3</sup> and Sips,<sup>4</sup> although it is recognized that coöperative interaction between the adsorbed molecules can be used as an alternative method in analyzing the same data.

Since none of the generally familiar isotherms adequately represented the experimental data, an equation was derived in a somewhat empirical manner, which has been found to be rather successful in analytically describing the adsorption isotherm in the region of the first monolayer. The thermodynamic and statistical development of the isotherm follows closely the arguments and methods

(1) This work was performed as part of the research project sponsored by the Reconstruction Finance Corporation, Office of Synthetic Rubber, in connection with the Government Synthetic Rubber Program.

(2) This research was conducted under the direction of Professor Harkins (deceased March 7, 1951), in his laboratories at the University of Chicago.

(3) (a) G. B. Halsey and H. S. Taylor, *J. Chem. Phys.*, **15**, 624 (1947); (b) G. B. Halsey, *ibid.*, **16**, 931 (1948); (c) G. B. Halsey, *J. Am. Chem. Soc.*, **73**, 2693 (1951).

(4) R. J. Sips, *J. Chem. Phys.*, **16**, 490 (1948).

used by Hill,<sup>5,6</sup> Tompkins,<sup>7,8</sup> and Everett.<sup>9</sup> In brief the method consists in finding an equation which represents the adsorption on a homogeneous surface and which can be explicitly solved for  $\theta$ , the surface coverage. This equation is then generalized for adsorption on a heterogeneous surface and the distribution of energy sites found by the formal mathematical method of Sips.<sup>4</sup> In order to perform the above operations it is necessary to make several assumptions and approximations. Therefore, the solution which is arrived at may be considered to have real physical significance only to the extent that the assumptions and approximations made are considered valid.

## II. The Isotherm for Adsorption on a Homogeneous Surface

The following assumptions are made concerning the nature of the two-dimensional adsorbed film supposedly being formed on a homogeneous surface: (a) that the film remains monomolecular until the fraction of surface covered,  $\theta$ , approaches unity, (b) that the adsorbed film is mobile rather than localized, (c) that there will be no phase change in the adsorbed film during the formation of the monolayer, and (d) that the film may be characterized by an equation of state for a two-dimensional imperfect gas.

The equation of state of the adsorbed film is taken to be

$$\phi = RT\Gamma(1 + \frac{\beta}{2}\Gamma) \quad (1)$$

where  $\phi$  is the two-dimensional spreading pressure,  $\Gamma$  is the surface excess of adsorbed molecules and  $\beta/2$  is given by the following expression of Fowler and Guggenheim<sup>10</sup>

$$\frac{\beta}{2} = -\frac{1}{2} \int_0^\infty \left[ \exp\left(\frac{-\omega'(r)}{kT}\right) - 1 \right] 2\pi r dr \quad (2)$$

Where  $\omega'$  is the potential energy of interaction between two molecules separated by a distance  $r$ , the integral expression in equation 2 is equivalent to  $(b' - a'/RT)$  where  $b'$  and  $a'$  are the two-dimensional van der Waals constants. From equation 1 and the Gibbs adsorption isotherm

$$d\phi = RT \Gamma d \ln p(\Gamma) \quad (3)$$

there is obtained

$$c'p = \Gamma \exp \frac{\beta\Gamma}{2} \quad (4)$$

which reduces to

$$C \frac{p}{p^\circ} = \theta \exp \omega \theta \quad (5)$$

when the constants are expressed in terms of  $\Gamma_m$ , the surface concentration of molecules at the completion of a monolayer, and  $p^\circ$  the equilibrium vapor pressure at the temperature of adsorption. Since  $1/\Gamma_m = b'$  where  $b'$  is the co-area of the adsorbed molecules

(5) T. L. Hill, *J. Chem. Phys.*, **14**, 441 (1946).

(6) T. L. Hill, *ibid.*, **17**, 762 (1949).

(7) F. C. Tompkins, *Trans. Faraday Soc.*, **46**, 569 (1950).

(8) F. C. Tompkins, *ibid.*, **46**, 580 (1950).

(9) D. H. Everett, *ibid.*, **46**, 942 (1950).

(10) R. H. Fowler and E. A. Guggenheim, "Statistical Thermodynamics," Cambridge University Press, London, 1949, Equation 1003-7, p. 424.

$$\omega = \beta\Gamma_m = 2 \left( 1 - \frac{a'}{b'RT} \right) \quad (6)$$

The integration constant,  $C$ , is according to the statistical mechanical treatment of Hill<sup>5</sup> given by

$$C = Z \exp (E_1 - \lambda)/RT \quad (7)$$

where the constant  $Z$  involves the ratio of the internal partition function of the adsorbed molecules to the internal partition function of the molecules in the liquid state,  $E_1$  is the molar heat of adsorption of the molecules in the first layer, and  $\lambda$  is the molar heat of vaporization of the liquid.

Equation 5 can be expressed in terms of the volume of gas adsorbed at S.T.P. by noting that  $\theta = V/V_m$  where  $V_m$  is the volume of gas required to form a monolayer.

In order to proceed further, and generalize equation 5 for adsorption on a heterogeneous surface, it is necessary to obtain an expression which can be explicitly solved for  $\theta$ . This is accomplished by expanding the exponential in equation 5 and noting that  $1/(1 - \omega\theta)$  when expanded will approximate the exponential series  $1 + \omega\theta + \omega^2\theta^2/2! + \omega^3\theta^3/3! \dots$  so that to a first approximation

$$C p/p^\circ = \theta/(1 - \omega\theta) \quad (8)$$

which, when solved for  $\theta$ , gives

$$\theta = C p/p^\circ / 1 + \omega C p/p^\circ \quad (9)$$

It should be noted that  $\theta/(1 - \omega\theta) > \theta \exp \omega\theta$  and that equations 5 and 9 become equal when  $\theta$  approaches zero or  $\omega$  is small. Having made the above mathematical approximation, it is interesting to note that the equation of state for a two-dimensional monolayer which would have led directly to equation 9 is

$$\phi = RT\Gamma(1 + \beta\Gamma/2 + \beta^2\Gamma^2/3 + \beta^3\Gamma^3/4 \dots) \quad (10)$$

where  $\phi$  is the two-dimensional film pressure. Equation 10 is equivalent to Fowler and Guggenheim's equation 1003-7<sup>10</sup> for the first two terms and contains additional empirical terms which may be considered as accounting for higher order interactions in terms of the two dimensional van der Waals constants. It should be emphasized that equation 10 has no physical basis but is the result of the desire to solve equation 5 for  $\theta$ .

## III. The Adsorption Isotherm for a Gas Forming a Mobile Monolayer on a Solid Surface Having a Heterogeneous Distribution of Energy Sites

If the surface is considered as being composed of a series of infinitely small Langmuir patches<sup>8</sup> such that

$$\theta = \sum_i f(M_i)\theta_i = \sum_i f(M_i)C_i \frac{p}{p^\circ} / 1 + \omega C_i \frac{p}{p^\circ} \quad (11)$$

where  $f(M_i)$  is the fraction of the total number of sites which may be characterized by the constant  $C_i$  of equation 9 and  $\theta_i$  is the fraction of these sites filled when the pressure is  $p(\Gamma T)$ . It is assumed that  $\omega$  is a constant presumably dependent only on the adsorbate and the temperature of adsorption. For simplicity it is also necessary to assume that the following relation holds

$$C_i = \bar{Z} \exp (E_i - \lambda)/RT \quad (12)$$

where  $\bar{Z}$  is assumed to be a constant independent

of the magnitude of the adsorption energies at a particular site. This is certainly a questionable assumption when it is considered that the rotational and vibrational characteristics of an adsorbed molecule cannot be independent of  $E_i$ .

If the summation in equation 11 is replaced by an integral and the limits set at  $-\infty$  to  $+\infty$  as is customary, then

$$\theta = \frac{1}{\omega} \int_{-\infty}^{+\infty} f(M_i) dq / 1 + \frac{\exp(-q_i)}{Z\omega p/p^\circ} \quad (13)$$

where

$$q_i = (E_i - \lambda) \quad (14)$$

If an expression can be found which represents the experimental adsorption data from  $\theta = 0$  to  $\theta = 1$ , then equation 13 can be solved for  $f(M_i)$  by the method of Sips.<sup>4</sup> To obtain an expression for  $\theta$ , the following empirical method is used.<sup>9</sup>

It is well known that the equation of state for a two-dimensional perfect gas

$$\phi = RT\Gamma = RTN/\mathcal{A} \quad (15)$$

leads to the isotherm

$$\theta = C'p \quad (16)$$

which is found to fit some experimental data at very low pressures, while the equation of state

$$\phi = \frac{1}{n} RT\Gamma \quad (17)$$

leads to the Freundlich isotherm

$$\theta = C''p^n \quad (18)$$

which has been found to fit the experimental data for many gases on a large number of solids over several decades in  $\log p$ . However, equation 18 often fails to hold as  $\theta \rightarrow 1$ , where adsorbate-adsorbate interactions become important. An improvement in the equation of state given by equation 17 may therefore be expected if equation 10 is multiplied by an arbitrary constant  $1/n$  to give

$$\phi = \frac{RT}{n} \Gamma \left( 1 + \frac{\beta}{2} \Gamma + \frac{\beta^2}{3} \Gamma^2 + \frac{\beta^3}{4} \Gamma^3 \dots \right) \quad (19)$$

Since

$$d\phi = RT\Gamma d \ln p(\Gamma) \quad (20)$$

we can eliminate  $\phi$  from 19 to obtain

$$n d \ln p(\Gamma) = \left[ \frac{d\Gamma}{\Gamma} + \frac{\beta d\Gamma}{1 - \beta\Gamma} \right] \quad (21)$$

or

$$\bar{C}' p^n = \frac{\Gamma}{1 - \beta\Gamma} \quad (22)$$

where  $\bar{C}'$  is the constant of integration.

Expressing the constants in terms of  $p^\circ$  and  $\Gamma_m$

$$\bar{C} \left( \frac{p}{p^\circ} \right)^n = \frac{\theta}{1 - \omega\theta} \quad (23)$$

and equation 23 can now be solved explicitly for  $\theta$

$$\theta = \frac{\Gamma}{\Gamma_m} = \frac{V}{V_m} = \bar{C} \left( \frac{p}{p^\circ} \right)^n / 1 + \omega\bar{C} \left( \frac{p}{p^\circ} \right)^n \quad (24)$$

Equation 24 is seen to be equivalent to the classical Langmuir equation when  $\omega$  and  $n$  are unity, and equivalent to the Freundlich equation when

$\omega = 0$  and to be equivalent to Henry's law when  $\omega = 0$  and  $n = 1$ .

Equation 24 may be equated to equation 13

$$\frac{\bar{C} \left( \frac{p}{p^\circ} \right)^n}{1 + \omega\bar{C} \left( \frac{p}{p^\circ} \right)^n} = \frac{1}{\omega} \int_{-\infty}^{+\infty} f(M_i) \frac{dq}{1 + \frac{\exp(-q_i)}{Z\omega p/p^\circ}} \quad (25)$$

which is similar to the integral equation used by Sips<sup>4</sup> to solve for  $f(M_i)$ , but differs by virtue of the constant  $\omega$  in the denominator. The solution to equation 25 can be approximated by the expression

$$f(M_i) = \frac{1}{2\pi RT} \left( \frac{\sin \pi n}{\exp \frac{y^2}{2} + \cos \pi n} \right) \quad (26)$$

where

$$y = \frac{n}{RT} (q_m - q_i) \quad (27)$$

and

$$q_m = \frac{RT}{n} \ln \omega\bar{C} - RT \ln Z \quad (28)$$

Equation 26 emphasizes the Gaussian character of the distribution function and shows that  $\bar{C}$  which was introduced as a constant of integration in equation 22 is related to the heat of adsorption,  $q_m$  at the maximum in the distribution curve, and that the constant  $n$  which was introduced as an empirical constant in equation 19 determines the width of the Gaussian distribution of energy sites. When  $n = 1$ ,  $f(M_i)$  is zero for  $q \neq q_m$  and  $\infty$  for  $q = q_m$ , while

$$\int_{-\infty}^{+\infty} f(M_i) dq_i = 1$$

which means that the Langmuir equation represents adsorption on a surface containing sites all of equal energy, the assumption made in the derivation of the Langmuir isotherm. As  $n \rightarrow 0$  the distribution curve becomes flat and

$$f(M_i) \simeq \frac{n}{RT}$$

When adsorption data are found to fit equation 44 it will be possible to calculate a distribution of energy sites which will of course not be necessarily unique.

#### IV. Experimental

The adsorption data were obtained by the standard volumetric procedure.<sup>11</sup> The sample was degassed at a temperature of 100° until a vacuum of better than 10<sup>-6</sup> mm. of Hg was obtained. Mercury was used as the confining liquid and in the manometers. Apiezon grease was used on all stopcocks. The adsorption of ethane and ethylene by the grease in the stopcocks was small compared to the volume of gas adsorbed at the equilibrium pressure by the high area solids. It will be noted that the error introduced in the total gas adsorbed cannot be larger than the experimental error since the nitrogen areas are the same as those determined with ethane. Precautions were taken to ensure that the partial vapor pressure of the mercury was reduced to that of the temperature of adsorption before the adsorbate was introduced into the adsorption bulb, by passing the gas through a tube packed with several centimeters of glass wool and immersed in the constant temperature bath. The pressure was not corrected for thermal transpiration; the error involved, however, is small compared to the error involved in the measurements.

(11) W. D. Harkins and G. Jura, *J. Am. Chem. Soc.*, **66**, 1366 (1944).

TABLE I  
 ADSORPTION OF ETHANE

| Pigment <sup>a</sup>      | Temp. of adsorption, °C. | BET area N <sub>2</sub> adsorption M <sup>2</sup> /g | Area, adsorption ethane M <sup>2</sup> /g | n    | U <sub>m</sub> , cal. | ω     | $\bar{C}$ | Range of fit, θ |
|---------------------------|--------------------------|--|---|------|-----------------------|-------|-----------|-----------------|
| Graphon                   | -78.8                    | 95   | 95  | 1.00 | 1420                  | ..    | 39.4      | 0.023-0.15      |
| Acetylene                 | -78.8                    | 64   | 59  | 0.80 | 1355                  | ..    | 16.6      | .029-0.50       |
| HAF-1                     | -78.8                    | 71   | 78  | .61  | 1200                  | 0.50  | 6.8       | .033-0.95       |
| HAF-2                     | -78.8                    | 81   | 82  | .68  | 1040                  | 0.65  | 6.2       | .041-0.98       |
| VFF-1                     | -78.8                    | 219  | 217                                       | .31  | 1355                  | 0.50  | 3.0       | .160-0.98       |
|                           | -64.0                    |  |   |      |                       |       |           |                 |
| EPC-1                     | -78.8                    | 111  | 100                                       | .36  | 700                   | 0-0.1 | 1.9       | .032-0.99       |
| MPC-1                     | -78.8                    | 121  | 129                                       | .40  | 630                   | 0-0.1 | 1.9       | .043-0.96       |
| TiO <sub>2</sub> (Rutile) | -78.8                    | ..   | 32  | .94  | 1050                  | 0.70  | 12.9      | .013-0.98       |
| Mixture                   | -78.8                    | 141  | 137                                       | .36  | 1080                  | 0.35  | 2.7       | 0.082-0.95      |
| (56 wt. % HAF-2)          |                          |  |   |      |                       |       |           |                 |
| (44 wt. % VFF-1)          |                          |  |   |      |                       |       |           |                 |

<sup>a</sup> HAF represents a high abrasion furnace black, VFF a very fine furnace black, EPC an easy processing channel black, MPC a medium processing channel black.

The adsorption was usually carried out at the Dry Ice temperature of -78.8° by maintaining a mush of solid carbon dioxide and methanol in a Dewar flask.

The ethane and ethylene, obtained from the Matheson Company, were dried over P<sub>2</sub>O<sub>5</sub>, condensed in liquid nitrogen and all air removed by repeated boiling in vacuum. The gases were 95% pure. No attempt was made to remove the methane, ethane, ethylene, propane and propylene given by the manufacturer as the impurities present.

Low pressures from 0.001 to 5 cm. were read to ±0.0005 cm. on a large bore manometer with a traveling microscope and the higher pressures with a cathetometer.

## V. Results and Discussions

A characteristic isotherm is shown in Fig. 1. Four constants determine the shape of the isotherm:  $\bar{C}$ ,  $V_m$ ,  $n$  and  $\omega$ . Reference to equation 44 shows that the limiting slope is determined by the value of  $n$  and that the value of  $\omega$  determines the degree of curvature. The value of  $\bar{C}$  is given by the intercept of the linear portion of the isotherm with the ordinate, when  $p/p^\circ$  is unity, divided by  $V_m$ . The value of  $V_m$  is taken as a point of inflection in the isotherm which, on a log-log plot, appears almost as a point of discontinuity.<sup>3c</sup> From the value of  $V_m$  the area of the solids may be calculated and compared with the area given by nitrogen and the BET theory.

The area of the adsorbed ethane molecule may be calculated from the density of the liquid assuming hexagonal close-packing,<sup>12</sup> or from the three-dimensional van der Waals constants.<sup>5,13</sup> The first method gives a value of 21.4 Å.<sup>2</sup> and the second method a value of 21.6 Å.<sup>2</sup> for the area occupied by an ethane molecule on a surface. In the calculations, the latter value has been used. For nitrogen, the first method gives a value of 16.2 Å.<sup>2</sup> while the second method gives a value of 15.4 Å.<sup>2</sup> For nitrogen it is customary to use the higher value.

In Table I, columns 4 and 5, are listed the areas calculated using nitrogen and ethane as the adsorbents. It is seen that the agreement is very good and that assigning a value of 15.4 Å.<sup>2</sup> to nitrogen would not appreciably alter the agreement. It, therefore, seems certain that the point of inflection observed in the isotherm does give a true

value for  $V_m$  and that the value of  $\Gamma_m = 1/b'_m$  may be considered as a constant for all the solids studied at the completion of monolayer.

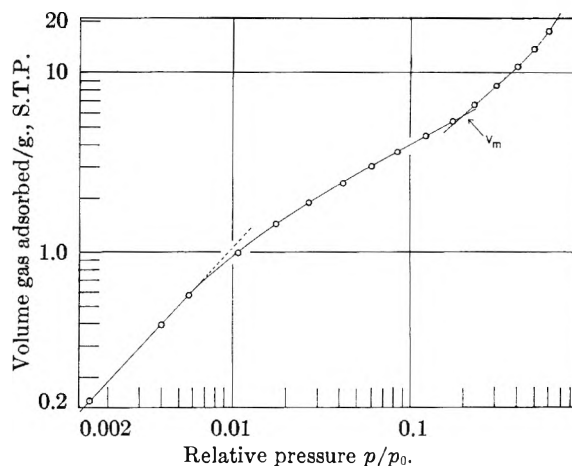


Fig. 1.—The adsorption isotherm of ethane on rutile at -78.8°.

Before proceeding further it will be profitable to present equation 24 in a modified form. The free energy of transfer of one mole of liquid from the bulk phase at  $p = p^\circ$  to the adsorbent surface where  $p = p_{(\theta)}$  is<sup>8,14,15</sup>

$$-(\bar{F}_\theta - \bar{F}_1) \equiv \Delta\bar{F}_\theta \equiv -RT \ln \frac{p}{p^\circ} = U_m - \frac{RT}{n} \ln \frac{\theta}{1 - \omega\theta} \quad (29)$$

where  $\bar{F}$  is the partial molar Gibbs free energy and  $U_m$  is given by

$$U_m = \frac{RT}{n} \ln \bar{C} \quad (30)$$

Equation 26 is often considered as giving the adsorption potential  $U_\theta$ . If the adsorption potential is plotted against  $\ln \theta/(1 - \omega\theta)$ , a straight line should be obtained with a slope of  $RT/n$  and a value of  $U_m$  given by the intersection of the line with the ordinate when  $\ln \theta/(1 - \omega\theta)$  is zero. Of the four constants in equation 24 only one,  $\omega$ , must be determined by approximation.

In Fig. 2 there are plotted adsorption data for

(12) S. Brunauer, P. H. Emmett and E. Teller, *J. Am. Chem. Soc.*, **60**, 309 (1938).

(13) T. L. Hill, *J. Chem. Phys.*, **16**, 181 (1948).

(14) V. A. Crawford and F. C. Tompkins, *Trans. Faraday Soc.*, **46**, 504 (1951).

(15) F. C. Tompkins and O. M. Young, *ibid.*, **47**, 77 (1951).

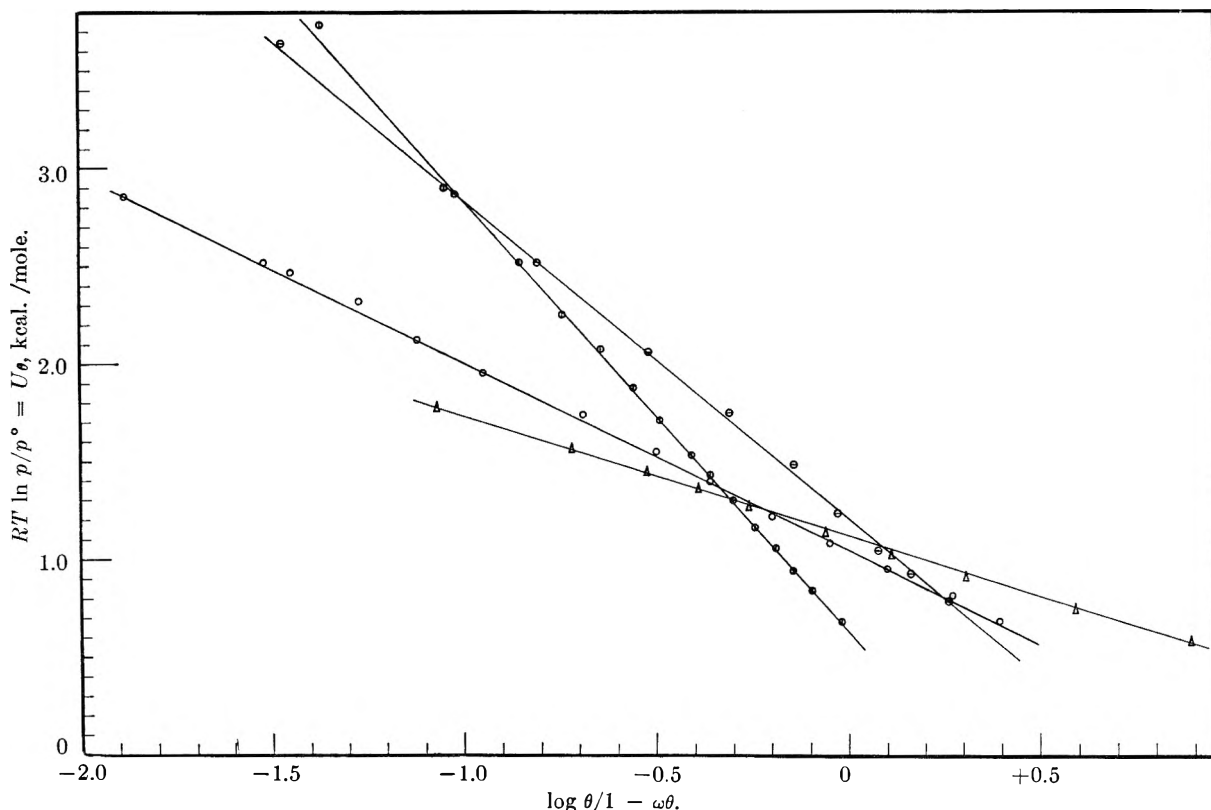


Fig. 2.—Adsorption isotherm of ethane at  $-78.8^\circ$  on:  $\circ$ , rutile;  $\diamond$ , MPC-1;  $\square$ , HAF-2;  $\triangle$ , oxygen on anatase at  $-195^\circ$ .

ethane on several solids. The data closely approximate straight lines as required by equation

29. The data in Fig. 3 represent adsorption at two temperatures; unfortunately, this is the only instance where the adsorption isotherm for ethane was obtained at more than one temperature. In this instance  $n$  is small, representing a broad distribution of energy sites, and as suggested by Tompkins,<sup>8</sup> the adsorption potential in this instance is found to be independent of temperature from  $\theta = 0.16$  to  $\theta = 0.98$ .

The data for the adsorption of ethane on nine solids are tabulated in Table I and for ethylene on five solids in Table II. The last column in Table I

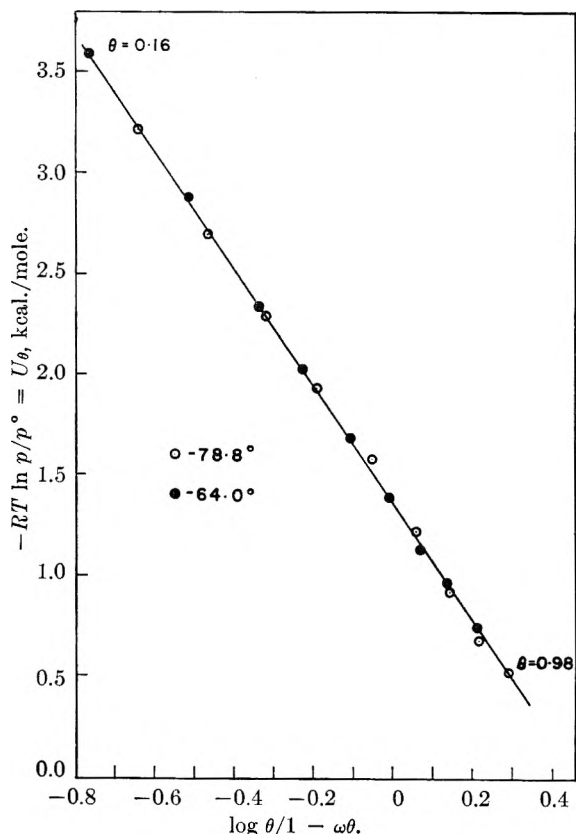


Fig. 3.—The adsorption isotherm of ethane on VFF-1 at  $-78.8^\circ$ ,  $\circ$ : and at  $-64^\circ$ ,  $\bullet$ .

TABLE II

| ADSORPTION OF ETHYLENE |   |      |              |          |           |
|------------------------|---|------|--------------|----------|-----------|
| Pig-ment               | Temp. of adsorption, $^\circ\text{C}$ . | $n$  | $U_m$ , cal. | $\omega$ | $\bar{C}$ |
| Graphon                | $-78.8$                                 | 1.00 | ..           | ..       | 56.2      |
| Acetylene              | $-78.8$                                 | 0.73 | ..           | ..       | ..        |
| HAF-2                  | $-78.8$                                 | .66  | 1070         | 0.40     | 6.1       |
| VFF-1                  | $-78.8$                                 | .31  | 1445         | 0.40     | 3.2       |
| EPC-1                  | $-78.8$                                 | .35  | ..           | 0-0.1    | 2.4       |

gives the range in  $\theta$  over which adsorption data were found to fit equation 29. Except in the case of Graphon and acetylene black the adsorption of ethane and ethylene was found to follow equations 24 and 29 for at least 95% of the monolayer. For these blacks,  $\omega$  was set equal to zero and the values of  $n$  and  $\bar{C}$  taken from the linear portion of the isotherm. The values of  $n$  for ethane and ethylene are very close together, as is to be expected since both these molecules have almost equal values of  $a'$  and  $b'$ .

To test the general applicability of equations 24

and 29 to other adsorbate-adsorbent systems, the data of Arnold<sup>16</sup> for N<sub>2</sub> and O<sub>2</sub> on Anatase at 78°K. have also been examined. The data for oxygen on Anatase are plotted in Fig. 2 and the constants are tabulated in Table III. The data for the adsorption of oxygen on Anatase are found to fit equation 29 over the entire monolayer in a satisfactory manner.

TABLE III

| ADSORPTION OF O <sub>2</sub> AND N <sub>2</sub> ON ANATASE AT 78°K. |       |              |          |           |                        |
|---|-------|--------------|----------|-----------|------------------------|
| Adsorbent   | $n$   | $U_m$ , cal. | $\omega$ | $\bar{C}$ | Range of fit, $\theta$ |
| N <sub>2</sub>  | 0.68  | 1740         | 1.45     | 2140      | 0.063-0.645            |
| O <sub>2</sub>  | 0.575 | 1110         | 0.90     | 61        | 0.079-0.972            |

At low surface coverage, a completely random distribution of adsorption sites (energies) cannot be expected, and at high coverage it is to be expected that second layer formation will begin before the monolayer has been completed.<sup>3a</sup> Therefore, equation 29 does well if it will represent the adsorption data over the range of surface coverage  $\theta = 0.05-0.95$ . This has been found to be the case for ethane on six carbon blacks and Rutile, for ethylene on three carbon blacks, and for oxygen on Anatase. When it is found that equation 29 represents the data only over a limited range, as for ethane and ethylene on Graphon and Acetylene black and for nitrogen on Anatase, it will be noted that the value of  $n$  is about 0.7 or greater and the value of  $\bar{C}$  large. Under these conditions, the surface is conceived of having a high degree of uniformity and the forces existing between the surface and the adsorbed molecules large. Since equation 29 should apply only to an adsorbed film following the equation of state for an imperfect monolayer as represented by equation 19, then failure of equation 29 to represent the adsorption data over the entire monolayer must imply, according to the model assumed, that either a phase change has taken place or more generally failure of equation 19 to express the equation of state of the monolayer. It would be of interest to study the effect of temperature on the range over which equation 29 represents the adsorption isotherm. For those adsorbate-adsorbent systems which appear to follow equation 29 a decrease in the temperature of adsorption should eventually result in the failure of equation 29 to represent the data over the entire monolayer region. While for the three cases noted where equation 29 was not applicable over the region of the first monolayer an increase in the temperature of adsorption should result in an increase in the range over which equation 29 represents the experimental data.

From the model assumed in the derivation of equation 24 it was anticipated that  $\omega$  would be independent of the adsorbent and dependent only on the adsorbate and the temperature of adsorption. Reference to Tables I and II shows that this is not true, since a very large variation in the value of  $\omega$  was found. If, now, the not unreasonable assumption is made that the value of  $\omega$  will be dependent on the magnitude and distribution of adsorption energies, then some combination of  $n$ ,

$\omega$  and  $\bar{C}$  may be expected to yield a constant. For those adsorbate-adsorbent systems where the data fit equation 29 over the entire monolayer so that  $1/\Gamma_m$  could be considered as equal to  $b'$  it was found that

$$n \frac{\omega}{\bar{C}} = \text{constant} = k \quad (31)$$

as shown in Table IV.

TABLE IV

| Ethane   | $k$       |
|----------|-----------|
| HAF-1    | 0.045     |
| VFF-1    | 0.052     |
| Rutile   | 0.051     |
| Mixture  | 0.047     |
|          | 0.049 av. |
| Ethylene |           |
| HAF-2    | 0.043     |
| VFF-1    | 0.039     |
|          | 0.041 av. |
| Oxygen   |           |
| Anatase  | 0.0085    |

Use of equation 31 to calculate  $\omega$  for the HAF and MPC blacks gives a value of 0.02-0.03. For these blacks any value of less than 0.05 will give a satisfactory fit to the data. Equation 31 can now be written

$$\omega = \frac{k\bar{C}}{n} = \frac{k}{n} \exp n \frac{U_m}{RT} \quad (32)$$

$$\beta = \frac{kb'\bar{C}}{n} = \frac{kb'}{n} \exp n \frac{U_m}{RT} \quad (33)$$

The constant  $k$  should be a function only of the adsorbate. Equation 33 shows that the product  $kb'$  has the dimensions of cm.<sup>2</sup>, which is in the same units as  $(\alpha)^{2/3}$ , where  $\alpha$  is the three-dimensional polarizability having units of cm.<sup>3</sup> For oxygen, ethane and ethylene it was found that the product  $kb'$  was proportional to the square root of the molar polarizability, a result which, if true, is not unexpected.

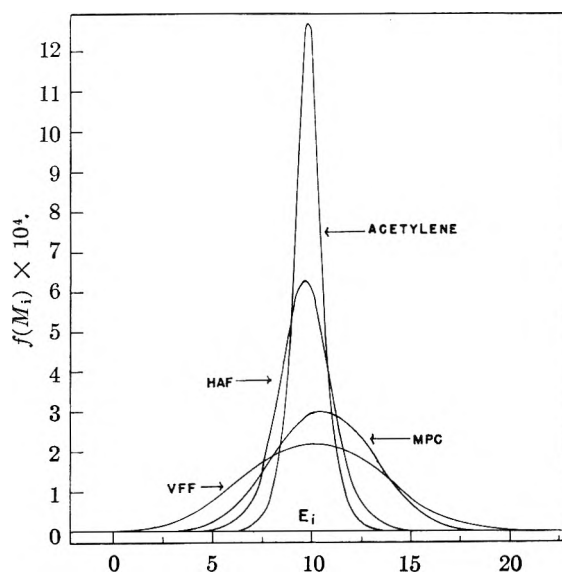


Fig. 4.—The apparent distribution of energy sites on several carbon blacks.

(16) J. R. Arnold, *J. Am. Chem. Soc.*, **71**, 104 (1949).

The values of  $n$  and  $U_m$ , recorded in Table I, allow the distribution of energy sites to be calculated through equation 25. Figure 4 shows several distribution curves calculated in this manner. Unfortunately it is not possible to evaluate  $\bar{Z}$ , with any degree of certainty. Calculated values in the literature range from  $1/1000$  to  $10$ .<sup>13,17,18</sup> It is, therefore, impossible to calculate  $E_i$  with any accuracy. It was found that  $\omega$  is also dependent on both the magnitude and distribution of adsorption energies, but for any surface it should be a constant providing the surface is completely random.

The limits of integration in equation 25 were taken as  $-\infty$  and  $+\infty$ . For the distribution to have any real physical significance, however, the curve should converge to zero as  $E_i \rightarrow 0$ . In the curves of Fig. 4 it has been assumed that  $E_0$  has a value of 5 kcal., which is 2.3 kcal. lower than the

(17) A. B. D. Cassie, *Trans. Faraday Soc.*, **41**, 450 (1945).

(18) G. L. Kington and J. G. Aston, *J. Am. Chem. Soc.*, **73**, 1934 (1951).

experimental value determined by Wiig and Smith<sup>19</sup> for the adsorption of ethyl chloride on charcoal. The heat of vaporization  $\lambda$  has been taken as 3,517 cal. Under these conditions  $f(M_i) \rightarrow 0$  when  $E_i = 0$ .

The conclusions which are drawn concerning the significance of the constants  $\bar{C}$ ,  $n$  and  $\omega$  are of course the direct result of the model assumed and considerable question may, therefore, be raised as to their actual physical significance. It should, therefore, be clear that equation 25 does not represent a true distribution of energy sites, if indeed it represents a distribution of energy sites at all. It is nevertheless a useful qualitative and schematic means of representing the differences between the surfaces of various solids which may be helpful in correlating various properties and behaviors in terms of what may be called a "distribution of energy sites."

(19) E. O. Wiig and S. B. Smith, *THIS JOURNAL*, **55**, 27 (1951).

## THE LOW TEMPERATURE REACTION OF WATER WITH CARBON<sup>1</sup>

BY R. NELSON SMITH, CONWAY PIERCE AND CLIFFE D. JOEL

*Chemistry Department, Pomona College, Claremont, California*

*Received March 19, 1953*

The heterogeneous reaction of water with different forms of carbon has been studied in the temperature range 25–200°. The products are H<sub>2</sub> and at least two surface oxygen complexes, one which decomposes easily to give CO<sub>2</sub> and a more stable one which may be thermally decomposed to give CO. Carbon surfaces containing sulfur or oxygen as impurities react much more readily and extensively than pure ones; those with sulfur also give H<sub>2</sub>S as a product. The results have been related to interpretation of water-carbon isotherm data and to the mechanism of the steam-carbon reaction.

In a previous paper<sup>2</sup> it was shown that the water isotherm of a graphite sample after exposure to water vapor at 80° was not the same as that for a fresh sample. The difference was ascribed to a reaction of carbon with water, with formation of a surface C–O complex that adsorbed more readily than a clean carbon surface. This paper describes additional work on the nature of this low temperature carbon-water reaction.

### Experimental

Some of the carbon samples in this study were treated before use with hydrogen at 1000°. After hydrogen treatment the samples were cooled to room temperature. This treatment appears to remove carbon-oxygen surface complexes. There is no indication that normal exposure to air at room temperature causes the carbon-oxygen surface complex to form again.

The sulfur content of the carbon samples was determined by the micromethods of Niederl and Niederl. Weighed samples were burned in a Parr oxygen bomb and the S determined gravimetrically as BaSO<sub>4</sub>, by precipitation of the sulfate from the bomb contents.

The following statements summarize the preparation and properties of the carbon samples used in the study.

**Spheron Grade 6:** a medium processing channel black manufactured by the Godfrey L. Cabot Co. The surface area is about 120 sq. m./g., and it contains 0.050% S before hydrogen treatment and 0.049% S after hydrogen treatment.

**G-1:** Graphon, a partially graphitized carbon black manufactured before 1951 by the Godfrey L. Cabot Co. by heat-

ing Spheron Grade 6 to approximately 3000° in an electric furnace. The surface area is about 80 sq. m./g. and it contains 0.039% S. It was hydrogen treated before use.

**G-2:** Graphon, a partially graphitized carbon black manufactured in 1951 by the Godfrey L. Cabot Co. by heating Spheron Grade 6 approximately 3000° in an electric furnace. The surface area is about 80 sq. m./g. and it contains 0.005% S. It was hydrogen treated before use.

**OG-1:** an oxidized sample of G-1 prepared by heating G-1 to about 600° and then pouring from one beaker to another as it cooled. Its surface area and sulfur content are essentially the same as G-1. It was not hydrogen treated before use.

**NC-1:** a very pure graphite furnished by the National Carbon Co. The surface area is about 4 sq. m./g. and it contains 0.002% S. It was not hydrogen treated before use.

**B:** an activated commercial nut charcoal, de-ashed with HCl in a Soxhlet extractor, dried and heated to 1000° *in vacuo*. The residual ash content is about 0.2%. The surface area is about 1050 sq. m./g. and it contains 0.02% S. It was not hydrogen treated.

For each run the weighed carbon sample was sealed into a small, well-cleaned Pyrex vessel which possessed a thin, sealed tip and a constricted lead. Except in the preliminary runs these bulbs all had a volume of  $11.3 \pm 0.6$  cc. After the absence of leaks had been ascertained, the sample was outgassed *in vacuo* for about one-half hour at a temperature just below the softening point of Pyrex. After the sample had cooled to room temperature, a weighed sample of water which had been freed of dissolved air was distilled into the reaction vessel and cooled by Dry Ice. The reaction vessel was then sealed at the constriction, removed from the vacuum system, and put into an oven at the desired temperature for a given length of time. The oven temperatures were  $200 \pm 4^\circ$  and  $100 \pm 3^\circ$ . It was not possible to measure the pressures reached during the reactions, but in a few instances at 200° it was high enough to shatter the sealed bulbs.

(1) This is a progress report of work done under Contract N8onr-54700 with the Office of Naval Research.

(2) C. Pierce, R. N. Smith, J. W. Wiley and H. Cordes, *J. Am. Chem. Soc.*, **73**, 4551 (1951).

After standing at temperature for the desired time, the vessel was sealed to a vacuum system containing a freeze-out trap and a Toepler pump. When the system had been outgassed with the Toepler pump, the thin, sealed tip was broken with a magnetically-operated glass-sheathed nail and the water was distilled from the reaction vessel to the freeze-out trap maintained at Dry Ice temperature. The Toepler pump was then used to transfer all the non-condensable gas to a gas cup for analysis. The carbon sample was again heated to a temperature just below the softening point of Pyrex and pumping continued until no further gas was evolved (15–20 minutes usually was required). This additional gas was collected in a separate gas cup. In some cases the second sample of gas was taken off at 100°, but the amount of gas evolved at this temperature was usually insignificant.

All of the gas samples were analyzed with the aid of a Blacet-Leighton microgas analysis apparatus (Arthur H. Thomas Co., Philadelphia, Pa.). All of the earlier analyses (including those upon which a preliminary statement<sup>2</sup> of results was based) were performed in the following sequence: CO<sub>2</sub> was removed with a KOH bead; H<sub>2</sub> and CO were burned with a measured excess of oxygen followed by water removal with a Mg(ClO<sub>4</sub>)<sub>2</sub> bead and measurement of contraction on combustion; CO was removed as CO<sub>2</sub> with a KOH bead. In practically all cases a residual volume remained unaccounted for; this is labeled "X" in the tables.

In all the earlier work it was observed that the gas contained some unidentified constituent that appeared to react slowly with mercury or to polymerize in the presence of mercury. At that time there was no evidence that the reaction involved anything except carbon and water. The combined gases obtained from G-1 by pumping at room temperature and pumping with flaming, were subjected to a mass spectrographic analysis (Consolidated Engineering Company, Pasadena, California). This analysis gave 49% H<sub>2</sub>S, 45% H<sub>2</sub>, 3% CO<sub>2</sub>, 1% CO, 1% N<sub>2</sub>, 1% CH<sub>4</sub>, and traces of CS<sub>2</sub>, COS and CH<sub>3</sub>SH, thus identifying the unknown constituent as H<sub>2</sub>S. It had been realized that carbon blacks contain sulfur, but it had been assumed that at the temperature of graphitization this sulfur would be removed. It is of interest to record that a 30-g. sample of G-2 which had been hydrogen-treated at 1000°, evacuated at 1000°, and then stored *in vacuo* for two weeks in the quartz tube in which it was treated, smelled of H<sub>2</sub>S when opened to the air. This odor was checked with lead acetate paper.

After it was learned that H<sub>2</sub>S was present in the gas, the analysis was modified. H<sub>2</sub>S was removed (before CO<sub>2</sub>) by a solution of acidified Hg(NO<sub>3</sub>)<sub>2</sub> held on a sintered glass bead. This treatment is not completely satisfactory but it appears to remove most of the H<sub>2</sub>S without affecting other constituents. To detect H<sub>2</sub>S a pink solution of *p*-aminodimethylaniline sulfate, ferric chloride and sulfuric acid<sup>3</sup> is put on a sintered glass bead and inserted into the sample. When H<sub>2</sub>S is present an intense blue color forms immediately.

In all the analyses reported, the combined percentages of H<sub>2</sub>S and CO<sub>2</sub> are believed to be accurate but there is some question about the individual values for these constituents.

The volumes of gases are reported at room conditions, about 730 mm. and 26°.

Several G-1 samples which had reacted with water vapor, but which had not subsequently been heated to the softening point of Pyrex, were submitted to carbon and hydrogen analysis; none of them showed a significant oxygen or hydrogen content. The sample of oxidized Graphon was analyzed as 98.3% C, 0.4% H and 1.3% O (by difference).

### Results

Typical results are given in Tables I-IV and Figs. 1-3. These include only a small portion of the many runs made, but illustrate the general trend and show the erratic variations from one run to another that hamper the formulation of the definite conclusions hoped for. In some runs the gas was pumped off while the sample was still at its reaction temperature. These runs are not significantly different from those in which the

sample was cooled to room temperature before sealing to the line and pumping. Samples G-2 and NC-1 have such a slow rate of reaction with water that no runs were made below 200°. The few runs made with G-1 at 100° with varying amounts of water gave the same general picture as that of Fig. 1, except that the gaseous products had a much smaller volume.

### Discussion

Interpretation is complicated by the presence of sulfur in samples G-1 and B but, except for H<sub>2</sub>S, the products from these samples are much the same as for those without sulfur. The reaction of water with carbon gives H<sub>2</sub> and a carbon-oxygen complex. There seem to be two types of complex, one that decomposes at room temperature to give CO<sub>2</sub> and another more stable complex that decomposes at high temperature with evolution of CO. The recovery of hydrogen is far below the stoichiometric amount. This suggests that the stable complex may contain OH and that on decomposition the hydrogen is reoxidized to water.

Comparison of Tables I and II shows that a trace of sulfur in the sample increases the reactivity to water enormously, not only in the reaction to give H<sub>2</sub>S but also in the reaction to give CO and CO<sub>2</sub>. In the case of G-1 there is one sulfur atom for every 6600 carbon atoms, yet there is about as much H<sub>2</sub>S produced as CO and CO<sub>2</sub>. The sulfur analyses show that hydrogen treatment seems to be relatively ineffective in reducing the sulfur content; this is to be expected if the sulfur is distributed uniformly throughout the sample and not located on the surface alone. Even the sulfur on the surface seems to be relatively unaffected by hydrogen treatment, for the ability of G-1 to produce H<sub>2</sub>S is about the same before and after treatment. The sulfur complex is heat-stable, for G-1 had been heated in its preparation to a temperature of 3000°. This information leads us to question that the previously published water isotherm of Graphon<sup>2</sup> is really the true water isotherm for a clean carbon surface. This isotherm showed the lowest water adsorption ever reported for a carbon, but even this may be too high.

When the carbon impurity is oxygen, the ease and extent of the water reaction is again enormously increased (Table IV and last run in Table III). It is evident that the C-O surface complexes are relatively stable at 100° on OG-1, and at about 550° on the non-hydrogen or heat-treated B. A larger volume of gas is naturally to be expected from B since its surface area is about thirteen times that of Graphon. In connection with the stability of the complex, it will be noted that hydrogen treatment at 1000° is appreciably more effective than heat treatment alone at 1000° in removing the carbon-oxygen surface complex. Even the hydrogen treatment has difficulty in completely removing this complex. One might use this reaction with water vapor as some measure of the amount of complex present on the surface.

Since a carbon-oxygen surface complex greatly increases the adsorption of water as well as the amount of reaction, it is probable that the water molecules react in large measure with their ad-

(3) F. Feigl, "Spot Tests," Elsevier Publishing Co., Ltd., London, 1939, p. 198.

TABLE I

## REACTION OF WATER WITH GRAPHON-1

Weight of Graphon-1 in each case = 0.42 g.; volumes of gas measured at room temperature and pressure.

| H <sub>2</sub> O,<br>g. | Hr.<br>reacted | Temp.,<br>°C. | V,<br>mm. <sup>3</sup> | Gases removed at room temp.<br>Composition, % |                 |                |      |      | V,<br>mm. <sup>3</sup> | Gases removed by heating<br>Composition, % |                 |                |      |      |
|-------------------------|----------------|---------------|------------------------|---|-----------------|----------------|------|------|------------------------|--|-----------------|----------------|------|------|
|                         |                |               |                        | H <sub>2</sub> S                              | CO <sub>2</sub> | H <sub>2</sub> | CO   | "X"  |                        | H <sub>2</sub> S                           | CO <sub>2</sub> | H <sub>2</sub> | CO   | "X"  |
| 0.1543                  | 48             | 200           | 69.90                  | 29.4  | 24.9            | 35.9           | 1.6  | 8.2  | 13.55                  | 15.8                                       | 11.1            | 55.6           | 11.8 | 5.7  |
| .1158                   | 48             | 200           | 74.45                  | 23.2  | 22.5            | 45.2           | 1.6  | 7.5  | 16.30                  | 21.2                                       | 24.6            | 52.7           | 0    | 1.5  |
| .1712                   | 12             | 200           | 69.35                  | 34.2  | 27.1            | 31.9           | 0.9  | 5.9  | 10.80                  | 12.0                                       | 2.3             | 53.7           | 7.9  | 24.1 |
| .1710                   | 12             | 200           | 63.30                  | 20.7  | 26.3            | 46.1           | 5.1  | 1.8  | 12.40                  | 15.3                                       | 26.6            | 38.7           | 20.6 | -1.2 |
| .1712                   | 72             | 100           | 17.20                  | 37.8  | 18.3            | 17.1           | 13.1 | 13.7 | 11.45                  | 32.3                                       | 17.0            | 26.2           | 19.2 | 5.3  |
| .1712                   | 742            | 25            | 8.45                   | 27.8  | 10.0            | 28.4           | 5.9  | 27.9 | 18.50                  | 32.2                                       | 36.0            | 16.0           | 7.6  | 8.2  |

TABLE II

## REACTION OF WATER WITH GRAPHON-2

Weight of Graphon-2 in each case = 0.416 g.; volumes of gas measured at room temperature and pressure.

| H <sub>2</sub> O,<br>g. | Hr.<br>reacted | Temp.,<br>°C. | V,<br>mm. <sup>3</sup> | Gases removed at room temp.<br>Composition, % |                 |                |    |     | V,<br>mm. <sup>3</sup> | Gases removed by heating<br>Composition, % |                 |                |    |     |
|-------------------------|----------------|---------------|------------------------|---|-----------------|----------------|----|-----|------------------------|--|-----------------|----------------|----|-----|
|                         |                |               |                        | H <sub>2</sub> S                              | CO <sub>2</sub> | H <sub>2</sub> | CO | "X" |                        | H <sub>2</sub> S                           | CO <sub>2</sub> | H <sub>2</sub> | CO | "X" |
| 0.1712                  | 6              | 200           | 1.30                   | 0   | 42              | 35             | 0  | 23  | 2.35                   | 0  | 11              | 38             | 13 | 38  |
| .1712                   | 12             | 200           | 2.00                   | 0   | 60              | 10             | 15 | 15  | 2.95                   | 0  | 36              | 14             | 20 | 30  |
| .1712                   | 24             | 200           | 3.60                   | 0   | 28              | 21             | 0  | 51  | 3.55                   | 0  | 28              | 37             | 21 | 14  |
| .1712                   | 48             | 200           | 1.70                   | 0   | 32              | 32             | 0  | 36  | 2.70                   | 0  | 15              | 70             | 0  | 15  |
| .2550                   | 12             | 200           | 2.00                   | 0   | 10              | 12             | 2  | 76  | 2.40                   | 0  | 0               | 100            | 0  | 0   |
| .3424                   | 12             | 200           | 1.70                   | 0   | 35              | 24             | 0  | 41  | 1.95                   | 0  | 28              | 72             | 0  | 0   |

TABLE III

## REACTION OF WATER WITH ACTIVATED CHARCOAL-B

Weight of charcoal in each case = 0.416 g.; volumes of gas measured at room temperature and pressure.

| H <sub>2</sub> O,<br>g. | Hr.<br>reacted | Temp.,<br>°C. | V,<br>mm. <sup>3</sup> | Gases removed at room temp.<br>Composition, % |                 |                |     |     | V,<br>mm. <sup>3</sup> | Gases removed by heating<br>Composition, % |                 |                |      |     |
|-------------------------|----------------|---------------|------------------------|---|-----------------|----------------|-----|-----|------------------------|--|-----------------|----------------|------|-----|
|                         |                |               |                        | H <sub>2</sub> S                              | CO <sub>2</sub> | H <sub>2</sub> | CO  | "X" |                        | H <sub>2</sub> S                           | CO <sub>2</sub> | H <sub>2</sub> | CO   | "X" |
| 0                       | 36             | 25            |                        |   |                 |                |     |     | 15.50                  | 0  | 10.3            | 5.3            | 77.8 | 6.6 |
| .1712                   | 15             | 25            | 1.70                   | 0   | 32              | 0              | 32  | 34  | 106.2                  | 0  | 15.0            | 2.4            | 80.0 | 2.6 |
| .1712                   | 12             | 100           | 3.70                   | 19  | 11              | 29             | 0   | 41  | 94.8                   | 0  | 13.1            | 9.3            | 69.5 | 8.1 |
| .1712                   | 12             | 200           | 39.70                  | 14  | 70              | 7              | 18  | -8  | 203.7                  | 8.2  | 3.7             | 26.7           | 59.0 | 2.4 |
| .1712 <sup>a</sup>      | 12             | 200           | 8.95                   | 0   | 83              | 9              | 0   | 8   | 330.8                  | 0  | 13.9            | 10.1           | 75.5 | 0.5 |
| .1712 <sup>b</sup>      | 12             | 200           | 855.3                  | 1.7   | 94.5            | 2.1            | 0.9 | 0.8 | 1897                   | 0  | 15.6            | 4.0            | 79.0 | 1.4 |

<sup>a</sup> Heat-treated at 1000° instead of hydrogen-treated. <sup>b</sup> Neither heat-treated nor H<sub>2</sub>-treated at 1000°. Heated only to softening point of Pyrex as in usual preparation for a run.

TABLE IV

## REACTION OF WATER WITH MISCELLANEOUS SAMPLES OF CARBON

Volumes of gas measured at room temperature and pressure.

| Sample            | C,<br>g. | H <sub>2</sub> O,<br>g. | Hr.<br>react. | Temp.,<br>°C. | V,<br>mm. <sup>3</sup> | Gases removed at room temp.<br>Composition, % |                 |                |     |      | V,<br>mm. <sup>3</sup> | Gases removed by heating <sup>b</sup><br>Composition, % |                 |                |      |      |
|-------------------|----------|-------------------------|---------------|---------------|------------------------|---|-----------------|----------------|-----|------|------------------------|---|-----------------|----------------|------|------|
|                   |          |                         |               |               |                        | H <sub>2</sub> S                              | CO <sub>2</sub> | H <sub>2</sub> | CO  | "X"  |                        | H <sub>2</sub> S  | CO <sub>2</sub> | H <sub>2</sub> | CO   | "X"  |
| OG-1 <sup>a</sup> | 0.416    | 0.171                   | 12            | 200           | 119.8                  | 2.9   | 71.2            | 1.0            | 6.1 | 18.9 | 2.70 <sup>a</sup>      | 0   | 18.5            | 5.6            | 33.3 | 46.2 |
|                   |          |                         |               |               |                        |   |                 |                |     |      | 150.0                  | 10.0  | 60.0            | 3.3            | 20.0 | 6.7  |
| OG-1 <sup>b</sup> | 0.516    | 0                       | 0             | ..            |                        |   |                 |                |     |      | 253.8                  | 7.0   | 51.0            | 27.5           | 4.5  | 10.0 |
| NC-1              | 3.461    | 0.171                   | 30            | 200           | 5.6                    | 0   | 65              | 10             | 4   | 21   | 3.9                    | 0   | 36              | 15             | 21   | 28   |

<sup>a</sup> Sample outgassed for one hour at 100° instead of at the softening point of Pyrex. <sup>b</sup> Sample heated to softening point of Pyrex.

sorbing sites to produce a new surface complex. This new surface complex appears to be less stable than the original one and decomposes rather easily on heating to give the observed gases (*vide infra*). Figure 3 indicates that for G-1 the CO complex sites are limited and about the same in number at each temperature (this may not be true at much higher temperatures). Figure 2, on the other hand, indicates that the CO<sub>2</sub> complex sites are not all the same, for as the temperature rises the reaction produces a larger total volume of gas. This tendency to form the CO<sub>2</sub> complex is not only a function of temperature but is also critically dependent on the water concentration. Figure 1

demonstrates that there is a very marked increase in the production of CO<sub>2</sub> when the water concentration has exceeded a certain value. There is no such effect in connection with the formation of the CO complex.

These observations emphasize the fact that interpretations of isotherm data for water on carbon must be made with great caution. If water isotherms are obtained at temperatures above room temperature, the surfaces will become altered as the adsorption proceeds and thus a true isotherm will not be obtained (the effect mentioned at the beginning of this paper). Moreover, if the carbon sample has not been treated with H<sub>2</sub>

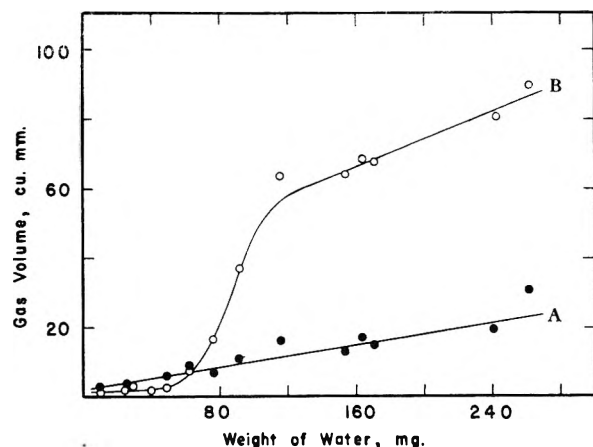


Fig. 1.—Combined volumes of  $\text{H}_2\text{S}$ ,  $\text{H}_2$ ,  $\text{CO}_2$  and  $\text{CO}$  produced by the reaction of different amounts of water with 0.42 g. of G-1 for 48 hours at  $200^\circ$ : (A) ●, volume removed at room temperature; (B) ○, volume removed by heating.

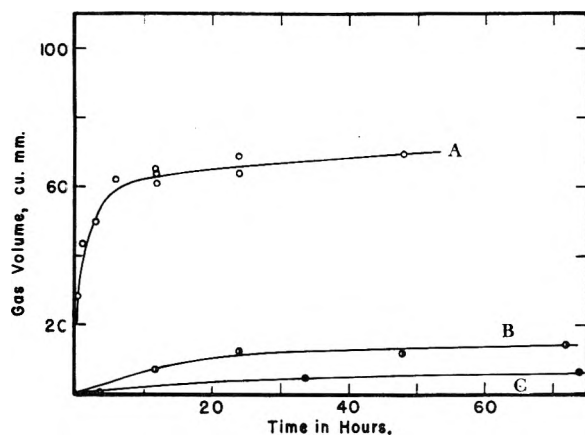


Fig. 2.—Combined volumes of  $\text{H}_2\text{S}$ ,  $\text{H}_2$ ,  $\text{CO}_2$  and  $\text{CO}$  removed at room temperature following the reaction of water with G-1 for different periods of time at various temperatures. For the reaction at  $25^\circ$ , the abscissa values are 200, 400, 600, etc., hours. For all reactions the weight of G-1 = 0.416 g. and the weight of water = 0.171 g.: (A) ○,  $200^\circ$ ; (B) ○,  $100^\circ$ ; (C) ●,  $25^\circ$ .

at a high temperature (a high-temperature treatment without hydrogen is not quite as good), an abnormally high adsorption of water will be observed and very extensive reaction of water with oxygen complex will occur. This will be especially important for activated charcoals as normally produced, or for any carbon sample which has been heated in air. Finally, most carbon blacks and gas carbons normally contain appreciable amounts of sulfur which may be very reactive, again leading to appreciable reaction of water with the surface at temperatures above room temperature. An important example in which these factors undoubtedly play a part is Coolidge's<sup>4</sup> water isotherms which have been cited by Brunauer<sup>5</sup> as showing that the differential net heat of adsorption of water by carbon may be positive. At low relative pressures the isotherms coincide in the temperature range of  $-30$  to  $20^\circ$ , but on progressing from  $60$  to  $218^\circ$  the adsorption at low relative

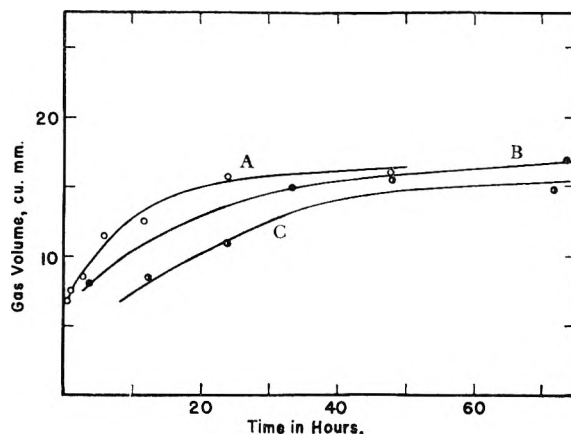


Fig. 3.—Combined volumes of  $\text{H}_2\text{S}$ ,  $\text{H}_2$ ,  $\text{CO}_2$  and  $\text{CO}$  which can be removed from G-1 only by heating following the reaction of water with G-1 for different periods of time at various temperatures. For the reaction at  $25^\circ$  the abscissa values are 200, 400, 600, etc., hours. For all reactions the weight of G-1 = 0.416 g. and the weight of water = 0.171 g.: (A) ○,  $200^\circ$ ; (B) ●,  $100^\circ$ ; (C) ○,  $25^\circ$ .

pressure rises as the temperature increases. At about  $P/P_0 = 0.4$  the isotherms at all temperatures show a sharp rise, and in this region and beyond, the amount of adsorption decreases with increase in temperature. Up to about  $P/P_0 = 0.4$ , adsorption at active sites is predominant and the nature of the surface is very important, but since the surface had been continually altered and made more adsorptive at the higher temperatures by reaction with water, this region of the isotherms cannot be used for calculations of isosteric heats of adsorption. It merely gives a qualitative measure of the extent of the reaction. Above  $P/P_0 = 0.4$  the filling of capillaries is important, and the continual changes in the character of the surface are not evident from the isotherms.

The present work has some bearing on the mechanism of the steam-carbon reaction. Many studies have been made of this reaction, the most recent and extensive being those by Long and Sykes,<sup>6</sup> Gadsby, Hinshelwood and Sykes,<sup>7</sup> Muller and Cobb<sup>8</sup> and Strickland-Constable.<sup>9</sup> Most of this work, however, was done in the temperature range of  $600$ – $1000^\circ$ , though some of Muller and Cobb's work went as low as  $300^\circ$ . These high temperature results are all summarized in the Long-Sykes mechanism, *i.e.*



The entities enclosed in parentheses are considered to be chemisorbed on the carbon surface. About 2% of the carbon surface studied was effective in the reaction and the hydrogen produced competed with water for these same sites. (Any  $\text{H}_2\text{S}$  which might have been produced in Long and Sykes work would have been computed as  $\text{CO}_2$  in their

(6) F. J. Long and K. W. Sykes, *Proc. Roy. Soc. (London)*, **A193**, 377 (1948).

(7) J. Gadsby, C. N. Hinshelwood and K. W. Sykes, *ibid.*, **A187**, 129 (1946).

(8) S. Muller and J. W. Cobb, *J. Chem. Soc.*, 177 (1940).

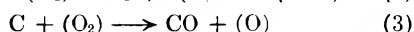
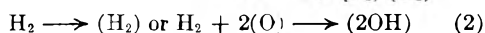
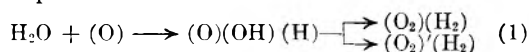
(9) R. F. Strickland-Constable, *Proc. Roy. Soc. (London)*, **A189**, 1 (1947).

(4) A. S. Coolidge, *J. Am. Chem. Soc.*, **49**, 708 (1927).

(5) S. Brunauer, "The Adsorption of Gases and Vapors," Princeton University Press, Princeton, New Jersey, 1943, p. 260.

analyses.) Long and Sykes speculated at length as to the nature of these active sites, and concluded that they must be due to the presence of surface carbon atoms which are attached to the rest of the lattice by only two or three bonds, leaving thus two or one bonds available for interaction with other molecules.

The samples used by Long and Sykes were impure commercial charcoals, not outgassed before use, and must certainly have possessed large amounts of a carbon-oxygen surface complex. Many descriptions of the properties and conditions of formation of such surface complexes have been published.<sup>10-16</sup> King<sup>17</sup> has been able to isolate measurable quantities of oxalic acid after exposure of charcoal to moist air, and both Jones and Townsend<sup>13</sup> and King<sup>17</sup> report the room temperature formation of carbon-oxygen complexes with peroxidic properties. Moreover, Muller and Cobb showed that the results of the steam-carbon reaction depend greatly on the forms and sources of carbon used and that wide variations were observed with samples of the same charcoal which differed only in heat treatment. In view of these facts and the enormous effect which the carbon-oxygen surface complex has on both the steam-carbon reaction and the adsorption of water, it seems probable that the initial step in the reaction is the absorption of a water molecule on a carbon-oxygen complex site and not on a carbon atom at all. The Long-Sykes mechanism might then be made more specific as



In addition to being more specific about the nature

(10) T. F. E. Rheac and R. V. Wheeler, *J. Chem. Soc.*, **103**, 461 (1913).

(11) H. H. Lowry and G. A. Hulett, *J. Am. Chem. Soc.*, **42**, 1408 (1920).

(12) E. A. Blench and W. E. Garner, *J. Chem. Soc.*, 1288 (1924).

(13) R. E. Jones and D. T. A. Townsend, *Trans. Faraday Soc.*, **42**, 297 (1946).

(14) S. Weller and T. F. Young, *J. Am. Chem. Soc.*, **70**, 4155 (1948).

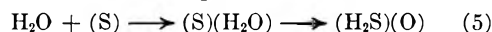
(15) R. B. Anderson and P. H. Emmett, *THIS JOURNAL*, **56**, 753 (1952).

(16) J. H. Wilson and T. R. Bolam, *J. Coll. Sci.*, **5**, 550 (1950).

(17) A. King, *J. Chem. Soc.*, 842 (1933).

of the active sites, this mechanism provides for two or more types of oxygen complexes (O), (O<sub>2</sub>), (O<sub>2</sub>'), (O<sub>2</sub>''), etc., the difference between them depending upon the state of the carbon atoms adjacent to the complexed adsorbing carbon atoms. This will in turn depend upon the previous heat treatment and degree of surface oxidation as well as upon the presence of ash and semi-volatile impurities. It also provides a reasonable possibility for the formation of CO<sub>2</sub>. In the earlier work at the higher temperatures it was judged that the small amounts of observed CO<sub>2</sub> were produced by the water gas reaction. This is no doubt the major cause at high temperature, but an improbable cause at low temperatures. The low-temperature results indicate that the CO complex, (O<sub>2</sub>), is more stable than the CO<sub>2</sub> complex, (O<sub>2</sub>)', and that the actual products of (3) can be obtained only by heating to over 500° (*i.e.*, to the softening point of Pyrex or higher). This same difference in stability of the complexes was observed by Wilson and Bolam<sup>16</sup> and by Anderson and Emmett.<sup>15</sup> Table II indicates that with pure carbon at low temperature (4) is more important than (3). The Long-Sykes type of active site may be responsible for the small quantities of gas produced from G-2, NC-1 or hydrogen-treated B, though there is evidence (#1, Table III) that the complex has not been completely removed from the latter. These changes do not alter the rate expression derived by Long and Sykes.

The carbon-sulfur complexes and their great reactivity with water have not previously been described. Perhaps the reaction occurring in this case consists of such steps as



in addition to reactions (1)-(4) utilizing (O) produced in (5). When a sample with a surface sulfur complex is oxidized and then treated with water, reactions (5) and (6) become less important than (1)-(4) because the concentration of (O) is raised through oxidation.

**Acknowledgment.**—The authors wish to acknowledge the help and suggestions of Dr. W. R. Smith of the Godfrey L. Cabot Co., Boston, Mass., who furnished the Graphon, and the help of Mr. Fred Geiger for the carbon-hydrogen analyses.

CHARGE EFFECTS IN LIGHT SCATTERING BY COLLOIDAL SOLUTIONS<sup>1</sup>

BY KAROL J. MYSELS

*Department of Chemistry, University of Southern California, Los Angeles, Calif.**Received August 10, 1953*

The classical fluctuation theory is applied to light scattering by ideal solutions of colloidal electrolytes in the presence of a simple salt. The necessity of introducing the condition of electroneutrality and of an equilibrium distribution of small ions is pointed out. This leads to a relatively simple expression for the turbidity as a function of the molecular weight, charge and concentration of the colloid and concentration of the simple salt. In agreement with previous results the charge  $p$  has no effect on the apparent molecular weight when the concentration of salt is very large compared to that of the colloid, but reduces it by a factor of  $(p + 1)$  when the salt concentration becomes negligible. In addition the intermediate region is covered. The effect of the various factors is presented graphically and is shown to agree qualitatively with pertinent experimental results, indicating that, as a first approximation, Debye-Hückel types of non-ideality are not involved.

Light scattering by solutions of small neutral particles can be explained fully and in relatively simple terms<sup>2,3</sup> by the fluctuation theory. The interference theory gives an alternate and concordant account of the phenomena. The situation becomes much more complicated when the particles are electrically charged. The interference approach has been applied to this problem<sup>4,5</sup> but encounters serious difficulties. The fluctuation theory has been applied to very dilute solutions by Edsall and co-workers<sup>6</sup> using a generalization of the simple theory to multicomponent systems obtained through statistical mechanics.<sup>7-10</sup> In a brief note T. M. Doscher and I<sup>11</sup> tried a more formal extension of the fluctuation theory to the whole range of concentrations of an ideal colloidal electrolyte. In the present paper I would like to explain and modify this approach and to present a solution of the problem in simple terms.

As is well known, light scattering by particles, small compared to the wave length of light, is caused by small local inhomogeneities of refractive index which are due (in fluids) to fluctuation of density or concentration caused by random thermal motion and counteracted by the increase in free energy caused by their occurrence. This increase may be measured by the work done against restraining pressures such as ordinary pressure developed when a pure fluid is compressed or the osmotic pressure arising when the concentration of a solution is changed. The fluctuations in concentration contribute to light scattering proportionally to the square of the resulting fluctuation in refractive index. Thus while all species present contribute to the scattering of a colloidal solution, it is the fluctuation of concentration of the colloidal particles which, as a first approximation, is the only significant one and I will discuss only this factor.

By slight modification of the reasoning of Her-

mans<sup>2</sup> it can be shown that the turbidity  $\tau$  of a liquid caused by its light scattering is given by

$$\tau = K(v\Delta^2/2F)$$

where  $K$  is a constant taking into account geometrical and refractive index factors and  $F$  the change in free energy caused by a fluctuation  $\Delta$  in a volume  $v$ .

If the fluctuating being considered can be imagined as caused by the reversible motion of an appropriate semipermeable piston

$$F = \frac{\partial\pi/\partial c}{c} \times \frac{v\Delta^2}{2}$$

where  $\partial\pi$  is the osmotic pressure corresponding to this piston when it separates concentrations  $c$  and  $c + \partial c$  of the fluctuating species. Combining the two equations one obtains the standard expression

$$\tau = \frac{Kc}{\partial\pi/\partial c}$$

I will try to apply these ideas to a simple ideal solution containing a colloidal electrolyte and a simple salt having a common ion.

Let the colloidal cation have a molecular weight  $M$ , charge  $p$  and concentration  $c$  grams,  $m$  moles and  $z$  equivalents, per liter. Let the small cation be univalent and its concentration  $x$  (equiv./l.). Let there be a single kind of anion which is also monovalent so that its concentration  $y$  must be

$$p(c/M) + x = z + x \text{ (equiv./l.)}$$

Let the weights of the small ions be negligible.

There are several ways in which fluctuations in concentration of the colloidal cation can be assumed to be produced and I shall discuss the main ones.

**A. The concentration of the colloidal cation fluctuates independently of all other ionic species:** in this case the osmotic pressure  $\pi = RTc/M$  is independent of the concentration of simple ions. This type of fluctuation, however, would produce very large changes in free energy due to electrostatic forces and, as has been shown by Hermans,<sup>4</sup> is negligible except perhaps at extreme dilution. Hence in the following I will consider only fluctuations which maintain electroneutrality, *e.g.*, involving  $p$  times as many small anions as colloidal cations.

**B. The concentration of the colloidal electrolytes as a whole fluctuates independently of the concentration of the simple salt, *i.e.*,  $c$  changes by  $\Delta$  and  $y$  by  $p(\Delta/M)$  while  $x$  remains unchanged.** Such a fluctuation cannot be produced by a single

(1) Presented in part at the J. W. McBain Memorial Symposium at the 24th Meeting of the American Chemical Society, Sept., 1953.

(2) J. J. Hermans in H. R. Krzyt, "Colloid Science," Vol. II, Elsevier-Publishing Co., New York, N. Y., 1949, p. 146.

(3) G. Oster, *Chem. Revs.*, **43**, 319 (1948).

(4) J. J. Hermans, *Rec. trav. chim.*, **68**, 859 (1948).

(5) P. Doty and R. F. Steiner, *J. Chem. Phys.*, **20**, 85 (1952).

(6) J. T. Edsall, H. Edelhoch, R. Lontie and P. R. Morrison, *J. Am. Chem. Soc.*, **72**, 4641 (1950).

(7) F. Zernike, *Arch. Neerland. Sci.*, [3A] **4**, 74 (1918).

(8) H. C. Brinkman and J. H. Hermans, *J. Chem. Phys.*, **17**, 574 (1949).

(9) C. G. Kirkwood and R. J. Goldberg, *ibid.*, **18**, 54 (1950).

(10) W. H. Stockmayer, *ibid.*, **18**, 58 (1950).

(11) T. M. Doscher and K. J. Mysels, *ibid.*, **19**, 254 (1951).

osmotic piston, but it can be produced by two: one impervious only to the colloidal cation, the other only to the small anion. To produce this fluctuation, the first one will have to move by  $v\Delta/c$ , the second by  $vp\Delta/M_y$ , while the corresponding  $\partial\pi/\partial c$  are  $RT/M$  and  $p(RT/M)$ . Hence

$$\Delta F = \frac{vRT\Delta^2}{2Mc} + \frac{vRTp^2\Delta^2}{2M^2y} = \frac{RT\Delta^2v}{2Mc} \left(1 + \frac{cp^2}{yM}\right) = \frac{RT\Delta^2v}{2Mc} \left(1 + \frac{pz}{y}\right)$$

so that

$$\tau = \frac{KcM}{RT\left(1 + \frac{pz}{y}\right)}$$

or in the more familiar form, if we define  $H = K/RT$

$$\frac{Hc}{\tau} = \frac{1}{M} \left(1 + \frac{pz}{y}\right) \quad (\text{Ia})$$

This can be written in equivalent forms, as

$$\frac{Hc}{\tau} = \frac{1}{M} \left(1 + p^2 \frac{m}{y}\right) \quad (\text{Ib})$$

which is the result obtained earlier by Doscher and myself<sup>11</sup> from a more formal treatment, or

$$\frac{Hc}{\tau} = \frac{1}{M} \left(1 + \frac{p}{1 + (x/z)}\right) \quad (\text{Ic})$$

and an especially convenient one is

$$\frac{Hc}{\tau} = \frac{1}{M} \left(1 + \frac{p}{1 + (xM/pc)}\right) \quad (\text{Id})$$

since  $c$  and  $M$  are much more accessible experimentally than  $z$ .

I doubt that fluctuations actually occur under the condition just assumed, *i.e.*, that the concentration of the simple salt is not an equilibrium one, but remains the same in the fluctuating volume as in the bulk of the solution. It seems much more likely that the concentration of the simple salt is given by an equilibrium distribution between the fluctuating volume and the bulk of the solution. This equilibrium is determined by Donnan conditions and is substantially influenced by the fluctuation of the colloid.

The relaxation times of fluctuations of any species are inversely proportional to their diffusion coefficients and hence in the ratio of about 20 to 1 for a typical small colloid such as albumin and an ordinary ion such as  $\text{Cl}^-$ . Hence the salt can follow without appreciable lag the fluctuation of the colloid and an equilibrium distribution of small ions is to be expected, at least on the average.

Another argument in the same direction is that the fluctuation of the small ions will be distributed around a value of minimum free energy. This value depends, however, on the concentration of the colloidal ions which itself is fluctuating. Hence, if we consider a very large number of small volumes and out of these we select those having a certain concentration  $c + \Delta$  of colloid, the average concentration of small ions in these selected volumes will be, on the average, that corresponding to minimum free energy, *i.e.*, to an equilibrium distribution.

Whether this expectation of an equilibrium distribution of ions is justified should be accessible to

experimental proof and in the meantime it may be worthwhile to examine its consequences.

The statistical mechanics treatments<sup>7-10</sup> seem to assume implicitly an equilibrium distribution of all species whatever the relaxation time of their fluctuation. This assumption seems much more questionable than the one I am making and is not necessary to solve the present problem. It leads to additional crossterms which are in general negligibly small and may be actually unnecessary.

**C. The concentration of the colloidal cation fluctuates while maintaining equilibrium with a salt solution:** this change corresponds to the movement of a piston impervious only to the colloidal cation while the other ions maintain equilibrium or, more exactly, fluctuate around equilibrium values. This is of course the classic condition of Donnan equilibrium in which the product of small ion concentrations (or activities) is constant throughout the system.

The osmotic pressure of a colloidal ion solution with respect to a simple salt solution of concentration  $x$  is well known and given by

$$\pi = RT \left[ \frac{c}{M} - 2x + \sqrt{z^2 + 4x^2} \right]$$

so that

$$\partial\pi/\partial c = \frac{RT}{M} \left[ 1 + \frac{p}{\sqrt{1 + (2x/z)^2}} \right]$$

and

$$\frac{Hc}{\tau} = \frac{1}{M} \left[ 1 + \frac{p}{\sqrt{1 + (2x/z)^2}} \right] \quad (\text{IIc})$$

which is equivalent to

$$\frac{Hc}{\tau} = \frac{1}{M} \left[ 1 + \frac{p}{\sqrt{1 + (2xM/pc)^2}} \right] \quad (\text{IIId})$$

This calculation still does not strictly correspond to our premises since it computes the differential osmotic pressure between two colloidal solutions both in equilibrium with a salt solution of concentration  $x$  rather than between two colloidal solutions, one of which has the concentration  $x$  of salt. An alternate point of view is that the salt solution considered should not have a concentration  $x$  but one which is in equilibrium with a colloid solution having a concentration  $x$  of simple salt and  $c$  of colloid. These two points of view are equivalent and I shall discuss them presently.

**D. The colloidal ion fluctuates while the small ions maintain equilibrium with the colloidal solution:** let  $C$  and  $X$  be the concentrations in the fluctuating volume while  $c$  and  $x$  are, as before, the ones in the bulk of the solution. Donnan equilibrium and electroneutrality require that

$$x \left( x + p \frac{c}{M} \right) = X \left( X + p \frac{C}{M} \right) \quad (1)$$

hence

$$X = \frac{-p \frac{C}{M} + \sqrt{p^2 \frac{C^2}{M^2} + 4x \left( x + p \frac{c}{M} \right)}}{2}$$

The osmotic pressure between the two solutions is

$$\pi = RT \left[ \frac{C}{M} + X + \left( X + p \frac{C}{M} \right) - \frac{c}{M} - x - \left( x + p \frac{c}{M} \right) \right] \quad (2)$$

or using (1) and rearranging

$$\pi = RT \left[ \frac{C}{M} - (p + 1) \frac{c}{M} - 2x + \sqrt{\frac{p^2 C^2}{M^2} + 4x \left( x + p \frac{c}{M} \right)} \right] \quad (3)$$

and its slope at  $C = c$  is

$$\frac{\partial \pi}{\partial C} = \frac{RT}{M} \left[ 1 + \frac{p}{\sqrt{1 + (4xM/pc) + (4x^2M^2/p^2c^2)}} \right] = \frac{RT}{M} \left[ 1 + \frac{p}{1 + (2xM/pc)} \right] = \frac{RT}{M} \left[ 1 + \frac{p}{1 + (2x/z)} \right]$$

hence

$$\frac{Hc}{\tau} = \frac{1}{M} \left[ 1 + \frac{p}{1 + (2x/z)} \right] \quad (IIIc)$$

or its equivalents

$$\frac{Hc}{\tau} = \frac{1}{M} \left( 1 + \frac{pz}{y + x} \right) = \frac{1}{M} \left( 1 + \frac{p}{1 + (2xM/cp)} \right) \quad (IIIa,d)$$

(IIIc) differs from (Ic) only by doubling the  $x/c$  factor and from (IIc) by the removal of the square and square root in the denominator.

**E. The colloidal ion fluctuates while the small ions maintain equilibrium with a salt solution in equilibrium with the bulk solution:** the concentration of the salt solution must be  $\sqrt{x(x + (pc/M))}$ .  $X$  is given by

$$x \left( x + \frac{pc}{M} \right) = XY = X \left( X + \frac{pC}{M} \right)$$

which is the same as 1.

The osmotic pressure is given by

$$\pi = RT \left[ \frac{C}{M} + X + \left( X + \frac{pC}{M} \right) - 2 \sqrt{x \left( x + \frac{pc}{M} \right)} \right]$$

which differs from 2 only by a constant. Hence  $\partial \pi / \partial c$  is the same as previously and therefore  $\tau$  is finally given again by equations III.

Thus far I have assumed implicitly that  $p$ , the charge of the colloidal cation, remains constant as the concentration of simple ions changes. This is not true in many systems and if equilibrium conditions are to be fully maintained, the change in charge should be taken into account. Since the establishment of charge depends on dynamic equilibrium with the small ions, this may be a rapid process compared to the main fluctuation.

**F. The concentration of colloidal cation fluctuates while both its charge and the concentration of small ions maintain equilibrium conditions:** this is closely related to the preceding case. If we call the charge in the fluctuating volume  $P$ , the basic equation becomes

$$x \left( x + p \frac{c}{M} \right) = X \left( X + P \frac{C}{M} \right)$$

hence

$$\pi = RT \left[ \frac{C}{M} + \sqrt{\frac{P^2 C^2}{M^2} + 4x \left( x + p \frac{c}{m} \right)} - 2x - (p + 1) \frac{c}{M} \right]$$

and its slope at  $C = c$  and  $P = p$

$$\frac{\partial \pi}{\partial C} = \frac{RT}{M} \left[ 1 + \frac{p + c(dp/dc)}{1 + (2x/z)} \right]$$

so that under these premises

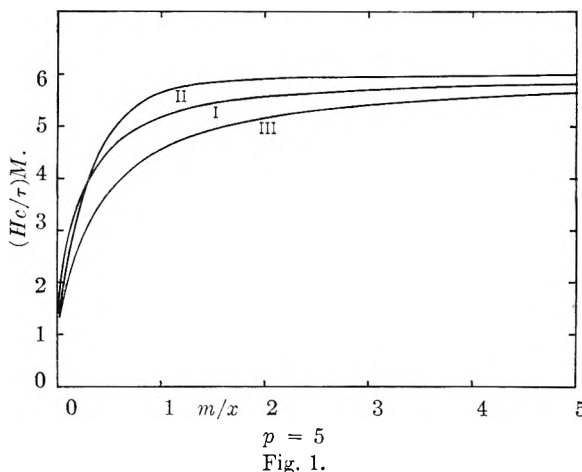
$$\frac{Hc}{\tau} = \frac{1}{M} \left[ 1 + \frac{p + c(dp/dc)}{1 + (2x/z)} \right] \quad (IVc)$$

which differs from (IIIc) only by the addition of  $c(dp/dc)$  to  $p$  in the numerator. As  $dp/dc$  is generally unknown, this equation can be applied only by successive approximations and is of lesser interest at present.

**Discussion of Formulas I, II and III**

In this section I shall point out some formal consequences of the three formulas corresponding to the three types of fluctuations at constant charge  $p$  discussed above, with special emphasis on III which seems to be the most probable.

Figure 1 shows the curves of light scattering *vs.* concentration  $c$  of colloid predicted by the three formulas for a constant charge  $p = 5$  and constant concentration of simple salt. It may be noted that all three give the same value,  $1/M$ , for  $c = 0$  and at high concentration tend to the same limit,  $(p + 1)/M$ , in agreement with Herman's results. They differ, however, at intermediate values: III predicts constantly a lower  $Hc/\tau$  and I approaches the horizontal limit much faster.



The initial slope is the same for II and III, namely

$$\left[ \frac{\partial (Hc/\tau)}{\partial c} \right]_{c=0} = \frac{p^2}{2xM^2}$$

which is the result obtained by Edsall and co-workers.<sup>6</sup> The initial slope according to equation I is twice the above value.

Since the difference between the three curves is not enormous, the remaining figures illustrate the effect of several factors only for formula III.

Figure 2 shows the effect of increasing charge  $p$  and the corresponding increase of  $Hc/\tau$  values and increasing sharpness of curvature.

Figure 3 shows the effect of changing the concentration  $x$  of the simple salt at constant charge  $p = 5$  upon the shape of the  $Hc/\tau$  *vs.*  $c$  curve. The reduction of initial slope and of curvature is clearly apparent.

Figures 2 and 3 both show that when the salt concentration  $x$  becomes large compared to that of the colloid, the charge effect disappears and  $Hc/\tau$  becomes  $1/M$  as in the case of uncharged colloids.

This "swamping electrolyte" situation pertains in aqueous solutions whenever the colloid concentration tends to zero because even in the absence of added electrolyte, the ionization products of water become swamping.

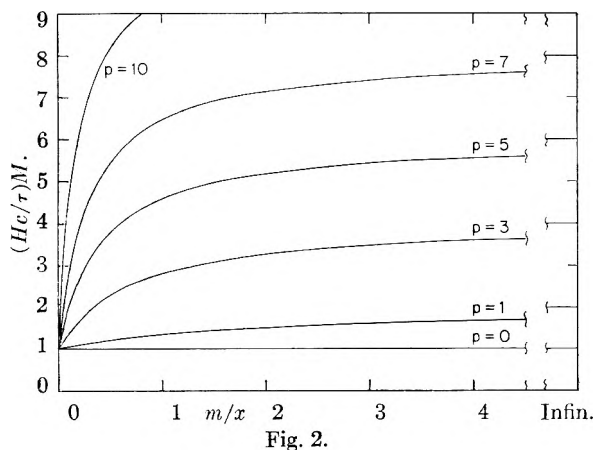


Fig. 2.

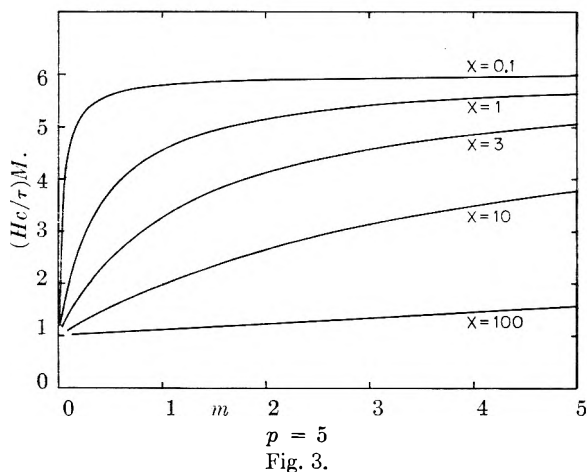


Fig. 3.

It also pertains, as already pointed out,<sup>11</sup> when the light scattering by micelles is extrapolated to the critical micelle concentration because then the unassociated ions are the swamping electrolyte.

Figure 4 shows the predicted effect of dilution of a solution containing originally a concentration  $x_0$  of simple salt and  $c_0$  of colloidal electrolyte of fixed charge  $p$  with solutions containing various concentrations  $x_1$  of simple salt. Under these conditions the actual concentrations are given by

$$x = \frac{c}{c_0}(x_0 - x_1) + x_1$$

and the turbidity for any  $c$  is given by

$$\frac{Hc}{\tau} = \frac{1}{M} \left[ 1 + \frac{p}{1 + \frac{2M}{p} \left( \frac{x_0 - x_1}{c_0} + \frac{x_1}{c} \right)} \right] \quad (\text{IIIe})$$

The slope of the  $Hc/\tau$  curve as  $c \rightarrow 0$  is, of course

$$\left( \frac{\partial Hc/\tau}{\partial c} \right)_{c \rightarrow 0} = \frac{p^2}{2M^2 x_1}$$

while the slope upon initial dilution at  $c = c_0$

$$\left( \frac{\partial Hc/\tau}{\partial c} \right)_{c_0} = \frac{2x_1}{c^2(1 + (2Mx_0/pc))^2}$$

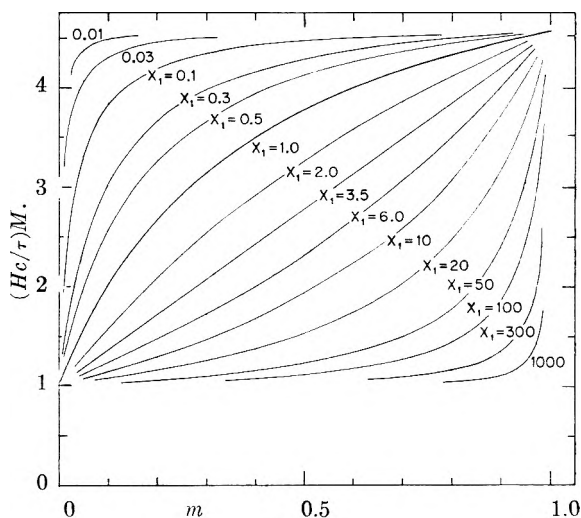


Fig. 4.

so that the ratio of initial slopes at  $c_0$  for dilutions with different salt concentrations  $x_1$  and  $x_2$  is simply the ratio of these concentrations

$$\left( \frac{\partial Hc/\tau}{\partial c} \right)_{c_0} \Big/_{(x_1)} \left/ \left( \frac{\partial Hc/\tau}{\partial c} \right)_{c_0} \Big/_{(x_2)} = \frac{x_1}{x_2}$$

This type of dilution with a salt solution gives an  $Hc/\tau$  vs.  $c$  curve which is either convex or concave to the abscissa, depending on the concentration of  $x_1$  of the diluting solution. It becomes a straight line when

$$x_1 = x_0 + p(m_0/2)$$

which is equivalent to keeping constant the concentration of the "salt component" in Scatchard's sense.<sup>12</sup>

**Non-Ideal Solutions.**—In the above I have considered implicitly solutions which are ideal in the sense that the activity and osmotic coefficients of the individual ions are unity. Their behavior deviates markedly from that of ideal uncharged systems due only to the condition of electroneutrality and Donnan equilibrium. If additional interactions between the particles are present such as the Debye-Hückel type, so that activity and osmotic coefficients depart from unity, the above reasonings become considerably more involved since electroneutrality requirements are not affected, Donnan considerations must be corrected by activity coefficients and osmotic terms by osmotic coefficients. While this can be done, it leads to very complex formulas which can have little interest at present. If the uncorrected formulas are used to calculate a charge  $p$  for non-ideal solutions, it must be remembered that this is an effective charge for light scattering and need not correspond exactly to the charge obtained by other measurements.

If the charge  $p$  is constant, it can, however, be obtained in principle accurately by a double extrapolation to zero colloid concentration when colloid-colloid interactions become negligible and zero salt concentration where colloid-salt interaction becomes negligible.

<sup>12</sup> G. Scatchard, *J. Am. Chem. Soc.*, **68**, 2315 (1946).

**Comparison with Experimental Data.**—The above reasoning excludes explicitly large polyelectrolytes whose dimensions are or may become comparable with the wave length of light. It can be applied to association colloids such as those studied by Debye<sup>13</sup> assuming micelles to be the colloidal species and unassociated ions the simple salt. These systems present, however, the difficulty that there is no *a priori* reason to assume either  $M$  or  $p$  to be constant and the evaluation of  $x$  is quite speculative. An attempt to treat this case quantitatively will be presented later,<sup>14</sup> but it may be noted qualitatively that Dr. Phillips in my laboratory has found for sodium lauryl sulfate a definite curvature and flattening of the  $H(c - cmc)/\tau$  vs.  $c$  curve at concentrations higher than those studied by Debye which makes it clearly belong to the family of Fig. 2 or 3.

Thus, pure proteins seem to be the only colloid suitable for comparison: Qualitatively, the curves (and particularly the points) presented in Figs. 1–3 by Edsall and collaborators<sup>6</sup> which show the effect of increasing  $x$  seem to belong in the family of curves shown in Fig. 3. The curves of Fig. 4 of Doty and Steiner<sup>5</sup> which show the effect of concentration and of  $pH$  (and hence  $p$ ) at low values of  $x$  seem to belong into Fig. 2 and curves of their Fig. 7 which show the effect of diluting with solutions of higher  $x$  seem to belong to Fig. 4.

Quantitative application to these systems is prob-

(13) P. Debye, *THIS JOURNAL*, **53**, 1 (1949).

(14) J. N. Phillips and K. J. Mysels, presented at 124th American Chemical Society Meeting, Chicago, September, 1953.

ably not justified. Nevertheless, it may be of interest to present some results: Doty and Steiner's<sup>5</sup> curve of turbidity vs. concentration at  $pH$  3.3 (Fig. 4) gives according to formula III an effective charge  $p$  decreasing linearly from 10.6 to 9.2 between 1.9 and 9.3 g./liter (points below 1.9/liter give rapidly decreasing values and are probably unreliable). If the change of  $p$  with concentration is taken into account by using formula IV, successive approximations give  $p$  decreasing from 11.1 to 10.4 over the same range of concentration. Since the concentration of  $Cl^-$  ions increases many-fold as the concentration of protein hydrochloride increases, the drop in  $p$  is not surprising, but the absolute value is remarkably low.

The curves obtained by the same authors for "isoionic" dilutions (Fig. 7) with salt solutions at  $pH$  3.3 give, by formula III, charges  $p$  which increase to about 13 in the most dilute solutions. I see no immediate explanation for such an increase.

In view of the experimental difficulties presented by these very dilute solutions, the highly disturbing effects of any electrolytic impurities or junction potentials and the uncertainties of their ideality, I do not think that these results can yet be taken as having a definite bearing on the value of the theory.

**Acknowledgment.**—I am grateful to the Bristol Myers Co. for support which gave me leisure for these thoughts, to Dr. J. N. Phillips and Professor A. W. Adamson for stimulating discussions and to Professor J. Th. G. Overbeek for helpful suggestions.

## EFFECT OF TEMPERATURE ON THE ADSORPTION OF *n*-DECANE ON IRON

BY PAUL R. BASFORD, WILLIAM D. HARKINS<sup>1</sup> AND SUMNER B. TWISS

*Contribution from the Chrysler Corporation of Detroit, Michigan, and the Department of Chemistry, University of Chicago, Chicago, Illinois*

Received September 4, 1953

Adsorption isotherms at temperatures from 70 to 125° have been measured for *n*-decane on iron. The results can be described very exactly in terms of the Polanyi theory. The data have been used to calculate the decrease in free surface energy of a solid due to an adsorbed film,  $\pi_s$ , and the work of adhesion,  $W_A$ , over the temperature range. Both quantities decrease moderately as the temperature increases.  $\pi_s$  and  $W_A$  values between 70 and 125° were also calculated from published data for *n*-heptane on iron, iron oxide ( $Fe_2O_3$ ), graphite and silver for comparison. With the exception of silver, which gave low results, these values were similar to the *n*-decane on iron. The isosteric heat and the three differential heats of adsorption were determined from the *n*-decane on iron data and compared. As expected, these heats of adsorption are quite different, and their relation to the adsorption process is discussed. Some experiments on the adsorption of *n*-hexyl alcohol on iron and *n*-propyl alcohol on  $Fe_2O_3$  at 100° are briefly described.

### I. Introduction

The effect of temperature on both activated and physical adsorption<sup>2–5</sup> has been extensively studied. In the latter field, with which this paper is concerned, it appears that Polanyi<sup>6</sup> and others fol-

lowing him<sup>7–11</sup> have established a valid theory to explain the observed temperature effects. However, it is to be noted that almost all the evidence for the theory involves adsorption on porous materials charcoal, silica gel and catalysts—where the

(1) Deceased.

(2) A. Titoff, *Z. physik. Chem.*, **74**, 161, 641 (1910).

(3) I. F. Homfray, *ibid.*, **74**, 129 (1910).

(4) J. McGavack and W. A. Patrick, *J. Am. Chem. Soc.*, **42**, 946 (1920).

(5) L. H. Ryerson and A. E. Cameron, *THIS JOURNAL*, **39**, 181 (1935).

(6) M. Polanyi, *Verh. deut. physik. Ges.*, **18**, 55 (1916)

(7) S. Brunauer, "The Adsorption of Gases and Vapors," Princeton University Press, Princeton, N. J., 1942, pp. 95–120.

(8) F. Goldmann and M. Polanyi, *Z. physik. Chem.*, **A132**, 313 (1928).

(9) H. H. Lowry and P. S. Olmstead, *THIS JOURNAL*, **31**, 1601 (1927).

(10) G. D. Halsey, *J. Chem. Phys.*, **16**, 931 (1948)

(11) T. L. Hill, *ibid.*, **17**, 590 (1949).

dissimilar processes of adsorption and capillary condensation, each differently affected by temperature, take place simultaneously. Obviously, it would be desirable to eliminate this source of uncertainty by working with non-porous adsorbents. The present study was undertaken for this purpose. The solid chosen was an electrolytic iron powder, known to be non-porous, and the adsorbate was *n*-decane.

This work has practical as well as theoretical importance because it is generally recognized that the effectiveness of a lubricant is related to the forces which hold it on the solid surfaces as a continuous film. However, there are few data on the magnitude of these forces, particularly at the higher temperatures normally encountered in the use of lubricants. From the adsorption isotherms at elevated temperatures, it is possible to calculate the free energy and heat of adsorption which determine the forces of adhesion in a representative case.

## II. Experimental

**A. Materials.**—The *n*-decane was a Bureau of Standards sample made available through the courtesy of Dr. M. L. Corrin of the University of Chicago. Since it was certified to be at least 99.5% pure, it was not purified further. It was dried over sodium hydride for an extended period and degassed immediately before use by repeated freezing and thawing under vacuum. The iron was an electrolytic powder, -325 mesh, which contained 0.3% impurities. The specific area, measured by adsorption of *n*-heptane, was 0.187 m.<sup>2</sup>/g.<sup>12</sup> No attempt was made to remove the thin oxide film on the surface. It was extracted with dry ether and dried under vacuum. The other materials referred to (*n*-heptane, Fe<sub>2</sub>O<sub>3</sub>,<sup>13</sup> iron,<sup>12</sup> silver<sup>14</sup> and graphite<sup>15</sup>) were those used by Harkins and Loeser in their experiments at 25°.

**B. Apparatus.**—In order to assure absolute accuracy in the adsorption measurements, the following precautions were taken: no part of the adsorbate vapor was exposed to a temperature below that at which it was to be adsorbed; no stopcocks were used, to eliminate any possible leakage of the stopcocks during extended use at high temperatures; mercury vapor was rigidly excluded during adsorption; the thermostat was capable of holding the temperature constant within 0.1° indefinitely; precision of measurement was comparable to that of volumetric adsorption apparatus at room temperature.

The apparatus finally adopted meets these requirements, but lacks speed and flexibility in consequence. Essentially it is a chamber of known volume containing the adsorbent and a series of samples of adsorbate which can be broken by magnet-operated plungers. A Bodenstein quartz spiral manometer is used to measure the pressure. An air thermostat controls the temperature. Outside the thermostat are a travelling microscope to measure the deflection of quartz fibers attached to the spiral, and a mercury manometer (read by means of a cathetometer) to measure the pressure in the outer chamber of the Bodenstein gage. A ballast bulb is provided to facilitate small pressure changes in the outer chamber. A 3-way stopcock connects this bulb either to the vacuum manifold or to a source of dry nitrogen.

Several difficulties with the design of the thermostat and the preparation of samples had to be overcome. It was found that extremely vigorous air circulation was necessary for precise temperature control. This was secured by an external duct and blower. In order to cut down thermal lag, two heaters were mounted in the duct—a large heater, constantly on, which supplied about 90% of the necessary heat, and a small heater controlled by a Wheelco 235-D

proportioning controller. Current to the two heaters was adjusted by means of Variacs so that the small heater was on about half the time. Under these conditions, the temperature could be held constant within ±0.03°. The samples of *n*-decane were prepared as follows: The sample tubes were made of very thin glass so they could be broken without danger to the rest of the adsorption apparatus. The empty tube was sealed to the male half of a ground joint, dried and weighed to 0.01 mg. It was then connected to a vacuum system, using a mercury seal but no lubricant. The assembly was evacuated thoroughly, and a small amount of *n*-decane distilled into the sample tube from the storage bulb. Repeated freezing, thawing and distillation under vacuum between two traps removed all dissolved gases. The liquid could be transferred to the sample tube by slightly warming the traps and leads with a hand torch while a slow stream of very cold air passed over the tip of the tube. When the tube was about half full (0.2 to 5.0 mg., depending on the diameter) it was sealed off, heated overnight at 150° and then weighed. The heating served to eliminate samples with walls so thin they would break prematurely when heated in the adsorption apparatus. Breakage averaged about 50%.

**C. Method.**—Before starting adsorption experiments, the sensitivity of the Bodenstein gage had to be measured. This amounted to 0.0524 mm. displacement of the fibers per mm. difference in pressure between the inner and outer chambers at all temperatures. The zero point (*i.e.*, the displacement of the fibers with vacuum in both chambers) shifted with temperature, and had to be measured before each set of experiments from 70 to 125°. Thereafter the travelling microscope could not be re-levelled or re-focused, since either would shift the zero point by an unknown amount.

Approximately 45 g. of iron powder was weighed into the sample tube, and outgassed by heating under vacuum at 200° in a small removable furnace until the residual pressure fell to 1 × 10<sup>-5</sup> mm. A McLeod gage was used for this measurement. Usually 16 to 24 hours heating was sufficient. The sample was then cooled to room temperature and the volume beyond the seal-off constriction was measured, using dry nitrogen and a gas buret. This volume was about 80 cm.<sup>3</sup>. Duplicate determinations usually checked within 0.03 cm.<sup>3</sup>. Pumping was resumed until the pressure again fell to 1 × 10<sup>-5</sup> mm. The system was then sealed off, the thermostat closed, and the temperature brought to 125 ± 0.5°, the highest temperature at which adsorption was measured. When temperature equilibrium had been established, one of the *n*-decane samples was broken. The magnet operating the breakers was so mounted that it could be manipulated from outside the thermostat. A period of 16 to 24 hours was allowed for adsorption equilibrium to be established. Numerous tests failed to show any measurable pressure drop beyond this period. The equilibrium pressure was then measured. In order to avoid errors of observation as far as possible, at least 50 readings of the displacement of the quartz fibers were averaged for each of 10 values of the pressure difference between inner and outer chambers. The displacement plotted against the pressure difference gave a straight line which was used to interpolate to the previously measured zero point. The temperature was measured on a thermometer which had been calibrated against one certified by the Bureau of Standards.

The amount adsorbed in cm.<sup>3</sup> (STP) per g. iron powder was calculated from the equation

$$V = \frac{V_m}{M_{Fe}} \left[ \frac{M_d}{341.82} - \frac{pV}{RT} \right] \quad (1)$$

where  $V_m$  = cm.<sup>3</sup> (STP) per mole,  $M_{Fe}$  and  $M_d$  the masses of the iron and *n*-decane samples, respectively,  $p$  the equilibrium pressure,  $V$  the volume of the system,  $R$  the gas constant and  $T$  the absolute temperature. The same *n*-decane sample was used to measure the adsorption at a series of progressively lower temperatures. Usually 5° decrements were used. The additional adsorption which takes place as the temperature is lowered is much more rapid than the desorption which would occur if the temperature were raised between successive measurements. The lowest temperature used was 70°. When the 70° measurement was complete, the thermostat was set at 125° again, the second *n*-decane sample broken, and the process above repeated. A set of ten samples could be mounted in the adsorption apparatus and used successively as described above. When

(12) W. D. Harkins and E. H. Loeser, *J. Chem. Phys.*, **18**, 556 (1950).

(13) G. Jura, E. H. Loeser, P. R. Basford and W. D. Harkins, *ibid.*, **14**, 117 (1946).

(14) *Ibid.*, **13**, 535 (1945).

(15) W. D. Harkins, G. Jura and E. H. Loeser, *J. Am. Chem. Soc.*, **68**, 554 (1946).

the set was completed, the apparatus was opened, a new set of *n*-decane samples installed, and the iron sample degassed as before. The first sample of each set contained an amount of *n*-decane sufficient to bring the equilibrium pressure to a value close to but below that for the last measurement of the previous set. This check served to show that the apparatus was working properly for both sets. Successive sets of *n*-decane samples were used until the pressure range from  $p/p_0 = 0.003$  to  $p/p_0 = 0.97$  was covered. The measurements at the highest relative pressure (above 0.95) are slightly low, probably because small thermal gradients in the apparatus led to some condensation of *n*-decane. These data were not included in the final analysis of the results.

It was found that the same apparatus could be used to follow the course of very slow surface reactions. Some experiments with *n*-hexyl alcohol on iron and *n*-propyl alcohol on iron oxide ( $\text{Fe}_2\text{O}_3$ ) are briefly noted below. The experimental technique was similar to that described above.

### III. Results and Discussion

The data are presented as adsorption isotherms at 70, 80, 90, 100 and 125° in Fig. 1. It should be pointed out that the volumes adsorbed were not necessarily measured at exactly those temperatures; the thermostat could be very quickly set to hold, *e.g.*, a temperature somewhere between 99.5 and 100.5°, but if it had to be set to hold exactly  $100 \pm 0.05^\circ$  much time was wasted. The small correction terms could be obtained with negligible errors by interpolation on a plot of equilibrium pressure *vs.* temperature for each series of results on a single sample (or combination of samples) of *n*-decane. The isotherms are all similarly shaped, and strongly resemble those observed for lower molecular weight hydrocarbons at lower temperatures. Presumably, only physical adsorption is taking place up to 125°, although attempts to prove this by demonstrating that the adsorption is completely reversible were inconclusive because of difficulties with the apparatus. Indirect evidence was obtained by showing that the data follow the Polanyi theory very closely. The postulates of the theory are such that it describes the adsorption of polar molecules only qualitatively, and breaks down completely for adsorbates which undergo reaction at the surface or so-called activated adsorption.

In order to apply the theory, it is necessary to know, in addition to the adsorption data at various temperatures,  $d$ , the density, and  $p_0$ , the vapor pressure of the liquid *n*-decane at the temperatures to be used. Data from several sources were evaluated, correlated, and finally used in the form of the two equations

$$d = 0.7460 - 0.00077t - 1.961 \times 10^{-6} t^2 \quad (2)$$

where  $t$  = temperature in degrees centigrade, and

$$\log p_0 = -8.6031101 \log T - \frac{3778.179}{T} + 34.13187 \quad (3)$$

According to the Polanyi theory, an adsorbate molecule originally at a distance,  $r$ , from the solid surface will require the expenditure of an amount of free energy,  $\Delta F$ , to remove it to an infinite distance, regardless of the temperature. If  $r$  is chosen at the boundary of the material adsorbed as a liquid

$$\Delta F = RT \ln p_0/p \quad (4)$$

when  $p_0$  and  $p$  are the vapor pressure and equilibrium pressure, respectively. The distance  $r$  can not be measured, but the thickness of the liquid layer,  $t$ , may be used equally well

$$t (\text{\AA.}) = \frac{V \times 10^8}{V_m \Sigma} V_{\text{ads.}} \quad (5)$$

where  $V$  = molecular volume of liquid adsorbate in  $\text{cm.}^3$ ,  $V_m$  =  $\text{cm.}^3$  (STP) per mole of vapor,  $\Sigma$  = specific area of adsorbent ( $\text{cm.}^2$  per g.) and  $V_{\text{ads.}}$  = volume adsorbed in  $\text{cm.}^3$  (STP) per g. The thickness calculated from this equation is slightly high, since the liquid is compressed by the forces holding it to the surface. The compressibility of *n*-decane is not known, but on the reasonable assumption that it is comparable to that of *n*-heptane, the error was evaluated, and found to be small in comparison with experimental errors. Equation 5 was therefore used without modification.

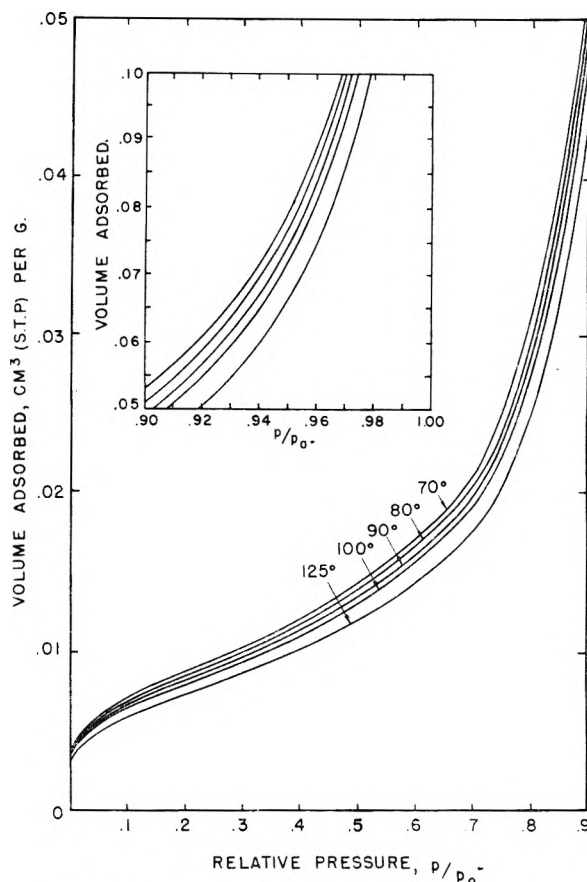


Fig. 1.—Adsorption isotherms, *n*-decane on iron.

Figure 2 shows  $\Delta F$  plotted against  $t$ , which Polanyi refers to as the characteristic curve. Since the experimental points for this curve are too numerous and too closely spaced to be reproduced, the expedient was adopted of showing the 90% confidence limits. Detailed analysis of this curve permits the following conclusions to be drawn.

1. All the data are self-consistent, and determine a single curve.
2. The points are distributed at random with respect to the temperature, *i.e.*, measurements at the highest temperatures show no tendency to be either higher or lower than those at lower temperatures.
3. Experimental errors, estimated from the scattering of points about the curve, are 1-2% at low pressures, and increase to about 4% at higher

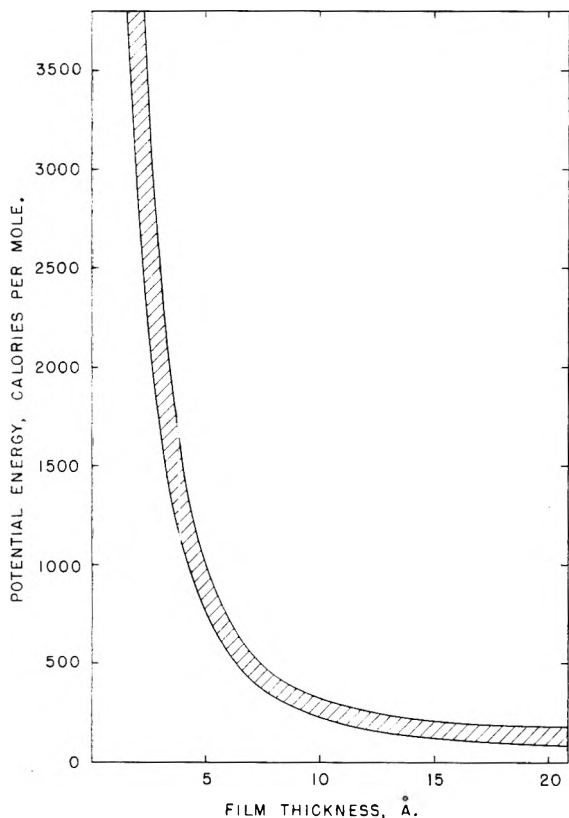


Fig. 2.—Characteristic curve, *n*-decane on iron. The two curves are so chosen that 90% of the observed points fall between them.

pressures. This is comparable to the precision attainable with the usual volumetric adsorption apparatus at room temperature.

4. The consistency of the data over a range of 55° indicates that the Polanyi theory is being followed very closely. This is true for multi-layer adsorption as well as for the monolayer. The same behavior was observed with nitrogen adsorbed on iron synthetic ammonia catalysts.<sup>16</sup>

5. Adsorption of a non-polar material such as *n*-decane is exclusively physical, at least up to 125°.

From the isotherms of Fig. 1 it is possible to determine the decrease of surface free energy ( $\pi$ ) due to the formation of adsorbed films<sup>17</sup>

$$\pi = \frac{RT}{V_m \Sigma} \int_0^p \frac{V_{ads}}{p^2} dp \quad (6)$$

where the symbols have the same meaning as in equation 5. Values of  $\pi$  calculated in this way at various temperatures are shown plotted against the relative pressure in Fig. 3. These curves can be used to extrapolate to  $p/p_0 = 1$  in order to obtain  $\pi_e$ , the free energy decrease due to an adsorbed film in equilibrium with the saturated vapor. Both  $\pi_e$  and a related quantity,  $W_A$ , the work of adhesion, are valid measures of the tightness of binding between solid and liquid

$$W_A = \pi_e + \gamma_L (1 + \cos \theta) \quad (7)$$

where  $\theta$  = contact angle (zero for *n*-decane on iron)

(16) P. H. Emmett and S. Brunauer, *J. Am. Chem. Soc.*, **57**, 2732 (1935).

(17) D. H. Bangham and R. I. Razouk, *Trans. Faraday Soc.*, **33**, 1462 (1937).

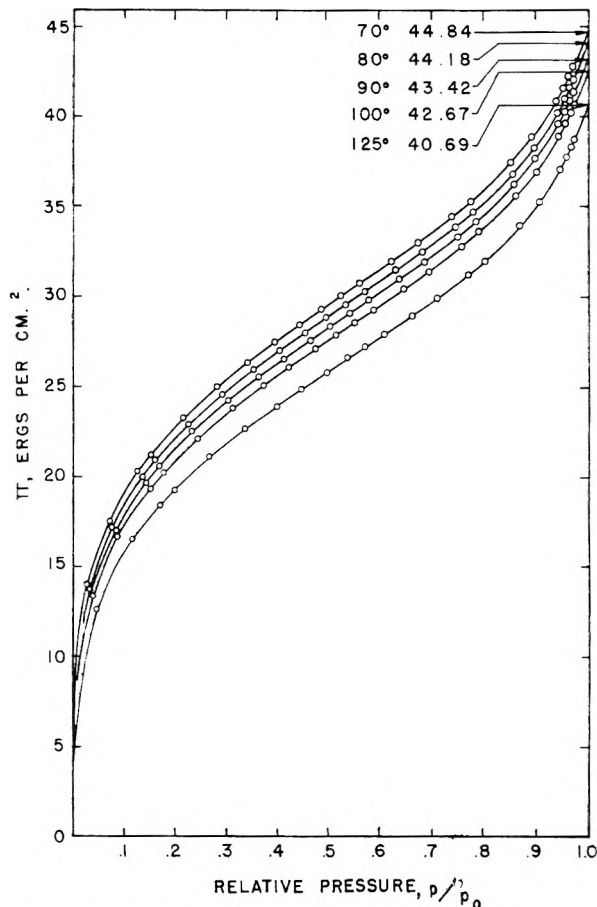


Fig. 3.—Decrease of free energy,  $\pi$ , for *n*-decane on iron.

and  $\gamma_L$  is the surface tension of the liquid adsorbate. The surface tension has been measured only at 20°, but its values at higher temperatures can be approximated by the Ramsey-Shields equation

$$\Gamma = \left(\frac{M}{d}\right)^{2/3} \gamma_L = K(T_c - T - 6) \quad (8)$$

since  $d$  and  $T_c$  are known.

$\pi_e$  and  $W_A$  are shown plotted against the temperature in Fig. 4. As expected, they decrease moderately as the temperature is raised. For comparison, similar curves for *n*-heptane on iron,<sup>12</sup> iron oxide ( $\text{Fe}_2\text{O}_3$ ),<sup>13</sup> silver<sup>14</sup> and graphite<sup>15</sup> are included in Fig. 4. They were calculated from the 25° adsorption data of Harkins and Loeser by means of the Polanyi theory. The characteristic curves can be obtained quite accurately, since the compressibility of the liquid is known over the whole temperature range.<sup>13</sup>

No estimate of errors can be made, so the curves must be regarded as qualitative only. The similar shape of all the curves, and the closeness of grouping, suggest that specific differences between hydrocarbons with respect to their adsorptive properties, and between different surfaces with respect to their effect on adsorption of hydrocarbons, are small. The failure of the curves for *n*-heptane on silver to fit into this pattern cannot be explained at present.

(18) L. B. Smith, J. A. Beattie and W. C. Kay, *J. Am. Chem. Soc.*, **59**, 1587 (1937).

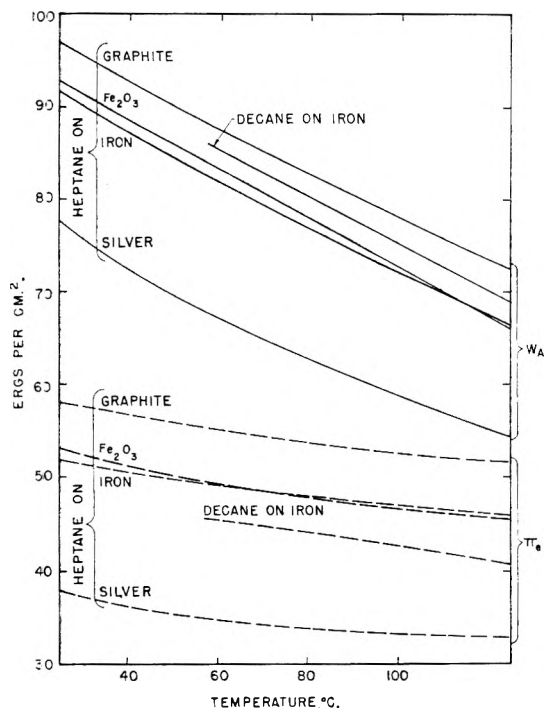


Fig. 4.—Change in  $\pi_e$  and  $W_A$  with temperature for various materials.

Adsorption data over a range of temperatures can be used to determine the heat of adsorption. Several different processes may be set up, each of which defines a different heat of adsorption. To avoid confusion, these will be discussed briefly before presenting the data.

The most commonly used heat of adsorption is the isosteric heat. This is defined, not by a process, but by the equation

$$\Delta H_{\text{iso.}} = T(S_G - \bar{S}_i) = R \left( \frac{\partial \ln p}{\partial 1/T} \right)_{n \text{ adsorbed}} \quad (9)$$

The significance of  $\Delta H_{\text{iso.}}$  can be brought out by making use of the exact analogy between the thermodynamics of adsorption and of solution.<sup>19</sup> If  $n_1$  moles of solvent and  $n_2$  moles of solute are combined to form a solution

$$\Delta H_{\text{soln.}} = n_1 \bar{H}_1 + n_2 \bar{H}_2 - n_1 H_1^0 - n_2 H_2^0 \quad (10)$$

Similarly, if  $n_1$  moles of gas at a pressure  $p$  are adsorbed on 1 sq. cm. of a clean solid surface to form an aggregate still in equilibrium with gas at the same pressure

$$\Delta H_{\text{total}} = n_1 \bar{H}_{1(\text{adsorbed})} + h_{n \text{ ads.}} - n_1 \bar{H}_1(\text{pressure} = p) - h_0$$

which can be rearranged to

$$\Delta H_{\text{total}} = n_1 \Delta H_{\text{iso.}} + (h_{n \text{ ads.}} - h_0) \quad (11)$$

The isosteric heat is therefore that part of the total heat of adsorption due to the change in heat content of the adsorbate; the simultaneous change in the heat content of the solid surface is not included in  $\Delta H_{\text{iso.}}$

Heats of adsorption which include the contributions of the solid as well as the adsorbate can be defined by any of the following processes.

- (a) 1 cm.<sup>2</sup> solid surface (0 moles adsorbed) +  $n$  moles adsorbate (liquid)  $\rightarrow$  1 cm.<sup>2</sup> solid surface ( $n$  moles adsorbed)

- (b) 1 cm.<sup>2</sup> solid surface (0 moles adsorbed) +  $n$  moles adsorbate (vapor, pressure =  $p_0$ )  $\rightarrow$  1 cm.<sup>2</sup> solid surface ( $n$  moles adsorbed)

- (c) 1 cm.<sup>2</sup> solid surface (0 moles adsorbed) +  $n$  moles adsorbate (vapor, at equil. pressure  $p$ )  $\rightarrow$  1 cm.<sup>2</sup> solid surface ( $n$  moles adsorbed)

The corresponding  $\Delta H$ 's are

$$\Delta H_a = -(h_{E(\text{SL})} - h_{E(\text{SfL})}) \quad (12)$$

$$\Delta H_b = -(h_{E(\text{SL})} - h_{E(\text{SfL})}) - n\lambda \quad (13)$$

$$\Delta H_c = -(h_{E(\text{SL})} - h_{E(\text{SfL})}) - n\lambda - nRT \ln p_0/p = -h_{D(\text{VS})} \quad (14)$$

where  $h_{E(\text{SL})}$  and  $h_{E(\text{SfL})}$  are the heats of emersion of the clean and the film covered solids, respectively,  $\lambda$  is the heat of condensation of the adsorbate, and  $h_{D(\text{VS})}$  is the total (calorimetric) heat of desorption.

The two-dimensional form of the Gibbs-Helmholtz equation<sup>20</sup>

$$(h_{E(\text{SL})} - h_{E(\text{SfL})}) = \pi - T \left( \frac{\partial \pi}{\partial T} \right)_n \quad (15)$$

was used to calculate  $(h_{E(\text{SL})} - h_{E(\text{SfL})})$  and  $h_{D(\text{VS})}$ .

The isosteric heat is shown in Fig. 5;  $h_{E(\text{SL})} - h_{E(\text{SfL})}$  and  $H_{D(\text{VS})}$  are shown in Fig. 6. Since  $(h_{E(\text{SL})} - h_{E(\text{SfL})})$  is an integral heat and the isosteric heat is a differential heat, they cannot be compared directly. In order to make this comparison, the differential heat of adsorption

$$\frac{d \Delta H_b}{dn} = \frac{d(h_{E(\text{SL})} - h_{E(\text{SfL})})}{dn} + \lambda \quad (16)$$

was calculated. It is shown in Fig. 5. The two curves are quite dissimilar, except that both approach  $\lambda$  as  $n$  becomes large.

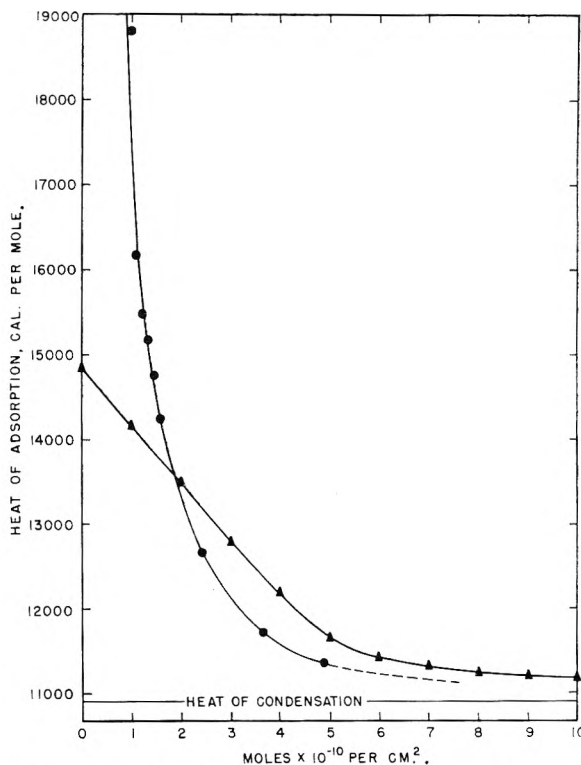


Fig. 5.—Isosteric heat of adsorption,  $\Delta H_{\text{iso.}}$ ,  $\bullet$  and decrease in surface heat content,  $d \Delta H_b/dn$ ,  $\blacktriangle$ , for *n*-decane on iron at 100°.

(19) T. L. Hill, *J. Chem. Phys.*, **18**, 246 (1950).

(20) W. D. Harkins, T. F. Young and G. E. Boyd, *ibid.*, **8**, 954 (1940).

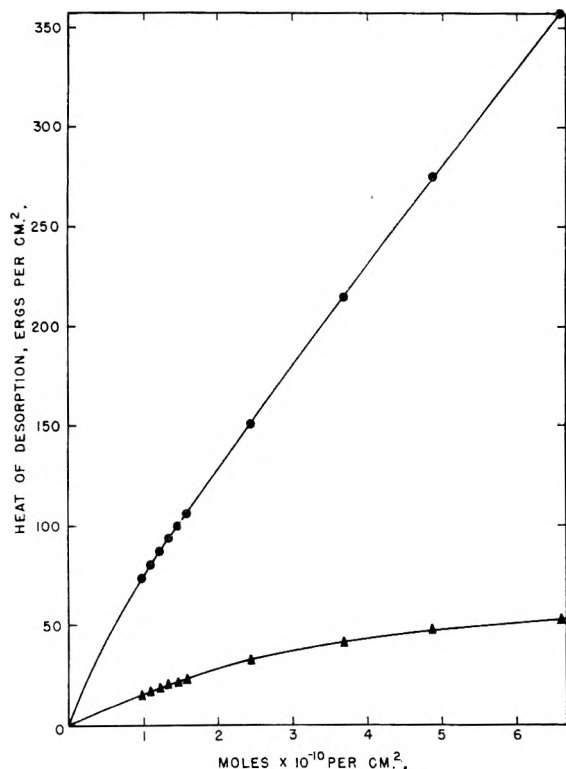


Fig. 6.—Heat of desorption for *n*-decane on iron at 100°: —●—,  $H_{D(7S)}$  and —▲—,  $(h_{E(SL)} - h_{E(SL)})$ .

It is evident that multiplication by the large factor  $T$  (373°K.) in equation 15 will greatly exaggerate any errors in the adsorption data, so that high accuracy is not to be expected. However, the consistency of the original data, and the relatively small scattering of points in Fig. 6, lead to the belief that  $(h_{E(SL)} - h_{E(SL)})$  and the isosteric heat are substantially correct.

The heat of adsorption of *n*-decane on iron at 100°, and its variation with the amount adsorbed, present no very unusual features. The initial (isosteric) heat of adsorption is high, at least 22,000–25,000 calories per mole. As more decane is adsorbed, this decreases regularly.

A high initial heat of adsorption is commonly ascribed to selective adsorption in pores and crevices. This is unlikely in the present case, since even if small pores were present, the decane molecules are too large to be adsorbed there. It is more probable that surface inhomogeneity, and the tendency of the decane molecules to lie flat on the sur-

face, are responsible. The latter point can be demonstrated easily; if the decane molecules were oriented and coiled as in the liquid, each would occupy an area of about 50 sq. Å. The area actually occupied is 92 sq. Å. A plot of  $p/V(p_0 - p)$  against  $p/p_0$  according to the Brunauer–Emmett–Teller theory gave a good straight line, from which it was found that 0.00754 cm.<sup>3</sup> (STP) per g. was necessary to complete the monolayer. Since the specific area was already known, the area occupied per molecule is thereby determined.

Neither the isotherms nor the heat curves show any evidence of discontinuities corresponding to phase changes. It is of course possible that they would be observed in the very low pressure region not accessible to the present apparatus.

It was planned originally to extend this study to polar adsorbates. *n*-Hexyl alcohol on iron at 100° was chosen for the first experiment. It was found that equilibrium was approached much more slowly than has ever been observed for physical adsorption; at the end of 5 days the pressure was still decreasing and the experiment was terminated. The alcohol vapor was removed by condensation in a trap submerged in liquid nitrogen, and the residual pressure (presumably due to hydrogen) measured. To judge from the amount of hydrogen, one half of the adsorbed molecules had reacted with the surface with evolution of hydrogen, and the other half either had not reacted, or had reacted without evolution of hydrogen. The reaction was not investigated further.

The adsorption of *n*-propyl alcohol on  $Fe_2O_3$  at 100° was investigated next, in the belief that physical adsorption alone would take place. Here also a very slow surface reaction was observed. The pressure had not reached a constant value at the end of 17 days, at which time a second increment was added, and the experiment continued another ten days. Both curves followed the rate equation  $dp/dt = -Kp(p - p_{eq.})$  very closely. It was possible to estimate  $p_{eq.}$  with fair accuracy; it was found that both curves approached the same equilibrium pressure. This suggests that the surface is homogeneous with respect to whatever reaction is taking place, and that if the isotherm could be measured it would resemble those observed by Loeser, *et al.*,<sup>13,15,21</sup> which exhibited first-order phase changes. It is not suggested that their discontinuities were due to surface reactions.

(21) E. H. Loeser, W. D. Harkins and S. B. Twiss, *THIS JOURNAL*, 57, 591 (1953).

# THERMODYNAMICS OF THE ADSORPTION OF WATER ON GRAPHON FROM HEATS OF IMMERSION AND ADSORPTION DATA

BY G. J. YOUNG, J. J. CHESSICK, F. H. HEALEY AND A. C. ZETTMEOYER

*Surface Chemistry Laboratory, Lehigh University, Bethlehem, Penna.*

*Received September 11, 1953*

Adsorption isotherms and heats of immersion were measured for the system Graphon-water. The very low adsorption of water by Graphon precluded reliable calculations of thermodynamic quantities from isotherms at two temperatures. Measurements of the heat of immersion as a function of the amount of water pre-adsorbed on the Graphon surface in combination with the results obtained from an adsorption isotherm at one temperature allowed the calculation of isosteric heats of adsorption and absolute entropies of the adsorbed state. The isosteric heats of adsorption were much less than the heat of liquefaction and had a minimum value of about 6.0 kcal. near the BET  $V_m$ . The thermodynamic criteria of a complete monolayer, the minimum in the  $S_3$  curve, corresponded closely to the BET value. This coverage amounted to only  $1/1500$  of the total Graphon surface area and lends support to the concept of cluster-wise adsorption of water on this surface.

**Introduction.**—The adsorption of water on Graphon has been measured previously by Pierce and Smith<sup>1,2</sup> and their results present several interesting features. Graphon appears to be a surface which, while generally considered homogeneous, does possess a small fraction of heterogeneous sites. These sites have been considered<sup>1</sup> to be primarily responsible for the adsorption of water at low relative pressures.

In view of the very small amount of water adsorbed by Graphon at pressures below saturation, thermodynamic quantities cannot be calculated with any precision by the usual method of measuring adsorption isotherms at two temperatures. However, by combining adsorption data with measurements of the heat of immersion of Graphon in water it has been possible to calculate both the absolute entropies of the adsorbed state and the isosteric heats of adsorption.

## Experimental

Water vapor adsorption isotherms were determined at temperatures of 10, 18 and 25° for Graphon.<sup>3</sup> This non-porous, graphitized carbon black had an area as determined by nitrogen adsorption of 83 m.<sup>2</sup>/g. The sample was degassed at 400° for 12 hours at  $10^{-5}$  mm. before use. The samples were not treated with hydrogen since it was desired to preserve any heterogeneous surface sites.

The amount of water adsorbed was determined volumetrically using a modified Orr apparatus previously described.<sup>4</sup> The deviation was about 0.005 ml. adsorbed per gram at lower coverages. Equilibrium pressures were read after one hour on a manometer filled with Apiezon "B" oil. To check the extent of water absorption by the oil, adsorption isotherms were also determined using a mercury manometer. In these instances, time intervals as long as 24 hr. were allowed before equilibrium pressures were read. No significant differences were found in the isotherms obtained by the two methods.

The calorimeter used in the heat of immersion studies has been described.<sup>4</sup> Values for the heat of wetting were obtained for evacuated Graphon and for Graphon with various amounts of adsorbed water on the surface. The water-coated Graphon samples were prepared on the adsorption apparatus and sealed off at the desired equilibrium pressure. Care was taken to ensure that the temperature of the sample was not altered during the sealing off process.

Two- to three-gram samples were used in the heat of

immersion studies. Samples were used only once, since it was found that after recovery and subsequent washing and drying, the reused sample often gave a slightly higher heat of immersion. This increase probably can be attributed to limited surface oxidation occurring in the presence of moisture and heat. Samples carefully recovered and immediately dried under vacuum gave no appreciable change in heat of immersion values. Samples activated at 400° for 4 hours gave essentially the same heat of wetting values as samples evacuated for 24 hours at 25°.

The calculated *maximum* deviation due to errors inherent in the calorimetric technique was about 2%. Actually the experimental deviation from a mean value was considerably better than this except for samples prepared at high relative pressures where the heat of wetting is strongly dependent on the relative pressure of the adsorbed film. The deviation from the best curve representing the data was  $\pm 0.07$  ergs./cm.<sup>2</sup> for coverages up to a relative pressure of 0.8.

## Results and Discussion

The isotherm for the adsorption of water on Graphon shown in Fig. 1 has predominant Type III

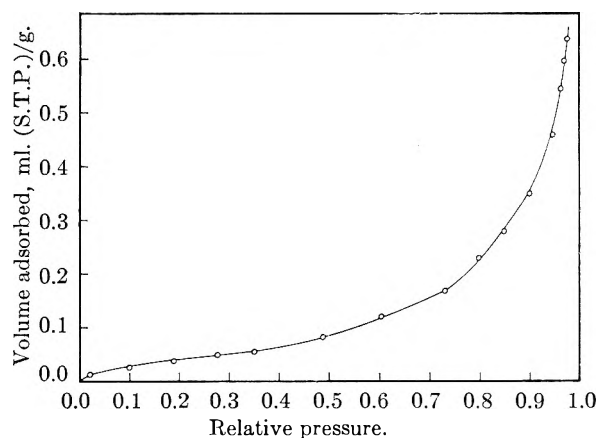


Fig. 1.—Adsorption of water on Graphon 18°.

character, despite the slight rise in the curve at low pressures. Only a few of the experimental points are shown. At a relative pressure of about 0.95 only about 1/30 of a statistical monolayer of water was adsorbed. Pierce and Smith<sup>2</sup> who studied the adsorption of water on a similar carbon adsorbent which had been treated with hydrogen at 1100° reported that a relative pressure of about 0.99 was required to form one statistical monolayer; two statistical monolayers were adsorbed at 0.997. Further, these workers concluded that their isotherms at 0 and 28.6° were identical up to about 0.93. Experimentally it was found for the samples used in this study of the same relative pressure

(1) Conway Pierce and R. Nelson Smith, *THIS JOURNAL*, **54**, 784 (1950).

(2) Conway Pierce and R. Nelson Smith, *ibid.*, **54**, 795 (1950).

(3) We wish to thank Dr. Walter Smith of the Godfrey L. Cabot Company, Boston, Mass., for furnishing the Graphon, L-2739 and Mr. William Shaefer for his sincere attention to our numerous requests during the course of this investigation.

(4) A. C. Zettlemoyer, G. J. Young, J. J. Chessick and F. H. Healey, *THIS JOURNAL*, **57**, 649 (1953).

range (up to 0.95) that slightly greater amounts of water were adsorbed at the higher temperature. Accurate isosteric heat calculations could not be made from the isotherm data at two temperatures because of the small amounts of water vapor adsorbed over a wide pressure range. However it was quite definite that the heat was well below the heat of liquefaction of water as would be required if more water vapor was adsorbed at a higher temperature for a given relative pressure. Approximate isosteric heat values calculated from the pressure change resulting from a change in temperature for a given amount adsorbed were also well below the heat of liquefaction of water.

A BET  $V_m$  value of 0.017 ml. was calculated from the adsorption data at 25°. The BET plot was fairly linear over the relative pressure region 0.07 to 0.4.

Values for the heats of immersion of Graphon in water are shown plotted in Fig. 2 as a function of the relative pressure to which the Graphon had been previously exposed. The curve differs markedly from the few curves for similar functions reported in the literature.<sup>4,5</sup> These latter curves were obtained for the immersion of hydrophilic solids on whose surfaces duplex films of water form at saturation. The heat curves for these hydrophilic materials are characterized by high values at low surface coverages, and decrease rapidly toward 118 ergs/cm.<sup>2</sup>; *i.e.*, the heat liberated when one square cm. of a water-air interface is destroyed at 25°. In sharp contrast, the heat values found for the water-Graphon system are about 32 ergs/cm.<sup>2</sup> near zero coverages and remain near this low value for samples exposed to water vapor over a wide range of relative pressures. Only at values of  $x = 0.90$  do the heat values increase significantly. The shape of the heat of immersion curve is not entirely unexpected since the hydrophobic Graphon surface does not adsorb to any appreciable amount except near saturation pressure.

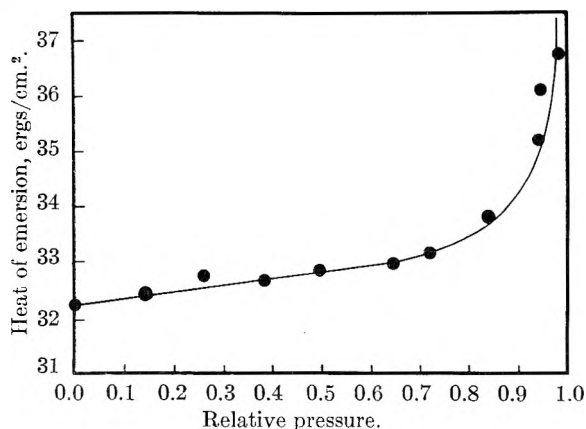


Fig. 2.

The isosteric heat values calculated from calorimetric data and an isotherm at one temperature are shown plotted as a function of volume adsorbed in Fig. 3. The heat values lie below the heat of liquefaction in agreement with the approximate isotherm data at two temperatures. The

error limits on the calculated points in Fig. 3 represent the maximum probable error as estimated from the maximum deviations of the heat of wetting and adsorption values.

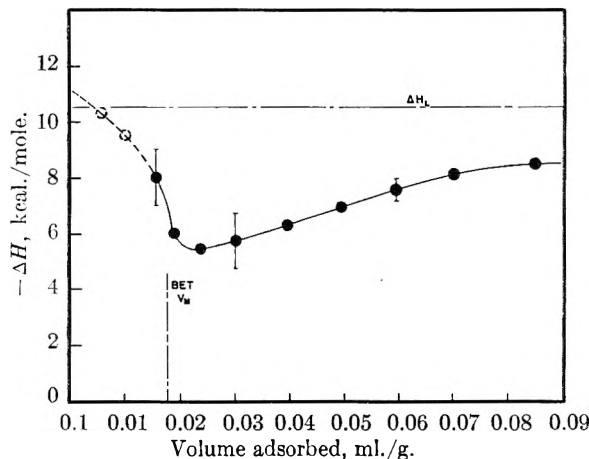


Fig. 3.

The difference in the internal energy  $E_L$ , per mole of liquid adsorbate in equilibrium with vapor at  $T$ , and the energy,  $E_S$ , per mole of adsorbed molecules is given by the relationship<sup>6</sup>

$$(U_0 - U)/N_S = E_L - E_S$$

where  $U_0 - U$  is the difference in the heat of immersion of the clean solid and a solid with  $N_S$  adsorbed molecules. The energy difference  $E_L - E_S$  is related to the isosteric heat,  $q_{st}$ , by an equation readily obtained from equation 91 of Hill<sup>7</sup>

$$E_L - E_S = 1/N_S \int_0^{N_S} q_{st} dN_S - \Delta H_V$$

where  $\Delta H_V$  is the molar heat of vaporization of water. The isosteric heat is thus obtained by a graphical differentiation of an  $N_S(E_L - E_S)$  vs.  $N_S$  plot. The calculated heat values are largely below the heat of liquefaction of water and pass through a minimum, near the calculated BET  $V_m$  value. The heat values then increase slowly toward the heat of liquefaction. The shape of the heat curve is strikingly similar to the curve for the adsorption of water on molybdenum sulfide which was reported recently by Ballou and Ross.<sup>8</sup>

The entropy of the adsorbed molecules,  $S_S$ , assuming an unperturbed adsorbent, was calculated from the equation

$$T(S_S - S_L) = \frac{U - U_0}{N_S} + \frac{\varphi}{\Gamma} - kT \ln x$$

as developed by Jura and Hill.<sup>6</sup> In this equation  $S_L$  refers to the entropy of the liquid,  $\varphi$  is the spreading pressure,  $\Gamma$  the surface concentration, and  $x$  the relative equilibrium pressure of the film coated solid.

The differential entropy  $\bar{S}_S$  was obtained directly from the isosteric heat values using the expression

$$\bar{S}_S = S_G - \Delta S = S_G - \frac{q_{st}}{T}$$

where  $S_G$  is the absolute entropy of gaseous water at  $T$  and  $p$ .

(6) G. Jura and T. L. Hill, *ibid.*, **74**, 1498 (1952).

(7) T. L. Hill, *J. Chem. Phys.*, **17**, 520 (1949).

(8) E. V. Ballou and Sydney Ross, *THIS JOURNAL*, **57**, 653 (1953).

(5) W. D. Harkins and G. Jura, *J. Am. Chem. Soc.*, **66**, 922 (1944).

The plots of  $S_S$  and  $\bar{S}_S$  as a function of the volume of water adsorbed are shown in Fig. 4. Both curves exhibit a minimum and it is to be noted that the curves intersect at the minimum of the  $S_S$  curve. This intersection follows as a mathematical consequence of the relation between the two quantities, but inasmuch as different methods of calculation were used for  $S_S$  and  $\bar{S}_S$  the correct intersection provides a check on the computations.

The minimum in the  $S_S$  curve has been taken<sup>9</sup> as a thermodynamic criterion for the completion of the first layer of adsorbed molecules, *i.e.*,  $V = V_m$ . This minimum  $S_S$  for water on Graphon is seen in Fig. 4 to be in excellent agreement with the value for  $V_m$  calculated from the BET equation. This close correspondence is worthy of special note since the amount of water adsorbed at the BET  $V_m$  amounts to only about 1/1500 of the value that would be expected from the nitrogen surface area. Thus, these two entirely independent approaches appear to indicate that the adsorbed water molecules begin to build up in a second layer when only a very small fraction of the surface has been covered.

It is apparent that such behavior can only be explained on the basis of at least two types of adsorption sites on the Graphon surface. The vast majority of the surface sites are hydrophobic and must correspond to the graphite-like array of carbon atoms. These sites show no tendency to adsorb water, at least up to pressures close to saturation. The hydrophilic sites are few in number and probably arise from traces of surface oxide such as might be expected to form at the edge atoms of the graphite planes. It would be these sites that would account for the initial Type II character of the water adsorption isotherm. These sites are probably of unequal energies as shown by the decrease in the isosteric heat below  $V_m$  (Fig. 3) but as a group are still vastly different from the remainder of the surface. After the adsorption of the first layer of water molecules on these sites the molecules build up additional layers on and around these sites rather than adsorb on the adjacent hydrophobic area.

The concept of cluster-wise adsorption also has been used by Pierce and Smith<sup>1</sup> to explain the hysteresis loop found in the water vapor isotherm on Graphon at high relative pressures and by Cassie<sup>10</sup> to explain contact angle hysteresis of water on graphite.

It may be surprising that the heat of adsorption on almost all of the hydrophilic sites is well below the heat of liquefaction. However, it must be remembered that the high heat of liquefaction of water is due largely to the formation of hydrogen bonds and that when no such bonding can take place in the adsorption process it is reasonable for the heat evolved to be considerably less. Indeed, a second molecule going down on top of the single adsorbed molecule should still have less opportunity for interaction than in the liquid. The heat of adsorption thus rises only gradually toward the heat of liquefaction.

(9) T. L. Hill, P. H. Emmett and L. G. Joyner, *J. Am. Chem. Soc.*, **73**, 5105 (1951).

(10) A. B. D. Cassie, *Discs. Faraday Soc.*, **3**, 11 (1948).

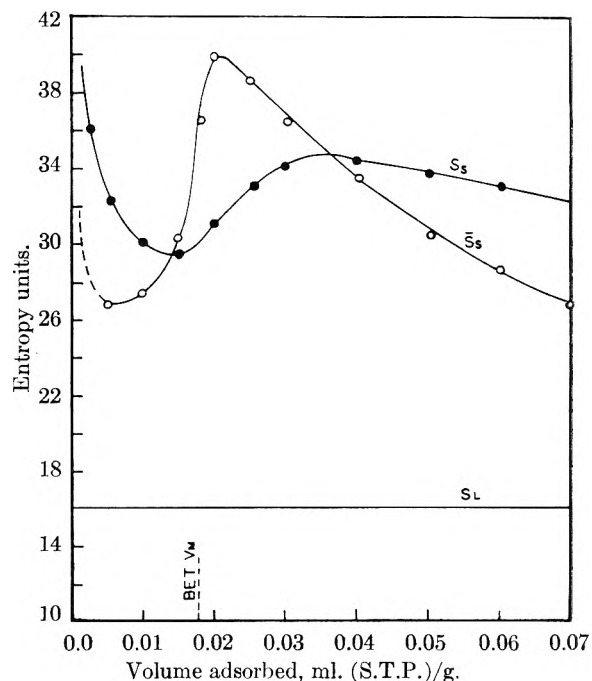


Fig. 4.—Entropy of adsorbed water on Graphon at 25°.

For the same reasons the entropy of the adsorbed water molecules is not as low as in liquid water. Inasmuch as the shape of the isosteric heat curve indicates that energies of these sites are not the same, it does not appear possible to account for the high entropy values by including a configuration entropy term for the ways in which the molecules could distribute themselves among the sites. If the sites are all of different energies there can only be one equilibrium distribution of identical molecules at a given pressure.

The surface of Graphon is generally considered<sup>11</sup> to be quite uniform. The present results do not, of course, contradict this conclusion since the heterogeneity reported here concerns only about 1/1500 of the surface. For adsorbents such as argon and nitrogen the effect of this minute fraction of the surface would be obscured even if the adsorption energies were quite different on the two types of surface sites. Nevertheless, the small amount of heterogeneity may be a critical factor in the observed properties of the material. It has been well demonstrated by Savage<sup>12</sup> that the wear properties and lubricating action of graphite are greatly improved by the presence of water vapor even at low pressures. Since both graphite and Graphon have similar crystalline arrays of carbon atoms, the water adsorption on graphite must also mainly occur on the hydrophilic oxide and impurity sites. It is indeed striking that, though little of the surface is covered by adsorbed water molecules, the presence of these few molecules is sufficient to prevent the rapid wear of carbon brushes in electric motors, and to allow the use of graphite as a lubricant.

**Acknowledgment.**—The authors are grateful for the support of the Office of Naval Research, Contract N8 onr-74300.

(11) R. A. Beebe, J. Bischoe, W. R. Smith and C. B. Wendell, *J. Am. Chem. Soc.*, **69**, 95 (1947).

(12) R. H. Savage, *Ann. N. Y. Acad. Sci.*, **53**, 862 (1951).

FUGACITY OF WATER AT HIGH TEMPERATURES AND PRESSURES<sup>1</sup>

BY WILLIAM T. HOLSER

*Department of Geology, Cornell University, Ithaca, New York**Received October 17, 1953*

Fugacities for water in the single phase range up to 1000° and 2000 bars are calculated by graphical integration of recently published  $p$ - $\bar{v}$ - $T$  data, and tabulated in terms of the fugacity coefficient. At high pressure and low temperature the fugacity coefficients are slightly less than the approximate values predicted by Newton's empirical graphs.

Reactions involving water at high temperatures and pressures are fundamentally important in geochemical processes, and are of increasing interest in other fields. Consideration of equilibria in such systems necessitates a knowledge of the fugacity of water.

## Method

Accurate values of the fugacity of water may be derived from  $p$ - $\bar{v}$ - $T$  data published recently by Kennedy.<sup>2</sup> These data are based on measurements up to 1000°, with an upper pressure limit decreasing from 2500 bars at 600° to 800 bars at 1000°; values for higher pressures were extrapolated assuming constant  $[\partial p/\partial T]_v$ . For the range to 460° and 350 bars, the previously published values<sup>3</sup> were taken by Kennedy as more accurate. The fugacity,  $f$ , is defined<sup>4</sup> with reference to the molal free energy in the standard (ideal gas) state at the same temperature,  $\bar{F}_T^\circ$ , by the equation

$$RT \ln f_{T,p} \equiv \bar{F}_{T,p} - \bar{F}_T^\circ \quad (1)$$

whence

$$RT \ln \frac{f_{T,p}}{f_{T,p_0}} = \int_{p_0}^p \bar{v} dp \quad (2)$$

where  $\bar{v}$  is the molal volume. Since Kennedy's data have not been reduced to an equation of state, the data were plotted on a large scale and integrated by planimeter along isotherms.

The results are most conveniently expressed<sup>5</sup> in terms of the fugacity coefficient

$$\nu \equiv f/p \quad (3)$$

as it changes less rapidly than  $f$  or  $\bar{F}$  with  $p$  and  $T$ , and is therefore more suitable for interpolation, extrapolation or graphical representation.

The mechanical integration is inconvenient for pressures lower than 100 bars (or perhaps 300 bars at high temperatures). Base values for these low pressures were calculated analytically from the equation<sup>6</sup>

$$RT \ln \nu_{T,p} = \int_0^p \left( \bar{v} - \frac{RT}{p} \right) dp \quad (4)$$

(1) This work was supported in part by the Geological Society of America and in part by the Office of Naval Research.

(2) G. C. Kennedy, *Am. J. Sci.*, **248**, 540 (1950).

(3) J. H. Keenan and F. G. Keyes, "Thermodynamic Properties of Steam," John Wiley and Sons, Inc., New York, N. Y., 1936.

(4) G. N. Lewis and M. Randall, "Thermodynamics," McGraw-Hill Book Co., Inc., New York, N. Y., 1923, p. 190.

(5) M. A. Paul, "Principles of Chemical Thermodynamics," McGraw-Hill Book Co., Inc., New York, N. Y., 1951, p. 236. The fugacity coefficient is equivalent to the "activity coefficient" of R. H. Newton, *Ind. Eng. Chem.*, **27**, 302 (1935).

(6) M. A. Paul, ref. 5, p. 237.

by substituting an equation of state<sup>7</sup> valid for this range

$$p = \frac{RT}{v - B_{T,p}} \quad (5)$$

where

$$B_{T,p} = B_{0T} + \frac{(B_{0T}p)^2 g_{1T}}{T} + \frac{(B_{0T}p)^4 g_{2T}}{T^3}$$

and

$$B_{0T} = 1.89 - \frac{2641.62 \times 10^{80870/T}}{T}$$

$$g_{1T} = \frac{82.546}{T} - \frac{1.6246 \times 10^6}{T^2}$$

$$g_{2T} = 0.21828 - \frac{1.2697 \times 10^5}{T}$$

giving

$$\ln \nu_{T,p} = \frac{1}{RT} \left[ B_{0T} + \frac{(B_{0T}p)^2 g_{1T}}{2T} + \frac{(B_{0T}p)^4 g_{2T}}{4T^2} \right] \quad (6)$$

The first term suffices at high temperatures.

At 200 and 300° the isotherms meet the saturation line at 15.55 and 85.91 bars, respectively, so that the above integration does not apply for the range 0-100 bars. At the saturation line the phase corresponding to the high pressure single phase is the denser of the two, but its fugacity must equal that of the lighter phase with which it is in equilibrium. Equation 6 is therefore solved for the saturation pressure, and extended from there by the graphical integration.

## Results

Fugacity coefficients calculated by the above process are shown in Table I. Multiplication by the pressure gives fugacity. If desired, equation (1) gives free energy in terms of the fugacity and the free energy in the standard state, taken from standard tables.<sup>8</sup>

If activities corresponding to liquid state definitions are preferred, it may be recalled that unit activity for a given temperature is defined as the fugacity at one atmosphere pressure and the same temperature.<sup>9</sup> Above the critical temperature the fugacity at such a low pressure is very nearly equal to the pressure, as shown in the first row of Table I, and the activity at higher pressure is

$$a_{T,p} \equiv \frac{f_{T,p}}{f_{T,1 \text{ atm}}} = \frac{\nu_{T,p} p}{1.013 \nu_{T,1 \text{ bar}}} \quad (7)$$

(7) F. G. Keyes, L. B. Smith and H. T. Gerry, *Am. Acad. Arts Sci.*, **70**, 319 (1936). Units for the constants are retained from the original;  $\bar{v}$  is specific volume in cc./g.,  $p$  is pressure in int. atm.,  $T$  is in °K.

(8) F. D. Rossini and others, "Selected Values of Chemical Thermodynamic Properties," Nat. Bur. Stds., Washington, 1949-, Ser. III, Vol. 1. Free energy (referred to liquid water in equilibrium with vapor at 0°) in the lower range of pressures and temperatures may be calculated directly from heat content and entropy data tabulated by J. H. Keenan and F. G. Keyes, ref. 3.

(9) G. N. Lewis and Merle Randall, ref. 4, p. 256.

TABLE I  
FUGACITY COEFFICIENT OF WATER

| Pressure,<br>bars | Temperature, °C. |       |        |       |       |       |       |       |       |       |
|-------------------|------------------|-------|--------|-------|-------|-------|-------|-------|-------|-------|
|                   | 200              | 300   | 400    | 500   | 600   | 700   | 800   | 900   | 1000  |       |
| 1                 | 0.995            | 0.998 | 0.999  | 0.999 | 1.000 | 1.000 | 1.000 | 1.000 | 1.000 | 1.000 |
|                   | *                | *     |        |       |       |       |       |       |       |       |
| 100               | .134             | .701  | * .874 | .923  | .952  | .969  | .980  | .987  | .993  |       |
| 200               | .0703            | .372  | * .737 | .857  | .909  | .938  | .960  | .975  | .985  |       |
| 300               | .0497            | .259  | .602   | .764  | .867  | .913  | .941  | .962  | .979  |       |
| 400               | .0392            | .204  | .483   | .735  | .830  | .886  | .923  | .950  | .963  |       |
| 500               | .0331            | .172  | .412   | .655  | .789  | .861  | .906  | .943  | .956  |       |
| 600               | .0290            | .150  | .361   | .599  | .751  | .838  | .890  | .931  | .951  |       |
| 700               | .0261            | .135  | .325   | .555  | .747  | .818  | .881  | .927  | .948  |       |
| 800               | .0253            | .124  | .299   | .517  | .693  | .800  | .868  | .919  | .947  |       |
| 900               | .0225            | .115  | .281   | .472  | .666  | .783  | .861  | .916  | .944  |       |
| 1000              | .0213            | .109  | .264   | .455  | .642  | .765  | .851  | .910  | .944  |       |
| 1100              | .0203            | .103  | .251   | .436  | .622  | .750  | .842  | .907  | .944  |       |
| 1200              | .0196            | .0991 | .241   | .420  | .604  | .737  | .834  | .904  | .945  |       |
| 1300              | .0190            | .0956 | .233   | .406  | .589  | .725  | .827  | .901  | .946  |       |
| 1400              | .0185            | .0928 | .226   | .395  | .577  | .715  | .821  | .899  | .948  |       |
| 1500              | .0181            | .0906 | .220   | .385  | .566  | .706  | .816  | .898  | .950  |       |
| 1600              | .0178            | .0887 | .216   | .377  | .556  | .698  | .811  | .897  | .952  |       |
| 1700              | .0176            | .0872 | .211   | .370  | .548  | .691  | .807  | .897  | .955  |       |
| 1800              | .0174            | .0860 | .208   | .365  | .542  | .685  | .803  | .896  | .957  |       |
| 1900              | .0173            | .0850 | .205   | .360  | .535  | .680  | .800  | .896  | .959  |       |
| 2000              | .0172            | .0843 | .203   | .356  | .530  | .676  | .798  | .896  | .962  |       |

\* Two phase region—do not interpolate.

Between 100 and 374°, high density ("liquid") water cannot be brought down to the 1 atm. standard state without a phase change. If activity is to have any meaning in this range, it must be in terms of the fugacity of hypothetical liquid water at 1 atm. An approximate value may be calculated by extrapolating the specific volume of liquid water from the empirical formula of Keenan and Keyes<sup>10</sup>

$$\bar{v} = 3.086 - 0.899017(374.1 - t)^{0.147168} - 0.4(385 - t)^{-1.6}(p - 218.5) + \delta \quad (8)$$

$\delta$  is a function of  $p$  and  $t$ , that was determined graphically by Keenan and Keyes. However, their determinations are not available so that this factor will have to be neglected here, although it is probably insignificant except close to the critical point. Integrating according to equation 2 from 1 atm. to the saturation pressure  $p_s$  gives

$$RT \ln \frac{f_{T,p_s}}{f_{T,1 \text{ atm.}}} = [3.086 - 0.899017(374 - t)^{0.147168} + 87.5(385 - t)^{-1.6}](p_s - 1) + 0.2(385 - t)^{-1.6}(p_s^2 - 1) \quad (9)$$

In conjunction with the fugacities at the saturation point already calculated above from equation 6, this gives fugacities  $f_{200^\circ, 1 \text{ atm.}} = 13.62$ , and  $f_{300^\circ, 1 \text{ atm.}} = 67.69$ . These values are used in the denominator of equation 7 to calculate activities at high pressure from the fugacity coefficients of the first two columns of Table I. Lewis and Randall<sup>11</sup> have pointed out the complications arising from multiple definitions of activity. Because of the hypothetical character of its definitive standard state and ambiguity of definition, activity is

(10) J. H. Keenan and F. G. Keyes, ref. 3, p. 20. Units for the constants are retained from the original:  $\bar{v}$  is specific volume in cc./g.,  $p$  is in int. atm.,  $t$  is in °C.

(11) Reference 4, p. 257.

probably a less satisfactory function than fugacity above the normal boiling point of a fluid.

### Discussion

The data of Table I do not all lie on smooth curves. Measurements and calculations have been double checked in all such cases. However, no attempt was made to redraw the  $p$ - $\bar{v}$  isotherms to give a smoother series of values. Some of the discrepancies may have originated in drawing the isotherm curves, and some may lie in the original data. Both could be corrected by reduction to an equation of state using least squares adjustment, as has already been done for the lower temperatures and pressures. In plotting the  $p$ - $\bar{v}$  isotherms no deviations from the smooth curves were noticeable except at 1000°, where the deviations from the regular curve were somewhat more than the stated precision of the measurements.

Newton has compared fugacity coefficients of various gases by means of the law of corresponding states.<sup>12</sup> At low temperatures and high pressures the values in Table I above are somewhat less than the average of the several substances used by Newton in constructing his curves. For example, at 400° and 2000 bars, Newton's curves predict  $\nu = 0.24$ , compared with 0.20 calculated (Table I). At high temperatures the calculated values are a little higher than predicted. The former discrepancy is not surprising in view of equation 5, which requires more than 3 independent constants for the equation of state, in which case the law of corresponding states would not be expected to hold exactly. At the low molal volume corresponding to this temperature and pressure, even equation 5 is inadequate as an equation of state.<sup>13</sup>

(12) R. H. Newton, ref. 5.

(13) F. G. Keyes, L. B. Smith, and H. T. Gerry, ref. 7.

## A SELECTIVITY SCALE FOR SOME MONOVALENT CATIONS ON DOWEX 50

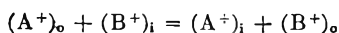
BY O. D. BONNER<sup>1</sup>*Department of Chemistry of the University of South Carolina, Columbia, S. C.**Received October 19, 1953*

Equilibrium studies involving lithium, hydrogen, sodium, ammonium, potassium and silver ions on Dowex 50 resins of approximately 4 and 16% divinyl benzene content have been made while maintaining a constant ionic strength of approximately 0.1 molar. These results are compared with those reported previously for an approximately 8% divinyl benzene resin, and a quantitative selectivity scale has been established for these resins.

**Introduction**

Although heterogeneous cation-exchange equilibria may be formulated in terms of the Langmuir adsorption mechanism<sup>2</sup> or of the Donnan membrane equilibrium,<sup>3</sup> perhaps the formulation most susceptible to simple thermodynamic treatment is that based upon the application of the law of chemical equilibrium to the exchange, regarded as a simple metathetical reaction.

Thus when both of the cations are univalent, let us consider the reaction to be that represented by the equation:



where  $A^+$  and  $B^+$  are the cations involved in the exchange and the subscripts  $i$  and  $o$  represent the resin phase and the outside solution, respectively. From a purely thermodynamic viewpoint, then, the following equation should be applicable

$$\frac{a_{(A^+)_{\text{i}}}a_{(B^+)_{\circ}}}{a_{(A^+)_{\circ}}a_{(B^+)_{\text{i}}}} = K \quad (1)$$

where  $a_{(A^+)_{\circ}}$  and  $a_{(B^+)_{\circ}}$  are the activities of the respective ions in the solution and  $a_{(A^+)_{\text{i}}}$  and  $a_{(B^+)_{\text{i}}}$  the activities of the two ions in the resin phase when equilibrium has been attained, and  $K$ , the activity quotient, must be constant at a fixed temperature. If the aqueous solution is sufficiently

dilute so that the ratio of the activity coefficients of the ions is approximately unity, the above relationship may be expressed by the equation

$$\frac{C_{(A^+)_{\text{i}}}C_{(B^+)_{\circ}}\gamma_{(A^+)_{\text{i}}}}{C_{(A^+)_{\circ}}C_{(B^+)_{\text{i}}}\gamma_{(B^+)_{\text{i}}}} = k \frac{\gamma_{(A^+)_{\text{i}}}}{\gamma_{(B^+)_{\text{i}}}} = K \quad (2)$$

where  $\gamma$  represents the activity coefficient of the ion in the resin phase and  $k$  is the experimental selectivity coefficient or equilibrium quotient.

At this point one must choose a standard reference state for the ions in the resin phase. Perhaps the preferable reference state from a theoretical viewpoint would be the infinitely dilute aqueous solution. For this choice,  $K$  would necessarily be unity, since at equilibrium  $a_{(A^+)_{\text{i}}} = a_{(A^+)_{\circ}}$  and  $a_{(B^+)_{\text{i}}} = a_{(B^+)_{\circ}}$ . The selectivity coefficient,  $k$ , would then be equal to the activity coefficient ratio  $\gamma_{(B^+)_{\text{i}}}/\gamma_{(A^+)_{\text{i}}}$ . From a practical viewpoint, however, it is preferable to choose as a standard reference state for the resin, the resin anion with only one associated cation,<sup>4,5</sup> so that the activity of each pure resin is unity. For this choice of standard states it is found that the equilibrium constant may be calculated from the equation<sup>4</sup>

$$\log K = \int_0^1 \log k \, dN \quad (3)$$

where  $N$  represents the molar fraction of the resin associated with  $A^+$ . Equation 3 was used for

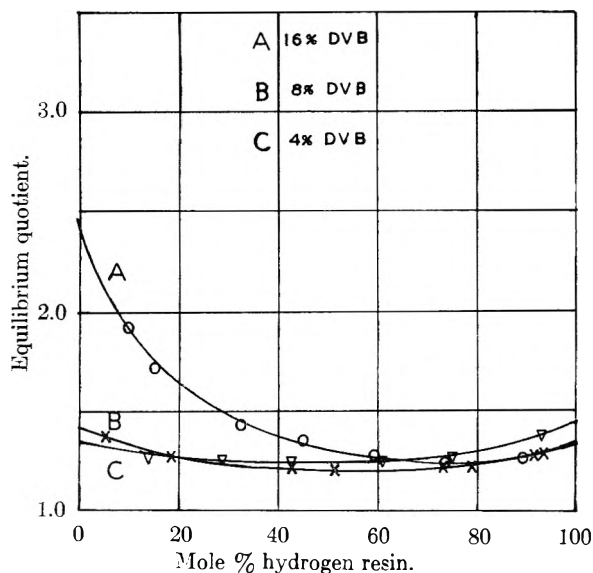


Fig. 1.—Hydrogen-lithium exchange.

(1) These results were developed under a project sponsored by the United States Atomic Energy Commission.

(2) G. E. Boyd, J. Schubert and A. W. Adamson, *J. Am. Chem. Soc.*, **69**, 2818 (1947).

(3) W. C. Bauman and J. Eichhorn, *ibid.*, **69**, 2830 (1947).

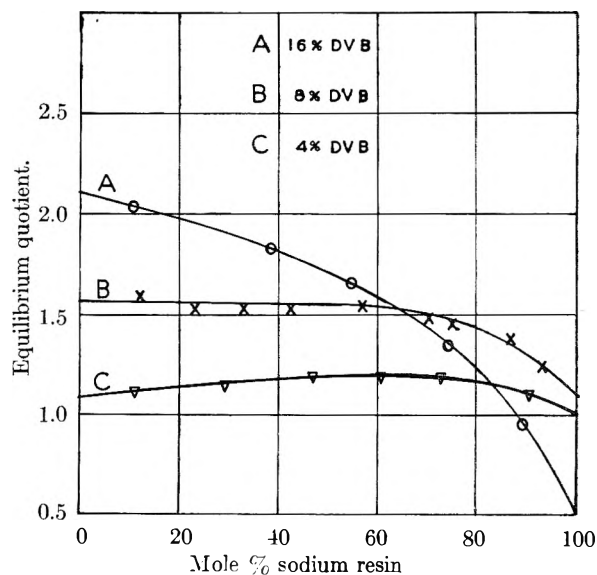


Fig. 2.—Sodium-hydrogen exchange.

(4) O. D. Bonner, W. J. Argersinger and A. W. Davidson, *ibid.*, **74**, 1044 (1952).

(5) E. Ekedahl, E. Högföldt and L. G. Sillén, *Acta. Chem. Scand.* **4**, 556 (1950).

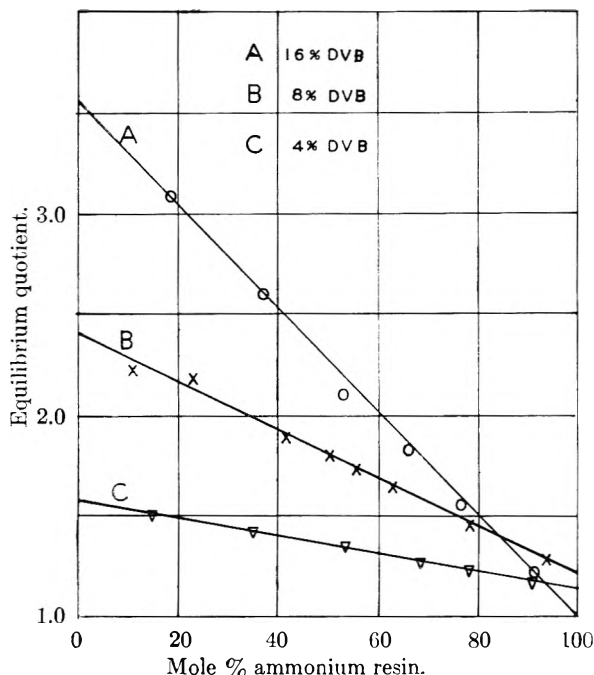


Fig. 3.—Ammonium-hydrogen exchange.

calculating the equilibrium constants presented in this paper.

**Experimental and Discussion**

Equilibrium studies involving exchanges of six monovalent cations on Dowex 50 resins of approximately 4 and 16% divinyl benzene content have been made at 25°. A description of this synthetic cation-exchange resin has been given by Bauman and Eichorn.<sup>3</sup> The experimental procedures have been described in detail previously.<sup>6,7</sup> The capacities of the 4 and 16% DVB resins in the dry acid form were 5.13 and 4.72 meq./g., respectively. These figures may be compared with 5.10 meq./g. for the 8% DVB resin previously reported.<sup>6</sup> While it is unfortunate that the capacity of the 16% DVB resin is low, probably due to incomplete sulfonation, it is believed that a significant comparison may be made between the affinities of these ions for the three resins.

The data representing the maximum water uptake of these resins in the various ionic forms and the selectivity of the resins for the ions relative to the lithium ion taken as unity are presented in Tables I and II (the values in Table II were calculated from the equilibrium constants for the various exchange reactions). The experimental selectivity curves (equilibrium quotient, *k*, vs. resin composition) are presented in Figs. 1-5. In each instance the corresponding data for the 8% DVB resins are given for convenience of comparison. The selectivity of the resin for any ion, relative to lithium, is noted to increase with increasing DVB content; *i.e.*, decrease in maximum water uptake. The hydrogen ion on the 8% DVB is an apparent exception. The maximum water uptake of each resin in any ionic form is noted to be inversely related to its affinity for these ions, hydro-

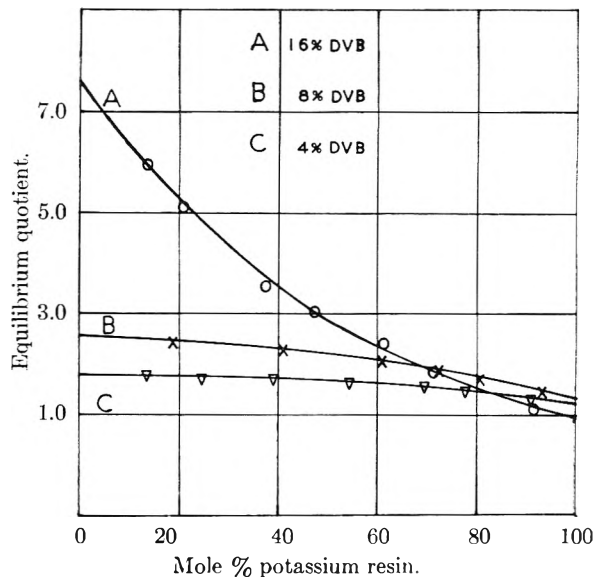


Fig. 4.—Potassium-hydrogen exchange.

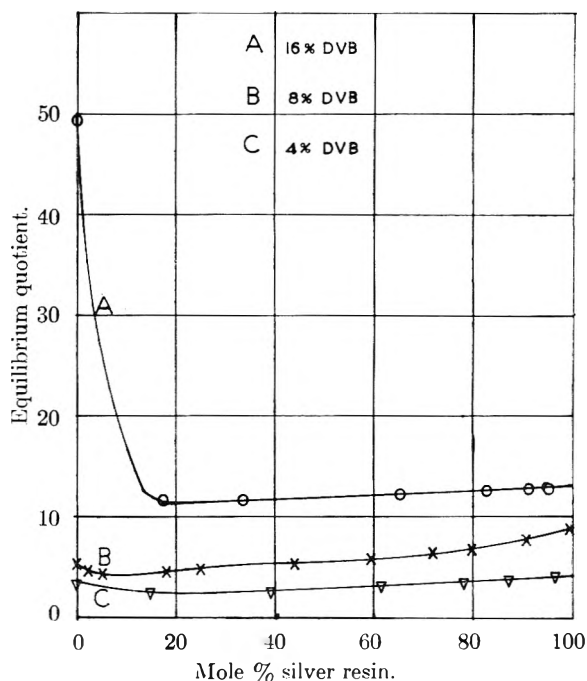


Fig. 5.—Silver-hydrogen exchange.

gen and lithium ions being apparent exceptions in the case of the 4 and the 16% DVB resins. These exceptions are believed to be real, as these data were reproducible. It is also of interest to note that the selectivity coefficient-resin composition curves for any pair of ions are similar, with the curve for the highest DVB content resin showing the greatest changes in slope. This fact results in a distinct reversal of selectivity in the sodium-hydrogen exchange on 16% DVB, the hydrogen ion being preferred by the resin when it is predominantly in the sodium form. For all of these exchanges except the silver-hydrogen and hydrogen-lithium exchanges, the 16% DVB resin exhibits less selectivity than the lower cross linked resins when it is predominantly in the salt form.

(6) O. D. Bonner and Vickers Rhett, *THIS JOURNAL*, **57**, 251 (1953).  
 (7) O. D. Bonner and W. H. Payne, *ibid.*, **58**, 183 (1954).

TABLE I

MAXIMUM WATER UPTAKE OF DOWEX 50 RESINS IN VARIOUS

|                              | IONIC FORMS (G./EQUIV.) |        |         |
|------------------------------|-------------------------|--------|---------|
|                              | 4% DVB                  | 8% DVB | 16% DVB |
| Li <sup>+</sup>              | 418                     | 211    | 130     |
| H <sup>+</sup>               | 431                     | 200    | 136     |
| Na <sup>+</sup>              | 372                     | 183    | 113     |
| NH <sub>4</sub> <sup>+</sup> | 360                     | 172    | 106     |
| K <sup>+</sup>               | 341                     | 163    | 106     |
| Ag <sup>+</sup>              | 289                     | 115    | 102     |

A final point of interest is the possible effect of the capacity of the resin upon its selectivity. In a previous paper<sup>6</sup> results were given for sodium-hydrogen and silver-hydrogen exchanges on a nominal 16% DVB resin having a capacity in the dry hydrogen form of 5.10 meq./g. The equilibrium constants were found to be 1.74 and 16.1

TABLE II

SELECTIVITY SCALE FOR DOWEX 50 RESINS

|                              | 4% DVB          | 8% DVB | 16% DVB |
|------------------------------|-----------------|--------|---------|
|                              | Li <sup>+</sup> | 1.00   | 1.00    |
| H <sup>+</sup>               | 1.30            | 1.26   | 1.45    |
| Na <sup>+</sup>              | 1.49            | 1.88   | 2.23    |
| NH <sub>4</sub> <sup>+</sup> | 1.75            | 2.22   | 3.07    |
| K <sup>+</sup>               | 2.09            | 2.63   | 4.15    |
| Ag <sup>+</sup>              | 4.00            | 7.36   | 19.4    |

for the sodium-hydrogen and silver-hydrogen exchanges, respectively. These results may be compared with the values of 1.54 and 13.4 for this resin of lower exchange capacity. Although both resins were classified as nominal 16% DVB, it is possible that a part of the difference in equilibrium constants for the same exchange reactions may be due to a slight difference in the cross-linkage.

## THE DIELECTRIC BEHAVIOR OF SORBED WATER ON SILICA GEL

BY SHIGEHICO KUROSAKI

*Department of Applied Physics, Central Research Laboratory, Hitachi, Ltd., Tokyo, Japan*

*Received October 28, 1953*

For the purpose of clarifying the state of sorbed water on silica gel, the sorption isotherms of water vapor on silica gel were obtained to determine the differential heat of sorption, as well as to measure the changes in the apparent dielectric constant of silica gel powder caused by an increase in water content and to calculate the specific polarization of the sorbed water. The apparent loss factor of silica gel having different moisture contents was also measured in the frequency range of 2 kc./sec.-1 Mc./sec. As a result, it has been ascertained that three different states exist for sorbed water on silica gel. In the first sorption stage (water content <15 mg./g.), the sorbed water indicates a very low specific polarization; it is firmly bound to the silica gel surface, and has a high heat of sorption. In the second sorption stage (15-94 mg./g.), the sorbed water is assumed to be in the condition similar to that of water dissolved in organic solvents. Sorbed water in the third sorption stage (>94 mg./g.), generally present in trimolecular layers or more, is considered as capillary condensed water, showing a maximum loss factor in the vicinity of 10 kc./sec. The  $\epsilon''_{\max}$  value can be explained semi-quantitatively by the theory of binary aggregates, and it is surmised that capillary condensed water on silica gel has a much more strongly developed hydrogen bonding (approaching that of ice) than liquid water.

### Introduction

In determining the states of gases or vapors sorbed on solids, the measurement of apparent dielectric constant is a very helpful method that has been employed by several researchers to date.<sup>1-7</sup> Especially when water vapor is the adsorbate, dielectric measurements are believed to be an effective means of determining the macroscopic or microscopic states of the water, because of its strong polarity.

In previous publications,<sup>8-10</sup> it was considered that water sorbed on solid polymers is similar in construction to water dissolved in organic solvents, and that interaction among the molecules of the sorbed water is not so strong. It has been established that the plots showing the relation between the dielectric constant and water content of vinyl

polymers are nearly linear, but that in the case of sorbed water on paper alone, the water is present in two different states separated by a certain water content.

The changes in the dielectric constant of silica gel due to differences in water content, already reported by McIntosh and others,<sup>6,7</sup> show that sudden variations in polarization of the sorbed water are observed before and after a certain moisture content, as in the case of water sorbed on paper. In this respect the results are similar to the facts observed by Higuti from the plots showing the apparent dielectric constant *vs.* moisture content relation of *n*-propyl alcohol adsorbed on titania gel, the only difference being that the polarization of the first stage sorbed water shows higher value than that of water sorbed after the first stage.

As for the absorption of electromagnetic energy by silica gel with a moisture content, the results of McIntosh's measurements do not indicate a Debye-type dispersion, and are therefore considered merely as showing dispersion caused by ion conduction at low frequencies. In this respect also further re-examination was desirable in connection with the restriction of the dipoles of sorbed water, and a detailed examination of the frequency characteristics of the loss factor has been made in this paper.

The fact that the molecules of water sorbed on solids are firmly bound to the surface of the solid

- (1) J. V. Zhilenkov, *Colloid J. (U.S.S.R.)*, **4**, 473 (1938).
- (2) I. Higuti, *Science Rep. Tohoku Univ.*, [1] **33**, 174 (1949).
- (3) *Ibid.*, **33**, 99 (1949).
- (4) M. Shimizu and I. Higuti, *THIS JOURNAL*, **56**, 198 (1952).
- (5) L. N. Kurbatov, *Zhur. Fiz. Khim.*, **24**, 899 (1950).
- (6) R. McIntosh, E. K. Rideal and J. A. Snelgrove, *Proc. Roy. Soc. (London)*, **A208**, 292 (1951).
- (7) J. A. Snelgrove, H. Greenspan and R. McIntosh, *Can. J. Chem.*, **31**, 72 (1953).
- (8) S. Kuroski, *J. Chem. Soc. Japan, Pure Chem. Sect.*, **71**, 522 (1950).
- (9) *Ibid.*, **72**, 688 (1951).
- (10) *Ibid.*, **72**, 990 (1951).

adsorbent is clear from the extremely high heat of sorption, and changes of the wave length of infrared absorption spectra accompanying the vibration of the OH bond in the molecules,<sup>11,12</sup> but observations of the loss factor for solids, having a moisture content to examine the restricted rotation of the OH dipoles are rather few in number, aside from the studies made by McIntosh and others. Takeda<sup>13</sup> has observed the dielectric dispersion of water sorbed on timbers, and discovered that the maximum loss factor,  $\epsilon''_{max}$ , was observed in the vicinity of 1000 Mc./sec., the maximum value shifting toward a higher frequency as the water content was increased. The same phenomenon was observed in the present study on silica gel sorbed water, and it is believed that success was obtained in clarifying to a certain extent the form of water vapor adsorbed by inorganic porous substances.

### Experimental

For the experiments, silica gel of 70 mesh or less was activated *in vacuo* at 250°. The sorption isotherms were obtained by measurements with a quartz spring balance at 25 and 35°. The dielectric cell consisted of two nickel coaxial cylinders covered by a glass receptacle, which could be joined to a vacuum system through a joint. The capacity of this cell in air was about 22  $\mu\text{f}$ .

The equipment for the measurement of the dielectric constant was a heterodyne beat apparatus in which the signal was supplied by a Hartley oscillator. Measurements were made at frequencies of 500 kc./sec. and 1 Mc./sec.

For measurements of the power factors ( $\tan \delta$ ), an electric bridge manufactured by the Yokogawa Electric Co. was used for the 1 kc./sec.-24 kc./sec. frequency range, while a Q-meter made by the same company and a resistance substitution type dielectric loss angle measurement apparatus made by the Riken Electric Instrument Co. were jointly used for the 80 kc./sec.-1 Mc./sec. frequency range. The amount of water sorbed on silica gel was not measured directly, but deduced from the isotherms, after causing the gel in the dielectric cell to reach the sorption equilibrium.

### Results

#### (1) Sorption Isotherms and Heat of Sorption.—

The sorption isotherms of silica gel at 25 and 35°,

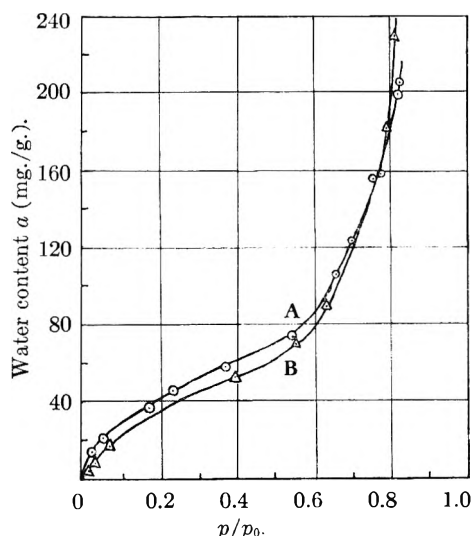


Fig. 1.—Isotherms of water-silica gel system: A, 25°; B, 35°.

(11) K. Kuratani, *Rep. Rad. Chem. Research Inst., Tokyo Univ.*, **3**, 14 (1948).

(12) R. Kawai, *Rep. Central Res. Lab. Hitachi*, 746 (1951).

(13) M. Takeda, *Bull. Chem. Soc. Japan*, **24**, 169 (1950).

shown in Fig. 1, indicate those of a sigmoid type. The moisture content  $a$  is shown by the amount of water in milligrams, adsorbed by 1 gram of dry silica gel. On the horizontal axis,  $p/p_0$  expresses the relative pressure, representing the ratio of the equilibrium water vapor pressure  $p$ , and the saturated vapor pressure of water  $p_0$  at the measuring temperature.

The differential heat of sorption can be obtained for each point on the isotherms shown in Fig. 1 by employing the Clapeyron-Clausius formula. If  $\bar{q}$  is taken to represent the difference between the differential heat of sorption and the heat of condensation in water, the relation between  $\bar{q}$  and  $a$  is as shown in Fig. 2. The first stage sorbed water indicates a heat of sorption higher by 10–20 kcal. than the heat of condensation, 9.7 kcal./mole for water, but this value decreases suddenly as the moisture content is raised, becoming several kilocalories in the moisture content range of 20–60 mg./g., and nearly coinciding with the heat of condensation of water in the vicinity of a moisture content of 100 mg./g. This indicates that sorbed water over this point is thermodynamically in the same state as liquid water.

(2) Surface Area of Silica Gel.—Examination as to whether Brunauer, Emmett and Teller's<sup>14</sup> theoretical formula of multimolecular layer adsorption conforms to the measured results as shown in Fig. 1 provides an useful reference for assuming the condition of the sorbed water. According to the BET formula, if  $a_m$  is the adsorbed amount of water necessary to form a monomolecular layer, we obtain the equation

$$p/a(p_0 - p) = 1/a_m c + \{(c - 1)/a_m c\}(p/p_0) \quad (1)$$

In the above,  $c$  is a constant. If formula 1 holds true, it follows that a linear relation should be obtained between  $p/a(p_0 - p)$  and  $p/p_0$ . Examination of the measured results shows that this linear relation clearly exists, as indicated in Fig. 3. The values  $a_m$  and  $c$  are obtained from this line. When  $a_m$  is obtained, the effective surface area of silica gel can be calculated from Emmett and Brunauer's formula,<sup>15</sup> yielding a value of approxi-

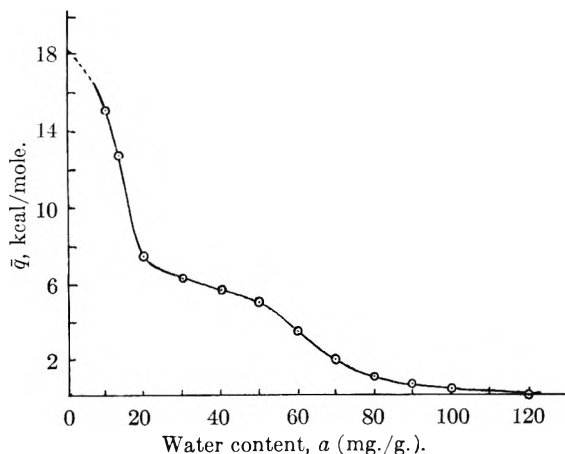


Fig. 2.—Differential heat of sorption.

(14) S. Brunauer, P. H. Emmett and E. Teller, *J. Am. Chem. Soc.*, **60**, 309 (1938).

(15) P. H. Emmett and S. Brunauer, *ibid.*, **59**, 1553 (1937).

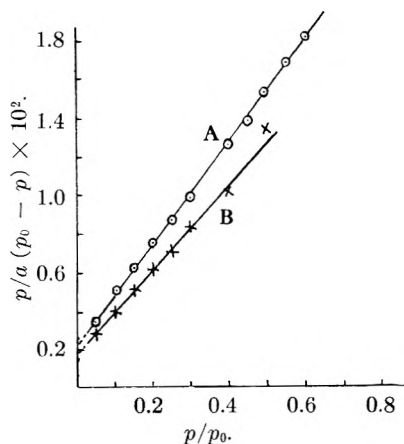


Fig. 3.—BET plots of sorption data: A, 35°; B, 25°.

mately 143 m.<sup>2</sup>/g. The surface area of silica gel recently has been obtained by Van Nordstrand and co-workers,<sup>16</sup> and the above value may be considered to be generally acceptable in point of order. When the value  $p/p_0$  is approximately 0.4 or less, the BET theory of multimolecular layer adsorption generally holds true, and it is believed that the sorption of water vapor may be safely taken as indicating the adsorption on the silica gel surface.

(3) **Differential Specific Polarization of Sorbed Water.**—Dry silica gel powder was placed within the dielectric cell previously described,<sup>8</sup> and tapped lightly to fill it solidly. The apparent specific gravity of silica gel is 0.37. Taking  $\epsilon_a$  as the apparent dielectric constant of this powder, the relation between  $\epsilon_a$  and the moisture content of the gel is presented in Fig. 4.

As may be seen from the above, the inclination of  $\partial\epsilon_a/\partial a$  indicates a sudden change with moisture contents of 15 and 94 mg./g. as dividing points. In a previous paper<sup>9</sup> reporting on the  $\epsilon$ - $a$  relation of vinyl polymers and condenser paper, it was stated that the  $\epsilon_a$ - $a$  relation of vinyl polymers is practically linear, showing no sudden changes in the  $\epsilon_a$ - $a$  relation, while a similar relation to present results has been obtained in the case of condenser paper. This is taken as a clear indication that sorbed water possessing different degrees of polarization is present. For the sake of explanation, we will divide the sorption condition into three stages, starting with the stage showing a low  $\partial\epsilon_a/\partial a$  gradient, namely, the first sorption stage (<15 mg./g.), second stage (15-94 mg./g.) and third stage (>94 mg./g.).

According to the Fuoss-Kirkwood theory,<sup>17</sup> the following relation exists between the specific polarization  $p_k$  of a substance and its dielectric constant  $\epsilon$ .

$$p_k = \frac{(\epsilon - 1)(2\epsilon + 1)}{9\epsilon} \frac{1}{\rho} \quad (2)$$

The increments  $\Delta\rho$ , and  $\Delta\epsilon$  of specific gravity and dielectric constant  $\rho$ ,  $\epsilon$  by the addition of an extremely small quantity of water  $\Delta w$ , g., having a polarization of  $p_w$  is expressed thus

(16) R. A. Van Nordstrand and co-workers, *THIS JOURNAL*, **55**, 621 (1951).

(17) R. M. Fuoss and J. G. Kirkwood, *J. Am. Chem. Soc.*, **63**, 385 (1941).

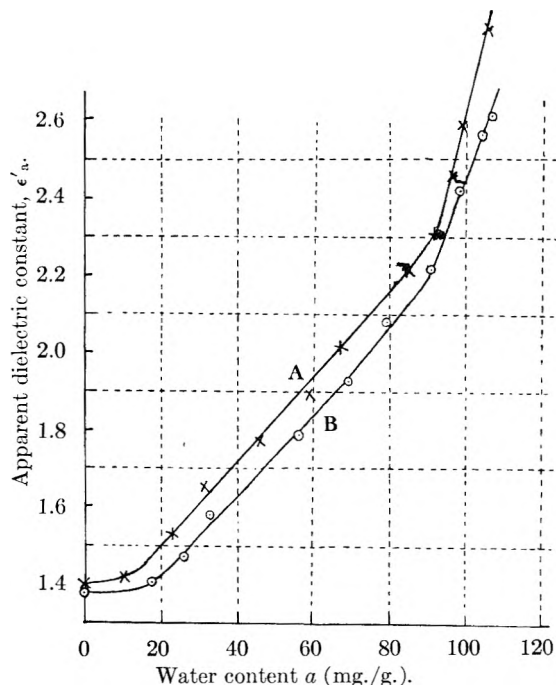


Fig. 4.—Relations between dielectric constants and sorbed amount of water (25°): A, 500 kc.; B, 1,000 kc.

$$p_w = \frac{1}{\rho\Delta w} \left\{ \frac{\partial p_k}{\partial \epsilon} \Delta\epsilon + \frac{\partial p_k}{\partial \rho} \Delta\rho \right\} \quad (3)$$

$$= \frac{1}{\rho\Delta w} \left\{ \frac{(2\epsilon^2 + 1)\Delta\epsilon}{9\epsilon^2} - \frac{(\epsilon - 1)(2\epsilon + 1)}{9\epsilon\rho^2} \Delta\rho \right\} \quad (4)$$

In the case of water, the second term of formula 4 is a value that may be neglected by approximation. Hence

$$p_w \approx \frac{2\epsilon^2 + 1}{9\epsilon^2\rho} \frac{\Delta\epsilon}{\Delta w} \quad (5)$$

Expressed as a differential equation, the differential specific polarization  $\bar{p}_w$  is shown as

$$\bar{p}_w = \frac{2\epsilon^2 + 1}{9\epsilon^2\rho} \frac{\partial\epsilon}{\partial w} \quad (6)$$

The differential specific polarization of sorbed water on silica gel can be calculated from the apparent dielectric constant  $\epsilon_a$ , and the apparent specific gravity  $\rho_a$ , which may be used instead of  $\epsilon$  and  $\rho$ , respectively, to obtain the differential specific polarization  $\bar{p}_w$  of adsorbed water. The differential specific polarizations of water adsorbed on the gel are listed in Table I.

TABLE I  
DIFFERENTIAL SPECIFIC POLARIZATION OF ADSORBED WATER

|                    | Water content, $a$ (mg./g.) | $\bar{p}_w$ |            |
|--------------------|-----------------------------|-------------|------------|
|                    |                             | 1 Mc./sec.  | 5 kc./sec. |
| 1st sorption stage | 0 ~ 15                      | 1.15        | ~ 1        |
| 2nd sorption stage | 20                          | 7.50        | ~ 8        |
|                    | 50                          | 7.02        | ~ 11       |
|                    | 80                          | 7.39        | ~ 9        |
| 3rd sorption stage | 93                          | 23.0        | ~ 23       |
|                    | 100                         | 22.2        |            |

(4) **Dielectric Losses of Water-Sorbed Gel.**—The apparent dielectric constant and loss factor

of moist silica gel were measured over a frequency range of 2-1,000 kc./sec. The results, shown in Fig. 5, indicate that water-sorbed silica gel in the 3rd sorption stage shows a maximum apparent loss factor  $\epsilon_a''$  between several kilocycles and ten-plus-several kilocycles. It was also observed that the maximum point shifts toward higher frequencies as the moisture content is increased.

Discussion

The specific polarization of sorbed water in the first sorption stage, as shown in Table I, shows a value in the vicinity of 1, and is very small. Water in gas phase, or in dissolved state in non-polar solvents shows a specific polarization of approximately 4, while similar values are obtained for water vapor adsorbed on organic high polymers. In the case of liquid water, with a more strongly developed hydrogen bond than the above, the value should be 17.7. The fact that sorbed water in the first sorption stage shows such a comparatively low polarization seems to suggest that the water molecules are firmly bound to the surface of silica gel. The fact that the value  $\epsilon_a''$  for gel having a moisture content of 15 mg./g. or less is nearly zero throughout the entire frequency range seems to prove the above assumption.

Adsorbed water in the second sorption stage possesses a specific polarization of approximately 8-11, which is somewhat higher than that of water molecules in the form of vapor or in dissolved state. Moreover, the value  $\epsilon_a''$  steadily increases as the frequency is lowered, and may be considered to increase until the frequency is decreased to fifty cycles, as has been observed by Brake-Schütze (1935) on timbers adsorbed water, leading to the belief that the loss is caused by ion conduction. It may be concluded therefore that adsorbed water in the second sorption stage does not possess a fixed time constant, and that interaction among the sorbed water molecules is slight, with different degrees of freedom in the dipole rotation of each molecule and a wide distribution of relaxation time.

The  $\epsilon_a''$  value of adsorbed water in the third sorption stage indicates a very distinctive tendency, which is very interesting when considering the state of sorbed water in excess of this stage. The maximum  $\epsilon_a''$  value occurs in the neighborhood of 10 kc./sec., and this phenomenon, indicating that the sorbed water possesses a fixed time constant, may be interpreted in two different ways. One method is to consider that the OH dipoles of the sorbed water have a restricted rotation. Takeda<sup>12</sup> assumes the relaxation time of the OH dipole rotation of sorbed water in timbers to be  $1.9-1.3 \times 10^{-10}$  sec. at a water content of 10-20%, resulting in an  $\epsilon''_{max}$  value at 840-1230 Mc./sec., and presumes a restricted rotation of the dipoles. Inasmuch as the same tendency is observed in the case of third stage sorbed water on silica gel, a similar explanation should hold true. Sorbed water in the third sorption stage is in a strongly bound condition, and since its specific polarization is ever greater than the 17.7 for liquid water, it is considered to have a much more strongly developed hydrogen bond than liquid water, the molecules being

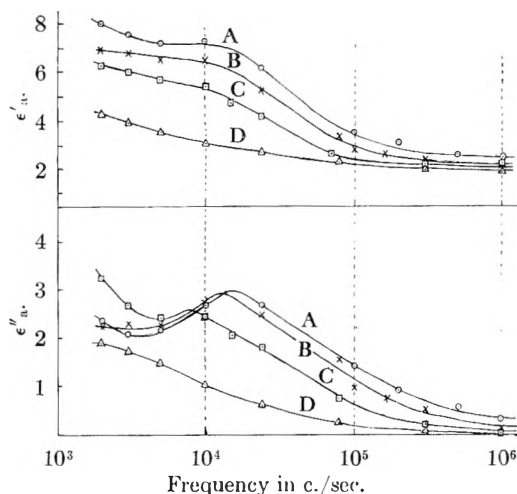


Fig. 5.—Upper part, dielectric constant; lower part, loss factor;  $\epsilon'_a$  and  $\epsilon''_a$  of water-sorbed silica gel at 12°: A, a = 143 mg./g.; B, 107; C, 93; D, 85.

oriented to some extent into a condition close to that of ice. According to results of experiments by Humbel, Jona and Scherrer<sup>18</sup> on a single crystal of ice, the  $\epsilon''_{max}$  value of ice at 0° is believed to occur in the vicinity of 20 kc./sec. The fact that the maximum points in the case of sorbed water in the third sorption stage also occur at nearly the same frequencies supports this assumption.

The second explanation is based on the formation of capillary condensed water. In this case, sorbed water is believed to condense as bulk water within the capillaries of silica gel, forming a different phase in relation to the silica gel, and causing the maximum  $\epsilon_a''$  value to occur. Examination of the surface of silica gel under an electron microscope reveals the presence of innumerable circular orifices showing that the capillaries of silica gel are mainly of the pinhole type. Consequently, the shape of the capillary condensed water may be approximated as elongated rotational ellipsoids, to which the Sillars<sup>19</sup> theory of the binary aggregate of dielectrics can be applied.

Using the Sillars theory as a binary aggregate model for silica gel and capillary condensed water, we obtain

$$\epsilon'_a = \epsilon_{a\infty} + \epsilon'_{a0}N/(1 + \omega^2\tau^2) \tag{7}$$

$$\epsilon''_a = \epsilon''_{a0}N\omega\tau/(1 + \omega^2\tau^2) \tag{8}$$

$$N = Vn^2\epsilon''_{a0}/\{\epsilon'_{a0}(n - 1) + \epsilon'_w\} \tag{9}$$

$$\tau = \{\epsilon'_{a0}(n - 1) + \epsilon'_w\}/4\pi\sigma_w \tag{10}$$

$$\epsilon_{a\infty} = \epsilon'_{a0}[1 + nV(\epsilon'_w - \epsilon'_{a0})/\{\epsilon'_{a0}(n - 1) + \epsilon'_w\}] \tag{11}$$

Where  $\epsilon'_{a0}$  represents the apparent dielectric constant of cumulated silica gel powder with no condensed water,  $\tau$  the relaxation time,  $V$  the volume fraction of condensed water in cumulated gel powder (including the air spaces between the particles of gel),  $\epsilon'_w$ ,  $\sigma_w$  the dielectric constant and specific conductivity of the condensed water, and  $n$  the form constant, which is a function of the axial ratio when the condensed water is considered as a rotational ellipsoid.  $\epsilon_{a\infty}$  is the apparent dielectric constant at the infinite frequency.

(18) F. Humbel, F. Jona and P. Scherrer, *Helv. Phys. Acta*, **26**, 17 (1953).

(19) R. W. Sillars, *J. Inst. Elec. Eng.*, **80**, 378 (1937)

As may be seen from formula 10, the higher the  $n$  value (that is, the longer and thinner the shape of the condensed water), and the smaller the  $\sigma_w$  value, the lower the frequency at which the maximum  $\epsilon_a''$  value is obtained. Again, when the frequency is sufficiently high ( $\omega\tau \gg 1$ ) and the value  $n$  is extremely great, formula 12 is obtained from formulas 7 and 11

$$\epsilon_a' \approx \epsilon_{a0}' + V(\epsilon_w' - \epsilon_{a0}') \quad (12)$$

This agrees with the formula used by Higuti and others<sup>20</sup> in obtaining the dielectric constants of sorbed substances. Application of formula 12 for calculation of third stage sorbed water on silica gel yields a  $\epsilon_w'$  value of approximately 90. In order to determine whether the measured results shown in Figs. 4 and 5 fulfill Sillars' formula above described, we will first take  $\epsilon_{a0}'$  as the  $\epsilon_a'$  value of 2.26 for  $a = 94$  mg./g. in the results shown for 1 Mc./sec. in Fig. 4. Since  $\epsilon_a'$  is 2.62 for a water content of 107 mg./g., and the apparent specific gravity of dry silica gel is 0.37, we obtain  $V \approx 0.0048$ , considering that the specific gravity of condensed water is generally equal to that of liquid water. Taking the dielectric constant of sorbed water to be the same as that for liquid water, we obtain from formula 11 the form constant value  $n \approx 600$ . Separately, using the value 4.2 representing the difference of  $\epsilon_a'$  before and after dispersion at 107 mg./g., as shown in Fig. 5, the value  $n$  can be obtained by employing formulas 7 and 9. Since  $\epsilon_a' - \epsilon_{a\infty}' \approx 4.2$  when  $\omega\tau = 0$ ,  $N \approx 1.86$ . Taking  $\epsilon_w' = 80$ , and introducing the value  $N$  into formula 9, we obtain  $n \approx 400$ . In any case, the fact that  $n$  indicates a high value of several hundred shows that the axial ratio of the condensed water is 40–50, indicating a long and narrow shape. Moreover, as the  $\epsilon_{a\max}''$  for this water content occurs at 13 kc./sec. (Fig. 5), the value  $\tau = 1.22 \times 10^{-5}$  sec. Consequently, if  $n = 600$ , from formula 10,  $\sigma_w = 9.3 \times 10^5$  e.s.u. or  $1 \times 10^{-6}$  mho; if  $n = 400$ ,  $0.7 \times 10^{-6}$  mho. These coincide, respectively, with the specific conductivity of water distilled in vacuum, or that of ice.

We may calculate the maximum value of  $\epsilon_a''$

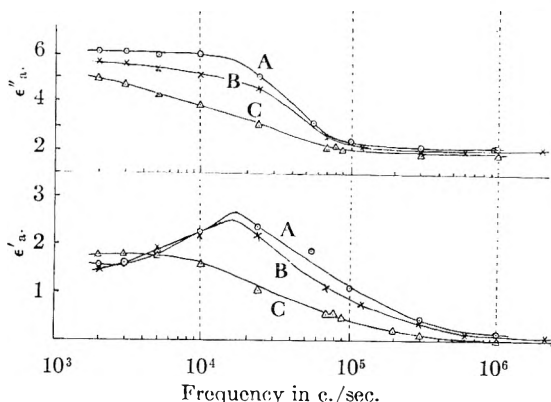


Fig. 6.—Upper part, dielectric constant; lower part, loss factor;  $\epsilon_a'$  and  $\epsilon_a''$  of water-sorbed silica gel containing NaCl (12°): A,  $a = 132$  mg./g.; B, 102; C, 86.

(20) I. Higuti, *Bull. Inst. Phys. Chem. Res. Japan*, **20**, 489 (1941); G. H. Argue and O. Mauss, *Can. J. Research*, **B13**, 156 (1935).

This can be obtained by including the values  $\omega\tau = 1$  and  $N = 1.86$  into the right side of formula 8, yielding a calculated value of 2.1. The observed value shown in Fig. 5 is slightly higher, being approximately 2.8, but since the  $\epsilon_a''$  of silica gel at the beginning of condensation of its water (at  $a = 94$  mg./g., 13 kc./sec.) requires a value of approximately 1, it will be seen that the observed value closely matches the calculated value when this value is subtracted.

As is clear from the above calculations, a quantitative explanation of the observed results can be made easily and readily if the adsorbed water in excess of 94 mg./g. is considered to exist in a phase having the same dielectric constant, specific gravity and electroconductivity as liquid water. This supposition is further borne out by the fact that the heat of adsorption begins to coincide with the heat of condensation of water starting at about this point.

However, this does not mean that adsorbed water in the third sorption stage can be identified as liquid water, because its specific polarization is higher than that of liquid water. In order to further examine the physico-chemical properties of so-called condensed water, the following experiment was carried out.

Activated silica gel was immersed in a 0.01  $N$  solution of NaCl and dried *in vacuo* at 250°. This desiccated material was allowed to absorb moisture and the same measurements as shown in Fig. 5 were made. If condensed water were identical with ordinary liquid water, it would dissolve the NaCl on the surface of the gel; consequently, the  $\sigma_w$  value would increase and the maximum point of  $\epsilon_a''$  in the gel having a water content corresponding to the third sorption stage should appear on a much higher frequency than shown in Fig. 5. However, the observed results, as shown in Fig. 6, indicated practically no change in the frequency, proving that so-called capillary condensed water exists in such a condition that is not able to dissolve an electrolyte. This fact, coupled with the observation that the polarization of adsorbed water in the third sorption stage is much stronger than that of liquid water, is believed to suggest that capillary condensed water is water in a more solid state than liquid water, and that it possesses characteristics approaching those of ice. This conclusion, in effect, is the same as that derived from the explanation based on restricted dipole rotation described earlier in this article.

Also, in Fig. 5, the maximum  $\epsilon_a''$  value is seen to shift gradually toward a higher frequency as the water content in the third sorption stage is increased. This is probably due to the fact that the average form constant  $n$  becomes smaller because of the condensation of water in capillaries of large diameter, which, according to formula 10, causes the value  $\tau$  to decrease gradually.

**Acknowledgment.**—The author is indebted to Dr. Rinjiro Kawai of the Central Research Laboratory for his guidance and helpful advice, and to Prof. Y. Toriyama of Tohoku University for his encouragement throughout this work.

## HYDROLYTIC BEHAVIOR OF METAL IONS. III. HYDROLYSIS OF THORIUM(IV)<sup>1</sup>

BY KURT A. KRAUS AND ROBERT W. HOLMBERG

*Oak Ridge National Laboratory, Chemistry Division, Oak Ridge, Tenn.*

*Received October 30, 1953*

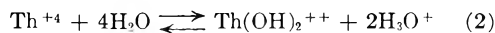
Hydrolysis of thorium(IV) in perchlorate and chloride solutions ( $\mu = ca. 1$ ) was studied potentiometrically with a glass-calomel electrode system as a function of thorium concentration ( $2.5 \times 10^{-4}$  to  $1.5 \times 10^{-2} M$ ) and acidity. The existence of the unhydrolyzed species  $Th^{+4}$  was confirmed. The hydrolytic reactions up to a hydroxyl number (average number of hydroxide ions per thorium)  $n = ca. 2$  were found to be readily reversible. The hydrolysis of thorium(IV) is concentration dependent, even in the early stages of hydrolysis. Even for  $n < 0.5$  several hydrolysis products must be postulated to explain the data. Of these, the species  $Th(OH)_2^{+2}$  and  $Th_2(OH)_2^{+6}$  seem to be definitely established, and estimates of their stability constants are given. The equilibrium constant for the reaction,  $Th^{+4} + 2H_2O \rightleftharpoons ThOH^{+3} + H_3O^+$ , was found to be surprisingly small ( $ca. 5 \times 10^{-5}$ ) compared with the constants for  $U^{+4}$  and  $Pu^{+4}$  ( $ca. 3 \times 10^{-2}$ ) and could not be established with certainty. Other species including higher polymers probably are formed during the hydrolysis. The thorium ion or a polymer of it ( $(Th(OH)_2)_x^{+2}$ ) does not show great stability. Hydrolytically thorium(IV) appears to be sufficiently different from  $U(IV)$  and  $Pu(IV)$  to make it questionable if it should be included in the same rare-earth-like series (actinide or thoride).

It has been shown that uranium(IV)<sup>2,3</sup> and plutonium(IV)<sup>2,4</sup> can exist as the hydrated and unhydrolyzed ions  $M^{+4}$  (or  $M(H_2O)_z^{+4}$ ) in acidic solutions and that their initial hydrolysis occurs according to the equilibrium



with equilibrium constants 0.032 ( $U^{+4}$ )<sup>2</sup> and 0.025 ( $Pu^{+4}$ )<sup>2,5</sup> at ionic strength  $\mu = 0.5$ . Since thorium has been considered a member of the same rare-earth-like series (actinide or thoride<sup>6</sup>), comparison of its hydrolytic properties with those of the other members of the series was of interest to determine if strict interpretation of a "rare-earth" hypothesis is supported by the behavior of the ions in aqueous solutions.

There is considerable disagreement in the literature regarding the mechanism of hydrolysis of  $Th(IV)$ . Kasper<sup>7</sup> concluded from measurements of the hydrogen ion concentrations of thorium nitrate solutions that the first step in the hydrolysis follows eq. 1, and estimated an equilibrium constant of  $ca. 4 \times 10^{-4}$ . However, his experiments were not carried out with sufficient precision or over a sufficiently wide range of conditions to establish this mechanism definitely. Chauvenet, Tonnet and Souteyrand-Franck<sup>8,9</sup> had earlier concluded from conductivity and thermochemical measurements of thorium chloride and thorium nitrate solutions that the principal hydrolytic reaction is



(1) This document is based on work performed for the Atomic Energy Commission at the Oak Ridge National Laboratory. This paper was presented in part at the Chicago Meeting of the American Chemical Society, 1950. Previous communication: K. A. Kraus and J. S. Johnson, *J. Am. Chem. Soc.*, **75**, 5769 (1953).

(2) K. A. Kraus and F. Nelson, *ibid.*, **72**, 3901 (1950).

(3) R. H. Betts and R. M. Leigh, *Can. J. Research*, **28B**, 514 (1950). See also (17).

(4) K. A. Kraus, "National Nuclear Energy Series," Div. IV, Vol. 14B, No. 3.16, McGraw-Hill Book Co., Inc., New York, N. Y., 1949.

(5) S. W. Rabideau and J. F. Lemons, *J. Am. Chem. Soc.*, **73**, 2895 (1951).

(6) For a summary, see G. T. Seaborg, *Nuclonics*, **5**, November 16 (1949).

(7) J. Kasper, Ph.D. Dissertation, The Johns Hopkins University, Baltimore, Md. (1941).

(8) E. Chauvenet and J. Tonnet, *Bull. soc. chim. (France)*, [4] **47**, 701 (1930).

(9) E. Chauvenet and Souteyrand-Franck, *ibid.*, **47**, 1128 (1930).

or



No equilibrium constant was given. Schaal and Faucher<sup>10</sup> concluded from pH measurements of partially neutralized thorium nitrate and thorium perchlorate solutions of various degrees of dilution that the tetramer  $Th_4O_4^{+8}$  is formed over a considerable range of hydrolysis. Souchay<sup>11</sup> gave supporting evidence for this tetramer on the basis of measurements of freezing point depressions. He also concluded that on further hydrolysis no other simple species is formed and that continuing polymerization takes place.

### Experimental

Anhydrous thorium tetrachloride was prepared from the metal by a procedure of Newton and Johnson.<sup>12</sup> The metal was converted to the hydride, which was converted to  $ThCl_4$  with dry HCl gas at  $ca. 350^\circ$ . It was purified by vacuum ( $< 10^{-4}$  mm.) sublimations. Only the well crystallized portions of the sublimate were used. The material was loaded into weighed small glass bulbs in a dry-box under a dry ( $Mg(ClO_4)_2$ ) nitrogen atmosphere. The ampoules were sealed and again weighed.

Purity was checked by gravimetric determination of the  $Th-Cl$  ratio (found  $3.98 \pm 0.03$ ) and by comparing (potentiometrically) the amount of acid liberated by successive sublimates dissolved in dilute  $HClO_4$  ( $\mu = 1$ ). The latter method is particularly convenient and sensitive since less than 1% hydroxide or oxide impurity yields considerable potential differences if the salt is dissolved in  $ca. 10^{-3} M$  acids to give  $ca. 10^{-2} M$   $Th(IV)$  solutions. If the second and third sublimates liberated the same amount of acid, they were assumed free of oxides and used in the measurements.

The degree of hydrolysis of  $Th(IV)$  at a supporting electrolyte concentration 1  $M$  (1  $M$   $HClO_4-NaClO_4$  or 1  $M$   $HCl-KCl$  mixtures) was determined, either by breaking ampoules of  $ThCl_4$  in solutions of known initial acidity or by adding to such solutions aliquots of  $ThCl_4$  stock solutions (0.015  $M$   $Th(IV)$ ) of known acidity and 1  $M$  supporting electrolyte concentration. Additions were made after the potential of a glass-calomel electrode system had become constant. The change in potential  $\Delta E$  was noted. The degree of hydrolysis was calculated from the potential change. In addition, some acid-base titrations were also carried out.

The acidities were measured with the automatically re-

(10) R. Schaal and J. Faucher, *ibid.*, **14**, 927 (1947); *Compt. rend.*, **225**, 118 (1947).

(11) P. Souchay, *Bull. soc. chim. (France)*, **15**, 143 (1948).

(12) A. S. Newton and O. Johnson, U. S. Patent 787,850; *Official Gaz. U. S. Pat. Office*, **651**, 615 (1951); *C. A.*, **46**, 7723e (1952).

cording vibrating reed electrometer previously described.<sup>13</sup> The Brown recorder had a full scale sensitivity of 1 mv. "Bucking potential" was supplied with a Leeds and Northrup type K potentiometer. The reference calomel half cells, which were made with saturated NaCl rather than KCl to prevent precipitation of KClO<sub>4</sub>, were mounted in small jacketed flasks and water (25 ± 0.05°) was pumped through the jackets. The measuring vessel, a deep beaker fitted with the electrodes, was immersed through a cover into a large Dewar flask through which the same thermostated water was pumped.

In many experiments two glass electrodes were used to estimate the reliability of the measurements. The standard deviation in the measurements of the potential differences was ca. 0.04 mv. and most of the larger deviations occurred when one electrode had not reached a completely constant potential. The electrode system was calibrated frequently with standardized 0.01 and 0.001 *M* acids at  $\mu = 1.00$ .

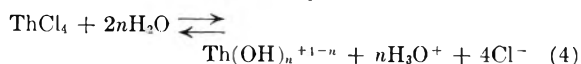
C.p. HClO<sub>4</sub>, HCl and KCl were used without further purification. The acids were titrated with NaOH, which was standardized with potassium acid phthalate. Sodium perchlorate was prepared by neutralizing HClO<sub>4</sub> with C.p. NaOH, filtering, acidifying to pH ca. 5 and flushing with nitrogen to remove carbon dioxide. The solutions were reacidified and flushed again, if necessary, to keep possible errors from carbonates to a minimum. The acidity of these solutions was estimated potentiometrically with the same electrode system used in the hydrolysis measurements.

## Results and Discussion

**1. Determination of the Hydroxyl Number. Identification of the Species Th<sup>+4</sup>.**—When thorium tetrachloride is dissolved in slightly acidic solutions of initial acidity  $h_1$ , the acidity increases to an equilibrium value  $h$  due to acid liberation from partial thorium hydrolysis. From this acid change and the total (stoichiometric) thorium concentration  $t$  the average number of moles of hydroxide ions per mole of thorium (hydroxyl number  $n$ ) can be determined by the equation

$$n = (h - h_1)/t \quad (3)$$

since the stoichiometry of the solution reaction can be described by the equation



Eq. 3 applies only if a pure salt is dissolved. When thorium is introduced as an acidic stock solution, computation of  $n$  also involves a correction for the amount of "free" acid (beyond the composition MX<sub>4</sub>) added.

The acid change  $\Delta h = h - h_1$  and  $h$  were calculated from  $h_1$  and the potential changes  $\Delta E$  of the glass-calomel electrode assembly by the equation

$$\log h/h_1 = (\Delta E - e)/S \quad (5)$$

where  $S$  is an empirically determined slope of  $E$  vs.  $\log h$  and where  $e$  is a correction term involving changes in activity coefficients of hydrogen ions and in liquid junction potentials due to the addition of the thorium salt. The slope  $S$  will be close to the "Nernst" slope ( $2.303RT/nF = 59.15$  mv.) if the electrode system acts as a perfect hydrogen electrode and if the concentration of the bulk electrolyte is so large compared to the acid and thorium concentrations that changes in activity coefficients and liquid junction potentials are negligible. The slope  $S$ , which was constant to ±0.1 mv. for any one glass electrode, was found to be in the neighborhood of 59.5 mv. for 1 *M*

HClO<sub>4</sub>-NaClO<sub>4</sub> and HCl-KCl solutions in the acid range 10<sup>-2</sup> to 10<sup>-3</sup> *M* H<sub>3</sub>O<sup>+</sup>.

The correction term  $e$  was assumed independent of the degree of hydrolysis and was evaluated from the observed potential changes on dissolution of ThCl<sub>4</sub> under conditions where hydrolysis appeared negligible. A typical series of experiments is shown in Fig. 1, where  $\Delta E$  for 1.5 × 10<sup>-2</sup> *M* ThCl<sub>4</sub> solutions in 1 *M* HClO<sub>4</sub>-NaClO<sub>4</sub> mixtures is plotted as a function of initial acidities  $h_1$ . With increasing acidity  $\Delta E$  first decreases rapidly and then approaches a constant value of 1.01 mv. at high acidities. This value was taken to be equal to  $e$  at this thorium concentration. Similarly  $e$  was evaluated at different thorium concentrations  $t$  (from 10<sup>-3</sup> to 2 × 10<sup>-2</sup> *M*) and was found to be proportional to  $t$ . The average values  $e/t = 68$  mv. for the HClO<sub>4</sub>-NaClO<sub>4</sub> solutions and  $e/t = 55$  mv. for the HCl-KCl solutions were obtained at a supporting electrolyte concentration of 1 *M*.

Although evaluation of  $e$  is necessary for an accurate determination of the degree of hydrolysis, its value is small enough to permit the conclusion that the principal uncomplexed species of Th(IV) in acidic solutions is Th<sup>+4</sup>. Setting the limiting value of  $\Delta E$  at high acidity equal to  $e$ , yields (for 0.015 *M* Th(IV) solution) the values of  $n$  shown in Fig. 1, while neglect of  $e$  (i.e., setting tentatively  $\log h/h_1 = \Delta E/S$ ) yields the values  $n^*$  also shown in Fig. 1. The latter reach the very low value of  $n^* = 0.03$  in ca. 10<sup>-2</sup> *M* H<sub>3</sub>O<sup>+</sup>, clearly indicating negligible hydrolysis of Th(IV) in acidic solutions. Similar low apparent degrees of hydrolysis in acidic solutions are obtained throughout the concentration range studied (2.5 × 10<sup>-4</sup> to 1.5 × 10<sup>-2</sup> *M*). One can thus conclude that Th<sup>+4</sup> is the principal species in perchlorate solutions if negligible complexing by perchlorate ions is assumed.<sup>14</sup> Similarly, since thorium forms only weak chloride complexes,<sup>15,16</sup> Th<sup>+4</sup> is probably the principal species in the ThCl<sub>4</sub>-perchlorate solutions studied here.

The existence of the species Th<sup>+4</sup> has been repeatedly assumed (see, e.g., ref. 7) and additional strong evidence for it based on solvent extraction experiments with thenoyltrifluoroacetone (TTA) was recently reported.<sup>17</sup> Regarding the existence of the species M<sup>+4</sup> in moderately acidic solutions, Th(IV) is thus similar to U(IV) and Pu(IV).

(14) This species is hydrated, i.e., Th(H<sub>2</sub>O)<sub>*x*</sub><sup>+4</sup>. The assignment  $x = 8$  for the coordination number appears reasonable since thorium has this coordination number with respect to oxygen in certain solids (e.g., oxides—W. H. Zachariassen (see ref. 22); basic salts—G. Lundgren and L. G. Sillén (see ref. 25)).

(15) R. A. Day and R. W. Stoughton, *J. Am. Chem. Soc.*, **72**, 5662 (1950); W. C. Waggener and R. W. Stoughton, *This Journal*, **56**, 1 (1952).

(16) E. L. Zebrowski, II, Walter and F. K. Heumann, *J. Am. Chem. Soc.*, **73**, 5646 (1951).

(17) Zebrowski, *et al.*, (ref. 16) demonstrated that the extraction of thorium follows approximately a fourth power dependence on acidity and TTA concentration and stated that the "data (are) considered to be in satisfactory agreement with the expected fourth power hydrogen ion activity dependence . . ." for Th<sup>+4</sup>. They apparently realized that this type of experiment does not conclusively establish the species Th<sup>+4</sup>, but only makes it highly probable since other ions of charge plus 4 (e.g., the polymeric species Th<sub>2</sub>(OH)<sub>4</sub><sup>+4</sup>) would give similar results if such species were extracted into the TTA-benzene phase.

(13) K. A. Kraus, R. W. Holmberg and C. J. Borkowski, *Anal. Chem.*, **22**, 341 (1950).

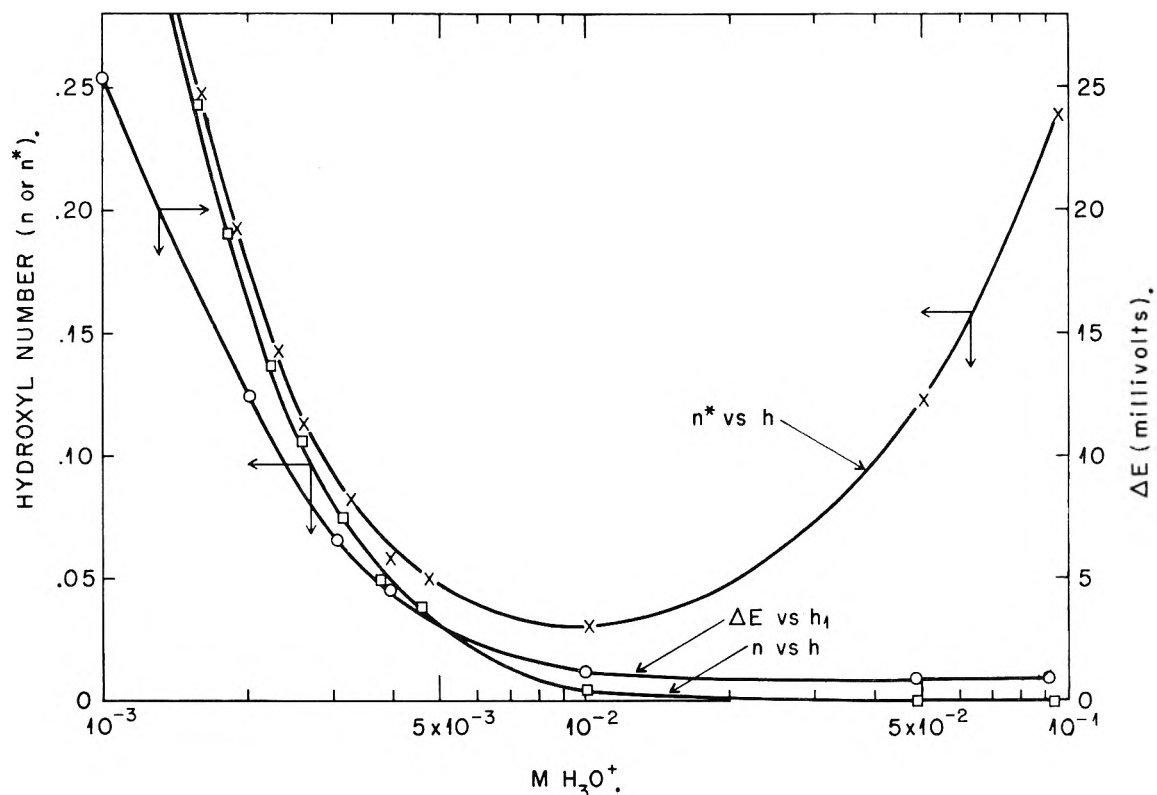


Fig. 1.—Effect of correction term on apparent hydroxyl numbers.

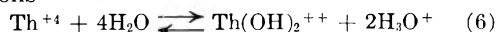
However, thorium differs from these elements in the  $pH$  range in which hydrolysis occurs and in the mechanism of hydrolysis, as will be discussed below.

**2. Reversibility of Hydrolytic Reactions.**—When  $\text{ThCl}_4$  is dissolved in slightly acidic media, a rapid potential change occurs. Steady state potentials are usually reached within a few minutes and no drifts are apparent over a period of several days. Equilibrium is thus rapidly established for the small hydroxyl numbers, which can readily be reached by this technique (see Table I). Furthermore, solutions with initial hydroxyl number  $n = ca. 2^{18}$  ( $t = 1.5 \times 10^{-2}$ ,  $1 M \text{HClO}_4\text{-NaClO}_4$ ) were titrated with  $\text{HClO}_4$  and back-titrated with  $\text{NaOH}$ . The solutions were clear for  $n < 2$ . The titrations (weight burets) were carried out with relatively concentrated acids and bases to avoid significant dilution of the solutions. The hydroxyl numbers for both types of titrations (Table I) agreed with each other and with those determined by dissolving samples of  $\text{ThCl}_4$ .

$\text{Th(IV)}$  differs greatly from  $\text{Pu(IV)}$  in the large hydrolysis range in which equilibrium is rapidly established.  $\text{Pu(IV)}$  near  $n = ca. 0.5^4$  apparently forms polymeric products which are only slowly depolymerized, even under extreme conditions (*e.g.*, with relatively concentrated nitric acid). Similarly, polymerization of  $\text{U(IV)}$ , although oc-

curing less readily than that of  $\text{Pu(IV)}$ , appears highly irreversible.<sup>19</sup>

**3. Hydrolysis in Perchlorate Solutions.**—Hydrolysis of  $\text{Th(IV)}$  in the concentration range  $2.5 \times 10^{-4}$  to  $1.5 \times 10^{-2}$  was studied in  $1 M \text{HClO}_4\text{-NaClO}_4$  mixtures by the dissolution and dilution techniques described in the experimental section and by acid-base titrations. The results are summarized in Table I. The data obtained by the dissolution techniques were satisfactory at higher concentrations. They scattered considerably at lower concentrations and hence for these only the more reproducible dilution experiments are recorded. Hydrolysis of  $\text{Th(IV)}$  was found to become appreciable near  $pH 3$ , in agreement with earlier work<sup>7,20</sup> and to be strongly dependent on the thorium concentration. From that dependence of  $n$  on  $t$ , one can conclude that monomeric hydrolysis products (*e.g.*,  $\text{ThOH}^{+3}$  or  $\text{Th(OH)}_2^{+2}$ ) are not sufficient to explain the data. As shown in Fig. 2, for low values of  $n$  ( $n < ca. 0.4$ , Region I),  $\log n$  varies approximately linearly with  $\log h$  with slope *ca.*  $-2$ . Thus, in this region the principal hydrolysis reactions probably involve the formation of two moles of hydrogen ions per mole of hydrolysis products as, *e.g.*, in the equations



(19) K. A. Kraus, F. Nelson and G. L. Johnson, *J. Am. Chem. Soc.*, **71**, 2510 (1950); K. A. Kraus and F. Nelson, *ibid.*, **72**, 3901 (1950).

(20) Recently J. Rydberg (*Acta Chem. Scand.*, **4**, 1503 (1950)) measured equilibria of  $\text{Th(IV)}$  with acetylacetonone and found negligible effect from thorium hydrolysis up to  $pH 6$ . This is in definite disagreement with the work reported here and apparently was in disagreement with work by Hietanen and Sillén, quoted by Rydberg as a private communication.

(18) These solutions were prepared by W. C. Waggner of the ORNL Chemistry Division from "thorium oxyperchlorate" samples obtained by fuming perchloric acid solutions of  $\text{Th(IV)}$  to dryness. The initial hydroxyl numbers were determined potentiometrically by determining the amount of acid consumed in bringing the solutions to *ca.*  $10^{-2} M \text{H}_3\text{O}^+$ .

and

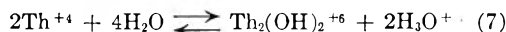


TABLE I

HYDROXYL NUMBERS  $n$  OF Th(IV) AS A FUNCTION OF ACIDITY  $h$  AND Th(IV) CONCENTRATION  $t$  IN 1 M NaClO<sub>4</sub>-HClO<sub>4</sub> MIXTURES

| A. Dissolution Experiments                 |                   |                           |                   |  |                   |  |       |
|--|-------------------|---------------------------|-------------------|--|-------------------|--|-------|
| $h \times 10^3$                            | $h_1 \times 10^3$ | $\Delta E, \text{mv.}$    | $n$               | $h \times 10^3$                            | $h_1 \times 10^3$ | $\Delta E, \text{mv.}$                     | $n$   |
| $t = 1.50 \times 10^{-2}$                  |                   |                           |                   | $t = 2.00 \times 10^{-2}$                  |                   |  |       |
| 4.36                                       | 3.806             | 4.52                      | 0.037             | 1.790                                      | 1.671             | 1.91                                       | 0.060 |
| 3.79                                       | 3.058             | 6.54                      | .049              | 1.216                                      | 1.008             | 4.98                                       | .104  |
| 3.144                                      | 2.018             | 12.47                     | .075              | 1.238                                      | 1.013             | 5.31                                       | .112  |
| 2.593                                      | 1.008             | 25.42                     | .106              | 0.868                                      | 0.457             | 16.73                                      | .205  |
| 2.223                                      | 0.173             | 66.96                     | .137              | .768                                       | .295              | 24.87                                      | .236  |
| 2.216                                      | .169              | 67.55                     | .136              | .671                                       | .050              | 67.22                                      | .311  |
| 2.154                                      | .083              | 85.28                     | .138              | $t = 1.00 \times 10^{-3}$                  |                   |  |       |
| $t = 7.00 \times 10^{-3}$                  |                   |                           |                   | 1.122                                      | 1.024             | 2.43                                       | 0.10  |
| 3.587                                      | 3.362             | 2.13                      | 0.032             | 1.110                                      | 1.015             | 2.39                                       | .10   |
| 2.517                                      | 2.075             | 5.47                      | .063              | 0.815                                      | 0.660             | 5.55                                       | .16   |
| 1.809                                      | 1.013             | 15.45                     | .114              | .876                                       | .706              | 5.62                                       | .17   |
| 1.782                                      | 0.962             | 16.33                     | .117              | .698                                       | .497              | 8.85                                       | .20   |
| 1.431                                      | .219              | 49.02                     | .175              | .672                                       | .459              | 9.93                                       | .21   |
| 1.396                                      | .079              | 74.71                     | .188              | .552                                       | .248              | 20.69                                      | .30   |
|  |                   |                           |                   | .501                                       | .135              | 33.97                                      | .37   |
|  |                   |                           |                   | .499                                       | .108              | 39.59                                      | .39   |
|  |                   |                           |                   | .480                                       | .074              | 48.26                                      | .41   |
| B. Dilution Experiments                    |                   |                           |                   |  |                   |  |       |
| $h \times 10^3$                            | $n$               | $h \times 10^3$           | $n$               | $h \times 10^3$                            | $n$               | $h \times 10^3$                            | $n$   |
| $t = 2.00 \times 10^{-2}$                  |                   | $t = 1.00 \times 10^{-2}$ |                   | $t = 5.00 \times 10^{-4}$                  |                   | $t = 2.50 \times 10^{-4}$                  |       |
| 1.200                                      | 0.119             | 1.171                     | 0.100             | 1.096                                      | 0.087             | 1.085                                      | 0.069 |
| 1.199                                      | .120              | 0.831                     | .148              | 0.824                                      | .135              | 0.797                                      | .120  |
| 1.013                                      | .160              | .752                      | .193              | .682                                       | .187              | .674                                       | .171  |
| 0.922                                      | .190              | .635                      | .248              | .532                                       | .261              | .641                                       | .178  |
| .825                                       | .226              | .626                      | .261              | .518                                       | .275              | .470                                       | .253  |
| .820                                       | .233              | .588                      | .281              | .474                                       | .306              | .454                                       | .276  |
| .785                                       | .242              | .520                      | .347              | .391                                       | .413              | .405                                       | .318  |
| .735                                       | .279              | .507                      | .368              | .376                                       | .451              | .303                                       | .464  |
| .719                                       | .287              |                           |                   |  |                   | .284                                       | .524  |
| C. Titrations                              |                   |                           |                   |  |                   |  |       |
| $h \times 10^3$                            | $n$               | $h \times 10^3$           | $n$               | $h \times 10^3$                            | $n$               | $h \times 10^3$                            | $n$   |
| $t = 15.9 \text{ to } 14.3 \times 10^{-3}$ |                   |                           |                   | $t = 7.00 \text{ to } 6.68 \times 10^{-3}$ |                   | $t = 2.00 \text{ to } 1.88 \times 10^{-3}$ |       |
| 5.79                                       | 0.02              | 0.741                     | 1.13 <sup>a</sup> | 1.782                                      | 0.12              | 1.200                                      | 0.12  |
| 3.98                                       | .04               | .664                      | 1.34 <sup>a</sup> | 1.573                                      | .15               | 1.151                                      | .13   |
| 3.52                                       | .07 <sup>a</sup>  | .651                      | 1.32              | 1.357                                      | .19               | 1.039                                      | .15   |
| 2.785                                      | .09               | .627                      | 1.45 <sup>a</sup> | 1.147                                      | .24               | 0.878                                      | .20   |
| 2.779                                      | .09               | .619                      | 1.40              | 0.985                                      | .32               | .794                                       | .23   |
| 2.241                                      | .15 <sup>a</sup>  | .588                      | 1.56 <sup>a</sup> | .886                                       | .39               | .683                                       | .30   |
| 2.225                                      | .14               | .552                      | 1.61              | .799                                       | .50               | .589                                       | .40   |
| 1.834                                      | .19               | .529                      | 1.72 <sup>a</sup> | .738                                       | .60               | .508                                       | .55   |
| 1.565                                      | .24               | .507                      | 1.72              | .621                                       | .90               | .440                                       | .77   |
| 1.542                                      | .26 <sup>a</sup>  | .466                      | 1.87 <sup>a</sup> | .450                                       | 1.52              | .386                                       | 1.02  |
| 1.351                                      | .31               | .449                      | 1.93              | .150                                       | 2.49              | .311                                       | 1.42  |
| 1.193                                      | .40 <sup>a</sup>  | .435                      | 1.94              |  |                   | .201                                       | 2.03  |
| 1.077                                      | .47               | .407                      | 2.04              |  |                   | .089                                       | 2.77  |
| 0.947                                      | .64               | .365                      | 2.16              |  |                   |  |       |
| .839                                       | .85               | .231                      | 2.37              |  |                   |  |       |
| .824                                       | .92 <sup>a</sup>  | .131                      | 2.59              |  |                   |  |       |
| .732                                       | 1.07              |                           |                   |  |                   |  |       |

<sup>a</sup> Titrations of "thorium oxyperchlorate" solutions with HClO<sub>4</sub>. The other values refer to titrations of ThCl<sub>4</sub> solutions with NaOH.

At higher values of  $n$  (Region II) an increase in slope (more negative) occurs followed by a decrease for  $n > 1$ . In Region II, which in general can only be reached by addition of base, a large number of species will probably have to be considered for complete interpretation, and hence at present discussion will be confined to Region I, where Th<sup>+4</sup> is still the principal species and where, thus, unambiguous interpretations appear feasible. Attempts were made to fit the data in

Region I by consideration of eq. 6 and 7 with equilibrium constants

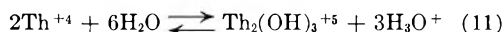
$${}^1k_2 = \frac{(\text{Th}(\text{OH})_2^{++})(\text{H}_3\text{O}^+)^2}{}_1G_2 \quad (8)$$

$${}^2k_2 = \frac{(\text{Th}_2(\text{OH})_2^{+6})(\text{H}_3\text{O}^+)^2}{}_2G_2 \quad (9)$$

where parentheses indicate molar concentrations of species and  $G$  the appropriate activity coefficient quotients. In the symbols  $k$  and  $G$  the subscripts refer to the number of hydroxide ions and the superscripts to the number of thorium ions in the hydrolysis products. Since the composition of the solutions changes only moderately throughout the series of experiments, the assumption was made that the activity coefficient quotients  $G$  are constant.<sup>21</sup> While neither eq. 6 or 7 by itself could explain the data, consideration of the two together with concentration quotients  ${}^1k_2^m = 3.4 \times 10^{-8}$  and  ${}^2k_2^m = 2.6 \times 10^{-5}$  (where  $k^m = k/G$ ) fitted the data fairly well, as illustrated in Fig. 2 for a few selected concentrations. The deviations probably could not all arise from changes in  $G$  and hence in addition eq. 1 with constant

$${}^1k_1 = \frac{(\text{ThOH}^{+3})(\text{H}_3\text{O}^+)}{}_1G_1 \quad (10)$$

was considered. By trial and error "best" fit was obtained with the concentration quotients  ${}^1k_1^m = 4 \times 10^{-5}$ ,  ${}^1k_2^m = 2 \times 10^{-8}$  and  ${}^2k_2^m = 2 \times 10^{-5}$ . This improved the fit at low  $t$  but increased the deviations at high  $t$ . Thus, if eq. 1 is of importance, only a four-parameter equation can satisfactorily explain the data, even in the narrow hydrolysis range of Region I. Consideration of the additional equilibrium



with constant  ${}^2k_3$ , together with eq. 1, 6 and 7, yielded satisfactory fit of the experimental data in Region I using  ${}^1k_1^m = 5 \times 10^{-5}$ ,  ${}^1k_2^m = 1.5 \times 10^{-8}$ ,  ${}^2k_2^m = 1.6 \times 10^{-5}$  and  ${}^2k_3^m = 1.0 \times 10^{-8}$  (Fig. 2). Since equilibrium 11 cannot account for the data at higher hydroxyl numbers there is little doubt that other species, e.g., Th<sub>2</sub>(OH)<sub>4</sub><sup>+4</sup> or trimers and tetramers must be postulated for interpretation of both Regions I and II. The use of eq. 11 should only be considered the introduction of an additional parameter to demonstrate that further equilibria occur. Consideration of additional equilibria or of an equilibrium different from 11 would affect the magnitude of all constants and hence the values given for  ${}^1k_1^m$ ,  ${}^1k_2^m$  and  ${}^2k_2^m$  are only approximate. However, it is felt that they are sufficiently accurate to permit the following conclusions: In the hydrolysis of Th(IV) polymeric equilibria are involved. A dimer is formed which contains two hydroxide ions. There is some indication for the existence of the species Th(OH)<sup>+3</sup>. The value of its formation constant

(21) As stated earlier, the experiments were not carried out at constant "ionic strength" but at an ionic strength (molarity scale)  $\mu = 1.000 + 10t$ . Since the highest thorium concentration was 0.015 M, the ionic strength range is 1.000 to 1.150. It is questionable if the assumption that the activity coefficient quotients are constant would be significantly better if the ionic strength had been kept at 1.000, since at these concentrations the principal effects on activity coefficients result from changes in medium rather than from changes in  $\mu$ .

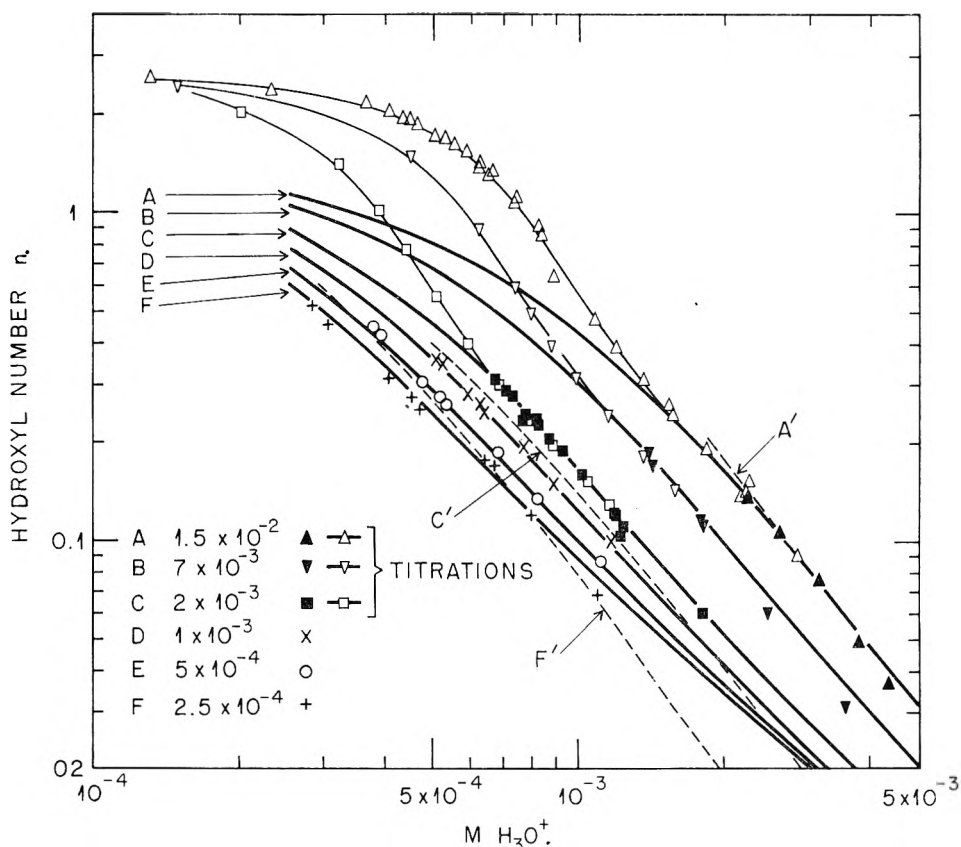


Fig. 2.—Hydrolysis of Th(IV): points, observed values; dotted lines (A',C',F') calculated for  ${}^1k_2^m = 3.4 \times 10^{-8}$  and  ${}^2k_2^m = 2.6 \times 10^{-6}$  at  $t = 1.5 \times 10^{-2}$ ,  $2 \times 10^{-3}$  and  $2.5 \times 10^{-4}$ ; heavy lines (A to F) calculated for  ${}^1k_1^m = 5.0 \times 10^{-5}$ ,  ${}^1k_2^m = 1.5 \times 10^{-8}$ ,  ${}^2k_2^m = 1.6 \times 10^{-6}$ ,  ${}^2k_3^m = 1.0 \times 10^{-8}$ .

${}^1k_1^m$  is surprisingly small (ca.  $5 \times 10^{-5}$ ) compared with the analogous constants for  $U^{+4}$  and  $Pu^{+4}$  (ca.  $3 \times 10^{-2}$ ). The constant  ${}^1k_1$  for Th(IV) would not be expected to be less than one-third of  ${}^1k_1$  for U(IV) if the slightly larger size of Th(IV)<sup>22</sup> is considered and a simple coulombic theory used.<sup>7,23</sup>

From the hydrolytic point of view the inclusion of Th(IV) with U(IV) and Pu(IV) in a rare-earth-like series appears thus very questionable. Rather it appears that Th(IV), on the basis of the differences in the values of  ${}^1k_1^m$  and in the mechanisms of hydrolysis, differs sufficiently from U(IV) and Pu(IV) to make its classification in a different group of elements plausible. Actually, the tendency of Th(IV) to form essentially reversibly low molecular weight hydrolytic polymers makes it appear similar to the considerably more acidic ions Zr(IV), Ce(IV) and Hf(IV), which also tend to form such low molecular weight hydrolytic polymers.<sup>24</sup> The hydrolytic properties thus lend further weight to the assumption that rare-earth-

like behavior of the heavy elements in aqueous solutions starts abruptly with uranium and not with actinium, as often proposed.

It may be noticed from Fig. 2 that the curve of  $\log n$  vs.  $\log h$  which seems to flatten near  $n = 2.5$  does not flatten near  $n = 2$ . Thorium ions ( $ThO^{+2}$  or  $Th(OH)_2^{+2}$ ), or their polymers ( $(Th(OH)_2^{+2})_N$ ), thus do not exhibit any striking stability. The formation of polymeric chains of  $(Th(OH)_2^{+2})_N$ , held together by hydroxide bridges, was recently made plausible by the work of Lundgren and Sillén<sup>25</sup> on the crystal structure of basic salts of Th(IV) and U(IV). Since the composition  $n = 2$  is not favored, one must conclude that should these polymeric chains exist in solution, they tend to hydrolyze further, e.g., by loss of protons from the water molecules coordinated to the metal ions of the chain.

In preliminary ultracentrifugations of Th(IV) perchlorate solutions,<sup>26</sup> aggregates were found in the vicinity of  $n = 2$  with tetramers possibly occurring for  $n$  just less than 2 and considerably larger polymers for  $n$  barely larger than 2. In the hydrolysis range where these polymers are formed, the number of possible species becomes very large, and a definitive interpretation does not appear feasible, at least until precise values of the degrees of polymerization are available. The use of a

(22) The metal-oxygen distances are 2.419, 2.363 and 2.332 Å. for  $ThO_2$ ,  $UO_2$  and  $PuO_2$ , respectively (W. H. Zachariasen, *Phys. Rev.*, **73**, 1104 (1948)).

(23) K. A. Kraus and J. R. Dam, "National Nuclear Energy Series," Div. IV, Vol. 14B, No. 4.15, McGraw-Hill Book Co., Inc., New York, N. Y., 1949, p. 496.

(24) Zr(IV): see footnote 28; Ce(IV): L. J. Heidt and M. E. Smith, *J. Am. Chem. Soc.*, **70**, 2476 (1948); D. Kolp and H. C. Thomas, *ibid.*, **71**, 3047 (1949); T. J. Hardwick and E. Robertson, *Can. J. Chem.*, **29**, 818 (1951); K. A. Kraus, R. W. Holmberg and F. Nelson, Abstracts, Portland Meeting, American Chemical Society (1947). Hf(IV): J. S. Johnson and K. A. Kraus, unpublished results.

(25) G. Lundgren and L. G. Sillén, *Arkiv. Kemi*, **1**, 277 (1950); G. Lundgren, *ibid.*, **2**, 535 (1951); **4**, 421 (1953).

(26) J. S. Johnson and K. A. Kraus, unpublished results.

simplified continuous polymerization hypothesis, such as that used by Granér and Sillén<sup>27</sup> in their interpretation of bismuth hydrolysis, does not appear justified at this time since, apparently, it can lead to erroneous conclusions regarding degrees of polymerization.<sup>28</sup>

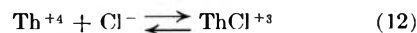
The hydrolysis products of thorium have been written as complexes with hydroxide ions (*e.g.*,  $\text{Th}(\text{OH})_2^{++}$  and  $\text{Th}_2(\text{OH})_2^{+6}$ ) rather than as complexes with oxide ions (*e.g.*,  $\text{ThO}^{++}$  and  $\text{Th}_2\text{O}^{+6}$ ). The techniques used here, of course, do not permit a decision as to which of these formulas is correct. However, recent work by Lundgren and Sillén<sup>25</sup> on basic salts of Th(IV) and U(IV) establishes the existence of hydroxide bridges in basic salts of these elements. Using these structure determinations as a guide, one may postulate that the hydrolysis products of thorium are complexes with hydroxide ions and that the polymeric species such as the dimer postulated in this work are held together by hydroxide bridges. In addition, the

(27) F. Granér and L. G. Sillén, *Acta Chem. Scand.*, **1**, 631 (1947).

(28) In preliminary ultracentrifugations of Bi(III)-perchlorate solutions under conditions where Granér and Sillén calculated a weight average degree of polymerization  $N_w = 20$ , a degree of polymerization of less than 6 was found, as well as considerably less polydispersity than indicated by Granér and Sillén (R. W. Holmberg, K. A. Kraus and J. S. Johnson, unpublished results). Similarly, zirconium perchlorate solutions were found to have a degree of polymerization of approximately 3 (K. A. Kraus and J. S. Johnson, *J. Am. Chem. Soc.*, **75**, 5769 (1953)) under conditions where Connick and Reas (*ibid.*, **73**, 1171 (1951)), also using a hypothesis of continuous polymerization, suggested a weight average degree of polymerization of *ca.* 300.

species are unquestionably hydrated and might be written as  $\text{Th}(\text{OH})_2(\text{H}_2\text{O})_6^{+2}$  and  $(\text{H}_2\text{O})_6\text{Th}_{\text{OH}}^{\text{OH}}\text{Th}(\text{H}_2\text{O})_6^{+6}$  if a coordination number of 8 is assumed.

**4. Hydrolysis in Chloride Solutions.**—The early steps in the hydrolysis of  $\text{ThCl}_4$  were studied in KCl-HCl solutions of total concentration 1 *M*. The data were obtained in an attempt to establish if hydrolysis of Th(IV) is sensitive to chloride complexing according to the equation



for which the concentration quotient

$$k_{01}^m = \frac{(\text{ThCl}^{+3})}{(\text{Th}^{+4})(\text{Cl}^-)} = 1.8 \quad (13)$$

had earlier been found by Waggener and Stoughton at  $\mu = 1.00$ .<sup>15</sup> Thorium was found to hydrolyze to approximately the same extent in chloride and perchlorate solutions. The effect of chloride complexing on *n* was estimated, and the predicted decrease in *n* was considerably outside the experimental error. If chloride complexing occurs as postulated by Waggener and Stoughton, one must conclude from the insensitivity of the hydrolytic reaction to chloride ions that basic chloride complexes of the type  $\text{Th}(\text{OH})_2\text{Cl}^+$  and  $\text{Th}_2(\text{OH})_2\text{Cl}^{+5}$ , etc., are formed and that the hydrolysis constants of such chloride complexes are approximately the same as those of the uncomplexed ions.

## THE ADSORPTION OF ARGON ON XENON LAYERS<sup>1,2</sup>

BY J. H. SINGLETON AND G. D. HALSEY, JR.

*Department of Chemistry, University of Washington, Seattle, Wash.*

*Received November 9, 1958*

The adsorption isotherms for argon on pre-adsorbed films of xenon have been measured on graphitized carbon black, silver iodide and anatase. The character of the isotherms change progressively as the amount of pre-adsorbed xenon is increased. The limiting isotherm with increase in amount of xenon is different for the three solids. This fact indicates that there is a limiting film thickness, beyond which the film of xenon is not stable.

### Introduction

Adsorption isotherms have been measured on a variety of substances in the past. Most of the surfaces have been poorly characterized and chemically complex. Even the ideal case of argon on potassium chloride is not free of difficulties. One may have a number of crystal faces exposed, frozen in defects in crystal structure, and adsorbed water, to mention a few. Such incidental factors make comparisons of isotherms taken on different surfaces difficult. Therefore we have measured a series of isotherms on a given solid covered with various thicknesses of xenon, deposited in a reproducible, reversible manner. The films thus formed are as pure as the bulk xenon itself, if we assume that any strongly adsorbed dirt remains on the surface of the solid, with which it presum-

ably has specific interaction. There is then an analogy with the technique of evaporating metal films for chemisorption studies,<sup>3</sup> with the difference that the xenon films are in equilibrium with the solid.

### Experimental

**Vacuum System.**—The adsorption measurements were made in a conventional constant volume system. Gas pressures were measured in manometers, 10 mm. in diameter, read with a cathetometer graduated to 0.05 mm.

**Gases.**—Tank helium, from Western Oxygen, Inc., was better than 99.9% pure. Nitrogen was produced by heating sodium azide to 350°. Xenon and argon of 99.9% purity were obtained in sealed glass bulbs from Air Reduction Sales Co.

**Adsorbents.**—Silver iodide was precipitated from hot 0.1 *M* HI by addition of 0.05 *M*  $\text{AgNO}_3$ . It was digested for six hours, filtered, washed with hot water and absolute alcohol, and dried in a vacuum desiccator. It was always shielded from light.

(1) This research was supported by Contract AF19(604)-247 with the Air Force Cambridge Research Center.

(2) Presented at the 123rd National Meeting of the American Chemical Society, Los Angeles, Calif., March 16-20, 1953.

(3) O. Beeck, A. E. Smith and A. Wheeler, *Proc. Roy. Soc. (London)*, **A177**, 62 (1940).

A sample of standard anatase,<sup>4</sup> surface area 13.8 m.<sup>2</sup>/g. was obtained from Professor George Jura, University of California, Berkeley.

A sample of graphitized carbon black<sup>5</sup> designated P-33-(2700°) was obtained from Dr. W. R. Smith, Godfrey L. Cabot, Inc., Cambridge, Mass. It has been shown<sup>5</sup> to have the characteristics of a nearly uniform surface.

The dead space of each sample was determined with helium at -195, -78 and 0°. The value of  $v_m$ , the volume of a monolayer, was determined with argon at -195° and with xenon at -124.6°. B.E.T. plots were used for anatase and silver iodide but the plot was unsatisfactory for carbon black, so "point B" was estimated directly from the isotherm. Areas were then obtained using the figures of Emmett and Brunauer.<sup>6</sup> The density of liquid xenon was taken from the "International Critical Tables" (1926). The results are tabulated in Table I.

TABLE I

|               | $v_m$ in ml./g. (areas in parentheses, m. <sup>2</sup> /g.) |             |                     |
|---------------|---|-------------|---------------------|
|               | Argon   | Xenon       | Nitrogen            |
| Carbon black  | 4.14 (11.9)   | 2.30 (11.6) | (12.5) <sup>5</sup> |
| Silver iodide | 0.47 (1.34)   | 0.26 (1.32) | 0.29 (1.27)         |
| Anatase       | 4.14 (11.9)   | 1.88 (9.50) | (13.8) <sup>4</sup> |

**Outgassing Procedure.**—Anatase and carbon black were heated to 300° and evacuated to 10<sup>-6</sup> mm. overnight, before use. Silver iodide was outgassed at room temperature; higher temperatures caused loss of area. The weight of each sample was chosen to give a total  $v_m$  of about 3 ml.

**Deposition of Xenon Layers.**—Preliminary experiments showed that a slow rate of cooling to liquid nitrogen temperature was necessary to obtain one or more equilibrium xenon layers. At the final temperature, the vapor pressure of the xenon is less than 10<sup>-3</sup> mm. and it will not redistribute at a reasonable rate. To facilitate controlled cooling the sample was enclosed in a small Dewar vessel shown in Fig. 1. The vertical temperature gradient was minimized by making the entry tubes long and thin. The horizontal gradient was controlled by evacuating the Dewar until the desired rate of cooling was achieved. The conductivity of the sample was maintained by including a few millimeters of helium with xenon. When the sample reached the temperature of liquid nitrogen (2-24 hours) the helium was removed and the outer jacket filled with hydrogen. Rough calculations indicated that the thermal gradients were small; however, the ultimate criterion of success in deposition was the reproducibility of the argon isotherm with further decrease in rate of cooling. Results reported here have all been reproduced in many cases with different sample bulbs of slightly changed shape and design.

**Measurement of Temperature and  $p/p_0$ .**—In the final design of the sample bulb (Fig. 1) an argon vapor pressure thermometer was located in the center of the sample. This constant indication of  $p_0$  was necessary for the carbon black isotherms, because of their complexity. For the other two samples  $p_0$  was obtained at the end of the isotherms, by introducing a large excess of argon; this produced some error in the results for  $p/p_0 < 0.9$ . A check isotherm, using the refined bulb with enclosed thermometer reproduced the silver iodide results exactly up to  $p/p_0 = 0.9$ . The temperature for the isotherms reported here was -195.8 ± 0.4°.

**Measurement of the Isotherm.**—Adsorption isotherms of argon on the bare surfaces and on a series of pre-adsorbed xenon layers were determined two or more times, usually with a second sample of the adsorbent. The graphs (Figs. 2-7) include only a portion of the actual points taken. The isotherms were reversible. For one or more layers of xenon the argon was removed completely by pumping for 15 minutes. The isotherm could then be reproduced showing that no xenon came off, and that the pre-adsorbed xenon was not rearranged by heat from the entering argon.

## Discussion of Results

### Isotherms on Graphitized Carbon Black (Fig. 2).

—Owing to the nearly uniform surface of this

(4) W. D. Harkins and G. Jura, *J. Am. Chem. Soc.*, **66**, 1362 (1944).

(5) M. H. Polley, W. D. Schaeffer and W. R. Smith, *THIS JOURNAL*, **67**, 46f (1953).

(6) P. H. Emmett and S. Brunauer, *J. Am. Chem. Soc.*, **59**, 1553 (1937).

sample great care was required to obtain reproducible results. Slight irregularity in the xenon layers creates heterogeneity and radically alters the isotherm for argon. In the initial experiments the xenon monolayer volume was estimated from the "point B" of the xenon isotherm at -124.6° (Table I). The argon isotherm taken on this nominal one-layer volume of xenon showed a pronounced "point B" at 0.15 nominal monolayers of argon (isotherm labeled 0.85 layer, Fig. 2). When 20% more xenon was pre-adsorbed, the "point B" disappeared (isotherm labeled 1.0, Fig. 2). This volume of xenon (1.20  $v_m$ ), was taken to be one layer and used to compute the number of layers pre-adsorbed (no similar adjustment was made for  $v_m$  for argon and the values of  $\theta$  are plotted in multiples of this volume). These two isotherms demonstrate the sensitivity of the results to slight changes in coverage, and explain the necessity for very careful cooling to ensure that all the xenon reaches its equilibrium location.

The isotherms will now be discussed in order. (The term "step" is used as a traditional way of referring to a pronounced point of inflection in the isotherm; it is not to be confused with a first-order transition, which is a real step.) With no pre-adsorbed xenon the presence of steps indicates that the argon is adsorbed more or less layer by layer as the pressure increases. With 0.43 layer of xenon a sort of dual surface has been prepared, half xenon and half carbon. The carbon half is covered at  $p/p_0 < 0.01$ , which creates a dual surface of xenon and argon. The step corresponding to the second layer of argon on the bare carbon occurred at  $p/p_0 = 0.35$ . Here a smaller step at  $p/p_0 = 0.2$  reflects the dual nature of the surface, and the greater van der Waals attraction of a mixed layer of xenon and argon, than that of a first layer of argon alone. Further steps are obscured, because of the mixed surface.

The isotherm with 1.0 layer of xenon shows the return of a larger step which is now at  $p/p_0 = 0.15$  because the first layer is all xenon. The step for the second layer of argon is very slightly lower than the third layer step for the bare surface ( $p/p_0 = 0.6$ ).

It is interesting that the isotherm for the 1.28 layers of xenon crosses and recrosses the one layer isotherm because the step in it is at a lower  $p/p_0$ , but smaller. Evidently the fraction of a second layer of xenon scattered over the first layer creates

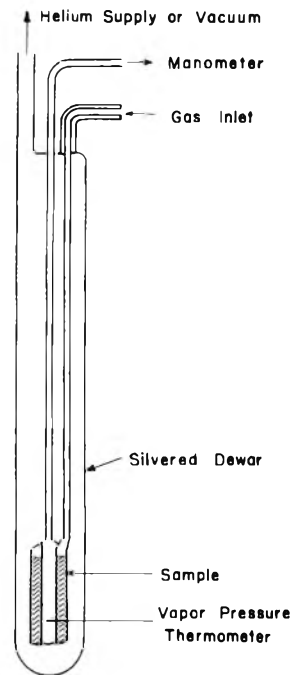


Fig. 1.—Dewar vessel for adsorption sample.

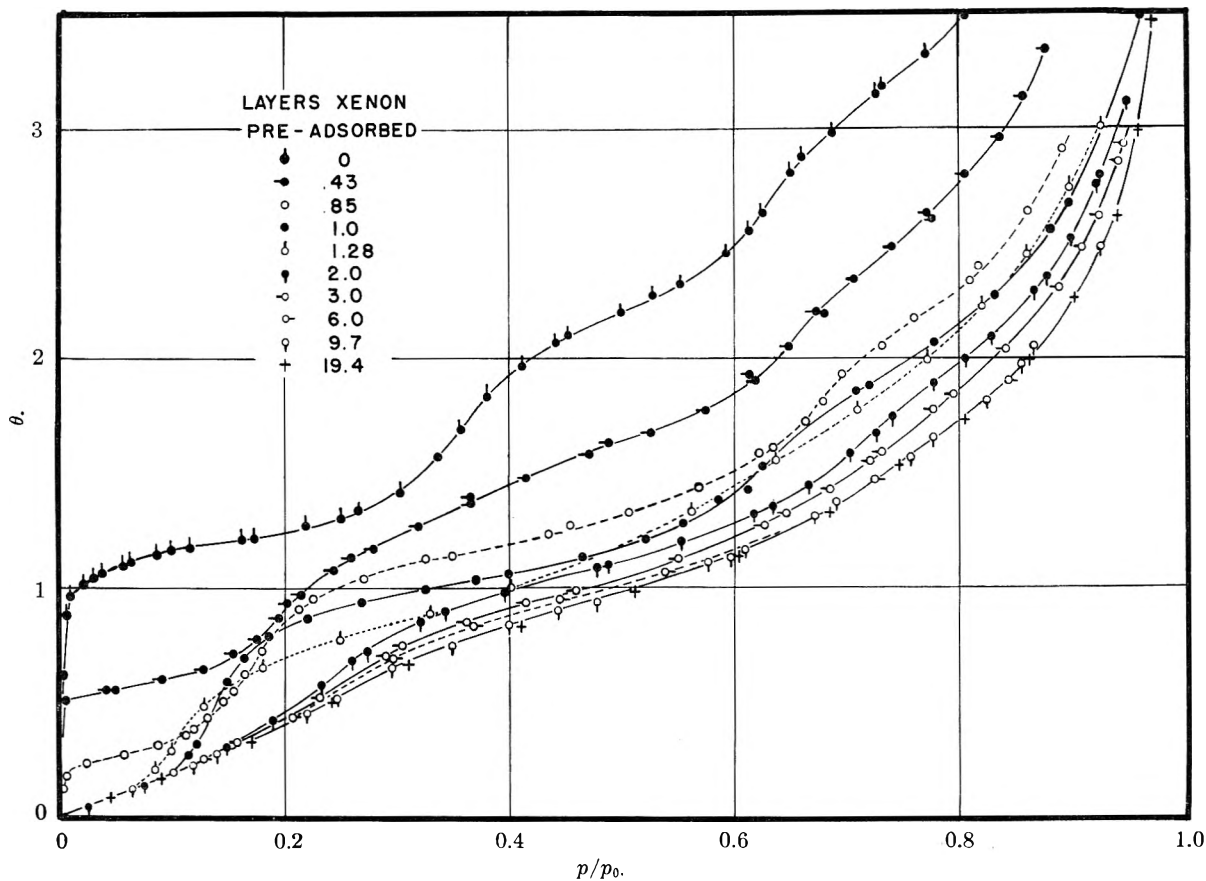


Fig. 2.—The adsorption of argon on layers of xenon on carbon black at  $-195^{\circ}$ .

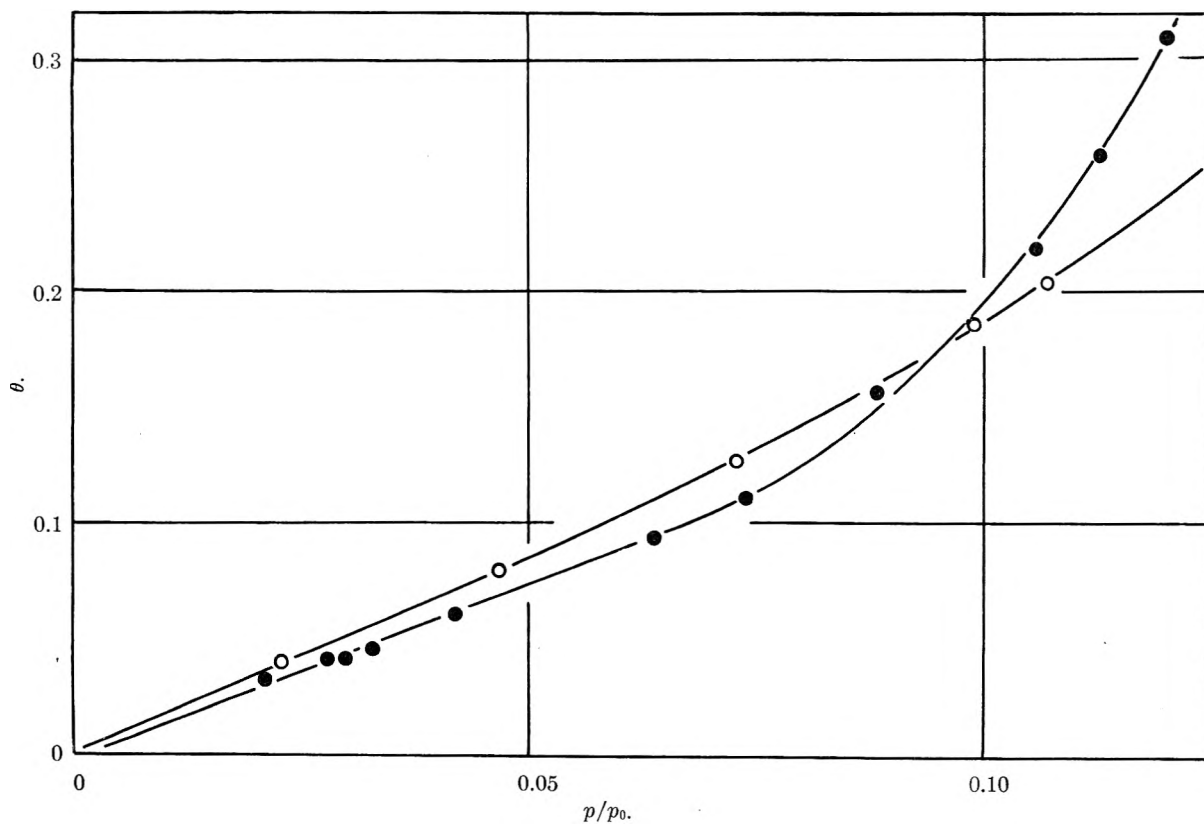


Fig. 3.—Argon isotherms on one and two layers of xenon on carbon black at low partial pressures ( $-195^{\circ}$ ): ●, one layer; ○, two layers.

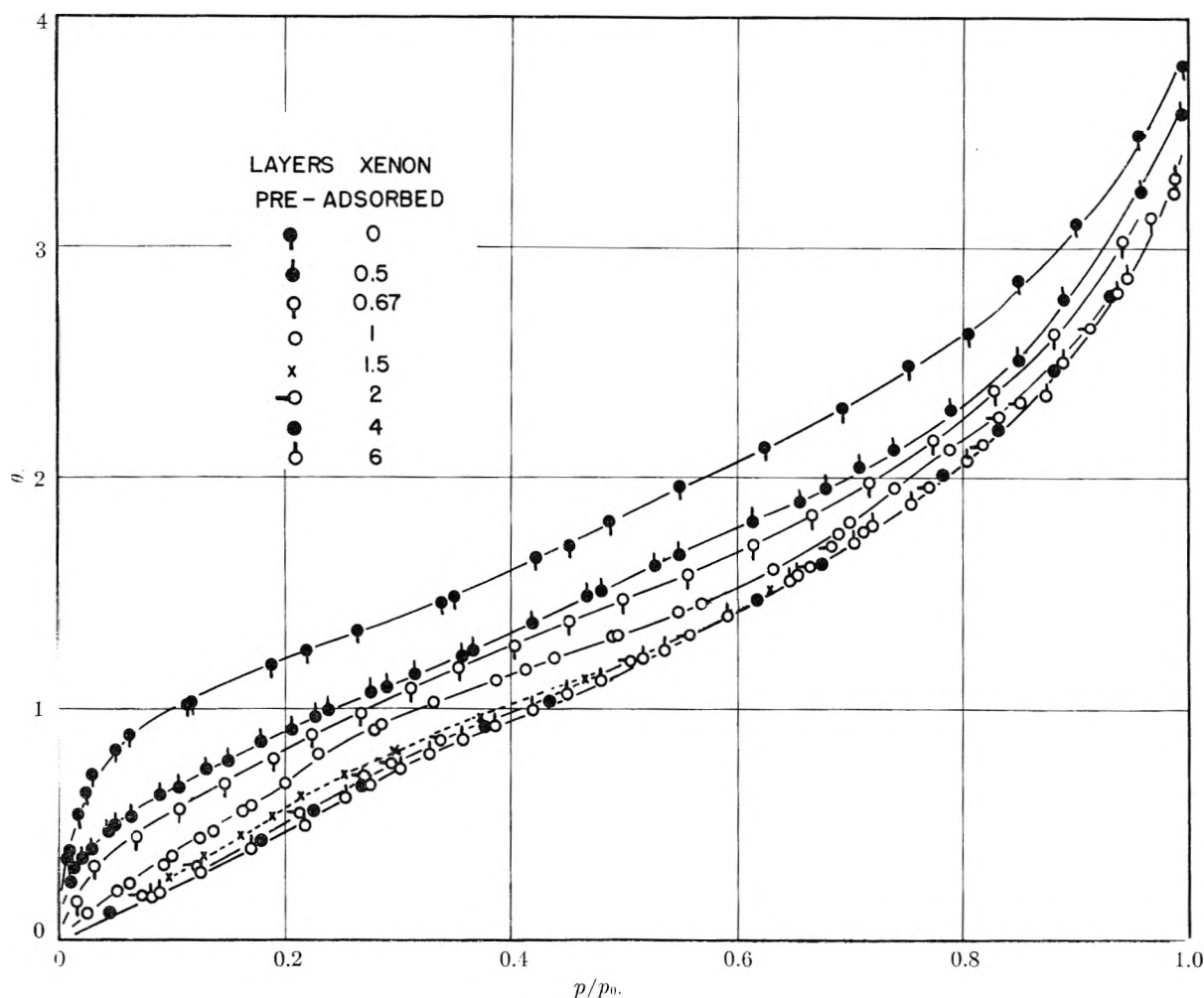


Fig. 4.—The adsorption of argon on layers of xenon on silver iodide at  $-195^{\circ}$ .

some higher energy sites at the same time as it takes up some of the available space in the second layer. The crossing is repeated near  $p/p_0 = 0.6$  and again faintly at 0.8.

The first step on two layers of xenon is near  $p/p_0 = 0.3$ , very much lower than the corresponding step on the bare adsorbent. The isotherms on 3.6 and 9.7 layers are only slightly different, showing that the van der Waals forces from the solid are almost negligible. The isotherm for 19.7 layers is indistinguishable from that for 9.7, which means that the surface forces are now completely negligible, or perhaps more likely that the extra layers condensed in low surface-area xenon crystals and never spread on the surface. It appears, however, that at least about six layers were successfully deposited.

Figure 3 shows argon isotherms on one and two layers for partial pressures up to 0.12. All isotherms for more than two layers lie on the curve for two layers, within experimental error. The isotherm for one layer is slightly, but definitely, below. It appears that a really complete, nearly uniform layer of xenon is produced only in the first layer, and that for higher layers a few xenon atoms are out of place, which creates a slight heterogeneity.

**Isotherms on Silver Iodide and Anatase.**—The isotherms on these solids (Figs. 4 and 5) are con-

siderably simpler than those for the carbon black. The isotherms show no steps, and the "point B" values are not as well defined. These observations suggest strongly heterogeneous surfaces. In the absence of a sharp "point B" an independent estimate of the  $v_m$  for xenon is not possible. The number of layers of xenon was calculated from the B.E.T.  $v_m$  values for xenon at  $-126.4^{\circ}$ . In the case of silver iodide there is some evidence that this value is correct. The isotherm labeled 1.0 shows a slight "point B" near  $\theta = 1$  at  $p/p_0 = 0.25$ , while the neighboring isotherms do not. Isotherms for more than one layer are Brunauer's Type III. There is no change in the isotherm beyond two layers of xenon.

In Fig. 6, the adsorption of nitrogen on silver iodide, with and without xenon, is compared with the argon isotherms. The isotherms are similar with nitrogen somewhat more strongly adsorbed. It is interesting to note that even for nitrogen, the "point B" values are poorly defined, and the nitrogen is weakly adsorbed. We have been informed<sup>7</sup> that this is an exception to the generalization that nitrogen is unique in giving good "point B" values and concomitant good B.E.T. plots and surface area measurements.

The argon isotherms on anatase are even simpler

(7) P. H. Emmett, private communication.

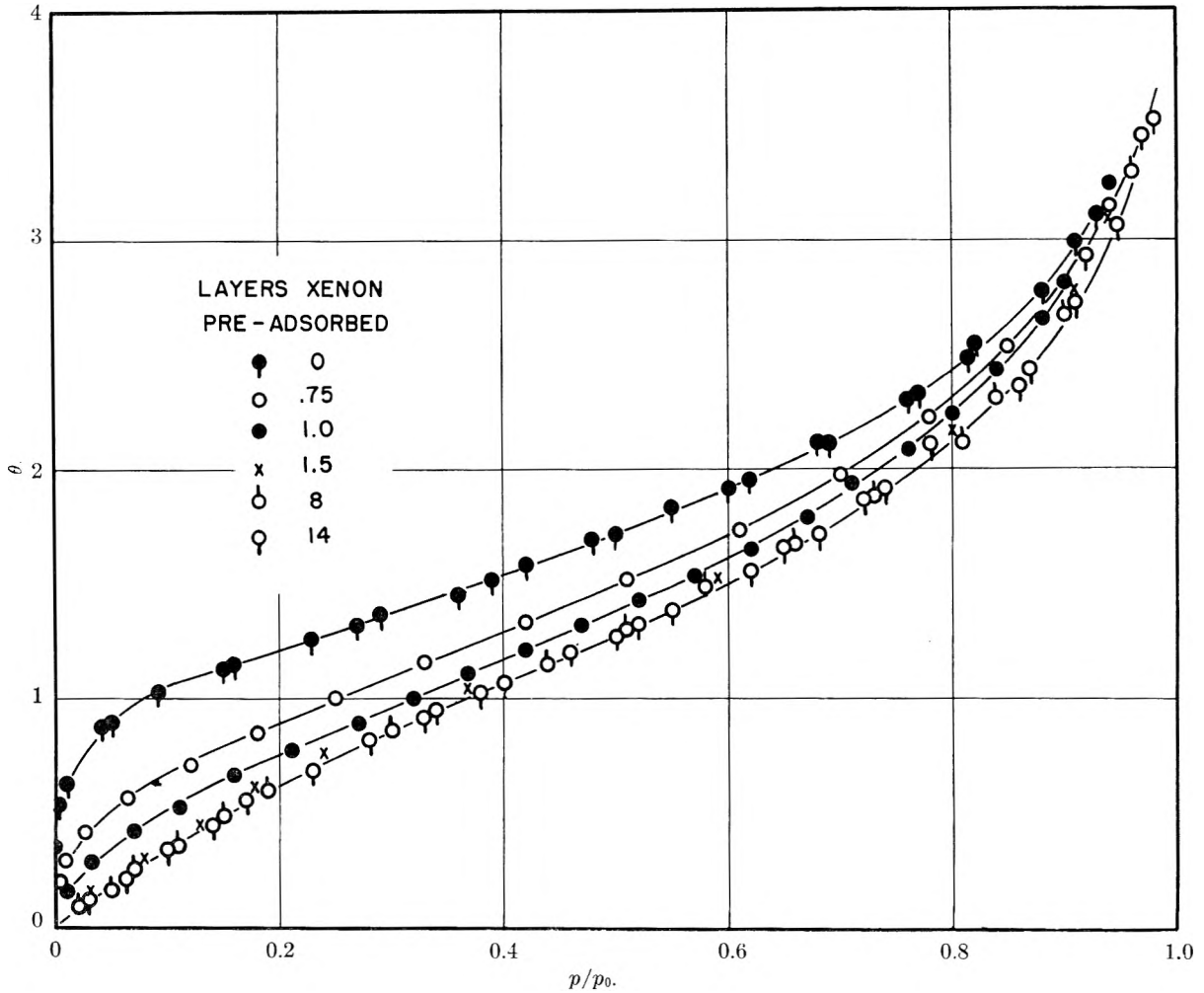


Fig. 5.—The adsorption of argon on layers of xenon on anatase at  $-195^{\circ}$ .

than those on silver iodide. There is a decline but no disappearance of a vague "point B" as coverage reaches one nominal layer. At 1.5 nominal layers the "point B" is gone, and beyond 1.5 layers there is no appreciable change in the isotherms.

**Comparison of the Isotherms on Three Solids.**—The three isotherms with no xenon and the limiting isotherms with many layers of xenon are compared in Fig. 7. Because of uncertainties inherent in

$v_m$  values for argon, it is possible that the limiting curves may be as much as 20% off in absolute value. However the shapes are different, and they cannot be made to coincide by a change in the  $\theta$  scale.

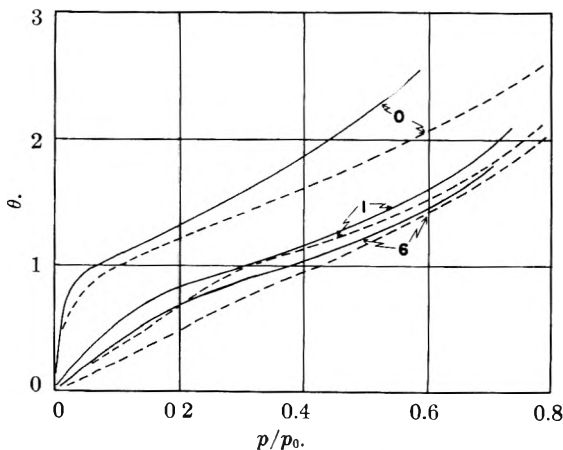


Fig. 6.—Comparison of the adsorption of nitrogen and argon on silver iodide at  $-195^{\circ}$ : —, nitrogen; ----, argon.

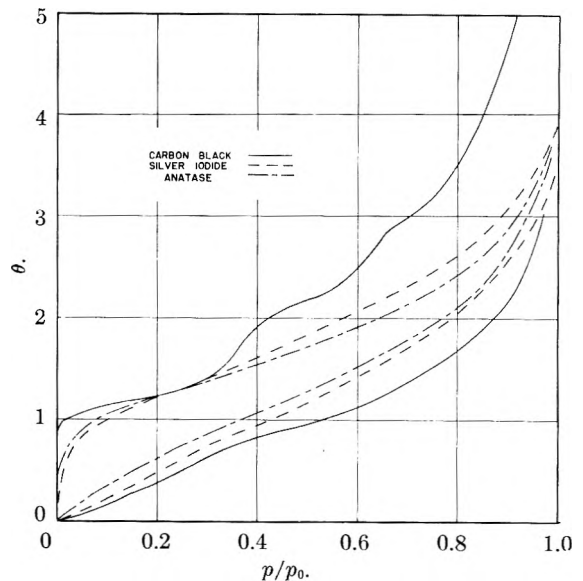


Fig. 7.—Comparison of argon isotherms on carbon black, silver iodide and anatase at  $-195^{\circ}$ .

There are two explanations of the difference in the limiting curves that come to mind: first, that only a few layers can be stabilized on the surface of silver iodide or anatase; that thicker layers are unstable with respect to a bulk crystal and the thinner layer; second, that a structure different on the different solids is established in the xenon and is transmitted out, layer by layer, indefinitely.

There are a number of difficulties that make the second alternative unlikely. The results on the graphitized carbon black are in harmony with the generally accepted view of the falling off of van der Waals forces<sup>8</sup> from the (original) surface with the inverse third power of the distance. Because of the non-specific nature of these forces, and the normal nature of the argon isotherms on silver iodide and anatase (bare of xenon) it is clear that a van der Waals field must extend from these surfaces also. It is unlikely that, in both cases, the hypothetical thickening film of xenon alters in exactly the right way to match this decaying field.

The proportionate change affected by the xenon is greatest for carbon black and least for anatase. This fact is in harmony with the proposed order of maximum layers pre-adsorbed: carbon, over six, silver iodide two or three, and anatase less than two.

Finally, on purely thermodynamic grounds, it is impossible that a film of different structure should be induced to grow indefinitely by a foreign body. The stability of the normal crystal favors a separation into a film of finite thickness and a bulk crys-

(8) T. H. Hill, *J. Chem. Phys.*, **17**, 590, 668 (1949).

tal, if it is impossible to make the transition from surface layer to bulk structure continuously.

**Conclusion.**—The results, especially on carbon black, support the general picture of adsorption as layer formation under the influence of transmitted van der Waals forces.<sup>9</sup> The difficulty in reproducing the isotherms, unless extreme care is taken, suggests that the ordinary preparation of adsorbents by chemical means is likely to create defects which cause heterogeneity, even in the absence of impurities.

Calculations have been made of the adsorption energy of argon on alkali halide crystals,<sup>10</sup> with the assumption that the ions behaved as rare gases. The isotherms on many layers of xenon reported here do not in the least resemble those on alkali halides, with which the calculations agree to a degree. Some doubt is thrown at once on both the assumption and the calculations themselves.

The technique of this paper provides a method of estimating the number of layers of an adsorbent that can be successfully preadsorbed. The impossibility of obtaining xenon films of indefinite thickness on some adsorbents suggests that a surface may be surrounded by a repulsive zone which will prevent the deposition of a solid from the gas phase. The looser structure of a liquid makes the continuous transition from adsorbed film to bulk phase easier, but if the bulk phase is solid,  $\theta$  may approach a limiting value, rather than infinity, as  $p/p_0$  approaches unity.

(9) G. D. Halsey, Jr., *J. Am. Chem. Soc.*, **73**, 2693 (1951).

(10) W. J. C. Orr, *Trans. Faraday Soc.*, **35**, 1247 (1939); *Proc. Roy. Soc. (London)*, **A173**, 349 (1939).

## THE BEHAVIOR OF COLLOIDAL SILICATE SOLUTIONS AS REVEALED BY ADSORPTION INDICATORS<sup>1</sup>

BY BENJAMIN CARROLL AND ELI FREEMAN

*Newark Colleges of Rutgers University, Newark, N. J.*

*Received November 10, 1953*

The adsorption and desorption of dyes, as reflected by spectral changes, were used to investigate the effects of pH, aging and ion exchange in colloidal solutions of sodium silicate. Aging effects were indicated by a loss in the absorption affinity for the dyestuffs. The addition of salts caused the absorption spectrum to shift back toward that of the free dye in water, indicating displacement of the dye by the salts. The nature of the anion appeared to be of minor importance, whereas the cation was found to be the significant factor in the binding affinity of salts for the silicate sol. The displacement series obtained with the alkaline earth and alkali elements was  $\text{Ca} > \text{Ba} > \text{Sr} > \text{K} > \text{Na} > \text{Li}$ . The effect of less than one part per million of divalent cations could be observed by this method. The adsorption isotherm for crystal violet indicated the maximum number of dye molecules which may be bound per formula weight of sodium silicate. The free energy of binding was obtained on the basis that the binding is of a statistical nature.

In a previous publication<sup>2</sup> it was shown that by the addition of a small quantity of suitable dye to a solution of a hydrous oxide, such effects as salt additions and aging upon the colloidal solution could be followed spectrophotometrically in a quantitative manner. An alternate procedure for this type of investigation is the use of equilibrium

(1) This material is taken from the dissertation submitted by Eli Freeman in partial fulfillment of the requirements for the Master of Arts degree of Brooklyn College, New York. Presented in part before the Division of Colloid Chemistry of the American Chemical Society, Atlantic City, N. J., September 14, 1952; *Abstr. Papers Am. Chem. Soc.*, 122, 2G (1952).

(2) B. Carroll and A. W. Thomas, *J. Chem. Phys.*, **17**, 1336 (1949).

dialysis. The latter method has the disadvantages of being time consuming and inexact for hydrous oxides. The inexactness is due in part to the necessity of using foreign electrolyte to suppress the Donnan effect, thus introducing appreciable changes in the colloidal system.

In this work a negative sol, sodium silicate, was investigated spectrophotometrically using the dyes crystal violet and methylene blue. These dyes were selected because it was found that they followed Beer's law reasonably well, up to a concentration of  $2 \times 10^{-5} M$ . Furthermore, the dyes alone showed inappreciable spectral shifts due to

the pH changes and salt additions employed in this work. Thus, the spectral changes in the dye-silicate solution brought about by various agents could be interpreted unambiguously. As an independent check, a few adsorption experiments were run using equilibrium dialysis and the resulting data were in qualitative accord with those obtained with the spectrophotometric method.

It should be stated that our work was aided by the results of Merrill and co-workers<sup>3</sup> who demonstrated that many cationic dyes exhibit spectral changes in sodium silicate solutions.

### Experimental

The sodium silicate solution, S-35 ( $\text{Na}_2\text{O}\cdot 3.75\text{SiO}_2$ ) of the Philadelphia Quartz Company which contained 25.3%  $\text{SiO}_2$  and 6.75%  $\text{Na}_2\text{O}$  was used in all experiments. The salts, potassium chloride, sodium chloride, lithium chloride, calcium chloride, barium chloride, strontium chloride and potassium acetate were all of reagent or C.P. grade. Methylene blue and crystal violet, of histological grade obtained from the National Aniline division of the Allied Chemical and Dye Corp., were used directly.

pH determinations were made with the Beckman Model G pH meter and the absorption measurements were taken with a Beckman Model DU Quartz spectrophotometer, provided with a cooling block. This permitted temperature control to  $\pm 0.2^\circ$ . One centimeter cuvettes were used for this work.

The molar extinction coefficients  $E$  were calculated from the equation  $E = 1/Cd \log (I_0/I)$  where the symbols have their usual significance.

Solutions were mixed immediately before spectral measurements were taken. Mixing and absorption measurements were usually completed within five minutes in order to minimize any drifts in optical density of the dye. Unless otherwise stated, measurements were taken at  $28^\circ$ .

### Results and Discussion

To use spectral measurements for determining quantitatively the extent of adsorption of dye in a colloidal solution, Beer's law must be followed by

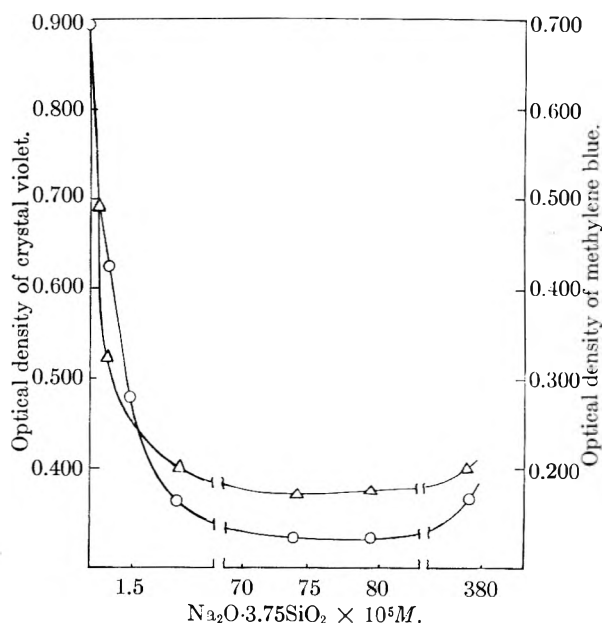


Fig. 1.—Optical density vs. concentration of  $\text{Na}_2\text{O}\cdot 3.75\text{SiO}_2$  in  $1 \times 10^{-5} M$  dye solution:  $\Delta$ , crystal violet at  $591 m\mu$ ;  $\circ$ , methylene blue at  $558 m\mu$ .

(3) R. C. Merrill, R. W. Spencer and R. Getty, *J. Am. Chem. Soc.*, **70**, 2460 (1948); R. C. Merrill and R. W. Spencer, *ibid.*, **70**, 3683 (1948); **72**, 2894 (1950).

the free dye and by the bound dye. To obtain the extinction coefficient of the latter, a large excess of sodium silicate is used. Constancy of the extinction coefficient in the presence of varying concentration of silicate may be taken as an indication that all the dye has been complexed and that Beer's law holds for the complexed dye.

Figure 1 is a plot of optical density at the spectral peaks of crystal violet and methylene blue at  $591$  and  $668 m\mu$ , respectively, versus concentration of  $\text{Na}_2\text{O}\cdot 3.75\text{SiO}_2$ . The concentration of dye is kept constant at  $1.0 \times 10^{-5} M$ . Upon increasing the concentration of the sol, there is a marked decrease in the optical density. As little as  $1 \times 10^{-5} \text{Na}_2\text{O}\cdot 3.75\text{SiO}_2$ , causes approximately a 50% decrease of the optical density. At sufficiently high concentrations of silicate, apparently all the dye is absorbed. The optical density in the plateau region may be used to determine the extinction coefficients of adsorbed dye molecules. This yields a value of 0.43 and 0.20 as the ratio of the extinction coefficients of the bound to free dye at the so-called  $\alpha$ -bands<sup>4,5</sup> for crystal violet and methylene blue, respectively.

It will be seen in Fig. 1 that a large excess ( $> 10^{-3} M$ ) of silicate produces a noticeable increase in the extinction coefficients. The reason for this is not clear. A few qualitative measurements using equilibrium dialysis indicated the increase in the  $\alpha$ -band value was not due to a decrease in the adsorption of the dye. This has also been the recent experience of Levene and Schubert.<sup>6</sup> It has been suggested<sup>7</sup> that high molecular weight polyelectrolytes may change their molecular shapes with increasing concentration. Such change in shape may conceivably affect the extinction coefficient of the bound dye. Also the dimeric form of the dye which seems to be the form adsorbed at low concentration of sodium silicate may tend toward the monomeric form when the interfacial area between the silicate phase and the solution is extended in the more concentrated silicate solutions.

Upon aging there is a considerable decrease in the amount of dye absorbed. This decrease is greater for more dilute silicate solutions. For example, a  $7.72 \times 10^{-4} M \text{Na}_2\text{O}\cdot 3.75\text{SiO}_2$  solution combined with 58% less crystal violet after standing for seven days at about a temperature of  $25^\circ$ . The decrease in binding of a more concentrated solution of the silicate ( $3.86 \times 10^{-2} M$ ) for crystal violet occurred at a lower rate, being 43% over a period of twenty-eight days. The dye concentration in both instances was  $1.0 \times 10^{-5} M$ .

Heating accelerates the aging process. When the sol ( $7.72 \times 10^{-4} M \text{Na}_2\text{O}\cdot 3.75\text{SiO}_2$ ) was aged from five to ten minutes at about  $80^\circ$  the amount of dye adsorbed decreased 23%. These observations may be accounted for by a decrease in the number of available binding sites, which may be due to an increase in the polymerization degree of the silicate. Other evidence that polymerization occurs upon aging has been obtained from light scattering meas-

(4) L. Michaelis and S. Granick, *ibid.*, **67**, 1212 (1945).

(5) L. Michaelis, *This Journal*, **54**, 1 (1950).

(6) A. Levene and M. Schubert, *J. Am. Chem. Soc.*, **74**, 5702 (1952).

(7) R. M. Fuoss and U. P. Strauss, *Ann. N. Y. Acad. Sci.*, **51**, 836 (1949).

urements.<sup>8</sup> The more dilute the solution and the higher the temperature, the more rapidly the process proceeds.

The addition of salts to a silicate-dye solution causes a reversal of the spectral shift in the direction of that for the dye alone. The effect increases with increasing salt concentrations, so that eventually the spectrum of the dye alone may be attained. Apparently, the salt displaces the dye from the sol, causing a reversal of the spectral change. These salt concentrations have little effect if any upon the spectrum of the free dye.

The effect of the nature of the anion on the interaction of salts with colloidal sodium silicate is illustrated in Fig. 2. A measure of the binding affinity is indicated by the amount of dye which is displaced from the sol. This is reflected by an increase in the optical density at the  $\alpha$ -band of the dyes. The broken line represents the limiting value of the optical density at the absorption maxima of  $1.0 \times 10^{-5} M$  crystal violet in water. Keeping the concentration of the dye and  $\text{Na}_2\text{O} \cdot 3.75\text{SiO}_2$  constant at  $1.0 \times 10^{-5}$  and  $7.72 \times 10^{-5} M$ , respectively, it is observed from the lower four curves of this figure that the nature of the anion, whether monovalent or divalent, plays only a minor role in the interaction of salts with sodium silicate. The effect of potassium acetate appears to be greater at concentrations higher than  $0.01 N$ . This is attributed to the effect of  $pH$  on the sodium silicate sol, due to the hydrolysis of the acetate ion.

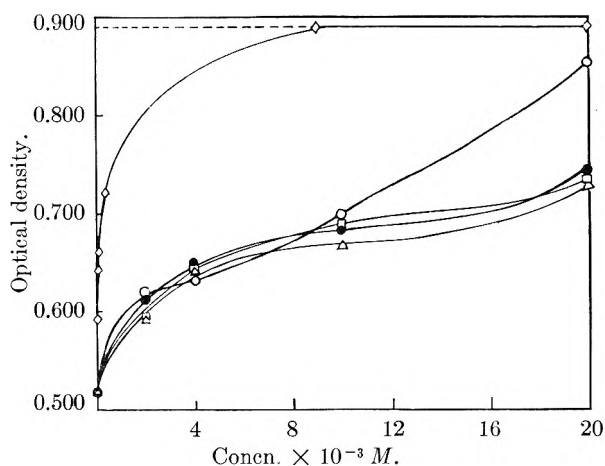


Fig. 2.—The effect of potassium salts on the binding of  $1 \times 10^{-5} M$  crystal violet to  $7.72 \times 10^{-5} M \text{Na}_2\text{O} \cdot 3.75\text{SiO}_2$ ; wave length at  $591 m\mu$ ; optical density vs. concentration of salts:  $\diamond$ ,  $\text{CaCl}_2$ ;  $\circ$ ,  $\text{KAc}$ ;  $\bullet$ ,  $\text{K}_2\text{SO}_4$ ;  $\square$ ,  $\text{KNO}_3$ ;  $\Delta$ ,  $\text{KCl}$ ; ---, dye alone in water.

In calcium solutions, represented by the uppermost curve, at a concentration of  $0.01 N$  all the dye is displaced. It appears that the nature of the cation is of major significance in the binding of salts. One part per million of calcium causes a 10% increase in the optical density, as illustrated in this figure. The average ratio of the number of moles of crystal violet displaced per mole of divalent cation seems to approach roughly one, as the salt concentration is decreased.

The effect of charge of cations in the interaction

with sodium silicate sol and the displacement of bound dye is illustrated in Fig. 3. Optical density versus concentration is plotted for several alkali and alkaline earth salts containing a common anion. The broken line represents the limiting optical density at the absorption maxima of crystal violet in water. The concentration of  $\text{Na}_2\text{O} \cdot 3.75\text{SiO}_2$  and dye are kept constant at  $7.72 \times 10^{-5}$  and  $1.0 \times 10^{-5} M$ . As a group, the alkaline earth salts of calcium, strontium and barium chloride are significantly more strongly bound by the sol, as represented by the top group of curves, than that of the alkali salts of potassium, sodium and lithium chloride, represented by the lower set of curves.

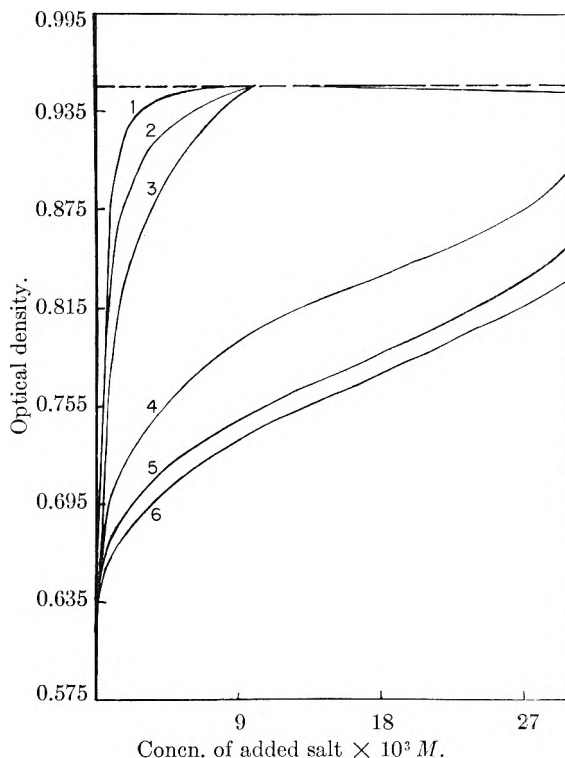


Fig. 3.—The effect of cations on the interaction of  $1 \times 10^{-5} M$  crystal violet and  $7.72 \times 10^{-5} M \text{Na}_2\text{O} \cdot 3.75\text{SiO}_2$ ; wave length at  $591 m\mu$ ; optical density vs. concentration of salts: 1,  $\text{CaCl}_2$ ; 2,  $\text{BaCl}_2$ ; 3,  $\text{SrCl}_2$ ; 4,  $\text{KCl}$ ; 5,  $\text{NaCl}$ ; 6,  $\text{LiCl}$ .

At a concentration of  $0.01 N$  all the dye is displaced by the alkaline earth elements, whereas, for the same normality, potassium displaces 58%, sodium 44% and lithium 41% of the dye. In  $0.03 N$  solution of the alkali salts all the dye is still not displaced. Apparently, there exists a definite order in the displacement ability for cations. For the alkaline earth elements, calcium appears to be the most strongly bound, followed by barium and strontium. For the alkali elements, potassium is the most strongly bound followed by sodium and lithium in order of decreasing affinity for the sol. The identical order was obtained substituting methylene blue for crystal violet. Ion-exchange studies reveal the same series, with the exception of calcium.<sup>9</sup> By means of electrometric titrations, Mukherjee and Chatterjee found that the intensity

(8) A. P. Brady, A. G. Brown and H. Huff, *J. Colloid Sci.*, **8**, 252 (1953).

(9) J. G. Vail, "Soluble Silicates," Vol. I, Reinhold Publ. Corp., New York, N. Y., 1952.

of the reaction of silicic acid sol with calcium, barium and sodium hydroxides decreased in the order of calcium, barium and sodium.<sup>10</sup> This is in agreement with the results in this paper. No data were reported for strontium, potassium and lithium. Merrill and co-workers in studying the relative affinity of the alkali salts and its interaction with sodium silicate sol, by following the changes in the absorption spectra of pinacyanol chloride revealed the order  $K > Li > Na$ . Their use of high concentrations of salt, sodium silicate and a dye which exhibits relatively large salt effects is probably responsible for this discrepancy. At these concentrations, they were unable to study the bivalent cations using this method due to precipitation.

Precipitation did not occur in this work. When the alkaline-earth cations are added to the silicate solution, the optical density of such a mixture in the absence of dye yields the same value as distilled water. This condition exists even at the cation concentration required to displace all the adsorbed dye as described for the results in Fig. 3.

The adsorption isotherm for crystal violet was determined. Assuming  $n$  binding sites per  $Na_2O \cdot 3.75SiO_2$  group, identical intrinsic binding constants for all sites, and the absence of interaction between successively bound dye ions, the adsorption data may be represented by the equation<sup>11</sup>

$$r/(A) = nk - rk$$

where

$$r = \frac{\text{moles of bound dye}}{\text{total moles of } Na_2O \cdot 3.75SiO_2}$$

$$(A) = \text{concn. of unbound dye}$$

$$k = \text{intrinsic binding constant}$$

The adsorption data are summarized in a graph  $r/(A)$  versus  $r$ , shown in Fig. 4. As is evident from

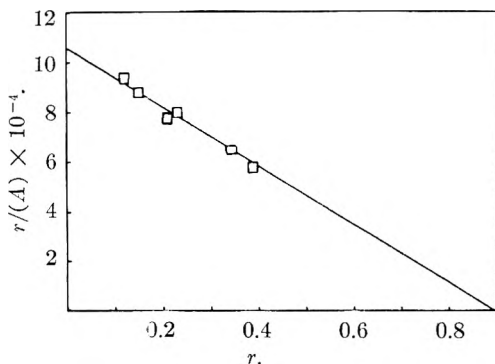


Fig. 4.—Adsorption of crystal violet by  $Na_2O \cdot 3.75SiO_2$  at  $28^\circ$ .

the absorption equation the extrapolated intercept on the abscissa of the graph is  $n$ , whereas the intercept on the ordinate is  $kn$ . Since the binding is ideal we have

$$nk = k_1$$

where  $k_1$  represents the equilibrium constant for the first complexed dye ion. The free energy  $\Delta F^0_1$  may be computed from the thermodynamic equation

(10) B. Chatterjee, *J. Indian Chem. Soc.*, **16**, 589 (1939); B. Chatterjee and A. J. Sen, *ibid.*, **19**, 17 (1942); J. Mukherjee and B. Chatterjee, *Nature*, **155**, 85 (1945).

(11) G. Scatchard, *Ann. N. Y. Acad. Sci.*, **51**, 660 (1949); also see I. M. Klotz and J. M. Urquhart, *J. Am. Chem. Soc.*, **71**, 847 (1949).

$$\Delta F^0_1 = -RT \ln k_1$$

The results in Fig. 4 yield a value of  $-6,960$  cal. for  $\Delta F^0_1$ . They indicate also an  $n$  value somewhat less than unity. Since dye occurs probably in dimeric form on the surface of the colloidal silicate, it would appear that some nine  $SiO_2$  groups are required to provide a site for crystal violet.

The adsorption data are too limited to establish the validity of the adsorption equation or the value of  $n$  since the latter is obtained by extrapolation to high values of  $r$  or  $(A)$ . This is a region where the spectrophotometric method does not provide adequate data. The free energy of binding may be more reliable since this value is based on a less extensive extrapolation.

An indication of the isoelectric point of the sol may be obtained from Fig. 5. This is a graph of the optical density at the absorption maximum of  $1.0 \times 10^{-5} M$  methylene blue versus pH of the dye in  $7.72 \times 10^{-5} M Na_2O \cdot 3.75SiO_2$ . These measurements are taken immediately after the addition of the acid to the silicate-dye solution. Increasing the acidity of the solution by the careful addition of HCl causes a sharp rise in the optical density until a pH is attained where the sol loses its ability to bind the dye. If this pH 2.9 is considered as the isoelectric point, it compares favorably with the values obtained by other workers. For example, using electrophoresis Gordon<sup>12</sup> observed that a silica gel membrane was negative at a pH of 3.17 and positive at a pH of 1.12.

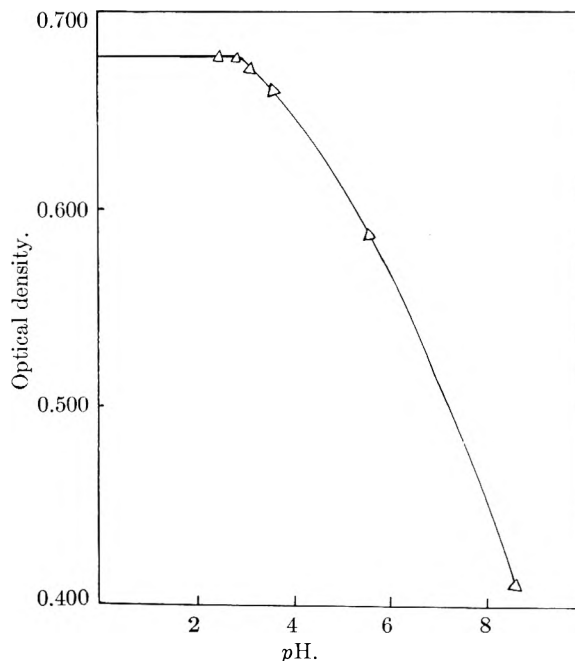


Fig. 5—Optical density vs. pH in solutions of  $1 \times 10^{-5}$  methylene blue and  $7.72 \times 10^{-5} M Na_2O \cdot 3.75SiO_2$  at wave length of  $668 m\mu$ .

**Acknowledgment.**—The authors wish to express their gratitude to the Research Corporation and to the Rutgers Research Council for grants which were used to defray part of the cost of the apparatus used in this study.

(12) N. E. Gordon, "Colloid Symposium Monograph," Vol. 2, Chemical Publishing Co., New York, N. Y., 1925, p. 119.

# THE POLAROGRAPHIC REDUCTION OF COPPER ETHYLENEDIAMINE TETRAACETATE

BY K. BRIL AND P. KRUMHOLZ

Research Laboratory of Orquima S.A., São Paulo, Brasil

Received November 24, 1953

A functional dependence of the half-wave potential of copper ethylenediamine tetraacetate (Enta) upon the pH, in well buffered solutions, is discussed. The formation of multiple waves in unbuffered solutions of copper Enta, containing small amounts of free hydrogen or metal ions capable of forming stable complexes with Enta has been studied. An approximate treatment of this effect is given based on the Ikovic theory and the assumption of depletion of hydrogen or metal ions from the solution-mercury interface. The interference of kinetic effects is stated.

It is known that the copper ethylenediamine-tetraacetate (Enta) complex produces a well defined polarographic wave.<sup>1</sup> Its half-wave potential in buffered solutions is shifted toward more negative values with increasing pH.<sup>1a</sup> Addition of small amounts of acids or metal ions, forming stable complexes with Enta, produces in unbuffered solutions of the copper-Enta complex a peculiar wave splitting.<sup>2</sup> Similar double or multiple waves have up to now been chiefly observed in organic systems.<sup>3</sup> In the following we report on this particular behavior of the copper-Enta system and its possible explanation.

## Experimental

The apparatus used was described in a previous communication,<sup>2</sup> as was also the preparation of Enta, copper, lead, cadmium, nickel and zinc solutions. The calcium nitrate solution was standardized according to the oxalate-permanganate method. The lanthanum nitrate was prepared from a pure oxide (purity 99%) calcinated at 950°.

The dropping mercury electrode had  $m^2/st^{1/6} = 2.53$  mg.<sup>2/3</sup> sec.<sup>1/6</sup> as determined in a solution 0.1 molar in potassium nitrate, 5 × 10<sup>-5</sup>% in methyl orange, oxygen free, at 20.0° in short circuit. Current measurements were made in general in 10-mv. potential intervals.

The pH of the solutions was maintained by the addition of potassium hydroxide or nitric acid with potentiometric control of the pH using a glass electrode mounted directly in the polarographic vessel. The pH of all solutions could thus be checked during the actual measurement. The reproducibility of the pH control in buffered solutions as well as in the unbuffered solutions in the pH range 3.5 to 4.5<sup>4</sup> was about ±0.02 pH unit. In unbuffered solutions in the pH range 5.5 to 6.5 the stability of the pH readings was about 0.1 pH unit.

All solutions were brought to equilibrium with respect to the exchange reaction (see ref. 2 and 4)



## Experimental Results

The half-wave potential of the copper-Enta complex at a given pH depends strongly upon the concentration of the buffer used, as well as upon

(1) (a) R. L. Pecsok, *J. Chem. Educ.*, **29**, 597 (1952); (b) H. Ackermann and G. Schwarzenbach, *Helv. Chim. Acta*, **35**, 485 (1952); (c) W. Furness, P. Crawshaw and W. C. Davies, *Analyst*, **74**, 629 (1949); (d) J. Koryta and I. Kossler, *Collection Czech. Chem. Commun.*, **15**, 241 (1950); (e) P. Souchay and J. Faucherre, *Anal. Chem. Acta*, **3**, 252 (1949); (f) *Bull. soc. chim. France*, 722 (1949); (g) R. Pribil and B. Matyska, *Chem. Listy*, **44**, 305 (1950); (h) E. I. Onstott, *J. Am. Chem. Soc.*, **74**, 3773 (1952).

(2) K. Bril and P. Krumholz, *THIS JOURNAL*, **57**, 874 (1953).

(3) (a) I. M. Kolthoff and J. J. Lingane, "Polarography," 2nd ed., Interscience Publishers, Inc., Chapter XIV and XV. (b) M. von Stackelberg, "Polarographische Arbeitsmethoden," W. de Gruyter, 1950, p. 309, etc.

(4) Actually in this pH range some buffering occurs due to the acid function of the copper Enta complex; see G. Schwarzenbach and E. Freitag, *Helv. Chim. Acta*, **34**, 1492 (1951). We found by potentiometric titration  $K_{\text{CuYH}} = 1.2 \times 10^3$  at 20° and 0.1 ionic strength.

the concentration of the supporting electrolyte. At constant ionic strength, it shifts toward more positive values with increasing buffer concentration (see Fig. 1). At constant buffer concentration it shifts toward more negative values with increasing ionic strength. Beyond the dotted line in Fig. 1, both the buffer concentration and the ionic strength increase, and it is actually probable that the apparently constant value of the half wave potential is only a result of a counterbalancing effect. Figure 1 shows that at low buffer concentrations the half-wave potential is almost independent of the concentration of copper-Enta. With increasing buffer concentration there appears an increasing shift of the half-wave potential toward more negative values as the copper Enta concentration is increased from 10<sup>-4</sup> to 10<sup>-3</sup> molar.

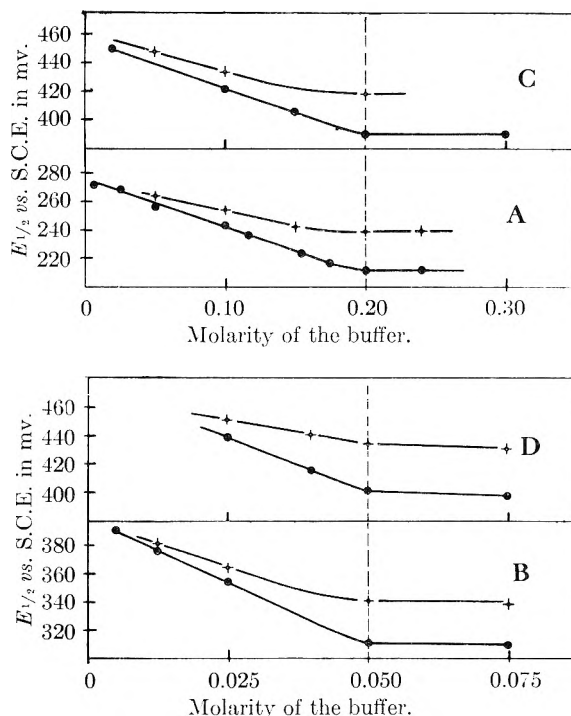


Fig. 1.—The influence of the buffer concentration upon the half wave potential of the copper-Enta complex. Left of the dotted line, the ionic strength is maintained constant ( $\mu = 0.10$ ) by suitable addition of potassium nitrate. Right of the dotted line the ionic strength, which is given by the buffer concentration, increases proportionally to the buffer concentration: A,  $\text{CH}_3\text{COOH} + \text{CH}_3\text{COONa}$  (pH 4.69); B,  $\text{NaH}_2\text{PO}_4 + \text{Na}_2\text{HPO}_4$  (pH 6.88); C, potassium tetraborate (pH 9.32); D,  $\text{NaHCO}_3 + \text{Na}_2\text{CO}_3$  (pH 10.08);  $t = 20.0^\circ$ . (All solutions contained 5 × 10<sup>-5</sup>% methyl orange.)

This shift reaches about 30 mv. for solutions where the total ionic strength is given by the concentration of the buffer. A further increase of the buffer concentration (and of the ionic strength) has no significant effect upon this shift.

The wave slope

$$\alpha = \frac{\Delta E}{\Delta \log i^2 / (i_d - i)}$$

in buffered solutions of constant ionic strength depends also upon the nature and the concentration of the buffer, decreasing slowly as the buffer concentration is increased, as shown in Table I.

TABLE I

DEPENDENCE OF THE WAVE SLOPE,  $\alpha$ , UPON THE CONCENTRATION OF THE BUFFER FOR A  $10^{-3} M$  COPPER-ENTA SOLUTION AT  $\mu = 0.1$ ,  $20.0^\circ$

| Buffer 1:1<br>pH  | CH <sub>3</sub> COOH<br>CH <sub>3</sub> COONa<br>4.69 | KH <sub>2</sub> PO <sub>4</sub><br>K <sub>2</sub> HPO <sub>4</sub><br>6.88 | H <sub>3</sub> BO <sub>3</sub><br>NaH <sub>2</sub> BO <sub>3</sub><br>9.32 | NaHCO <sub>3</sub><br>Na <sub>2</sub> CO <sub>3</sub><br>10.08 | $\alpha$ |
|-------------------|---|--|--|--|----------|
| 0.24 <sup>a</sup> | 0.030   |  |  |  |          |
| .20               | .031  |  |  |  |          |
| .10               | .038  |  |  |  |          |
| .05               | .039  |  | 0.035  |  |          |
| .037 <sup>b</sup> |   | 0.030  |  | 0.035  |          |
| .025              |   | 0.032  | 0.036  | .036   |          |
| .020              |   |  |  | .036   |          |
| .012              |   | 0.040  | 0.037  | .039   |          |
| .0062             |   | 0.042  |  | .043   |          |

<sup>a</sup>  $\mu = 0.12$    <sup>b</sup>  $\mu = 0.15$ .

In unbuffered solutions of the copper-Enta complex containing very small amounts of free acid the polarographic wave shows a peculiar wave splitting illustrated in Figs. 2 and 3. Two distinct pre-waves appear clearly. The height of these waves, at constant copper-Enta concentration is approximately proportional to the hydrogen ion concentration.

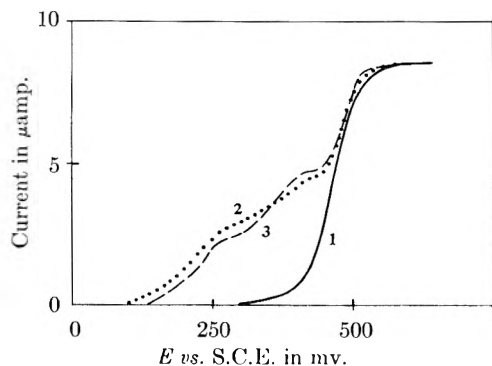


Fig. 2.—Wave splitting in slightly acid unbuffered solutions of copper-Enta in  $0.1 M$  potassium nitrate, copper-Enta concentration  $10^{-3} M$ ,  $5 \times 10^{-5}\%$  methyl orange,  $t = 20.0^\circ$ : 1, copper-Enta wave at pH 7.1; 2, copper-Enta wave at pH 3.99; 3, the calculated current-potential curve (for  $E_1$  the value  $-464$  mv. was used).

In the absence of maximum suppressors two very prominent maxima appear in these solutions, as shown in Fig. 3. Methyl red, methyl orange,  $\alpha$ -naphthol, caffeine and gelatin, all can be used to suppress these maxima. For methyl red and methyl orange the polarographic wave is independent of the concentration of the maximum sup-

pressor in the concentration range of  $5 \times 10^{-5}$  to  $15 \times 10^{-5}\%$ . By further increasing this concentration the prewave is depressed and suffers a shift to more negative potentials. This effect is essentially the same for all suppressors used.

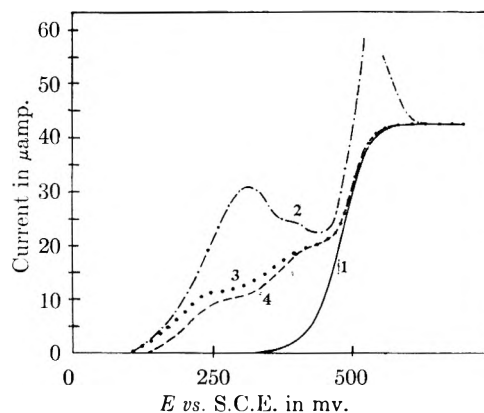


Fig. 3.—Wave splitting in slightly acid unbuffered solutions of copper-Enta in  $0.1 M$  potassium nitrate, copper-Enta concentration  $5 \times 10^{-3} M$ ,  $t = 20.0^\circ$ : 1, copper-Enta wave at pH 7.1,  $5 \times 10^{-5}\%$  methyl orange added; 2, copper-Enta wave at pH 3.62, no maximum suppressor added; 3, copper-Enta wave at pH 3.62,  $5 \times 10^{-5}\%$  methyl orange added; 4, calculated (see text) current-voltage curve for pH 3.62 (for  $E_1$  the value  $-464$  mv. was used).

In almost neutral copper-Enta solutions the double wave formation disappears completely (see Fig. 2 and 3). Also, in solutions containing sufficient excess of acid over the copper-Enta concentration the double wave formation does not occur. There appears only a continuous shift of the half-wave potential toward more positive values, with increasing acidity.

Upon addition of salts of cadmium, calcium, lanthanum, lead and zinc, all capable of complexing the Enta ion, to a nearly neutral solution ( $pH \geq 6$ ) of copper-Enta, a single prewave is produced as shown in Fig. 4.<sup>5</sup> In more acid solution the hydrogen prewave adds to the metal induced wave.

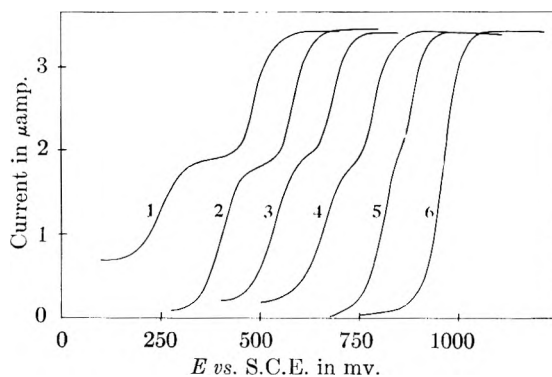


Fig. 4.—Wave splitting in a  $0.4$  mM copper-Enta solution,  $0.2$  mM in metal nitrate,  $0.1 M$  in potassium nitrate,  $t = 20.0^\circ$ ,  $pH 6.1 \pm 0.2$ : 1, lead nitrate; 2, lanthanum nitrate; 3, cadmium nitrate; 4, zinc nitrate; 5, calcium nitrate; 6, no metal added. Abscissa scales for curves 2, 3, 4, 5, 6, start at 100, 200, 300, 400 and 500 mv., respectively, to the right of curve 1. (All solutions contained  $5 \times 10^{-5}\%$  methyl orange.)

(5) No wave splitting could be observed upon addition of nickel salts.

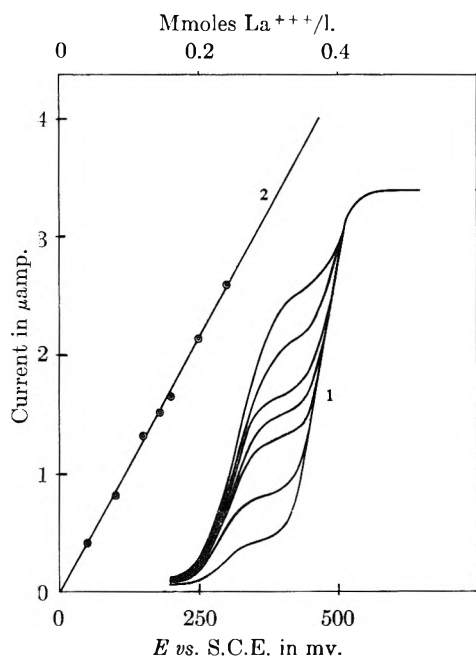


Fig. 5—Wave splitting produced by various concentrations of lanthanum nitrate in a 0.4 mM copper-Enta solution in 0.1 M potassium nitrate at 20.0°, pH 6.2 ± 0.1: 1, current-potential plots; 2, diffusion current (induced by the metal)-concentration plot.

Figure 5 shows the dependence of the height of the metal induced wave upon the concentration of the metal ion in the case of lanthanum at pH 6.2 ± 0.1. A very good proportionality is observed. The same was found for all other metals studied here.<sup>6</sup> The height of the metal induced wave shows no marked dependence upon the concentration of the copper-Enta complex. It has a normal temperature coefficient as shown by the fact that, all other conditions being maintained constant, the relation between the height of the first wave and the total height of the wave is, within the experimental error, independent of the temperature in the range of 0° to about 50°.

In the case of the metal induced wave as well as in that of the hydrogen prewave the total ionic strength exerts a pronounced effect upon the wave separation: the higher the total ionic concentration the poorer the wave separation. Thus in the case of calcium, the double wave formation apparently disappears, in 0.5 M potassium nitrate. It manifests itself only by broadening the derivative polarograms (see Fig. 6). As shown by this figure the half-wave potential of the second wave remained almost unaltered by the change in the ionic strength, whereas that of the first wave is shifted by about 40 mv. toward more negative potentials with increasing ionic strength. Values ranging up to 70 mv. (for lead) were found for the

(6) Actually the metal induced wave is proportional to the concentration of the free metal ion. This, in general, is different from the added, because of the exchange equilibrium  $\text{CuY}^- + \text{Me}_{(2)}^{n+} = \text{Me}_{(2)}^{(n-2)+} + \text{Cu}^{++}$ . Only in the case of lead, however, does this correction become important. In all other cases studied here it can be neglected, within the experimental error, when the wave height of the induced wave is measured from zero current line up (corrected for the residual current). This is due to the fact that the diffusion coefficients of the metal ions studied here, with the exception of lead, are almost equal (see ref. 3a, p. 52) to each other (see also ref. 2).

other metals, and of about 60 mv. for the hydrogen induced wave.

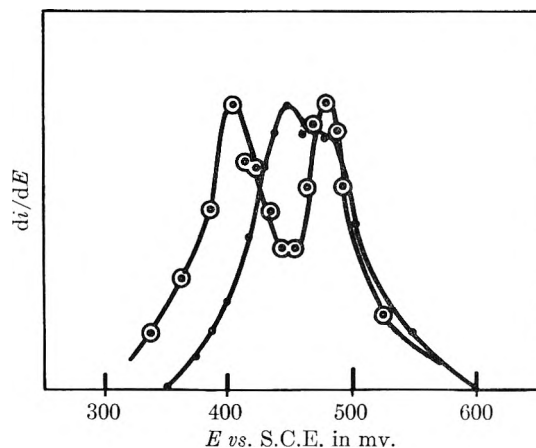
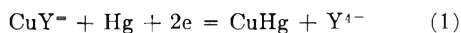


Fig. 6.—Derivative polarogram of a  $4 \times 10^{-4}$  M copper-Enta solution containing  $2 \times 10^{-4}$  M calcium nitrate at 20.0°;  $\mu = 0.1$  (○);  $\mu = 0.5$  (●).

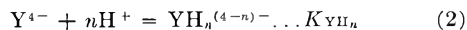
Some experiments were performed using the streaming mercury electrode for comparison (see ref. 2). The wave separation is in all cases poorer at this electrode than at the dropping mercury electrode. Thus, in the case of zinc even in 0.1 M potassium nitrate the wave splitting at the jet electrode manifests itself only on the derivative diagrams. Raising the temperature seems to improve the wave separation. Only lead gives at the jet electrode a clean wave splitting, a good proportionality existing between the free lead concentration (see ref. 6) and the height of the induced wave.

## Discussion

**A. Well Buffered Solutions.**—The diffusion current constant of the copper-Enta complex is only about 10% smaller than the diffusion current constant for copper in nitrate medium.<sup>7</sup> In acetate solutions the difference observed is of about 5% only. This indicates a two-electron electrode process which can be tentatively formulated as



Except in very alkaline solutions the Enta ion,  $\text{Y}^{4-}$ , will react with hydrogen ions, free or furnished by proton donors as buffers or water, according to



Assuming as a first approximation the reduction to be reversible, the potential of the mercury electrode should be given at 20° by

$$E = E_0 - 0.029 \log \frac{(\text{CuHg})_0 (\text{Y}^{4-})_0}{(\text{CuY}^{2-})_0} F \quad (3)$$

where  $F$  is an activity factor and the  $(X)_0$  indicates concentrations at the electrode surface.

If reaction 2 as well as the dissociation of the proton donors occurs instantaneously, then the concentration  $(\text{Y}^{4-})_0$  of the Enta ion at the interface can be expressed as a function of the total analytical concentration of Enta at the interface  $(\text{Y}^*)_0$ , the concentration of the hydrogen ions, and

(7) See also ref. 1b, p. 487.

of the acid dissociation constants of Enta<sup>8</sup> according to

$$(Y^*)_0 = \sum_0^4 (YH_n)_0 = (Y^{4-})_0 \mathcal{f}(H^+)_0 \quad (4)$$

where

$$\mathcal{f}(H^+)_0 = 1 + K_1(H^+)_0 + K_1K_2(H^+)_0^2 + \frac{K_1K_2K_3(H^+)_0^3}{K_1K_2K_3(H^+)_0^3 + \dots} \quad (4a)$$

By following a treatment similar to that proposed by Tomes<sup>9</sup> in the discussion of the polarographic reduction of mercury cyanide equation 3 can be put into the form<sup>10</sup>

$$E = E_1 + 0.029 \log \mathcal{f}(H^+)_0 - 0.029 \log \frac{i^2}{i_4 - i} \quad (5)$$

Equation 5 presumes the validity of the Ilkovic equation for the diffusion of all components of the electrode process.

Equation 5 predicts a 29 mv. negative shift of the half-wave potential with a tenfold increase of the copper-Enta concentration. This was experimentally verified only at the highest buffer concentration compatible with the given ionic strength (see Fig. 1). The half-wave potentials of copper-Enta in solutions where the total ionic strength is that from the buffer components, are plotted against  $p(H)$  (see ref. 8) in Fig. 7. A very

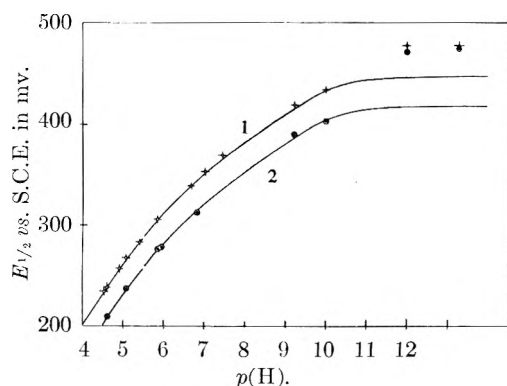


Fig. 7.—Dependence of the half-wave potential of the copper-Enta complex upon the  $p(H)$  in buffered solutions. Ionic strength (0.10) from the buffer components,  $t = 20^\circ$ ; copper-Enta concentration: 2( $\odot$ ),  $10^{-4} M$ ; 1( $\square$ ),  $10^{-3} M$ . Full drawn curves were calculated according to equation 5 using  $E_1 = -428$  mv. (All solutions contained  $5 \times 10^{-5}\%$  methyl orange.)

good agreement with the dependence predicted by equation 5 is found in the  $p(H)$  range of 4 to about 10 using the value  $E_1 = -428$  mv. The increase of the half-wave potential in alkaline medium is not predicted by equation 5. It might be accounted for by the formation of hydroxo complexes of the copper ion and/or of the copper-Enta complex in alkaline solutions.

Equation 5 does not account for the strong de-

(8) G. Schwarzenbach and H. Ackermann, *Helv. Chim. Acta*, **30**, 1768 (1948); values reported by these authors are concentration constants; in the following we shall use the value of  $\gamma_{H^+} = 0.81$  for hydrogen ions at 0.1 ionic strength. The symbol  $p(H)$  will be used whenever the concentration (and not activity) of the hydrogen ions is considered.

(9) J. Tomes, *Collection Czech. Chem. Commun.*, **9**, 12, 81, 150 (1937).

(10) The interaction of the copper-Enta complex with hydrogen ions can be neglected as numerically insignificant at  $pH$  higher than 5 (see ref. 4 and 2).

pendence of the half-wave potential upon the buffer concentration.<sup>11</sup> The strong shift of the half wave potential toward more positive values with decreasing ionic strength may only in part be accounted for by considering the change of the activity factor in equation 3 and of the  $K_{YHn}$ <sup>12</sup> values in equation 4.

**B. Wave Splitting in Unbuffered Slightly Acid Solutions.**—In unbuffered solutions of the copper-Enta complex the  $p(H)$  at the interface will obviously increase with increasing current, due to the increasing consumption of the hydrogen ions by reaction 2. The relation between the interfacial hydrogen ion concentration  $(H^+)_0$ , and the current can be expressed in terms of the concentrations and diffusion coefficients of all proton donors, water included, assuming the validity of the Ilkovic equation, according to

$$i\bar{n} = i \frac{\sum_1^4 n(YH_n)_0}{\sum_1^4 (YH_n)_0} = K [D_{H^{1/2}}(H^+) - (H^+)_0] + D_{CuYH^{1/2}}\{(CuYH^-) - (CuYH^-)_0\} + D_{OH^{1/2}}\{(OH^-)_0 - (OH^-)\} \quad (6)$$

This equation results from the condition of stationarity which presumes that under equilibrium conditions the diffusion fluxes of all proton donors have to equal those of the proton acceptors.<sup>13</sup> The first and second right hand members of equation 6 represent, respectively, the Ilkovic fluxes of free hydrogen ions, and of the copper-Enta acid (see ref. 4); the third term represents the contribution of water (as proton donor) in terms of the hydroxyl ions flux (see ref. 13b);  $\bar{n}$  is the mean number of hydrogen ions bound per ion of Enta; it varies with  $p(H)$  (see ref. 8) according to Fig. 8 which was computed using the dissociation constants of Enta acid as determined by Schwarzenbach.<sup>8</sup> The last term in equation 6 can be dropped as long as the interface remains acid. Then the current can be expressed more simply by

$$i\bar{n} = K \left[ D_{H^{1/2}}(H^+) \left\{ 1 + \frac{D_{CuYH^{1/2}}}{D_{H^{1/2}}} K_{CuYH}(CuY^-) \right\} - D_{H^{1/2}}(H^+)_0 \left\{ 1 + \frac{D_{CuYH^{1/2}}}{D_{H^{1/2}}} K_{CuYH}(CuY^-)_0 \right\} \right] \quad (7)$$

where  $K_{CuYH}$  is the stability constant of the copper-Enta acid (see ref. 4) and the diffusion coefficients of copper-Enta anion and copper-Enta acid are assumed to be equal.

(11) As pointed out by O. H. Müller in A. Weissberger, "Physical Methods of Organic Chemistry," Part II, 2nd Ed., 1949, p. 1833, adequate buffering is provided when the concentration of the active partner of the buffer is in a hundred-fold excess over that of the reducible species; the hydrogen ion concentration at the electrode surface should then be within about 1% that of the bulk of the solution. This evaluation is based of course upon the hypothesis of instantaneous attainment of all proton equilibria. In our case a solution of  $10^{-4} M$  copper-Enta in 0.02 M 1:1 acetate buffer exhibits a half-wave potential which corresponds to a concentration of the free Enta ion  $(Y^{4-})_0$  at a  $p(H)$ , by about two  $p(H)$  units more alkaline than in the bulk of the solution (compare Figs. 1 and 7).

(12)  $K_{YHn}$  values at 0.5 ionic strength were reported by S. F. Carini and A. E. Martell, *J. Am. Chem. Soc.*, **74**, 5745 (1952).

(13) Similar relations are to be found in the literature. See, i.e., (a) E. F. Orlemann and I. M. Kolthoff, *ibid.*, **64**, 1044 (1942); (b) P. Ruetschi and C. Trümpler, *Helv. Chim. Acta*, **35**, 1021, 1486, 1957 (1952).

Equations 5 and 7 can be solved graphically for  $(H^+)_0$  and allow calculating the current-potential curve for a particular solution. This curve fits reasonably well the experimental results (see Figs. 2 and 3), considering the approximations introduced by using the Ilkovic equation<sup>13,14</sup> and the assumption of instantaneous equilibria.

The appearance of the double pre-wave can be explained qualitatively as follows. Let us consider a  $10^{-3}$  molar solution of copper-Enta complex at a  $p(H)$  of about 3.5 (see Fig. 2). At this  $p(H)$  the  $\bar{n}$  value will be about two (see Fig. 8). Now as the current increases  $(H^+)_0$  as well as  $(CuYH^-)_0$  will decrease. At a  $p(H) = 5.5$  both will be already negligible as compared with the bulk hydrogen ion and copper-Enta acid concentrations. Until that point the  $\bar{n}$  value will suffer no marked change and consequently the polarographic current will reach a diffusion plateau. As the hydrogen ion concentration at the electrode surface will decrease further,  $\bar{n}$  will start to diminish also, until reaching a new steady value of about one in the  $p(H)$  range 7.5 to 9.5. Thus the current should start to increase again after having reached the first plateau and attain a second one at twice the value of the first diffusion current. This second plateau, however, should be rather indistinct as at  $p(H) 7$  the current will soon further increase due to the  $OH^-$  term in equation 6.

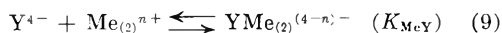
The numerical value of the total height of the prewave should be given by

$$i_{d1,2} = KD_H^{1/2}(H^+) \left\{ 1 + \frac{D_{CuYH^{1/2}}}{D_H^{1/2}} K_{CuYH}(CuY) \right\} \quad (8)$$

This equation is in a good quantitative agreement with the experiment (see Figs. 2 and 3). The first part of the prewave is found to be somewhat higher than was to be expected.

The shift of the half-wave potential of the prewave toward more positive values with decreasing ionic strength (see Experimental results) can be accounted for only qualitatively on the basis of the foregoing discussion.

**C. Wave Splitting in Neutral Unbuffered Solutions of Copper-Enta Complex by Metal Ions.**—If a nearly neutral solution of the copper-Enta complex contains metal ions  $Me_{(2)}^{n+}$  capable of forming stable complexes with Enta, then the following reaction should be considered in addition to reaction 2



In the following we shall neglect the formation of ion pairs between the metal Enta complexes and metal ions, as well as the presence of the  $Me_{(2)}Y$  complex in the bulk of the solution which is appreciable only for lead under our experimental conditions (see ref. 2 and 6). Then the current observed should vary according to

$$i = KD_{MeY}^{1/2} (MeY)_0 - (MeY) - KD_Y^{1/2} (Y^{4-})_0 \mathcal{F}(H^+)_0 \\ \approx KD_{Me}^{1/2} \{ (Me) - (Me)_0 \} - KD_Y^{1/2} \alpha (Y^{4-})_0 \mathcal{F}(H^+)_0 \quad (10)$$

In all cases studied here the metal complexes have

(14) (a) J. Koutecky and R. Brdicka, *Collection Czech. Chem. Commun.*, **12**, 337 (1947); (b) P. Delahay and col., *J. Am. Chem. Soc.*, 1949-1953; (c) P. Delahay *ibid.*, **74**, 3497 (1952); (d) see also ref. 3.

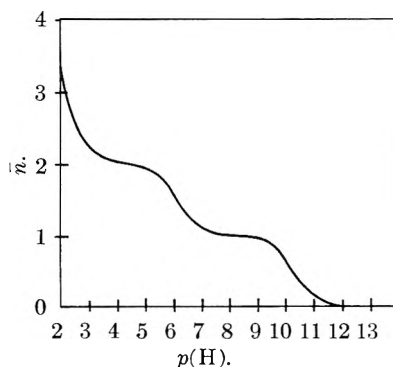


Fig. 8.—The variation of the mean number of hydrogen ions bound per ion of Enta with  $p(H)$ ; calculated according to Schwarzenbach<sup>8</sup> values of the dissociation constants of Enta acid;  $t = 20^\circ$ ,  $\mu = 0.1$ .

stability constants higher than  $10^{10}$  (see ref. 4). In nearly neutral solutions, the reaction of Enta ions (liberated at the drop surface) with hydrogen ions can thus be neglected until the concentration of the metal ions in the interface drops below a very small value. Under those conditions (10) reduces to

$$i \approx KD_{Me}^{1/2} \{ (Me) - (Me)_0 \} \quad (11)$$

According to this equation, the current should reach a steady value, when the metal ion concentration at the interface becomes small in comparison with the concentration in the bulk of the solution. A further increase of the current should then occur due to the increasing contribution of the second term in equation 10. The usual diffusion plateau of the copper-Enta complex should be reached finally. The first diffusion current should be proportional to the metal concentration, in agreement (see ref. 6) with the experiment (see fig. 5).

The wave splitting of course will occur only if the concentration of the metal ion is smaller than the concentration of the copper-Enta complex. As a matter of fact at higher metal concentration a single wave appears, whose half-wave potential shifts toward more positive values with increasing metal ion concentration.

In order to express the potential of the dropping mercury electrode as a function of the current, equation 4 should be substituted by

$$(Y^*)_0 = (MeY)_0 + \sum_0^4 (YH_n)_0 = \{ \mathcal{F}(H^+)_0 + \\ K_{MeY}(Me)_0 \} (Y^{4-})_0 \quad (12)$$

Combining equations 3 and 12 one gets the following simple expression for the half-wave potential of the metal induced wave

$$E_{1/2} = E_1 + 0.029 \log K_{MeY} + 0.029 \log \frac{2i_d - i_{d1}}{i_{d1}} \quad (13)$$

where  $i_{d1}$  is the diffusion current of the metal induced wave. It follows from (13) that the greater the stability constant of the metal ion complex with Enta, the better the separation of the metal induced wave. Actually the shift predicted by equation 13 is only in a rough qualitative agreement with the experiment. Figure 4 shows a half-wave potential separation of about: 250, 190, 160, 140 and 90 mv. for lead, lanthanum, cadmium,

zinc and calcium, respectively, whereas the predicted values are (see ref. 4): 530, 450, 480, 470 and 310 mv.

According to equation 13 the half-wave potential of the metal wave should shift at a constant metal concentration to more positive values with increasing copper-Enta concentrations. At a constant copper-Enta concentration the half-wave potential should shift toward more negative values with increasing metal concentrations. Both predictions are fulfilled at least in a qualitative way (see Fig. 5).

The dependence of the half-wave potential on the ionic strength (see Experimental part) can only partly be accounted for by considering the influence of the ionic strength upon the equilibria involved.

**D. Interference of Reaction Rates in the Polarographic Reduction of the Copper-Enta Complex.**—It seems that at least some of the discrepancies observed between theory and experiment can be attributed to the influence of non-equilibrium conditions in the mercury-solution interface (see ref. 3 and 14a, b, c).

It was found that nickel ion does not produce the wave splitting observed with all other metals studied here. This indicates the possibility that the equilibrium 9 is not very rapid. This possibility is further confirmed by the fact that for all metals studied here the wave splitting is much less

clean at the jet electrode than at the dropping mercury electrode. As pointed out previously<sup>15</sup> at the jet electrode only very fast reactions can manifest themselves fully.

The strong dependence of the half-wave potential upon the buffer concentration indicates that slow proton equilibria in the mercury-solution interface can also interfere kinetically in the observed phenomena. In addition to reactions 2 one should consider here also the dissociation equilibria of the buffer<sup>16</sup> as well as the possibility of a direct reaction between the acid component of the buffer and the Enta ion liberated in the electrode process (see *i. e.*, ref. 16a). Each of these reactions can be slow enough to disturb the overall process.

Finally the rather strong dependence of the half-wave potential upon the ionic strength could be interpreted partly at least in terms of the Bjerrum-Brønsted concept of ionic reactions: the increase of the ionic strength accelerating or retarding the rates according to the charges of the reaction partners.<sup>17</sup>

(15) (a) J. Heyrovsky and J. Forejt, *Z. physik. Chem.*, **193**, 77 (1943); (b) see also ref. 2.

(16) (a) C. R. Castor and J. H. Saylor, *J. Am. Chem. Soc.*, **75**, 1427 (1953); (b) O. H. Müller, *ibid.*, **62**, 2434 (1940); (c) see also ref. 14c.

(17) See, *i. e.*, S. Glasstone, K. J. Laidler and H. Eyring, "The Theory of Rate Processes," McGraw-Hill Book Co., Inc., New York, N. Y., 1941, Chapter VIII.

## THE ADSORPTION OF GASES ON CALCIUM FLUORIDE<sup>1</sup>

BY HAROLD EDELHOCH AND HUGH S. TAYLOR

*Frick Chemical Laboratory, Princeton University, Princeton, N. J.*

*Received November 27, 1953*

Isotherms of argon and oxygen, nitrogen and carbon monoxide, xenon and propane, in the neighborhood of liquid oxygen and nitrogen boiling points, on sintered and ground calcium fluoride powders have been determined. Marked inflections in the isotherms for argon and oxygen were found. Nitrogen and carbon monoxide conformed to the BET equation (Type II). With xenon and propane the data fall on a single smooth curve of adsorbed volume *versus* relative pressure. The data have been examined in terms of two-dimensional changes of state, horizontal interactions and derived thermodynamic data.

Recently, Young and Tompkins<sup>2,3</sup> examined and augmented the observations and calculations of Orr<sup>4</sup> pertaining to the interactions of gases with surfaces possessing periodic structures, such as ionic crystals. In a re-evaluation of Orr's work with non-polar gases on CsI, Tompkins and Young<sup>3</sup> suggest that adsorption was taking place on the (110) plane of CsI. As adsorption progressed to the more uniform parts of the surface, horizontal interaction effects became significant and the localized (square) array of molecules condensed to an hexagonally close-packed layer. This rearrangement in molecular orientation was associated with a phase change. These events con-

tribute an additional heat term based on lateral interactions to the predominant one occurring between the adsorbed molecules and the adsorbent. If the latter heat effects are sensibly constant, a maximum in the heat curve will be evident.

Crawford and Tompkins<sup>5</sup> have measured the adsorption of polyatomic molecules on BaF<sub>2</sub> and CaF<sub>2</sub>. They have concluded that the adsorbed molecules formed a localized layer on the crystal planes with their distribution fixed by the lattice structure of the adsorbent.

The nature of the adsorbed phase has received considerable attention, notably by Hill,<sup>6</sup> Gregg,<sup>7</sup> and Jura and Harkins.<sup>8</sup> The latter have postu-

(1) Abstracted from a thesis by Harold Edelhoch, presented in partial fulfillment of the requirements for the Ph.D. degree in Princeton University, 1947.

(2) D. M. Young, *Trans. Faraday Soc.*, **47**, 1228 (1951); **48**, 548 (1952).

(3) F. C. Tompkins and D. M. Young, *ibid.*, **47**, 77 (1951).

(4) W. J. C. Orr, *ibid.*, **35**, 1247 (1939); *Proc. Roy. Soc. (London)*, **A173**, 349 (1939); J. K. Roberts and W. J. C. Orr, *Trans. Faraday Soc.*, **34**, 1346 (1938).

(5) V. A. Crawford and F. C. Tompkins, *ibid.*, **44**, 698 (1948); **46**, 504 (1950).

(6) T. L. Hill, *J. Chem. Phys.*, **14**, 441 (1946); **15**, 767 (1947); **17**, 520 (1949). For a critical review of physical adsorption theory see chapter by T. L. Hill, in "Advances in Catalysis," Academic Press, Inc., New York, N. Y., 1952.

(7) S. J. Gregg, in "Surface Chemistry," Butterworths Scientific Publications, London, 1949.

(8) G. Jura and W. D. Harkins, *J. Am. Chem. Soc.*, **68**, 1941 (1946).

lated a one to one correspondence between the various states of adsorbed gases with those of insoluble films on liquid subphases. Principally employing organic vapors and working near room temperature, they have noted many cases of discontinuities and inflections in their isotherms which they related to two-dimensional phase transitions.<sup>9</sup> Halsey<sup>10</sup> has considered the mechanics of isothermal adsorption processes revealing inflections, etc., in terms of cooperative phenomena.

The following paper presents the results of measurements of the adsorption of a series of gases on a single sintered and ground surface of CaF<sub>2</sub>. These results are similar to those observed by Orr<sup>1</sup> and Ross.<sup>11</sup> A recent report by Ross<sup>12</sup> offers confirmatory evidence of the presence of discontinuities and inflections in physical adsorption isotherms.

### Experimental

**Materials.**—Nitrogen, oxygen, argon and xenon were commercial preparations of the "spectroscopically pure" grade. These gases were used directly from their glass containers. Carbon monoxide, propane, helium and methane were of tank origin and were dried by passing through a CaCl<sub>2</sub>, ascarite and P<sub>2</sub>O<sub>5</sub> train. Propane was fractionally distilled several times in the all-glass manifold. Helium was purified further by passing over copper at 500°, CuO at 300°, and activated carbon at -195°.

Ethyl iodide and ethyl ether were standard materials of reagent grade and were used without further treatment. Solid CO<sub>2</sub> was purchased locally.

Baker's C.P. grade of CaF<sub>2</sub> was used. A small sample was sintered at 410° for two hours in a stream of hydrogen and then milled in a stone ball mill for 12 minutes at room temperature. All measurements in this paper were performed on this sample (no. 1, Table I) except those included in Fig. 2. These latter samples (no. 2-5, Table I) of CaF<sub>2</sub> differed only in variation of the sintering temperature and the grinding time.

TABLE I

EFFECTS OF SINTERING AND GRINDING ON ADSORPTIVE CAPACITY AND MAGNITUDE OF INFLECTIONS

| Sample no. | Sintering temp., °C. | Grinding time, min. | Surface area, <sup>a</sup> m. <sup>2</sup> /g. |
|------------|----------------------|---------------------|--|
| 1          | 410                  | 12                  | (9.6) <sup>b</sup>                             |
| 2          | 250                  | 0                   | 14.1   |
| 3          | 500                  | 4000                | 4.9  |
| 4          | 500                  | 100                 | 2.8  |
| 5          | 850                  | 200                 | 0.8  |

<sup>a</sup> Surface areas calculated by using "B" point method for definition of monolayer coverage. <sup>b</sup> Determined from  $V_m$  of nitrogen isotherm.

**Methods. A. Preparation of Constant Temperature Baths.**—Liquid oxygen and methane were prepared by condensing tank gases in Pyrex tubes, suspended in a thermos flask containing liquid nitrogen. Freezing mixtures of ethyl iodide and of ethyl ether were obtained by cooling with liquid nitrogen until a viscous two phase mixture of solid-liquid resulted.

**B. Temperature Control and Measurement.**—Nitrogen, oxygen, argon and carbon monoxide isotherms were measured at liquid nitrogen and oxygen temperatures. Temperature fluctuations during experiments were followed with an oxygen vapor pressure thermometer. Where small temperature changes were observed average values were used for determining the saturated vapor pressures ( $p_0$ ). Acetone-CO<sub>2</sub> mixtures provided temperature control for the propane run.

(9) G. Jura, W. D. Harkins and E. H. Loeser, *J. Chem. Phys.*, **14**, 344 (1946); G. Jura, E. H. Loeser, P. R. Basford and W. D. Harkins, *ibid.*, **14**, 117 (1946).

(10) G. Halsey, *ibid.*, **16**, 931 (1948).

(11) S. Ross, *J. Am. Chem. Soc.*, **70**, 3830 (1948).

(12) S. Ross, *ibid.*, **75**, 6081 (1953).

**C. Adsorption Measurements.**—An all glass adsorption apparatus of conventional design gave pressures to 10<sup>-6</sup> mm. Adsorption pressures were read from a mercury manometer. Adsorption isotherms were obtained by the successive addition of small increments of gas to an adsorption chamber at constant volume and temperature. All adsorption measurements attained equilibrium within the time required to adjust the mercury level and read the manometer.

### Results

**Argon and Oxygen.**—Four independent runs including three adsorption and one adsorption-desorption, were performed on sample no. 1 to verify the reproducibility and reversibility of the adsorption behavior of argon near 79°K. This series of experiments is summarized in Fig. 1, and Table II contains a sample of the experimental points collected from the three adsorption isotherms. The magnitude of the inflections could be modified appreciably by varying the sintering and/or grinding treatment of the CaF<sub>2</sub>. These samples were treated under the conditions listed in Table I and their isotherms appear in Fig. 2. The relative pressure and coverage at the inflection point appear to remain moderately constant with the change in surface area incurred by the sintering process. A complete isotherm of sample 5 (to  $p/p_0 \sim 0.95$ ) resembled Type II in Brunauer's classification<sup>13</sup> and showed very little, if any, inflection. Argon isotherms at several temperatures on CaF<sub>2</sub> sample no. 1 appear in Fig. 3.

TABLE II

SAMPLE OF ARGON ADSORPTION DATA AT 78.8°K. ON 410°-SINTERED CaF<sub>2</sub>

$$V_m = 2.66 \text{ cc. (S.T.P.)}, P_0 = 24.4 \text{ cm.}$$

| $V_1$<br>cc. S.T.P. | $P_1$<br>cm. | $\theta$ | $\log \frac{\theta}{1-\theta}$ | $V_1$<br>cc. S.T.P. | $P_1$<br>cm. | $\theta$ | $\log \frac{\theta}{1-\theta}$ |
|---------------------|--------------|----------|--------------------------------|---------------------|--------------|----------|--------------------------------|
| 0.336               | 0.32         | 0.126    | -0.84                          | 1.87                | 1.68         | 0.702    | 0.373                          |
| .456                | .49          | .171     | -.69                           | 2.10                | 1.93         | .787     | .570                           |
| .635                | .88          | .238     | -.50                           | 2.27                | 2.32         | .850     | .754                           |
| .750                | 1.10         | .282     | -.40                           | 2.35                | 2.86         | .880     | .866                           |
| .882                | 1.29         | .330     | -.31                           | 2.46                | 3.42         | .922     | 1.073                          |
| .941                | 1.39         | .353     | -.26                           | 2.48                | 3.71         | .932     | 1.137                          |
| 1.32                | 1.54         | .495     | -.008                          | 2.62                | 4.95         | .980     | 1.690                          |
| 1.65                | 1.66         | .620     | .213                           | 2.66                | 5.35         | 1.00     |                                |

When oxygen was substituted as the adsorbate, substantially similar effects to those observed with argon were evident (see Fig. 4).

**Nitrogen and Carbon Monoxide.**—The isotherms observed with nitrogen and carbon monoxide as adsorbates appear in Fig. 5. The adsorption data fit well the usual BET plots from which a surface area of 9.6 m.<sup>2</sup>/g. has been calculated, using 16.2 Å.<sup>2</sup> as the cross-sectional area of nitrogen.<sup>14</sup> To calculate the surface coverage ( $\theta$ ) with argon,

TABLE III

BET PARAMETERS

| Adsorbate                     | $V_m$<br>cc. (S.T.P.) | $C$  | $E_1$<br>kcal./mole | $E_L$<br>kcal./mole |
|-------------------------------|-----------------------|------|---------------------|---------------------|
| N <sub>2</sub>                | 2.35                  | 1700 | 2.5                 | 1.33                |
| CO                            | 2.68                  | 750  | 2.5                 | 1.41                |
| Xe                            | 1.19                  | 2.6  | 3.5                 | 3.25                |
| C <sub>3</sub> H <sub>8</sub> | 0.60                  | 5.2  | 8.2                 | 7.55                |

(13) S. Brunauer, "Adsorption of Gases and Vapors," Princeton University Press, Princeton, 1943, p. 150.

(14) P. H. Emmett and S. Brunauer, *J. Am. Chem. Soc.*, **69**, 1553 (1937).

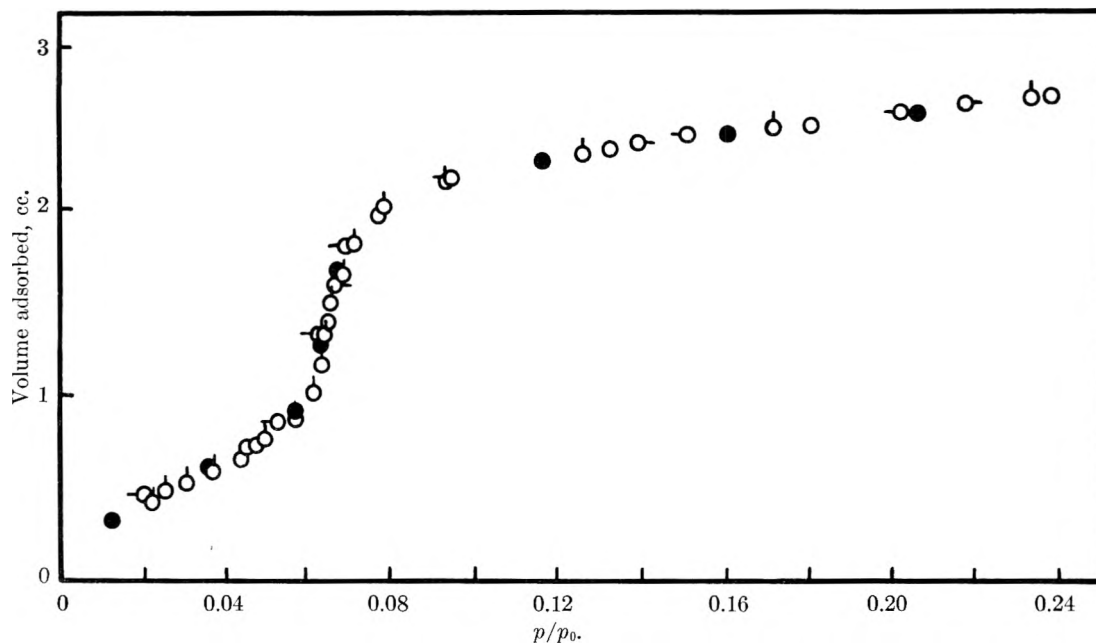


Fig. 1.—The results of three independent adsorption runs and one adsorption-desorption run of argon on  $\text{CaF}_2$  at  $78.8^\circ\text{K}$ .  
 ●, ○, ◇, □, represent the adsorption-desorption points, respectively.

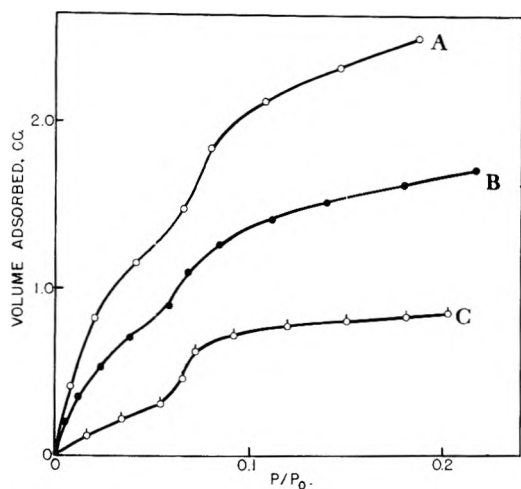


Fig. 2.—Argon adsorption isotherms near  $79^\circ\text{K}$ . on sintered  $\text{CaF}_2$  samples of different surface areas: sample no. 2, ○ (A); 3, ● (B); 4, ◇ (C).

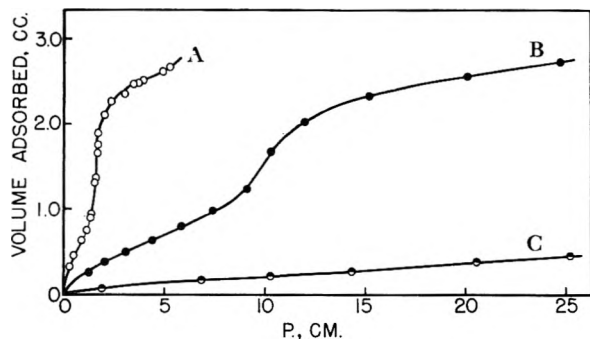


Fig. 3.—Variation of argon adsorption with temperature: (A) ○,  $78.8^\circ$ ; (B) ●,  $89.7^\circ$ ; (C) ●,  $112^\circ\text{K}$ .

$V_m$  (monolayer volume) was obtained by adjusting the nitrogen value of  $V_m$  (see Table III) by the ratio of cross-sectional areas for the two gases, *i.e.*,  $16.2/14.4$ .<sup>14</sup>

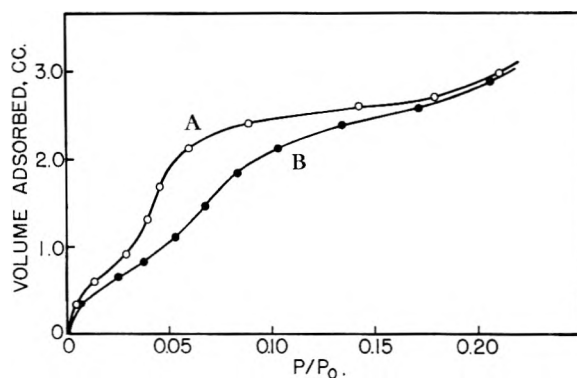


Fig. 4.—Oxygen adsorption isotherm on  $\text{CaF}_2$  plotted against relative pressure: (B) ●,  $89.5^\circ\text{K}$ .; (A) ○,  $78.0^\circ\text{K}$ .

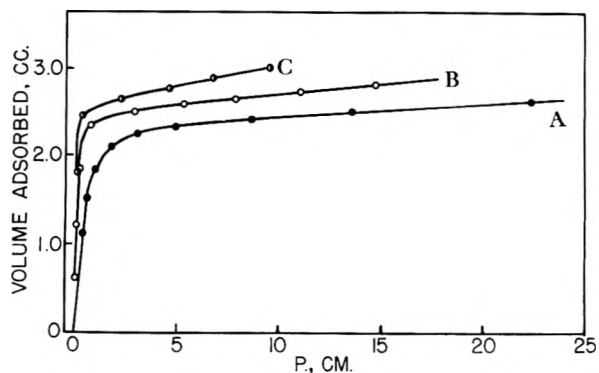


Fig. 5.—Isotherms of nitrogen at:  $78.3^\circ$ , ● (A);  $89.8^\circ\text{K}$ ., ○ (B), and carbon monoxide at  $77.9^\circ\text{K}$ ., ● (C).

**Xenon and Propane.**—Xenon isotherms were measured at three temperatures. All the data could be fitted by a single smooth curve when the adsorbed volume was plotted against relative pressure, as shown in Fig. 6. The results of a propane isotherm, extending close to saturation pressure, are shown in Fig. 7.

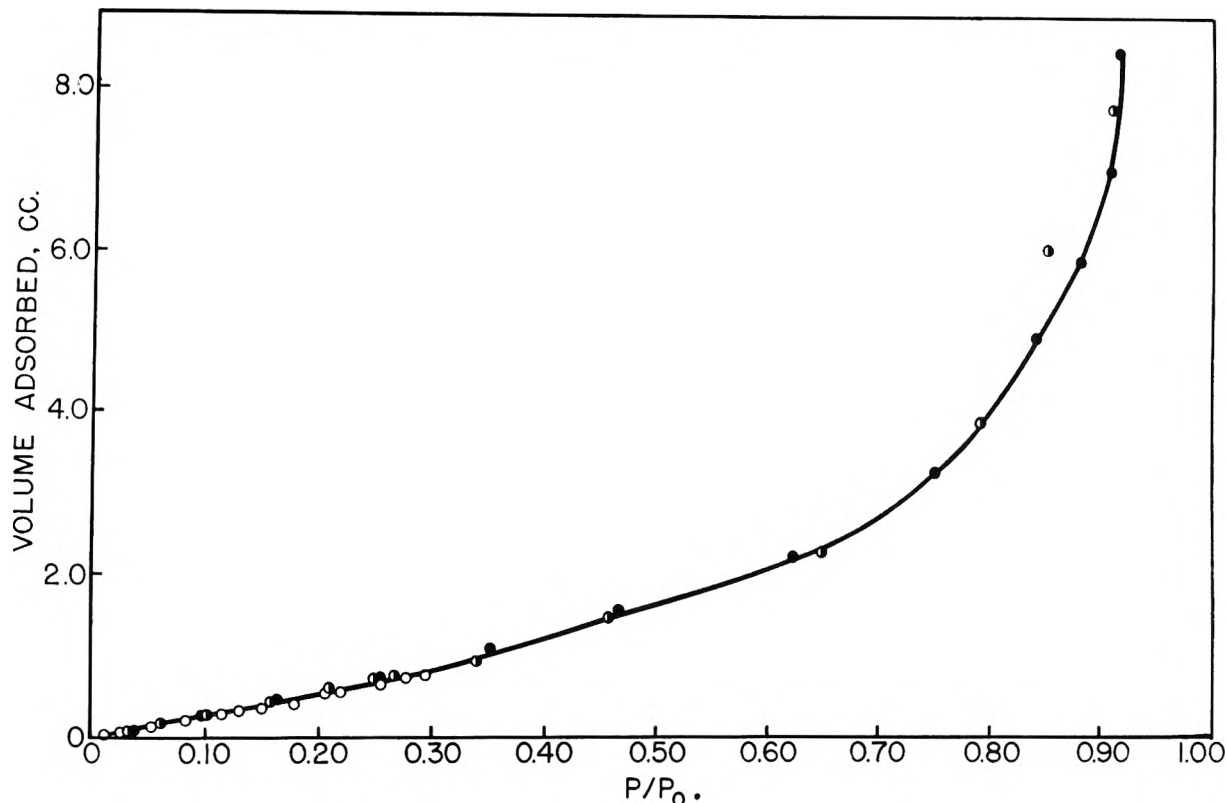


Fig. 6.—Xenon adsorptions plotted against relative pressures: ●, 157.0°K.; ◐, 161.0°K.; ○, 189.2°K. The points at 161.0° and 189.2°K. represent the sum of two independent isotherms obtained under identical conditions.

**Thermodynamic Calculations.**—Since important information concerning the mechanism of adsorption processes may be acquired from considerations of heat and entropy contributions to the free energy, isotherms for argon, nitrogen and xenon were measured at several temperatures. The differential thermodynamic constants of adsorption for these gases on  $\text{CaF}_2$ , as a function of coverage, have been computed from equations (1, 2 and 3)<sup>15</sup> and are shown in Figs. 8, 9, 10, respectively. The saturated vapor pressures were taken as the standard state.

$$H_G - \bar{H}_S = \frac{1}{RT^2} \left( \frac{\partial \ln p}{\partial T} \right)_\theta \quad (1)$$

$$F_G - \bar{F}_S = RT \ln p_0/p \quad (2)$$

$$S_G - \bar{S}_S = (H_G - \bar{H}_S) - (F_G - \bar{F}_S)/T \quad (3)$$

### Discussion

**Test of Adsorption Equations.**—From the work of Hill,<sup>6</sup> Tompkins and Young,<sup>3</sup> Gregg,<sup>7</sup> and Jura and Harkins,<sup>8</sup> it is evident that a two-dimensional change of state occurs with argon and oxygen in the region where the isotherm shows an inflection. Accordingly, those theories of adsorption that neglect to account for the possibility of horizontal interactions, phase changes and coöperative effects will be incapable of representing the adsorption data.<sup>16</sup> Since the BET theory does not provide for these contingencies, it will fail.

(15) T. L. Hill, *J. Chem. Phys.*, **17**, 520 (1949).

(16) O. Theimer (*Trans. Faraday Soc.*, **48**, 326 (1952)) has presented an interesting discussion of the adsorbent surface properties requisite for fulfillment of the BET theory.

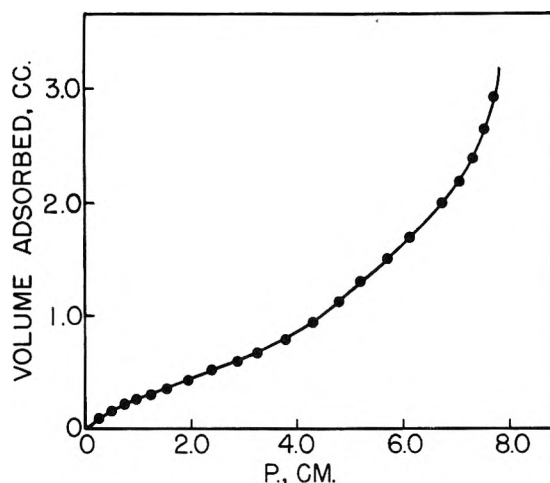


Fig. 7.—Complete propane adsorption isotherm on  $\text{CaF}_2$  at 193°K.

A solution to the problem of nearest neighbor interactions for localized molecules on a uniform surface is the quasi-chemical approximation<sup>17</sup>

$$p = p^0 \frac{\theta}{1-\theta} \exp - \left( \frac{2w\theta}{kT} \right) = p^0 \frac{\theta}{1-\theta} \exp - (\alpha_1\theta) \quad (4)$$

where  $p$  is the gas pressure,  $\theta$ , the fraction of sites occupied by molecules,  $k$ , the gas constant,  $T$ , the temperature,  $w$ , the interaction energy of two adsorbed molecules on nearest neighbor sites and  $p^0$  is a constant at a particular temperature.

(17) See R. H. Fowler and E. A. Guggenheim, "Statistical Thermodynamics," Cambridge University Press, Cambridge, 1939, Chapter 10.

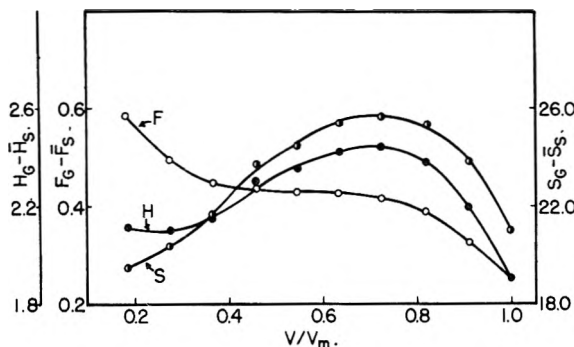


Fig. 8.—Differential thermodynamic functions of argon calculated from 78.8 and 89.7°K. isotherms.

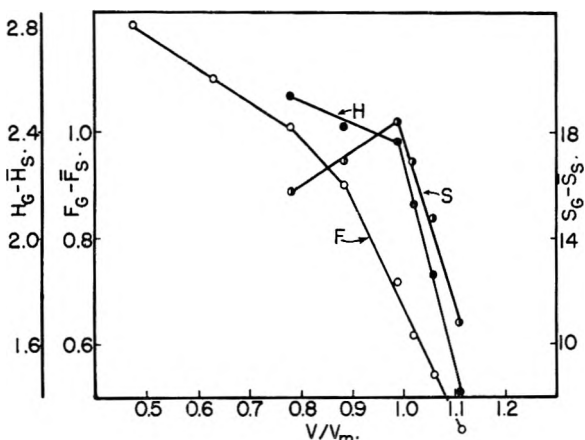


Fig. 9.—Differential thermodynamic functions of nitrogen on  $\text{CaF}_2$ .

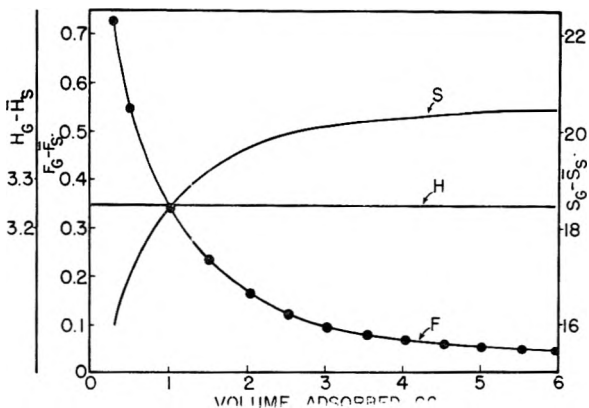


Fig. 10.—Differential thermodynamic functions of xenon on  $\text{CaF}_2$  ( $V_m = 1.19$  cc. STP).

If  $\log p$  is compared with  $\log \theta / 1 - \theta + \alpha_1 \theta$  a rectilinear relationship should result with a slope of unity. When  $\alpha_1 = 0$  equation 4 reduces to the Langmuir isotherm equation. The influence of several values of  $\alpha_1$  on the argon data at 78.8°K. is shown in Fig. 11.

Hill, employing an equation of state for a two-dimensional van der Waals gas, has derived equation 5 for adsorption on most of the first layer.

$$xC = \frac{\theta}{1 - \theta} \exp\left(\frac{\theta}{1 - \theta} - \alpha\theta\right) \quad (5)$$

where  $x = p/p_0$ ;  $\theta = Nb'/A = V/V_m$ ;  $C = \text{constant} \exp(\epsilon_1 - \epsilon_L)/RT$ ;  $\alpha = 2a'/b'kT$ ,  $p$  is the pressure and  $p_0$  the saturated pressure;  $V$

is the adsorbed volume and  $V_m$  is the volume of gas necessary to form a unimolecular volume on the adsorbent surface;  $A$  is the adsorbent surface area;  $a'$  and  $b'$  are two-dimensional van der Waals constants;  $-\epsilon_1$  and  $-\epsilon_L$  represent the potential energy of a molecule in the first layer and the potential energy of molecules in higher layers, respectively.

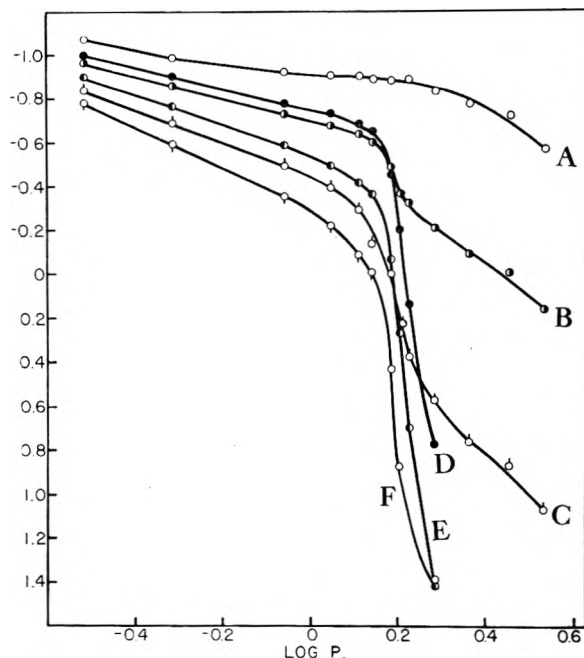


Fig. 11.—Langmuir, van der Waals and Lennard-Jones and Devonshire plots of argon adsorption data at 78.8°K. The ordinate has the following significance: Langmuir plot,  $\log \theta / (1 - \theta)$ ,  $\circ$  (C); quasi-chemical approximation,  $\log \theta / (1 - \theta) - 0.435 \alpha_1 \theta$ ;  $\alpha_1 = 2.30$ ,  $\bullet$  (B);  $\alpha_1 = 4.14$ ,  $\circ$  (A); van der Waals plot,  $\log \theta / (1 - \theta) + 0.435 (\theta / (1 - \theta - \alpha\theta))$ ;  $\alpha = 0, \circ$  (F);  $\alpha = 2.3$ ,  $\bullet$  (E);  $\alpha = 4.14$ ,  $\bullet$  (D).

Figure 11 shows the results of applying equation 5 to the argon data with the same three values of the attractive interaction parameter ( $\alpha$ ) as was employed with equation 4. It is apparent from inspection of the curves in Fig. 11 that neither the quasi-chemical nor van der Waals approximations offer much hope in characterizing the argon adsorption data. Similar interpretation proved inadequate for the 89.8°K. argon isotherm data.

**Two-dimensional Critical Constants.**—Hill<sup>6</sup> has explored some of the properties of the isotherm which can be derived from Devonshire's two-dimensional analog of the Lennard-Jones and Devonshire (LJD) equation of the liquid state. Inspection of the argon isotherm at 78.8°K. suggests a closer correlation with the LJD theory, in that the critical area ( $\theta_c$ ) appears to be nearer the LJD value of 0.71 than the 0.33 value of van der Waals theory, or the 0.50 value of the quasi-chemical analysis.

Since so few two-dimensional critical constant data are available, especially for permanent gases, it seemed of interest to compute these quantities for argon. Actually, judging from the steepness of the inflection argon shows at 78.8°K., it appears

to be sufficiently close to critical behavior to yield critical constant data of some significance.

To calculate surface pressures by the Bangham-Gibbs equation very low pressure isotherm data should be available. These data are lacking in the argon isotherms. Since the initial slope is relatively small, it was considered that this region could be represented by a suitable extrapolation, for computational purposes. A quadratic extrapolation of the low pressure argon data to zero pressure was performed. Surface pressures ( $\phi$ ) were calculated, using Hill's notation<sup>15</sup> as in equation 6, by numerical integration of the isotherm data and these appear in Fig. 12. Critical

$$\phi = KkT \int_0^p V d \ln p \quad (6)$$

constants, recorded in Table IV, correspond to values of  $\phi$  and  $A/N$  at the maximum in the compressibility ( $\beta$ ) curve of equation 7<sup>7</sup>

$$\beta = \frac{A}{RT} \frac{1}{V^2} \frac{dV}{d \ln p} \quad (7)$$

Also listed in Table IV are the theoretical critical constant values of van der Waals and LJD theory.

TABLE IV  
ARGON CRITICAL CONSTANTS

|   | $T_c$ ,<br>°K. | $\phi_c$ ,<br>dynes/cm. | $A_c/N$ ,<br>Å. <sup>2</sup> |
|---|----------------|-------------------------|------------------------------|
| This paper                                | 78.8           | 3.9                     | 25                           |
| van der Waals <sup>a</sup>                | 75             | 0.9                     | 35                           |
| Lennard-Jones and Devonshire <sup>a</sup> | 79             | 1.9                     | 26                           |

<sup>a</sup> The expressions for the critical constants of van der Waals and Lennard-Jones and Devonshire two-dimensional equations of state were taken from reference 9.

The critical constant values for argon are in best accord with LJD theory. In view of the strong periodic surface forces and equivocal planar structure prevailing on the surface of the doubly charged ionic adsorbent, further speculations hardly seem warranted.

**Comparison of Gases.**—It is manifest from Fig. 4 that oxygen parallels argon in its adsorption characteristics on CaF<sub>2</sub>. This was to be expected since the cross-sectional areas and potential energy curves of oxygen and argon are very similar. Orr<sup>4</sup> found that the behavior of these two gases on KCl (and CsI) was almost identical. He observed that the characteristic maxima in the  $\Delta H-\theta$  curves differed by approximately 100 calories, while the adsorbed volumes were only  $\sim 1\%$  displaced from each other. Our results show a variation of about 50 calories in heat and less than 1% in volume for these two gases. The oxygen isotherms bear a close resemblance to those of argon but are of less general interest since they lack the sharp vertical inflection noted with argon. For this reason, calculations and discussion have been concentrated on argon.

Nitrogen and carbon monoxide show more typical behavior and constitute a second type of adsorption on CaF<sub>2</sub>. As with argon and oxygen, their size and potential energy parameters closely resemble each other. They are more strongly adsorbed, and evidently do not show the pronounced inflections at comparable coverages found with

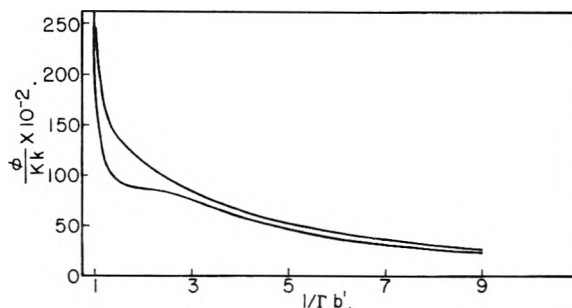


Fig. 12.—Surface pressure-area curves of argon at 78.8° (lower curve) and 89.7°K. (upper curve), following Hill,<sup>6</sup>  $K = 1/V_m b^1$ ;  $\Gamma = N_s/A$ .

argon and oxygen. This may be a reflection of the fact that the nitrogen and carbon monoxide isotherms are considerably above their two-dimensional critical temperatures ( $T_{2c} \sim 0.5T_{3c}$ ). However, it should be noted that the first observation for nitrogen at 89.8°K. occurred at about  $1.1 \times 10^{-3}x$  and  $0.45\theta$  (see Fig. 5). If adsorbed nitrogen formed a van der Waals layer, the critical pressure and area constants would occur near  $5 \times 10^{-3}x_c$  and  $\theta_c/3^6$ .

Although Orr<sup>4</sup> groups nitrogen in the same class with argon and oxygen for KCl and CsI as adsorbents, he states, "In some unpublished, adsorption experiments on LiCl, nitrogen and carbon monoxide isotherms behaved very similarly and differed quite markedly from the shape of the argon isotherms." In the present series on CaF<sub>2</sub>, a similar division was found.

From theoretical arguments Orr has concluded that the maximum in the heat curve coincided with the completion of a monolayer. If the  $V_m$  calculated for nitrogen by BET theory is adjusted by the ratio of the diameters of nitrogen and argon, the maximum in the heat curve occurs at  $0.72\theta$  for argon (and for oxygen). The nitrogen value of  $V_m$  is supported by the sharp change in the shape of its heat curve at this value (see Fig. 9), as would be expected for strongly adsorbed molecules.<sup>18</sup>

These results may be compared with observations by Keenan and Holmes<sup>20</sup> of argon adsorption on KCl where a maximum in the heat curve occurred at 70% of the BET  $V_m$  value. In fact, Tompkins and Young<sup>3</sup> have calculated for weakly adsorbed oxygen on CsI at 80°K. (BET value of  $C = 200$ ) that the maximum in the heat curve should occur at 80–85% of the BET value. With higher values of  $C$ , as observed with nitrogen and carbon monoxide, a more abrupt change in  $\Delta H$  should occur close to a  $\theta$  value of unity. By

(18) There is some evidence<sup>19</sup> indicating that on crystal faces containing a particular geometry (i.e., 100 face of Cu) nitrogen may be oriented with its long axis normal to the surface. If this occurs on CaF<sub>2</sub>, then the maximum in the heat curves would occur close to  $\theta \approx 1$  if we use Rhodin's suggested value of 12.2 Å, as the cross-sectional area of nitrogen.

(19) T. N. Rhodin, Jr. in "Advances in Catalysis," Vol. 5, Academic Press, Inc., New York, N. Y., 1953.

(20) A. G. Keenan and J. M. Holmes, THIS JOURNAL, 53, 1309 (1949). The surface areas of Keenan and Holmes' samples of KCl, calculated from the nitrogen isotherms, are about 20% smaller than those obtained from argon (and oxygen). Hence if the nitrogen surface areas were used with the argon adsorption data, the maximum in the heat curve would appear much closer to monolayer coverage.

considering the adsorbed volume at the point of maximum slope in the heat curve as the termination of monolayer coverage, Tompkins and Young were able to obtain consistent values for the surface area of CsI based on the cross-sectional areas of argon, oxygen, nitrogen and carbon monoxide.

All the xenon data may be fitted by a single curve when the adsorbed volume was plotted against relative pressure. The BET theory describes this type of adsorption when  $C$  is close to 1, *i.e.*, Type III in Brunauer's classification.<sup>13</sup> Consequently the heat of adsorption is of the same magnitude as the heat of liquefaction. From a consideration of the compressibility curves of the various types of isotherms depicted by Brunauer, Gregg and Jacobs<sup>21</sup> deduce that with the Type III isotherm the adsorbed gas molecules do not tend to complete a first layer and therefore are not likely to show phase transformations.

**Thermodynamic Considerations.**—The adsorption isotherms of argon, nitrogen and xenon on a single sample of sintered and ground  $\text{CaF}_2$  represent three divergent types of adsorptive behavior. Each gas possesses a distinctive thermodynamic pattern in all three functions, *i.e.*, free energy, heat and entropy. It should be noted that the nitrogen data are limited to the region near the completion of the monolayer; the argon and xenon data include observations on most of the first adsorbed layer, while xenon adsorption also extends considerably into the multilayer region.

The free energy curves of nitrogen and xenon appear to change monotonically with surface coverage, with increasing and decreasing slopes, respectively. Argon free energy changes, however, pass through a broad region with a slope near zero, indicative of a phase change.

Similarly, the isosteric heat curves of each gas are characteristic of each type of adsorption process. As already mentioned, the nitrogen heat curve displays a sharp change in slope close to the completion of a monolayer, while the heat curve of xenon remains essentially invariant over several layers of gas adsorption.<sup>22</sup> Argon, however, ex-

hibits a broad maximum which cogently reflects the magnitude of the horizontal interactions between adsorbed molecules.

Maxima in heats of adsorption have been reported for a number of gases on a variety of surfaces.<sup>23-25</sup> With nitrogen on graphon<sup>23,24</sup> the maxima in the heat curve occurred at  $\sim 0.70-0.75\theta$ . With krypton<sup>25</sup> on nylon, polyethylene and collagen, a multiplicity of heat effects were encountered in the first layer. For all these systems the BET equation was found applicable. The free energy in most instances decreased almost monotonically without any evidence of a phase transformation.

A comprehensive, detailed study of the variation of heats with coverage for specified faces of single crystal surfaces of copper and zinc has been presented by Rhodin.<sup>26,27</sup> Maxima in the heat curves have been observed close to monolayer coverage. These maxima were ascribed to lateral interaction effects and are significantly greater in magnitude than those observed by us for argon and oxygen. Considerable evidence, both from consideration of packing and coordination numbers between surface atoms and adsorbed atoms and from energetics (variation of intensity of maxima with crystal face) is suggestive of localized adsorption on specific lattice sites. It is of interest to find localized adsorption accompanied by strong lateral interactions with no evidence of an inflection or phase change. It is also apparent that the BET equation (but not the assumptions) readily fits the data since Rhodin found agreement with theory from  $p/p_0 = 0.05$  to  $0.40$ .<sup>19</sup>

**Acknowledgments.**—Our best thanks are expressed to Dr. George G. Joris, who assisted considerably in the supervision of this project. The work was carried out during World War II with the facilities made available by the Manhattan District Project under Contract No. W7405—Eng 98 at Princeton University.

157–161°K. isotherms average about five times as great as when employing the 189°K. isotherm. The heat range of the second cc. of adsorbed gas is  $3600 \pm 300$  cal./mole. Above the second cc. the calculated heats remain surprisingly uniform at  $3200 \pm 50$  cal./mole. In view of these minor discrepancies a single average value of 3250 cal./mole has been assumed for the heat of adsorption of xenon for the entire isotherm.

(23) R. A. Beebe, J. Biscoe, W. R. Smith and C. B. Wendell, *J. Am. Chem. Soc.*, **69**, 95 (1947).

(24) L. G. Joyner and P. H. Emmett, *ibid.*, **70**, 2353 (1948).

(25) A. C. Zettlemyer, A. Chand and E. Gamble, *ibid.*, **72**, 2752 (1950).

(26) T. N. Rhodin, Jr., *ibid.*, **72**, 5691 (1950).

(27) T. N. Rhodin, Jr., *This Journal*, **57**, 143 (1953).

(21) S. J. Gregg and J. Jacobs, *Trans. Faraday Soc.*, **44**, 574 (1948).

(22) The heat of adsorption of xenon on  $\text{CaF}_2$ , for  $V = 0.04$  to  $0.80$  cc. ( $V_m = 1.19$  cc.), calculated from either the 157–189°K. or 161–189°K. isotherms fall in the range  $3250 \pm 50$  cal./mole; the 157–161°K. isotherm data give values of  $3400 \pm 100$  cal./mole. 0.80 cc. represents the limit of the 189°K. isotherm data. Above this volume the experimental curves diverge from linearity and interpolation of pressure values becomes less precise. Moreover, for a given error in a pressure value, the error in the heat values calculated from the

THE STABILITY OF SiO SOLID AND GAS<sup>1</sup>BY LEO BREWER AND RUSSELL K. EDWARDS<sup>2</sup>*Department of Chemistry and Radiation Laboratory, University of California, Berkeley, California**Received December 1, 1953*

There is considerable confusion in the literature in regard to the properties of SiO solid and to the question of its thermodynamic stability. The available data have been critically reviewed and experiments designed to clarify the behavior of SiO. The conclusions reached may be summarized as follows: A mixture of Si and SiO<sub>2</sub> will vaporize to form pure SiO gas which has a  $\Delta H_{298}^\circ$  of formation of  $-21,411 \pm 570$  cal. or a dissociation energy to the gaseous atomic elements of  $169,300 \pm 3100$  cal. SiO<sub>2</sub> vaporizes under neutral conditions predominately to SiO and O<sub>2</sub> gases. Solid SiO may be prepared in a metastable amorphous or poorly crystallized form by condensation of SiO gas upon a cold surface. The most characteristic property of this solid, useful in its identification, is an electron or X-ray diffraction ring corresponding to a d-spacing of  $3.60 \pm 0.05$  Å. SiO is found to be optically isotropic and X-ray data indicate a cubic symmetry for the better crystallized samples. This solid is completely soluble in HF and is believed to have an average heat capacity at constant pressure of  $9.19 \pm 0.16$  cal./deg./mole in the region of 338°K. The metastable SiO solid prepared by quenching of SiO gas begins to disproportionate to Si and SiO<sub>2</sub> at an appreciable rate at around 400–700°. SiO solid appears to be thermodynamically unstable at all temperatures below 1450°K. Experimental evidence is offered which indicates that at some higher temperature SiO solid becomes stable with respect to Si and SiO<sub>2</sub> and has a melting point higher than 1975°K.

**Stability of SiO Gas.**—The existence of gaseous SiO has been established unequivocally by spectroscopic investigations.<sup>3–7</sup>

The first recognition of the chemical importance of the gaseous molecule SiO was by Potter<sup>8,9</sup> who found that a sublimate of the composition SiO could be obtained by heating mixtures of Si and SiO<sub>2</sub>. Since then five<sup>10</sup> different pairs of investigators have studied equilibria involving gaseous SiO and their data allow one to calculate the heat of formation of SiO gas. The data have been evaluated, using the free energy functions tabulated as a function of temperature by the National Bureau of Standards<sup>11</sup> for Si (solid), H<sub>2</sub>(gas), O<sub>2</sub> (gas) and H<sub>2</sub>O (gas).

In the calculations which are to follow, the free energy functions for SiO<sub>2</sub> (tridymite and cristobalite) were obtained by combining the values of  $S_T^\circ - S_{298}^\circ$  and  $H_T^\circ - H_{298}^\circ$  from Kelley<sup>12</sup> with the values of  $S_{298}^\circ$  listed by Kelley,<sup>13</sup> and the following  $H_{298}^\circ - H_0^\circ$  values which were obtained by graphical inte-

gration of the heat capacity data of Anderson<sup>14</sup>: tridymite,  $1701 \pm 10$  cal./mole and cristobalite,  $1667 \pm 10$  cal./mole.

The spectroscopic data listed by Herzberg<sup>15</sup> were used to calculate thermodynamic functions for SiO by the common methods described by Kelley.<sup>12,13</sup> All fundamental constants were taken to agree with the values given by the National Bureau of Standards.<sup>11</sup> Only the  $^1\Sigma^+$  electronic state need be considered as the nearest known state,  $^1\pi$ , is 42835.3 cm.<sup>-1</sup> higher and by analogy with CO, there is no reason to expect any other low lying levels.<sup>15</sup> No anharmonicity corrections were used as high vibrational levels are not largely populated even at the higher temperatures. (The vibrational contribution to the entropy at 1400°K. is only 0.655 entropy unit.) The functions so derived are tabulated in Table I.

TABLE I

## THERMODYNAMIC FUNCTIONS FOR GASEOUS SiO

| T, °K. | $\frac{F_T^\circ - H_0^\circ}{T}$<br>cal./mole/°K. | $\frac{H_T^\circ - H_0^\circ}{T}$<br>cal./mole/°K. | $S_T^\circ$<br>cal./mole/°K. |
|--------|--|--|------------------------------|
| 298.16 | -43.548  | 6.986  | 50.534                       |
| 900    | -51.524  | 7.587  | 59.111                       |
| 1000   | -52.328  | 7.673  | 60.001                       |
| 1100   | -53.062  | 7.751  | 60.813                       |
| 1200   | -53.739  | 7.821  | 61.560                       |
| 1300   | -54.368  | 7.884  | 62.252                       |
| 1400   | -54.954  | 7.941  | 62.895                       |
| 1500   | -55.504  | 7.992  | 63.496                       |
| 1600   | -56.021  | 8.039  | 64.060                       |
| 1700   | -56.510  | 8.081  | 64.591                       |
| 1800   | -56.973  | 8.120  | 65.093                       |
| 1900   | -57.413  | 8.156  | 65.569                       |
| 2000   | -57.832  | 8.188  | 66.020                       |

When considering a particular equilibrium the  $(\Delta F_T^\circ - \Delta H_0^\circ)/T$  values were calculated at even temperatures and then interpolation to the desired temperatures was done graphically. Tridymite was taken as the form of silica in the range 1143–1743°K. and cristobalite was taken as the stable form from 1743–1983°K.<sup>16</sup>

(14) C. T. Anderson, *J. Am. Chem. Soc.*, **58**, 568 (1936).

(15) G. Herzberg, "Molecular Spectra and Molecular Structure," Vol. I, Spectra of Diatomic Molecules," D. Van Nostrand Co., New York, N. Y., 1950.

(16) F. P. Hall and H. Insley, *J. Am. Ceramic Soc.*, Part II, 19 (1947).

(1) (a) Presented at Symposium on "High Temperature Chemistry" sponsored by the A.E.C. and O.N.R., Chicago, April, 1952. (b) Based on thesis by R. K. Edwards, submitted to the University of California in partial fulfillment of the requirements for the Ph.D. degree, September, 1951. (c) This research performed under A.E.C. Contract No. W-7405-eng-48 and described in detail in declassified report UCRL-1639, March 12, 1952.

(2) American Chemical Society Predoctoral Fellow, 3 years.

(3) A. de Gramont and C. de Watteville, *Compt. rend.*, **147**, 239 (1908).(4) W. Jevons, *Proc. Roy. Soc. (London)*, **106**, 174 (1932).(5) P. G. Saper, *Phys. Rev.*, **42**, 498 (1932).(6) K. F. Bonhoeffer, *Z. physik. Chem.*, **131**, 363 (1928).(7) D. Sharma, *Proc. Nat. Acad. Sci. India*, **A14**, 37 (1944).(8) H. N. Potter, *Trans. Am. Electrochem. Soc.*, **12**, 191, 215, 223 (1907).(9) Earlier work by Potter appears in the patent literature and is cited in the review by C. A. Zapffe and C. E. Sims, *Iron Age*, **149**, [4] 29, [5] 34 (1942).(10) The data from a subsequent paper, N. C. Tombs and A. J. E. Welch, *J. Iron Steel Inst.*, **172**, 69 (1952), became available since the presentation of this work at the High Temperature Chemistry Symposium and have been treated in the present paper.

(11) "Selected Values of Chemical Thermodynamic Properties," National Bureau of Standards, loose leaf tabulations.

(12) K. K. Kelley, "Contributions to the Data on Theoretical Metallurgy. X. High Temperature Heat Content, Heat Capacity and Entropy Data for Inorganic Compounds" (Bull. 476, Washington, 1949).

(13) K. K. Kelley, "Contributions to the Data on Theoretical Metallurgy. XI. Entropies of Inorganic Substances" (Bull. 477, Washington, 1950).

The heat of formation of cristobalite determined by Humphrey and King<sup>17</sup> was used together with the low temperature heat contents to obtain  $\Delta H_0^\circ = -208,020 \pm 180$  cal./mole for cristobalite. From transition temperature data and free energy function data the value  $\Delta H_0^\circ = 457 \pm 520$  cal./mole for  $\text{SiO}_2$  (cristobalite) =  $\text{SiO}_2$  (tridymite) was calculated. Thus  $\Delta H_0^\circ = -207,633 \pm 730$  cal./mole was used for the formation of tridymite.

The first reaction we will consider is  $\text{H}_2(\text{g}) + \text{SiO}_2(\text{s}) = \text{SiO}(\text{g}) + \text{H}_2\text{O}(\text{g})$  which was studied by Grube and Speidel<sup>18</sup> by a flow method in an alumina tube between 1473 and 1773°K. Eleven measurements up to 1673°K. yield  $\Delta H_0^\circ = 134,749 \pm 1400$  cal.<sup>19</sup> with  $\text{SiO}_2(\text{s})$  in the tridymite form. Three measurements at 1773°K. yield  $\Delta H_0^\circ = 136,853 \pm 700$  cal. with  $\text{SiO}_2(\text{s})$  in the cristobalite form. They observed attack of their alumina tubes by SiO and it seems likely that their SiO pressures are low, but no correction is made for this. Using these data and the heat of formation of silica, one obtains for  $\text{Si}(\text{s}) + \frac{1}{2}\text{O}_2(\text{g}) = \text{SiO}(\text{g})$ ,  $\Delta H_{298}^\circ = -15,291 \pm 2000$  cal. per mole.

The second reaction is  $\text{SiO}_2(\text{cristobalite}) = \text{SiO}(\text{g}) + \frac{1}{2}\text{O}_2(\text{g})$  as measured by Brewer and Mastick<sup>20</sup> using an effusion method. Three measurements between 1840–1951°K. yield  $\Delta H_0^\circ = 186,578 \pm 2,700$  cal. from which one obtains  $\Delta H_{298}^\circ = -21,159 \pm 2900$  cal. for the formation of  $\text{SiO}(\text{g})$  from the elements. This value differs from the value they give because of an error in the free energy function for SiO gas that they used.

The third reaction is  $\text{Si}(\text{s}) + \text{SiO}_2$  (tridymite) =  $2\text{SiO}(\text{g})$  as measured by Schäfer and Hörnle<sup>21</sup> using an effusion method. Seventeen measurements between 1336 and 1429°K. yield  $\Delta H_0^\circ = 164,242 \pm 450$  cal. from which one obtains  $\Delta H_{298}^\circ = -21,411 \pm 570$  cal. for the formation of  $\text{SiO}(\text{g})$  from the elements. Four determinations at 1460°K. diverge from the determinations at lower temperatures yielding  $\Delta H^\circ = 165,546 \pm 630$ . These uncertainties include assumed uncertainties in the  $(\Delta F^\circ - \Delta H_0^\circ)/T$  functions used. For comparison purposes, the actual probable error in the data alone,  $\pm 160$  cal. for the low temperature data and  $\pm 340$  cal. for the 1460°K. data, should be considered since the error in the functions would cancel. Thus the divergence of these data is beyond experimental error and is considered suggestive of the formation of a solid SiO phase from Si and  $\text{SiO}_2$  at the higher temperature.

Gel'd and Kochnev<sup>22</sup> have also studied the vaporization of SiO from a mixture of Si and  $\text{SiO}_2$  by an effusion method. They believed that they

(17) G. L. Humphrey and E. G. King, *J. Am. Chem. Soc.*, **74**, 2041 (1952).

(18) G. Grube and H. Speidel, *Z. Elektrochem.*, **63**, 341 (1949).

(19) The probable error used throughout except as otherwise noted is defined by the equation

$$r = 0.6745 \sqrt{\frac{\sum \Delta_i^2}{(n-1)}}$$

where  $r$  is probable error,  $i$  is deviation of  $i$ 'th result from average, and  $n$  is total number of results.

(20) L. Brewer and D. Mastick, *J. Chem. Phys.*, **19**, 834 (1951).

(21) H. Schäfer and R. Hörnle, *Z. anorg. allgem. Chem.*, **263**, 261 (1950).

(22) P. V. Gel'd and M. K. Kochnev, *Zhur. Priklad. Khim.*, **21**, 1249 (1948)

had a solid SiO phase present, but at their temperatures, as will be shown later, solid SiO is unstable with respect to Si and  $\text{SiO}_2$ , and their data have been treated as those of Schäfer and Hörnle.<sup>21</sup> Eleven measurements between 1173 and 1428°K. yield  $\Delta H_0^\circ = 170,644 \pm 1200$  cal. for  $\text{Si}(\text{s}) + \text{SiO}_2(\text{tridymite}) = 2\text{SiO}(\text{g})$  or  $\Delta H_{298}^\circ = -18,212 \pm 960$  cal. for the formation of  $\text{SiO}(\text{g})$  from solid Si and gaseous  $\text{O}_2$ .

Tombs and Welch<sup>10</sup> studied the same reaction as Grube and Speidel, also by the flow method. Their ten data in the 1501°K. through 1742°K. range have been recalculated, assuming the equilibrium to be with the  $\text{SiO}_2$  in the tridymite form. The thirteen data in the 1758 to 1926°K. range are recalculated, assuming cristobalite as the stable  $\text{SiO}_2$  form. The first set of data yields  $\Delta H_0^\circ = 124,414 \pm 1700$  cal. and leads to  $\Delta H_{298}^\circ = -26,004 \pm 2400$  cal. for the heat of formation of  $\text{SiO}(\text{g})$  from the elements. The second set yields, respectively, the values  $129,503 \pm 1300$  cal. and  $21,269 \pm 1500$  cal. The latter measurements were in a temperature range which permitted better gas ratio analyses. Their measurements of the  $\text{SiO}(\text{g})$  pressure over a mixture of Si and  $\text{SiO}_2$  by the flow technique will be discussed later.

Baur and Brunner<sup>23</sup> have determined the vapor pressure of Si from which one can obtain  $\Delta H_0^\circ = 88,962$  cal. for the heat of sublimation. They used an alumina container which can be reduced by silicon but the rate seems to be small enough not to cause interference in the dynamic method of boiling temperature observation that they used, and this heat of sublimation is not believed to be in error by more than  $\pm 2500$  cal. Using this value and the heat of dissociation of oxygen given by the Bureau of Standards,<sup>11</sup> one can calculate the dissociation energy of SiO gas to the gaseous atoms. The results are given in Table II.

From these data one may take  $H_{298}^\circ = -21,411 \pm 570$  cal. as the best value for the heat of formation of  $\text{SiO}(\text{g})$  and the dissociation energy is taken as  $7.34 \pm 0.13$  e.v. This is in good agreement with the  $D_0$  of 7.4 e.v. obtained by Herzberg<sup>15</sup> from a linear Birge-Sponer extrapolation.

From the agreement among the various data, the behavior of SiO gas appears well established. The thermodynamic data demonstrate that a mixture of Si and  $\text{SiO}_2$  yields virtually pure SiO gas while the vaporization of  $\text{SiO}_2$  under neutral conditions yields SiO and  $\text{O}_2$  gases as the main species. The  $\text{SiO}_2$  molecule could not be as important as the SiO molecule under neutral conditions although it might be more important under highly oxidizing conditions. The gas SiO is a monomer.

**Preparation of SiO Solid.**—Since a mixture of Si and  $\text{SiO}_2$  vaporizes to pure SiO, one would expect to be able to obtain SiO solid by quenching SiO vapor. Tone<sup>24</sup> and Winkler<sup>25</sup> could only obtain a mixture of Si and  $\text{SiO}_2$  by such a procedure, but Potter<sup>8,9</sup> claimed to be able to prepare SiO solid by suitable quenching. He reported that this solid disprop-

(23) F. B. Baur and R. B. Brunner, *Helv. Chim. Acta*, **17**, 958 (1934).

(24) F. J. Tone, *Trans. Am. Electrochem. Soc.*, **7**, 243 (1905); further work done on Tone's original preparations is given by H. N. Baumann, Jr., *ibid.*, **80**, 95 (1941).

(25) C. Winkler, *Ber.*, **23**, 2642 (1890).

TABLE II

| Investigators and equilibrium studied  | Si(s) + $\frac{1}{2}$ O <sub>2</sub> (g) = SiO(g)<br>$\Delta H_{298}^{\circ}$ , cal. | SiO(g) = Si(g) + O(g)<br>$\Delta H_0^{\circ}$ , cal. or e.v. |
|--|--|--|
| Grube and Speidel<br>H <sub>2</sub> (g) + SiO <sub>2</sub> (I, II) <sup>a</sup> = H <sub>2</sub> O(g) + SiO(g) | -15,291 ± 2000   | 163,175 ± 4600 or 7.074 ± 0.200                              |
| Brewer and Mastick<br>SiO <sub>2</sub> (II) = Si(g) + $\frac{1}{2}$ O <sub>2</sub> (g)                         | -21,159 ± 2900   | 169,043 ± 5400 or 7.328 ± 0.240                              |
| Gel'd and Kochnev<br>Si(s) + SiO <sub>2</sub> (I) = 2SiO(g)  | -18,212 ± 960  | 166,096 ± 3500 or 7.200 ± 0.150                              |
| Schäfer and Hörnle<br>Si(s) + SiO <sub>2</sub> (I) = 2SiO(g)   | -21,411 ± 570  | 169,296 ± 3100 or 7.339 ± 0.130                              |
| Tombs and Welch<br>H <sub>2</sub> (g) + SiO <sub>2</sub> (I) = H <sub>2</sub> O(g) + SiO(g)                    | -26,004 ± 2400   | 173,889 ± 5000 or 7.537 ± 0.220                              |
| H <sub>2</sub> (g) + SiO <sub>2</sub> (II) = H <sub>2</sub> O(g) + SiO(g)                                      | -21,269 ± 1500   | 169,154 ± 4000 or 7.333 ± 0.170                              |

<sup>a</sup> (I) refers to tridymite. (II) refers to cristobalite.

portionated to Si and SiO<sub>2</sub> upon annealing. Since Potter's work a voluminous literature has accrued. SiO solid is usually prepared by heating SiO<sub>2</sub> with some reducing agent such as Si, C or SiC or by heating Si with some oxidizing agent such as a metallic oxide and condensing the resulting SiO gas by rapid quenching. There is now a multiplicity of evidence from X-ray diffraction and electron diffraction studies<sup>26-31</sup> which leaves little room for doubt that a diffraction ring corresponding to a d-spacing of  $3.60 \pm 0.05$  Å. is to be associated with SiO solid. This ring, which will hereinafter be referred to as the "characteristic ring," is almost always quite broad and most often alone so that the amorphous appearance long attributed to solid SiO finds agreement with this evidence of lack of appreciable long-range order. Hass<sup>31</sup> has presented the electron diffraction pattern for amorphous Si and König<sup>28</sup> has tabulated both the electron and X-ray diffraction patterns of amorphous SiO<sub>2</sub> and one can eliminate the possibility that the characteristic diffraction ring of SiO could be due to amorphous Si or SiO<sub>2</sub>.

**Properties of SiO Solid.**—Because solid SiO has a very similar appearance to the mixture of Si and SiO<sub>2</sub> which often results if the quenching of SiO vapor is not rapid enough, many of the properties ascribed to SiO are actually due to these mixtures. If the criterion of possessing the characteristic diffraction ring of SiO is used, one can establish some other properties which belong decisively to SiO solid.

The physical appearance of SiO solid has been variously reported. In cases where identification has been probably assured, the range in color runs from "brown transparency"<sup>28</sup> for thin film to "dark brown to black, massive, glass-like,"<sup>31</sup> "fine dark powder,"<sup>26</sup> "black glassy,"<sup>32</sup> and "black resinous-looking"<sup>30</sup> for the heavier deposits. Deposits which have decomposed to Si and SiO<sub>2</sub> seem to be more often of a lighter brown color. However, many indications lead one to suppose that the color of pure SiO solid or a mixture of Si and SiO<sub>2</sub> can fall within a range of light brown to black.

Erasmus and Persson<sup>30</sup> found that material having the characteristic ring was completely soluble in HF while a mixture of Si and SiO<sub>2</sub> dissolves only partially, leaving the Si as a residue. Inuzuka<sup>26</sup> confirmed this. Potter<sup>8,9</sup> carefully measured the average specific heat of his "brown

powder" in the interval 30–99° and he compared his results with several reference runs on crystalline Si and SiO<sub>2</sub> and amorphous Si and SiO<sub>2</sub>. The results of his reference runs are in very good agreement with the accepted values today and it is believed that the increase in heat capacity of 1.14 cal./mole/deg. of the "brown powder" over that of Si–SiO<sub>2</sub> mixtures is significant. This conclusion is substantiated by the measurements which showed the heat capacity of the "brown powder" to decrease after annealing at 400° becoming essentially that of a Si–SiO<sub>2</sub> mixture after four hours. Since Potter's "brown powder" did not completely dissolve in HF, his SiO undoubtedly was contaminated with some Si and SiO<sub>2</sub>. Thus the heat capacity at constant pressure of  $9.19 \pm 0.16$  cal./mole/deg. that one obtains from his data should represent an upper limit to the value.

The density of SiO appears to be about  $2.15 \pm 0.03$  g./cc. This property does not seem useful for distinguishing between SiO and mixtures of Si and SiO<sub>2</sub> as Hass<sup>31</sup> has reported considerable variations of the bulk density with variation of rate of condensation from the gas phase. Erasmus and Persson<sup>30</sup> report a dielectric constant of 5.0 for a frequency of 0.05 megacycle and a power factor of 0.011 for a sample which can be characterized as SiO on the basis of other properties reported.

SiO oxidizes readily. Thus the powder is pyrophoric. König<sup>28</sup> demonstrated the oxidation of SiO films at room temperature. Hass<sup>31</sup> found rate oxidation at room temperature as high as 100 Å. per hour and careful techniques are required to obtain SiO samples with the correct composition.

**Crystal Structure of Solid SiO.**—Inuzuka<sup>26</sup> in 1940 was the first to present X-ray and electron diffraction data on solid SiO. His work has received insufficient recognition in the literature because of the unavailability of his publications.

His work is of special interest in that he obtained several diffraction rings in addition to the characteristic ring subsequently reported several times. He prepared SiO gas by vaporization in vacuum from a mixture of SiO<sub>2</sub> and C in a graphite crucible. The SiO was condensed on the water cooled walls. His sample had less than 0.5% carbon. His procedure yielded a "fine dark powder" and apparently a higher degree of lattice order than did other methods. He found SiO to be optically isotropic,

(26) H. Inuzuka, *Mazda Kenkyu Zihō*, **15**, 161, 237, 305, 374 (1940).

(27) Private communication from Dr. Inuzuka.

(28) H. König, *Optik*, **3**, 419 (1948).

(29) G. Hass and N. W. Scott, *J. Optical Soc. Am.*, **39**, 179 (1949).

(30) H. Erasmus and J. A. Persson, *J. Electrochem. Soc.*, **95**, 316 (1949).

(31) G. Hass, *J. Am. Ceram. Soc.*, **33**, 353 (1950).

(32) G. Grube and H. Speidel, *Z. Elektrochem.*, **53**, 339 (1949).

as was found later by Beletskii and Rapoport.<sup>33</sup> Because of the high symmetry, Inuzuka was able to evaluate his X-ray data to obtain a cubic lattice of  $a_0 = 6.4 \text{ \AA}$ . with eight molecules per unit cell with the  $T_h^6$  space group. On the other hand, Beletskii and Rapoport,<sup>33</sup> who have supposed Inuzuka had only a mixture of Si and SiC, report that their own X-ray work establishes a cubic lattice with  $a_0 = 5.16 \text{ \AA}$ . However, they present no data and many of the lines indicated by their lattice constant are found among Inuzuka's patterns. The carbon analysis on the latter's material seems to rule out the finding of SiC.

**Rate of Disproportionation of SiO Solid and its Stability Range.**—As noted earlier, SiO solid oxidizes at an appreciable rate even at room temperature. The first evidence of decomposition was reported by Pctter<sup>8,9</sup> who observed a conspicuous change in the specific heat after four hours at  $400^\circ$  in sealed glass or silver containers. Hass<sup>31</sup> found SiO films to be converted to amorphous Si and amorphous SiO<sub>2</sub> after two hours at  $700^\circ$ . Similar treatment at  $900^\circ$  yielded crystalline Si and amorphous SiO<sub>2</sub>. Erasmus and Persson<sup>30</sup> and Schäfer and Hörnle<sup>21</sup> heated SiO samples to temperatures ranging from  $1000$  to  $1375^\circ$  and obtained silicon, indicating disproportionation. We have heated intimate mixtures of Si and SiO<sub>2</sub> at  $1300^\circ$  for periods from 20 to 30 minutes in argon. Upon cooling to room temperature, the mixtures were X-rayed and the X-ray diffraction results showed the major phases to be silicon and  $\alpha$ -cristobalite with some  $\alpha$ -quartz present. The results are in agreement with the results obtained when SiO was used as the starting material.

On the other hand, Grube and Speidel<sup>32</sup> and König<sup>34</sup> claim that SiO is stable below  $900^\circ$  for periods of time as long as  $1/4$  hour. It is difficult to explain the disagreement. The SiO used by König was  $70 \text{ \AA}$ . thick and was on a platinum sheet. It is conceivable that a thin film of SiO might be stabilized by the supporting material under conditions where the bulk phase would be unstable.

The results, showing disproportionation of SiO after high temperature treatment, do not necessarily prove the instability of SiO at the high temperatures. They only indicate that there is at least a region of instability between room temperature and  $1000^\circ$ . The SiO actually might be stable at the high temperatures but disproportionate during the cooling.

Because it is difficult to quench the solid samples rapidly enough to retain any SiO that might be stable at high temperatures, it is necessary to use some method that can detect SiO at the high temperature. The high-temperature X-ray camera is a logical tool to use for such problems.

**High Temperature X-Ray Examination of SiO-Si Samples. Experimental.**—Mixtures of Si and SiO<sub>2</sub> were examined in a high-temperature X-ray camera to determine the stability range of SiO solid. 99.87% silicon powder containing 0.007% carbon, less than 0.015% Mn, less than 0.01% Ca and P, and less than 0.004% Cr, Ti, Zr, Co and Ni was used. The SiO<sub>2</sub>, in the form of silica gel, was extremely

flocculent and finer than 400 mesh. It contained less than 0.01% Mg and less than 0.1% each of Al, Ca, Fe and Na according to spectroscopic analysis. A modified Unicam<sup>35</sup> high-temperature X-ray camera of 19 cm. diameter was used. Experiments were limited to a maximum temperature of  $900^\circ$  by failure of the windings at higher temperatures.

The samples were contained in silica glass capillaries of about 0.2 mm. outside diameter with walls as thin as possible. Copper X-ray radiation was used. Before X-ray examination, the mixture of Si and SiO<sub>2</sub> in an equal molar ratio was degassed for ten minutes at  $1400^\circ$  in an alumina crucible and only that material not in contact with the alumina was used.

The samples were heated in the high-temperature X-ray camera to allow opportunity for reaction before the X-ray exposure. Total heating times up to 44 hours at  $900^\circ$  were used.

**Discussion of Results.**—No X-ray evidence for formation of a new phase or for any lessening of the Si concentration was found. All X-ray diffraction lines could be attributed to Si plus a mixture of  $\beta$ -tridymite and  $\beta$ -cristobalite. The lattice parameters of the silica forms were the same to within  $\pm 0.0005 \text{ kX}$ . whether heated alone or with silicon. Likewise no evidence for appreciable solid solubility of oxygen in silicon was found. The lattice constant of silicon in these mixtures was found to be  $5.4200 \pm 0.0005 \text{ kX}$ . unit at  $9^\circ$  and  $5.4367 \pm 0.0005 \text{ kX}$ . at  $900^\circ$ , in good agreement with values from which Becker<sup>36</sup> and Hölbling<sup>37</sup> obtained their thermal expansion coefficients for pure silicon if one corrects their "brightness" temperatures to true temperatures. These observations confirm that SiO solid is not a stable phase at temperatures up to  $900^\circ$ .

**Thermodynamic Stability of SiO Solid.**—Von Wartenberg<sup>38</sup> has determined the heats of solution of SiO, Si and SiO<sub>2</sub> in AgClO<sub>4</sub>-HF solutions. Wartenberg's data yield for the reaction  $\text{Si(s)} + \text{SiO}_2(\text{cristobalite}) = 2\text{SiO}(\text{amorphous})$ ,  $\Delta H_{298}^\circ = 0.0 \pm 3.0 \text{ kcal}$ . Within the experimental error, SiO gave the same heat of solution as a mixture of Si and SiO<sub>2</sub>. König<sup>34</sup> has indicated that he had examined Wartenberg's SiO and found the characteristic diffraction ring which would distinguish the SiO from a mixture of Si and SiO<sub>2</sub>. The data, then, indicate that SiO is just on the verge of stability, and thus this situation is analogous to the cases of FeO, GeO and SnO where only limited temperature ranges of stability are observed. We have demonstrated by our high-temperature X-ray camera observations that SiO is unstable at  $900^\circ$  and is undoubtedly unstable in the range  $400$ – $900^\circ$ . Taking this observation together with limits to the heat of formation of SiO fixed by the data of Wartenberg, it is of interest to see if reasonable values of the heat capacity and entropy of SiO will predict its stable existence at other temperatures. The entropy will be the decisive factor and it must be considered carefully. As a first approximation, Latimer's rule<sup>39</sup> was used. Values obtained by this rule for oxides of Ti and Si were compared with the experimental values and a correction applied to the value calculated for SiO. The entropy of

(35) Obtained from Unicam Instruments, Ltd., Arbury Works, Cambridge, England.

(36) K. Becker, *Z. Physik*, **40**, 37 (1926).

(37) R. Hölbling, *Z. angew. Chem.*, **40**, 655 (1927).

(38) H. Von Wartenberg, *Z. Elektrochem.*, **53**, 343 (1949).

(39) W. M. Latimer, *J. Am. Chem. Soc.*, **73**, 1480 (1951).

(33) M. S. Beletskii and M. B. Rapoport, *Doklady Akad. Nauk. S.S.S.R.*, **72**, 699 (1950).

(34) H. König, private communication, July 20, 1951.

crystalline SiO is taken as 6.4 entropy units at 298° K. and is not believed to be uncertain by more than  $1\frac{1}{2}$  entropy unit. We must consider that SiO as actually produced is amorphous and could have a higher entropy by as much as  $R \ln 2$  as a maximum. This randomness entropy was roughly estimated as 0.9 e.u. on the assumption that it would be about the same as given by Simon and Lange<sup>40</sup> for SiO<sub>2</sub> glass. Thus the entropy of amorphous SiO is taken as 7.3 e.u. at 298°K. Combining these data, we can write for the reaction,  $\frac{1}{2}\text{Si}(s) + \frac{1}{2}\text{SiO}_2(\text{cristobalite}) = \text{SiO}(\text{amorphous})$ .  $\Delta S_{298}^\circ = -0.05 \pm 1.0$  e.u., and  $\Delta F_{298}^\circ = 0.0 \pm 3.3$  kcal. The result is indecisive as far as stability at room temperature is concerned. The reaction would have slightly less tendency to go if quartz were considered instead of cristobalite.

It now becomes necessary to estimate the effect of increasing the temperature. The heat capacity of SiO has been determined at 338°K. by Potter.<sup>8,9</sup> The heat capacity of TiO is given by Kelley.<sup>12</sup> Lewis and Randall<sup>41</sup> point out that many isotropic crystalline substances have  $C_V$  values which are the same function of  $T/\theta$  where  $\theta$  is a characteristic constant for the particular solid. Using the known heat capacity for SiO at one temperature with the value for TiO at the same temperature, the ratio of characteristic constants was determined and applied to obtain the following equation for crystalline SiO:  $C_P = 10.57 + 2.98 \times 10^{-3}T - 2.72 \times 10^5 T^{-2}$ . From the equation can be calculated that the entropy at 1200°K. is 22.4 e.u. for crystalline SiO and 23.3 e.u. for amorphous SiO. This value may be checked by the same use of Latimer's rule that would be used to obtain  $S_{298}^\circ$  but by using entropies at 1200°K. Considering all uncertainties, the entropy at 1200°K. should not be in error by more than 3 e.u. Finally, one obtains for  $\frac{1}{2}\text{Si}(s) + \frac{1}{2}\text{SiO}_2(\text{cristobalite}) = \text{SiO}(\text{amorphous})$ ,  $\Delta S^\circ = 1.5 \pm 3.0$  e.u.,  $\Delta H^\circ = 1.0 \pm 3.0$  kcal., and  $\Delta F^\circ = -0.9 \pm 6.6$  kcal. The errors indicated are not probable errors but are believed to be the maximum derivations possible. Nevertheless, the uncertainty is too large to allow any decisive conclusion from the thermodynamic data alone. However, it will be noted that there is a definite trend toward increase in stability as the temperature is increased as one finds for FeO. Taking the observation of instability at 900°, one can confidently say that there will be no region of thermodynamic stability at lower temperatures. There remains the intriguing possibility that SiO may be stable at temperatures higher than 900°. We have previously shown that mixtures of Si and SiO<sub>2</sub> heated to 1300° gave no evidence of SiO upon cooling to room temperature, but any SiO that might form would undoubtedly disproportionate upon cooling with the quenching rates used.

It is of interest to examine the data of Schäfer and Hörnle<sup>21</sup> for the reaction  $\text{Si}(s) + \text{SiO}_2(\text{tridymite}) = 2\text{SiO}(g)$  that was considered earlier in the paper. If SiO becomes a stable solid phase in the temperature range of their experiments, their

data might give some indication of this. As noted earlier their measurements between 1336 and 1429°K. were very concordant, but their four measurements at 1460°K. diverged from the other determinations by an amount that seemed to be outside the experimental uncertainty. This might be due to SiO becoming the stable phase between 1429 and 1460°K.

**Melting Point of SiO.**—Potter<sup>8</sup> has presented one important observation tending to indicate the stability of SiO at high temperatures. He reported that he could not liquefy SiO at 1700°. If SiO were not stable at this temperature and he had a mixture of Si and SiO<sub>2</sub>, he would have observed some melting since SiO<sub>2</sub> glass softens below 1700° and silicon melts well below this temperature. It appeared worthwhile to attempt verification of Potter's observation.

**Experimental.**—A SiO<sub>2</sub> tube of 13 mm. inside diameter and 1 mm. wall thickness was filled with the same mixture (Si + SiO<sub>2</sub>) as used in the previous X-ray work, except that no preheating had been done. The bottom end of the tube, Fig. 1a, was heated by two oxy-hydrogen torches while a vacuum (mechanical pump) was being drawn on the system. Heating in this fashion allows gradual collapse of the tube from the bottom upwards so that sintering takes place under compression and finally complete constriction of the upper tube is achieved (Fig. 1b). An additional SiO<sub>2</sub> glass rod working handle was fused on to the other end of the cylindrical ampule thus prepared (Fig. 1c). Now, using the arrangement illustrated in Fig. 1d, an attempt was made to draw off the ampule in the middle section where the heat from the two torches was concentrated. In spite of the fact that the center section was the hottest region, the drawing off occurred at the ends (A and B of Fig. 1d).

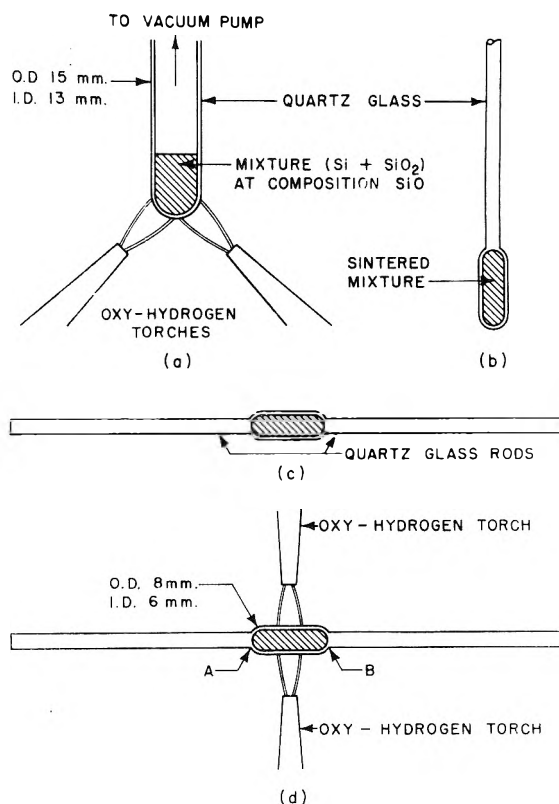


Fig. 1.—Melting point apparatus.

**Discussion of Results.**—The results seem to indicate that the solid mixture has a melting point higher than either of its components and that

(40) F. Simon and F. Lange, *Z. Physik*, **15**, 312 (1923).

(41) C. N. Lewis and M. Randall, "Thermodynamics and the Free Energy of Chemical Substances," McGraw-Hill Book Co., Inc., New York and London.

hence a new phase such as the solid SiO may have replaced the mixture.

### The Thermoelectrovalve Effect, Experimental

**Introduction.**—Examination of all the data to this point indicates that SiO solid is thermodynamically unstable at all temperatures below 1200°K. and undoubtedly below 1450°K. On the other hand the available thermodynamic data would not be inconsistent with a stable SiO at temperatures above 1450°K. The data of Schäfer and Hörnle<sup>21</sup> have an anomaly between 1429 and 1460°K. which may be an indication of the formation of stable SiO. Our experiments have confirmed the observation of Potter<sup>8</sup> that a mixture of Si and SiO<sub>2</sub> does not show the melting behavior expected of such a mixture and it appears that a high melting SiO phase is formed. Thus it was considered worthwhile to devise an experiment to test the formation of SiO at high temperatures.

It would be expected that SiO would have a different electrical conductivity than a mixture of Si and SiO<sub>2</sub>. Gel'd and Kochnev<sup>22</sup> report that material which they believe to be SiO has an electrical resistivity of about  $5 \times 10^6$  ohm-cm. Erasmus and Persson<sup>30</sup> found that SiO samples with the characteristic diffraction ring were almost non-conductors while disproportionated SiO samples that were mixtures of Si and SiO<sub>2</sub> were electrical conductors with high resistance. It is believed that ordinary silicon with the usual small metallic impurities would be a much better conductor than SiO. If this were so, a rod of a sintered mixture of Si and SiO<sub>2</sub> used as an electrical heating element would heat to the temperature at which transformation to SiO takes place. The transformation to SiO would increase markedly the resistance and prevent any further heating.

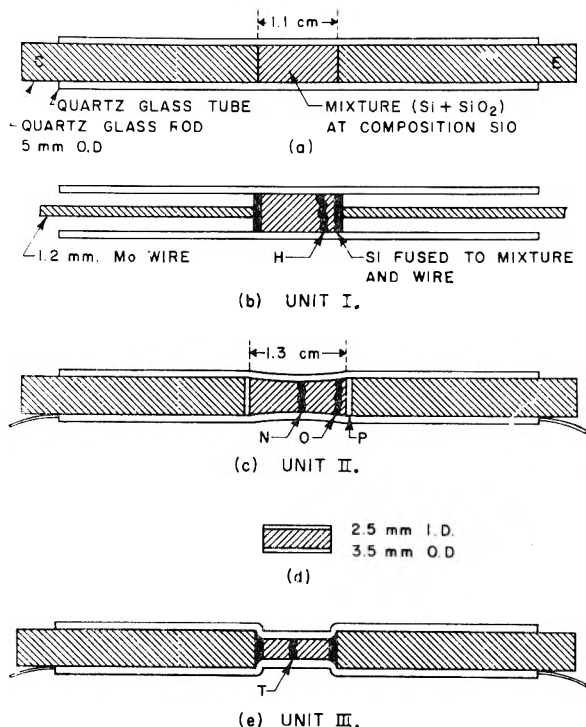


Fig. 2.—Thermoelectrovalve elements.

If the reversible transformation were extremely rapid, one would observe a fixed transition temperature independent of reasonable variation in the applied voltage. If the transformation were relatively slow, one might expect oscillations in the current drawn and the temperature of the rod, since overheating would occur before transformation had taken place and then undercooling would occur due to lagging of the disproportionation reaction. The quenching experiments previously discussed would certainly indicate that the disproportionation reaction at least would be rapid.

**Materials.**—The silicon used was the same as used in the high-temperature X-ray experiments and was passed through a 200-mesh screen. The silica was high purity cristobalite<sup>42</sup> that had been passed through a 325-mesh screen.

**Preparation of Resistance Elements.**—Several different resistance elements were developed in the course of exploring different facets of the phenomenon. Three units are shown in Fig. 2.

All resistance rods were made up of mixtures of SiO<sub>2</sub> and Si in equal molal percentages so that the over-all compositions would correspond to the stoichiometry of SiO. Outer envelopes of the resistance rods were made of quartz glass.

Unit I (shown in Fig. 2b) was prepared by heating the mixture section as hot as possible with a pair of oxy-hydrogen torches while at the same time pressure was exerted by means of the two close-fitting quartz glass rods (C & E of Fig. 2a). The quartz rods were then removed, a small amount of Si powder sprinkled on one end of the sintered mixture and a Mo wire electrode inserted. The tube was held in a vertical position and treated in the oxy-hydrogen torch until the Si fused to both the Mo wire and the mixture. The process was repeated for the other end. Several attempts were necessary before sufficiently sturdy and satisfactory contacts were achieved.

An improved and simple technique of introducing the refractory metal electrode was used in the preparation of Unit II (Fig. 2c), which was prepared in the same manner as Unit I with the exception that thin tungsten ribbon electrodes were lapped over the ends of the close-fitting quartz glass rods and thus held against the silicon powder during fusing. The quartz glass rods fused in place and a sturdy unit with flexible electrode leads was achieved. This particular unit was purposely slightly constricted during the early stages of sintering the mixture, for reasons which will be apparent later.

Unit III (shown in Fig. 2e) differed from Unit II only in that special care was taken to obtain a uniform core of as dense a sintered mixture as possible by using a small diameter mixture section prepared as in Fig. 1. Then a section was broken out (Fig. 2d) and placed in a larger tube, the walls of which were collapsed down around the small tube section and fused to it.

**Apparatus and Calibration.**—The refractory metal electrodes were connected to a 60 cycle a.c. power source with variable voltage of up to 457 volts. Voltages were observed on an R. C. A. Volt Ohmyst Junior electronic voltmeter.

An electrical switch arrangement was used to introduce to the circuit either a 0-10 ampere ammeter, or this ammeter in series with a Weston Model 476 milliammeter of 0-250 milliamperes range.

Temperature readings were taken with a Leeds and Northrup optical pyrometer mounted about two feet from the heating rod. Correction of temperature readings for non-black body conditions were made, based on calibration of the pyrometer at the freezing point of Si. The Si in a quartz glass tube of the same dimensions as the resistance elements was heated with the oxy-hydrogen torch and "brightness temperature" readings were taken at the freezing point arrest 1683°K. It was seen that the Si-quartz tube interface surface was of the same light brown, non-glossy character as the heating element quartz tube interface, as one would expect. In consequence, identical emissivities were assumed and the relationship obtained was

$$\frac{1}{T'} - \frac{1}{S} = -1.74 \times 10^{-5} \text{ deg.}^{-1}$$

(42) The authors are grateful to Dr. K. K. Kelley of the U. S. Bureau of Mines, Berkeley, California, who furnished this material.

where  $T$  is the true temperature and  $S$  is the brightness temperature (on the absolute scale).

**Experimental Results.**—The first experiments were performed with Unit I. Approximately 400 volts were applied across the tube and the sintered mixture section was observed to rapidly heat up to a dull red and then suddenly to form a bright boundary zone (H of Fig. 2b) approximately one to two millimeters thick and extending completely around the tube. At the time of the formation of the bright boundary zone, the electrical current began to oscillate between the values 75 and 150 milliamperes. The frequency of oscillation was approximately one per second.

A few simple tests were performed to see if their results would also be in accord with expectations. Heating of the mixture by use of a torch caused the current to fall quickly to approximately 75 milliamperes—the lowest value for the usual oscillation. More intensive heating caused the current to decrease slowly, but the current could not thus be extinguished. When the torch was removed the bright boundary was seen to reappear and the oscillation again set in. On the other hand, if cold air were blown across the tube the current increased to the high value, 150 milliamperes, and remained there without detectable oscillation. In this case the bright boundary did not disappear. When the blowing of cold air across the tube was ceased, oscillation again set in. The voltage across the tube was varied from 457 to 330 volts, and the temperature of the hot boundary zone was found to remain constant at 1463°K., within experimental error of measurement. At voltages lower than about 300, the process was unable to maintain itself and the tube cooled down. It is important to note that any time a rod cooled down to the point of the disappearance of the bright boundary it would not again begin to conduct current and form the bright boundary (even when full voltage was applied across the tube) unless auxiliary heating was done with a torch.

The bright boundary zone extending around the tube is a wavy line whose small nodes are apparently constantly shifting in position. Measurement with a pyrometer was difficult since a pulsing fluctuation within the boundary zone itself can be seen to be constantly taking place. An attempt was made to see if the bright boundary might be caused to shift in position by applying intensive heating toward the end of the mixture more remote from the boundary. This did cause the original boundary to disappear, but when the heat was removed the new bright boundary, where the torch had been applied, shifted by jumps until it was essentially in its original position. The frequency of oscillation was found to be inversely related to the applied voltage and directly related to the cooling convection air currents in the room. The frequency of oscillation varied from about 120 oscillations per minutes for a voltage of 457 to zero, in some cases, at 300 volts.

Measurements made of the temperatures as a function of voltage throughout the course of two days showed that there was no systematic variation of temperature within the range of voltages 300 to 457.

Later the tube was broken open for inspection. A conspicuous ring of recrystallization around the interior of the quartz glass envelope was noted and this corresponded in position and width to the former bright boundary zone. This opaque ring was noted before the tube was broken open but it was then thought to belong to the mixture. A void core down about half the length of the mixture zone was found. It is supposed that the mixture had not been as well sintered as previously thought and that gradual transference of the mixture from the central core to its outer extremes took place. The cross sectional area of the void was about one-fourth the total cross sectional area of the sintered mixture.

In the core area the mixture was a rich golden brown when viewed under the microscope. It appeared decidedly homogeneous, but X-ray diffraction showed clearly that silicon was present. The other lines in the pattern were not very distinct but it appeared that each of the three room temperature modifications of SiO<sub>2</sub> were probably present. The exterior of the mixture zone was light brown and as such answered the general description of the amorphous mixture that has often been reported in the literature.

A new tube, Unit II of Fig. 2c, was made. It was quite uniform but with a slight constriction in the center section so that one might test as to whether the bright boundary zone did not necessarily form at the narrowest cross sectional area. When about 385 volts were applied across the

tube, considerable arcing took place in the region of the mixture-electrode interface. This was allowed to continue, and after about 15 seconds a bright boundary formed right at the mixture-silicon interface, P of Fig. 2c. After about ten minutes this bright boundary zone was observed to have shifted slowly until it had moved about three millimeters toward the center section, O of Fig. 2c. The current was then shut off for a time. Reapplication of voltage across the tube did not result in spontaneous heating and the torch was applied to the center section. The boundary then formed at the center section, N of Fig. 2c, but for a short time a partial second boundary coexisted at O. This tube was not broken apart for inspection since it was desired for laboratory demonstration. The average temperature of the bright boundary was 1447°K.

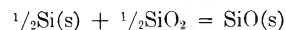
The Unit III tube, as noted above, was constructed to obtain an especially well-sintered rod of uniform cross section. It was desired to find out if one could obtain uniform heating instead of only localized bright boundary zone heating. Furthermore, it was desired to see if the void core previously mentioned could be eliminated through having the mixture sufficiently well sintered.

That the rod was well sintered and without initial void was established by microscopic examination during the preparation of the unit. When 350 volts was applied across the tube as usual, spontaneous heating occurred. Very uniform heating took place, and the mixture reached a temperature of 1323°K. at 350 volts at almost two amperes. Since the system was electrically fused at two amperes, it was necessary to turn off the power and insert a larger fuse. Four hundred and forty volts were applied and considerable arcing took place for a few seconds; then the current suddenly went to 60 milliamperes and the usual bright boundary zone formed at approximately the mid-point of the mixture section, T of Fig. 2e. The temperature of the bright zone was 1459°K.

The tube was broken open after it had been in operation only a few minutes and an inspection was made for voids. Only a very small pinhole void was found.

The mean bright boundary temperature was 1461°K., based on all (84) temperature observations made with all tubes used. The average deviation from the mean was  $\pm 22^\circ\text{K.}$  and the maximum deviation from the mean was  $+78^\circ\text{K.}$

**Discussion of Results.**—The agreement of the bright boundary temperature of  $1461 \pm 18^\circ\text{K.}$  with the value  $1445 \pm 15^\circ\text{K.}$  which one would infer, based on the anomaly in the vapor pressure data of Schäfer and Hörnle, is impressive. The conformity of the behavior of the thermoelectrovalve experiments with predictions seems to clearly indicate that SiO solid becomes stable at about 1450°K. and above, by the reaction



and that the reaction is quite rapidly reversible. The latter is in agreement with the fact that quenched solid phase preparations have always revealed the disproportionation products.

Since the time of the earlier presentation of this work,<sup>1</sup> Hoch and Johnston<sup>43</sup> have conducted a study, using a high temperature X-ray camera, and they confirm the existence of a new high temperature phase in the Si-SiO<sub>2</sub> system. They were unable to find the new phase at a temperature as low as 1520°K., however. As mentioned previously, Tombs and Welch<sup>10</sup> have conducted flow method SiO(g) pressure measurements (1573–1920°K.) over material nominally a mixture of Si and SiO<sub>2</sub>. They assumed that an experimental error of  $\pm 20\%$  accounted for the discrepancy be-

(43) Michael Hoch and Herrick L. Johnston, "Formation, Stability, and Crystal Structure of Solid Silicon Monoxide," presented at the 123rd American Chemical Society National Meeting, March, 1953, Los Angeles.

tween their work and that of Schäfer and Hörnle.<sup>21</sup> It is now clear that the data of Tombs and Welch belong to the reaction  $\text{SiO}(s) = \text{SiO}(g)$  and they lead to mean values of  $\Delta H^\circ = 58,550$  cal./mole and  $\Delta S^\circ = 25.45$  cal./mole/deg. for this process in the temperature range of the study. The entropy which this value would imply for either solid SiO or a mixture of Si and SiO<sub>2</sub> seems much too high. Extrapolation of the data of Tombs and Welch<sup>11</sup> and of Schäfer and Hörnle<sup>21</sup> to convergence would predict a transition temperature for the reaction,  $\frac{1}{2}\text{Si}(s) + \frac{1}{2}\text{SiO}_2(s) = \text{SiO}(s)$ , of approximately 1560°K., but the entropy consideration does not permit reliance on the extrapolation.

The new phenomenon of the thermoelectrovalve effect is itself interesting to discuss since it has not been previously reported. The formation of a bright boundary rather than a uniformly hot section of the heating rod is easily understood. As the first few nuclei of solid SiO are formed, greater electrical resistance is encountered in the given cross sectional zone and continued catastrophic formation of solid SiO results in the formation of the boundary. The experiments show that although the boundary may form initially any place it none the less migrates to the limiting cross sectional area.

The frequency of the current oscillation seems to be governed by the balance between the rate of power input and the rate of heat loss. Thus cooling the tube by blowing cold air over it caused the frequency to go to zero and the tube to require maximum power input. Heating the tube caused the frequency to go to zero at minimum power input. Other things being held constant, the oscillation frequency increased as the voltage was increased or as the current carried decreased.

It is to be noted, however, that intense heating of the mixture section did not reduce the current carried much below the minimum value existing during normal operation, and it is necessary then to suppose that the conductivity of the solid SiO probably becomes appreciable at higher temperatures.

The voids formed at the cores of the rods are presumed to be due to a vaporization and recondensation process of SiO to form a more dense mixture.

The necessity for heating a tube to initiate conduction on the occasion of any reuse is not clear. If it may be assumed that conduction is principally by means of silicon-to-silicon particle contacts, one might suppose that operation of the process resulted in reduced particle size (as evidenced by microscopic homogeneous appearance) and as a consequence SiO<sub>2</sub> insulation between silicon particles could take place. Since the conductivities of both Si and SiO<sub>2</sub> increase with temperature, heating would tend to break down the barriers.

During the course of the experimentations, alternate explanations for the supposed thermoelectrovalve effect were considered. The temperature calibration work was done in order to eliminate the possibility of the phenomenon being associated with the melting of silicon and the decrease in conduction which would result in the contraction on melting of the silicon. Experiments conducted verified the work of von Wartenberg<sup>44</sup> as to the large volume contraction undergone by silicon on melting, but the temperature of the thermoelectrovalve phenomenon is too far removed from the melting point of silicon to permit the supposed alternate mechanism.

(44) H. von Wartenberg, *Naturwissenschaften*, **36**, 373 (1949).

## INFLUENCE OF ADSORPTION OF WATER AND QUINOLINE ON THE SURFACE CONDUCTIVITY OF A SYNTHETIC ALUMINA-SILICA CATALYST

BY MELVIN A. COOK, REX O. DANIELS, JR.,<sup>1</sup> AND J. HUGH HAMILTON

*University of Utah, Salt Lake City, Utah*

*Received December 3, 1958*

A method is described for the simultaneous measurement of the adsorption and resistivity at constant temperature and relative pressure for the adsorbates water and quinoline on a synthetic alumina-silica catalyst adsorbent. Measurements were made over a range of temperatures and relative pressures, thus providing, in addition to a series of adsorption isotherms, resistivity-surface coverage isotherms corresponding to the adsorption isotherms and the resistivity-temperature relations at constant adsorption. In this way it was possible to determine the surface component of the total resistivity and show the relations between surface resistivity and adsorption at various temperatures. The results show that surface resistivity is critically dependent upon the amount of gas adsorbed on the surface of the catalyst. Moreover, it is shown that quinoline in the low surface coverage ranges enhances surface conductivity much more strongly than water at comparable surface coverage. This remarkable effect is attributed to the influence of quinoline on the shift in coordination of surface aluminum ions from the 6- to the 4-coordinated state. Interesting unexplained correlations between the resistivity and relative pressure also are shown.

The conductivity in polar crystals is believed to be composed of two parts, (1) the bulk conductivity associated with the migration of ions through the bulk solid by way of lattice defects of the Schottky

and Frenkel types, and (2) the conductivity associated with free surfaces and interfacial boundaries. The former follows generally the Arrhenius law,  $A_1 e^{-E_1/RT}$ , and gives a straight line on a plot of  $\log \sigma_b$  vs.  $1/T$ . The latter, however, is quite erratic according to most experimental observation concerning the low temperature conductivity of

(1) This paper is based on the thesis presented by Rex O. Daniels in partial fulfillment of the requirements for the degree of Doctor of Philosophy, June, 1952.

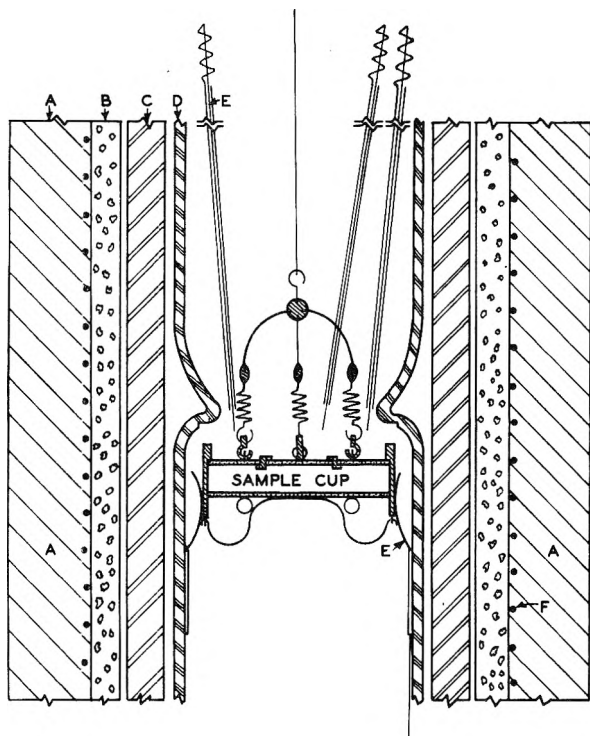


Fig. 1.—Sample cup and its position in furnace: A, insulation; E, ceramic tube; C, aluminum block; D, glass adsorption tube; E, tungsten contacts to resistance meter; F, heating element.

polar crystals. Even so, it is possible to express the conductivity of polar crystals approximately by the equation

$$\sigma = A_b e^{-E_b/RT} + A_s e^{-E_s/RT} \quad (1)$$

where the first term on the right refers to the bulk, and the second to the surface (or interfacial) conductivity. In general  $A_b \gg A_s$ , and  $E_b \gg E_s$  hence the high temperature conductivity involves effectively only the bulk conductivity while at sufficiently low temperature the bulk conductivity may be neglected in favor of the surface conductivity. Also, there exists a temperature region of 50–100° where both terms need to be taken into account; an equation of this sort does not lead to a sharp discontinuity in the  $\log \sigma$  vs.  $1/T$  curve.<sup>2</sup>

Most studies of the conductivity of polar crystals have ignored the influence of adsorbates on the surface conductivity. Recent studies<sup>3</sup> have shown, however, that adsorbates can and do influence the low temperature conductivity profoundly. This is shown clearly by the work of Schmidt who studied the influence of water vapor pressure on the conductivity of a synthetic catalyst.<sup>4</sup> One suspects as a result

(2) For a review of conductivity in polar crystals see N. F. Mott and R. W. Gurney, "Electronic Processes in Ionic Crystals," Oxford University Press, New York, N. Y., 1940.

(3) J. F. Chittum, J. H. Hamilton and H. J. White, unpublished Laboratory Reports on Temperature and Humidity Effects on the Resistivities of Dusts as Applied to Cottrell Precipitation Operation.

(4) W. A. Schmidt, *Ind. Eng. Chem.*, **41**, 2428 (1949).

of these studies that much of the erratic behavior of  $\log \sigma$  vs.  $1/T$  curves at low temperatures found in the literature may be associated with inadequate control of atmospheric conditions.

This investigation was undertaken as the beginning of an anticipated long-range project to provide a better understanding of surface conductivity in view of the importance of this factor in dust precipitation by means of the Cottrell pre-

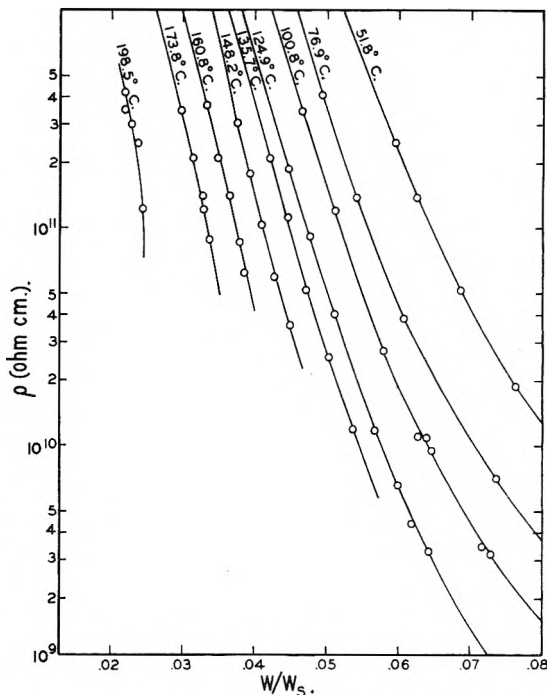


Fig. 2.—Resistivity against weight adsorbed per gram for water adsorption on synthetic catalyst.

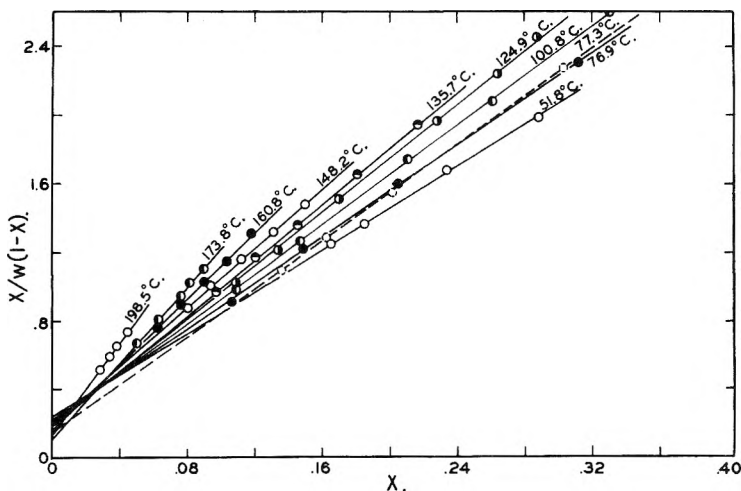


Fig. 3.—B.E.T. plot for water adsorption on synthetic catalyst.

cipitator. It is believed also that the results of fundamental studies of surface conductivity may find important applications in various other fields, e.g., heterogeneous catalysis where ion mobilities are no doubt of great importance. Furthermore, if it were possible to provide a relationship between surface conductivity and the adsorption isotherm, an important new tool would be provided in studies

of surface chemistry. One purpose of this paper is therefore to provide (empirically) expressions for the following three relations

$$w/w_s = f(x) \quad (2)$$

$$\sigma = g(w/w_s) \quad (3)$$

$$\sigma = h(x) \quad (4)$$

for the particular systems under investigation. Here  $w$  is the weight of adsorbate adsorbed on the solid of weight  $w_s$ ,  $x$  is the relative pressure of the adsorbate,  $f$ ,  $g$ , and  $h$  are functions to be determined experimentally.

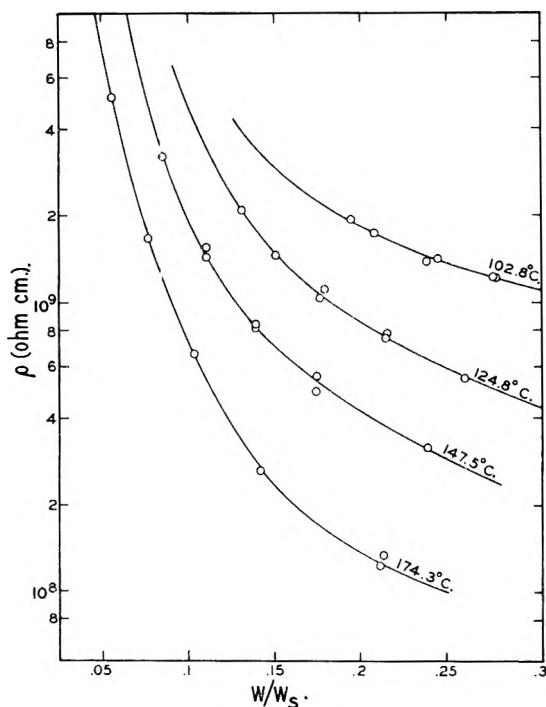


Fig. 4.—Resistivity against weight adsorbed per gram for quinoline adsorption on synthetic catalyst.

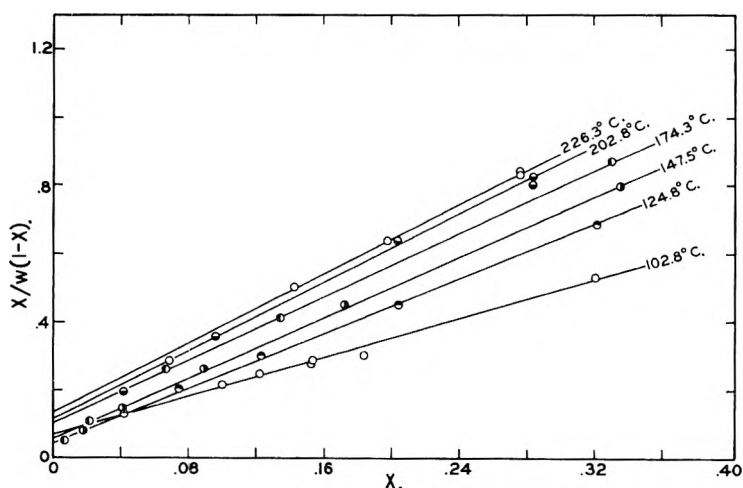


Fig. 5.—B.E.T. plot for quinoline adsorption on synthetic catalyst.

### Experimental Methods and Results

The adsorbent used in this study was a synthetic alumina-silica catalyst used by the petroleum industry in fluidized catalytic cracking columns. It was prepared by the simultaneous precipitation of silica and alumina from solution giving a mixture of approximately 90% silica and 10%

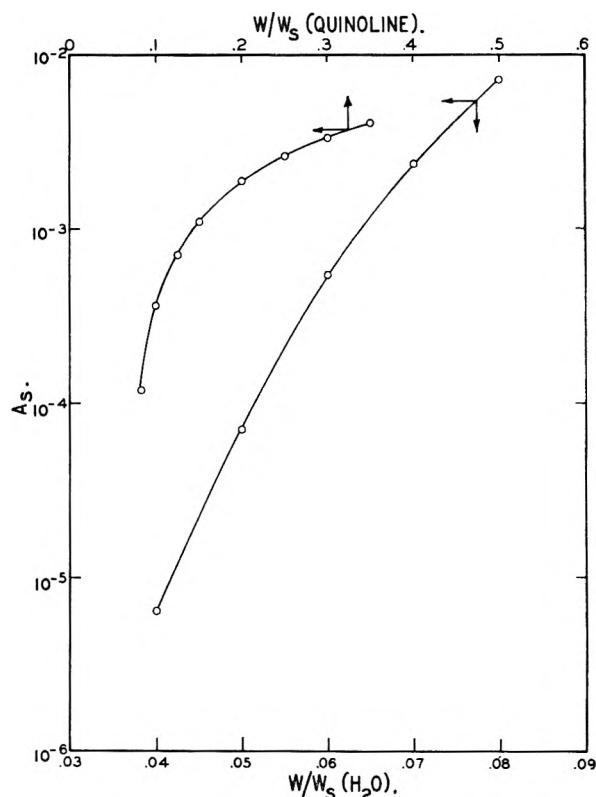


Fig. 6.—Plot of  $\log A_s$  vs.  $w/w_s$  for both water and quinoline adsorption on synthetic catalyst.

alumina. Its size was about 200 mesh. Adsorbates were water and quinoline.

The method used for measuring adsorption isotherms was an adaptation from the technique of Mills, Boedeker and Oblad.<sup>5</sup> The sample was maintained at a fixed temperature in an atmosphere of inert gas pre-saturated with the adsorbate at a predetermined temperature. The amount adsorbed by the sample was measured by a direct weighing technique using nitrogen and (in some cases) air as the carrier gas.

An important modification to the method of Mills, *et al.*, developed here was the use of a porous sample cup for rapid attainment of equilibrium. The sides of the sample cup were made of 0.012" lead-free glass and the bottom and top (electrodes) of porous stainless steel of 35 micron porosity. The coefficients of expansion of the glass side walls and the porous steel ends were similar permitting operating temperatures greater than 300° without damaging the cup. The glass sides and metal discs were machined to close tolerances to prevent the powder from passing between them. A silver strip (1/2-inch wide) was painted about the outside of the cup, touching platinum loops. This made electrical contact with the bottom disc through a tungsten clip holding the bottom in place; and consequently, with the resistance measuring circuit when the cup was pulled into position. To eliminate stray currents and glass surface effects, a guard circuit was provided by placing a guard ring around a small disc of known area, the small disc being insulated from the guard ring by a glass insert. During the pre-saturation period, the porous sample cup was seated against a ground glass joint projecting downward in the adsorption chamber. This forced the gas stream to pass through the sample and thereby greatly shortened the time required for equilibration of the sample. Measurements were made after lowering the sample cup from a support which held it against the ground glass joint (Fig. 1).

(5) G. A. Mills, E. R. Boedeker and A. G. Oblad, *J. Am. Chem. Soc.*, **72**, 1554 (1950).

TABLE I  
RELATIVE INFLUENCE OF WATER AND QUINOLINE ON SURFACE CONDUCTIVITY OF CATALYST

| $x$ | $t, ^\circ\text{C.}$ | $w/w_s$ |           | Moles/ $w_s$ |           | Resistivity, ohm cm. |                   | $\rho_w/\rho_q$ |
|-----|----------------------|---------|-----------|--------------|-----------|----------------------|-------------------|-----------------|
|     |                      | Water   | Quinoline | Water        | Quinoline | Water                | Quinoline         |                 |
| 0.1 | 125                  | 0.0435  | 0.170     | 0.00242      | 0.00131   | $2.5 \times 10^{10}$ | $1.2 \times 10^9$ | 208             |
|     | 175                  | .035    | .122      | .00195       | .00094    | $7.0 \times 10^{10}$ | $3.9 \times 10^8$ | 180             |
| 0.2 | 125                  | .0535   | .210      | .00297       | .00162    | $2.0 \times 10^{10}$ | $7.7 \times 10^8$ | 26              |
| 0.3 | 125                  | .063    | .253      | .00350       | .00195    | $3.7 \times 10^9$    | $5.8 \times 10^8$ | 6.3             |

While a large amount of data were accumulated in this study, in the interest of brevity only the results of the final runs are presented here. The  $\sigma, x, w/w_s$  data for water on the catalyst are shown in Figs. 2 and 3 while those for quinoline are given in Figs. 4 and 5. The reproducibility of results may be judged somewhat from the smoothness of the curves of Figs. 2 and 5.

Discussion of Results

The  $\sigma(T)$  data calculated from the isotherms at constant  $w/w_s$  were found for water as the adsorbate to follow approximately

$$\sigma = 5.3 \times 10^{21} e^{-32,200/T} + A_s(w/w_s) e^{-5,980/T} \quad (1a)$$

with the  $A_s(w/w_s)$  relationship given in Fig. 6. While equation 1a expressed the experimental data quite reliably, it was actually not possible from the data to evaluate each of the three constants  $A_b, E_b$  and  $E_s$  within limits of less than about 25%, due to the experimental error and compensating effects between the constants. It is an interesting and significant fact that equation 1a also applied, with the same values of  $A_b, E_b$  and  $E_s$ , to the system in which quinoline was the adsorbate. Again  $A_s(w/w_s)$  for quinoline is given in Fig. 6. The experimental method used here was inapplicable above 200° for quinoline because of electrical leakage. These results show that absorption is an important factor in the low temperature conductivity of ionic crystals and that the log  $\sigma$  vs.  $1/T$  plot (Figs. 7 and 8), in the region where

bulk conductivity is negligible, is linear only when the ratio  $w/w_s$  is held constant.

Table I shows an interesting phenomenon with regard to the influence of water and quinoline on the surface conductivity of the catalyst. The lower conductivity of the adsorbed water is very apparent in the lower relative pressure regions.

Bernal and Fowler<sup>6</sup> accounted for surface conductivity by the so-called "proton-jump" mechanism due to adsorbed water. This theory may account for the results with water as adsorbate, but, of course, not in the case of quinoline. It is surprising indeed that the conductivity at a given coverage was several times greater with quinoline than with water. This result suggests a mechanism for surface conductivity in the alumina-silica system based on the theory of Milliken, Mills and Oblad.<sup>7</sup> According to their theory, the calcined catalyst is a potential Lewis acid in an octahedral or 6-coordinated configuration. Under the influence of a Lewis base such as quinoline, the structure shifts to a tetrahedral or 4-coordinated one. Assuming that the conductivity of the catalyst is due primarily to the interstitial migration of

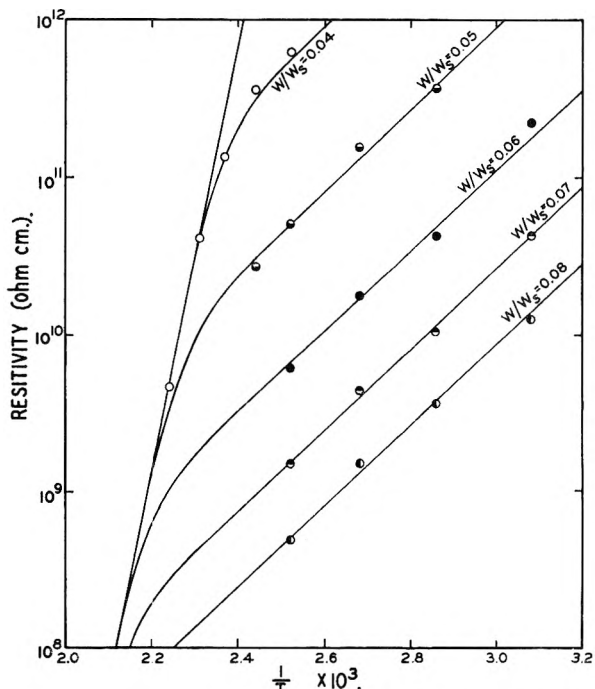


Fig. 7.—Surface conductivity resulting from adsorption of water on synthetic catalyst (lines calculated from equation 1a, circles represent experimental values).

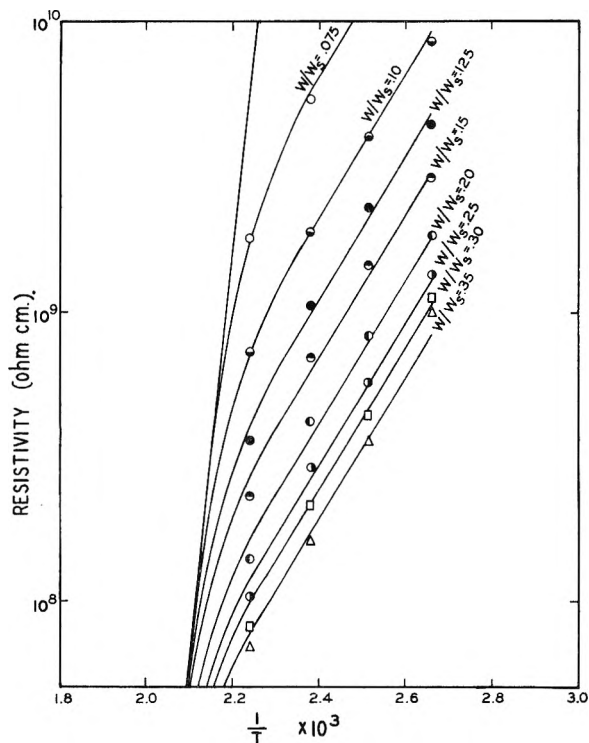
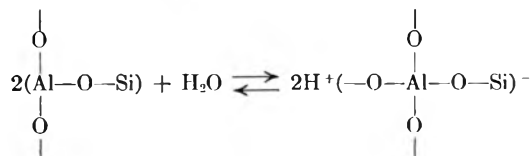


Fig. 8.—Surface conductivity resulting from adsorption of quinoline on synthetic catalyst (lines calculated from equation 1a, symbols represent experimental values).

(6) J. D. Bernal and R. H. Fowler, *J. Chem. Phys.*, **1**, 515 (1933).  
 (7) T. H. Milliken, Jr., G. A. Mills and A. G. Oblad, *Faraday Soc Disc.*, No. 8, 279 (1950)

Al<sup>+++</sup>, one would expect the conductivity in the 4-coordinated alumina to be much greater than that in the 6-coordinated state because the former would be a more open structure. Since quinoline is a strong Lewis base, it would tend to convert the surface states largely to the 4-coordinated structure, leaving the Al<sup>+++</sup> in the surface layer highly mobile. On the other hand, water would act as a much weaker base and would probably convert only a small fraction of the states to the 4-coordinated structure by an equilibrium of the type



in which the equilibrium is shifted to a limited extent to the right depending on the structural influence of the cristobalite silica, *i.e.*, upon the catalytic activity. The extent of the shift would depend on the extent of activation of the catalyst. This suggests that the same factors which would tend to displace the above equilibrium to the right would also tend to promote catalytic activity. This theory is subject to two types of direct evaluation. First, one may measure directly the ion mobilities, and second the conductivities of catalysts under varying degrees of activation. No attempt has yet been made to apply these tests.

The  $g(w/w_s)$  function (equation 3) was not obtained in completely analytical form. Equations 1a and Fig. 6 will, however, suffice to describe this function. The  $h(x)$  functions found empirically in this study were interesting indeed, but no explanation of them was readily apparent. For

water as adsorbent, it was found that the equation

$$\sigma = \alpha(T)e^{+ax^{1/2}} = \rho^{-1} \quad (4a)$$

gave a satisfactory representation of the  $h(x)$  function of equation 4. Here  $\alpha(T)$  is a temperature dependent constant determined at constant  $x$  by means of equation 1a, and  $a$  is a temperature independent constant the value of which was  $8.3 \pm 2.0$  for water. For quinoline the corresponding relationship for  $h(x)$  was found to be

$$\sigma = \alpha(T)e^{+ax^{1/10}} = \rho^{-1} \quad (4b)$$

with  $\alpha(T)$  again dependent only on temperature through equation 1a and  $a$  was again a constant of value approximately  $4.0 \pm 1.0$ .

Finally, it is of interest to note that the surface area  $\Sigma$ , computed from the isotherm by the B.E.T. method fell off (approximately) linearly with increasing temperature from about 250 m.<sup>2</sup>/g. at 40° to 100 m.<sup>2</sup>/g. at 200° with water as adsorbate. In the case of quinoline, according to computations by the B.E.T. method,  $\Sigma$  changed from about 400 m.<sup>2</sup>/g. at 100° to 250 m.<sup>2</sup>/g. at 200°. While the same trends were observed with water and quinoline, the observed values of  $\Sigma$  were about twice as large with quinoline as with water, indicating an error or errors in the assigned area per molecule for quinoline and/or water. It should be noted that the present technique, while considered good for the present purpose, does not claim the accuracy of the low temperature, high vacuum, nitrogen absorption method. Even in the latter, it is difficult to achieve a reproducibility of better than 20%. Hence, it is possible that the indicated variation of  $\Sigma$  with temperature may be spurious.

## CALCIUM SILICATE HYDRATE (I)

BY SIDNEY A. GREENBERG

Contribution from the Johns-Manville Research Center, Manville, New Jersey

Received December 10, 1953

Dehydration curves, surface area measurements and differential thermal analyses were made on calcium silicate hydrate (I) compounds formed in dilute suspension and hydrothermally up to 186° from CaO:SiO<sub>2</sub> mole ratio mixtures of 1:1, 1:2, 1:4, 2:1 and 4:1. Various forms of calcium silicate hydrate (I) including crestmoreite were prepared. Evidence was obtained which showed that the 3:2 CaO:SiO<sub>2</sub> ratio is maximum in the hydrate except under extreme reaction conditions. Chemical evidence also is presented which substantiates the presence of Ca[SiO<sub>2</sub>(OH)<sub>2</sub>] groups in the hydrate structure. In dilute suspension at 93° calcium hydroxide was found to react completely with equimolar or excess amounts of hydrated silica.

In this paper, a report is given on a study of some of the conditions under which calcium silicate hydrate (I) (CSHI) is synthesized and on an examination of the products formed. It has already been shown<sup>1</sup> that calcium silicate hydrate (I) is formed at room temperature from calcium hydroxide and silica gel and on the hydrolysis of tricalcium silicate. The compound has also been formed hydrothermally<sup>2-4</sup> from the same reactants. Calcium sili-

cate hydrate (I) is reported<sup>5</sup> to have a composition of 0.8-1.5 CaO·SiO<sub>2</sub>·XH<sub>2</sub>O with  $X$  approximating 0.5, 1.0 and 2.5. An orthorhombic unit cell has been proposed<sup>5,6</sup> for this compound with  $a = 5.62$  Å,  $b = 3.66$  Å, and  $c$  or interlayer spacings of 9.3, 10.4 and 14.0 Å, depending upon the water contents ( $X$ ) which are given above. No conclusive evidence exists<sup>5</sup> on whether Ca<sup>++</sup>SiO<sub>2</sub>(OH)<sub>2</sub><sup>-2</sup> or

(1) H. F. W. Taylor, *J. Chem. Soc.*, 3682 (1950).

(2) L. Heller and H. F. W. Taylor, *ibid.*, 2397 (1951).

(3) *Ibid.*, 1018 (1952).

(4) *Ibid.*, 2535 (1952).

(5) H. F. W. Taylor, *ibid.*, 163 (1953); "Proceedings of the Third International Symposium on the Chemistry of Cements," London, 1952, in press.

(6) J. D. Bernal, J. W. Jeffery and H. F. W. Taylor, *Mag. Concrete Research*, 49 (1952).

TABLE I  
SUMMARY OF EXPERIMENTAL CONDITIONS AND RESULTS

| Sample no. | Hydrothermal conditions °C. | Time, hr. | CaO:SiO <sub>2</sub> ratio | Reagents + hydrated silica | X-Ray and optical results   | Surface area (sq. m./g.) |
|------------|-----------------------------|-----------|----------------------------|----------------------------|---|--------------------------|
| A-1        | 186                         | 15        | 1:1                        | CaO                        | CSHI <sup>a</sup> —strong pattern; calcite trace                    | ...                      |
| B-1        | 170                         | 24        | 1:1                        | Ca(OH) <sub>2</sub>        | CSHI + trace calcite  | 90                       |
| B-2        | 170                         | 48        | 1:1                        | Ca(OH) <sub>2</sub>        | CSHI + trace calcite  | 49                       |
| B-4        | 170                         | 96        | 1:1                        | Ca(OH) <sub>2</sub>        | CSHI + trace calcite  | 31                       |
| B-18       | 170                         | 432       | 1:1                        | Ca(OH) <sub>2</sub>        | CSHI + trace calcite  | 25                       |
| C-1        | 148                         | 18.5      | 2:1                        | CaO                        | Ca(OH) <sub>2</sub> —strong pattern; CSHI and calcite—weak patterns | 75                       |
| C-2        | 148                         | 18.5      | 4:1                        | CaO                        | Ca(OH) <sub>2</sub> —strong pattern; CSHI and calcite—weak patterns | ...                      |
| C-3        | 170                         | 24        | 2:1                        | Ca(OH) <sub>2</sub>        | Ca(OH) <sub>2</sub> —strong pattern; CSHI and calcite—weak patterns | ...                      |
| C-4        | 170                         | 24        | 4:1                        | Ca(OH) <sub>2</sub>        | Ca(OH) <sub>2</sub> —strong pattern; CSHI and calcite—weak patterns | ...                      |
| D-1        | 148                         | 24        | 1:2                        | Ca(OH) <sub>2</sub>        | CSHI and calcite—not well defined                                   | 161                      |
| D-2        | 148                         | 24        | 1:4                        | Ca(OH) <sub>2</sub>        | CSHI—weak pattern   | 40                       |
| D-3        | 170                         | 24        | 1:2                        | Ca(OH) <sub>2</sub>        | CSHI, 14.5 and 8.5 Å. spacings                                      | ...                      |
| D-4        | 170                         | 24        | 1:4                        | Ca(OH) <sub>2</sub>        | CSHI, 14.5 and 8.5 Å. spacings                                      | ...                      |
| E-1        | Heated in suspension at 93° |           | 1:1                        | CaO                        | Ca(OH) <sub>2</sub> —strong pattern; CSHI and calcite—weak patterns | ...                      |
| E-2        | Heated in suspension at 93° |           | 1:1                        | Ca(OH) <sub>2</sub>        | Ca(OH) <sub>2</sub> —strong pattern; CSHI and calcite—weak patterns | 26                       |

<sup>a</sup> CSHI = calcium silicate hydrate (I).

Ca<sup>++</sup>(SiO<sub>3</sub>OH)<sup>-1</sup>(OH)<sup>-1</sup> groups are present in the hydrate.

The hydrate has been found to be stable to between 750 and 800°, in which temperature range it converts to  $\beta$ -wollastonite.<sup>5,7</sup> The calcium silicate hydrate (I) compounds reported here were formed at 93° at atmospheric pressure and with hydrothermal conditions in saturated steam at 148, 170 and 186°. CaO:SiO<sub>2</sub> mole ratios of 1:4, 1:2, 1:1, 2:1 and 4:1 were used in the reaction mixtures. The products were examined and identified by Debye-Scherrer patterns. Thermal dehydration curves, differential thermal analyses and surface area measurements were used to study the properties of calcium silicate hydrate (I) formed under the variety of conditions mentioned above.

### Experimental

**Materials.**—The calcium hydroxide of analytical reagent grade, the calcium carbonate and hydrated silica (83.2% SiO<sub>2</sub>) of standard luminescent grade were purchased from Mallinckrodt. The mineral wollastonite was obtained from Cabot. The calcite studied by thermal decomposition measurements was a single crystal of Iceland Spar. By heating the calcium carbonate four hours at 1000°, it was converted to calcium oxide. The calcium hydroxide used in the dehydration experiment was prepared from this calcium oxide. The purity of the calcium oxide and hydrated silica was carefully examined chemically and spectrographically, and the reagents were found to be very pure.

**Preparation at Atmospheric Pressure.**—Equimolar mixtures of calcium oxide or hydroxide and hydrated silica in dilute water suspension were heated on a steam-bath at approximately 93°. After three hours of heating the products were filtered, washed with acetone and dried in a vacuum-desiccator over calcium chloride. Reactions were carried out in Pyrex, platinum and stainless steel vessels, but no differences in the products were found.

**Preparations under Hydrothermal Conditions.**—Mixtures of calcium oxide or hydroxide and hydrated silica were heated on a steam-bath for three to four hours. The products were filtered and then treated hydrothermally in steam under equilibrium conditions. After hydrothermal treatment,

the hydrates formed were washed with acetone and dried in a vacuum-desiccator over calcium chloride. Very little of the original mixture was found to be lost by this treatment, and it is, therefore, assumed that the products have the same CaO:SiO<sub>2</sub> ratios as the reaction mixtures.

**X-Ray Apparatus.**—Debye-Scherrer diagrams were obtained with nickel-filtered copper radiation in a 114.59 mm. diameter camera. Exposures of four hours were usually adequate, but products formed at atmospheric pressure were irradiated for 20 hours to obtain more intense patterns. In order to reduce stray radiations a nickel-foil filter was placed in contact with the film. This procedure was previously used by Heller and Taylor.<sup>2</sup>

**Thermobalance Measurements.**—Weight loss curves were made with a Chevenard thermobalance according to the procedure outlined by Duval.<sup>8</sup> Sample weights of 0.7236 g. were generally used and exceptions are noted. A controlled heating rate of 8°/min. was employed. Because calcium silicate hydrates continue to lose weight to 1000°, it was necessary to estimate the slope of their curves to 1000° in the presence of calcium hydroxide and carbonate decomposition breaks in order to determine the concentration of the latter compounds.

**Surface Area Measurements.**—The measurements were made by the nitrogen gas adsorption method.<sup>9</sup> The samples were degassed at room temperature to avoid any thermal changes in the hydrates.

**Differential Thermal Analysis.**<sup>10</sup>—Alumina was used as a standard. A controlled heating rate of 12.5°/min. was employed. Measurements were made at the Rutgers School of Ceramics by Mr. M. G. McLaren through the courtesy of Professor J. Koenig.

### Results and Discussion

The experimental conditions, reagents and a summary of the results are presented in Table I.

**Products Formed Hydrothermally (186°).** CaO:SiO<sub>2</sub>, 1:1.—A hydrated calcium silicate (sample no. A-1) was prepared hydrothermally at 186° after 15 hours of reaction from an equimolar mixture of calcium oxide and hydrated silica.

(8) C. Duval, "Inorganic Thermogravimetric Analysis," Elsevier Publishing Co., New York, N. Y., 1953.

(9) P. H. Emmett and T. Dewitt, *Ind. Eng. Chem., Anal. Ed.*, **13**, 28 (1941).

(10) W. J. Smothers, Yao Chiang and Allen Wilson, "Bibliography of Differential Thermal Analysis," University of Arkansas, Institute of Science and Technology, Research Series No. 21, 1951.

(7) E. Thilo, H. Funk and E. M. Wichmann, *Abhand. Deut. Akad. Wiss. Berlin*, No. 4, 1 (1950).

The Debye-Scherrer pattern of the hydrate was found to follow closely that of the calcium silicate hydrate (I) previously reported.<sup>11,12</sup> A trace of calcite could be identified by the doublet at 1.87 and 1.92 Å.<sup>13</sup> No calcium hydroxide lines were found.

Thermal dehydration curves of calcium silicate hydrate (I), hydrated silica, calcite, calcium hydroxide and wollastonite were obtained. The curves (except wollastonite) are shown in Fig. 1.

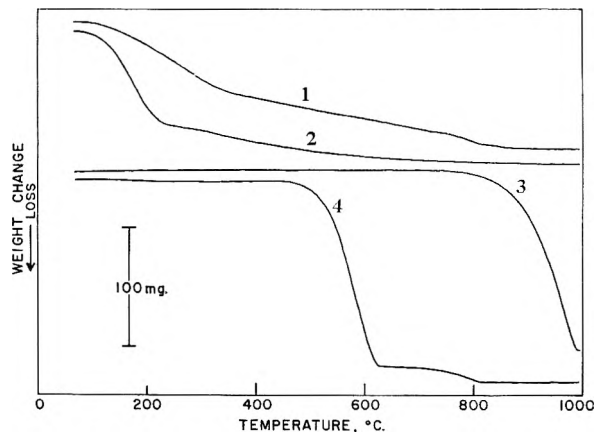


Fig. 1.—Dehydration curves: 1, calcium silicate hydrate (I) (sample no. A-1); 2, hydrated silica; 3, calcite; 4, calcium hydroxide.

The thermal dehydration curve of the calcium silicate hydrate is continuous, which is characteristic of the zeolites.<sup>14</sup> A similar continuity may be noted in the dehydration curve 2 of hydrated silica. The completeness of the calcium hydroxide reaction in the calcium silicate hydrate is apparent since no calcium hydroxide break is observed in the 450 to 650° range. The calcium hydroxide breakdown may be noted in curve 4. However, a break in the hydrate curve between 750 and 825° is also present in the calcite and calcium hydroxide curves (3 and 4) and is obviously due to carbonate decomposition. The per cent. of calcium carbonate was found to be 1.7 in the hydrate, none in the hydrated silica, 3.5 in the calcium hydroxide and 96.5 in the calcite. The curve for the mineral wollastonite showed a weight loss only in the range of the breakdown of calcium carbonate. Total water contents were 15.0% in the calcium silicate hydrate (I) and 16.8% in the hydrated silica.

The resemblance is marked between the dehydration curves of the hydrate and hydrated silica. Both lose the majority of their water below 300° and then a more gradual almost constant loss is maintained to approximately 850°. A loss of 57% of total water is found below 300° in the hydrate and hydrated silica loses 75% of its water in this temperature range.

Differential thermal analysis curves are presented in Fig. 2 of the calcium silicate hydrate (I), of an unreacted equimolar mixture of calcium hydroxide and hydrated silica, of hydrated silica and

of wollastonite. An endothermic peak at 865° and an exothermic peak at 965° will be noted in the DTA curve of the hydrated silicate. The 865° endothermic peak could immediately be ascribed to the breakdown of calcite, which has been found to decompose in this temperature range.<sup>15</sup> The unreacted mixture of calcium hydroxide and hydrated silica showed no energy change to 1000° as can be seen in the DTA curve 2 except for the decomposition of calcium hydroxide at 560°.<sup>16</sup> Wollastonite, similarly, was not found to have a marked energy change up to 1000° (curve 4). Hydrated silica presented a usual DTA curve<sup>17</sup> with no marked peaks (curve 3).

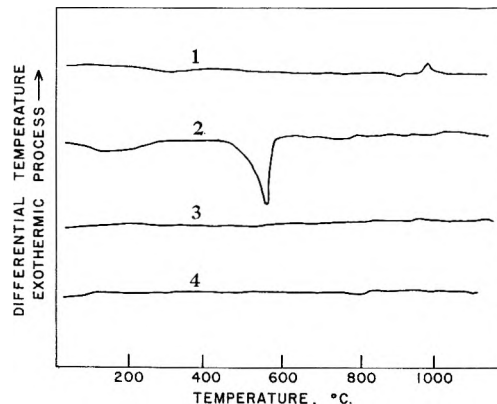


Fig. 2.—Differential thermal analysis curves: 1, calcium silicate hydrate (I) (sample no. A-1); 2, calcium hydroxide and hydrated silica; 3, hydrated silica; 4, wollastonite.

In an effort to establish the origin of the 965° peak, samples of calcium silicate hydrate (I) (sample no. A-1) were heated at 8°/min. to 700, 750, 800, 900 and 1000°. Debye-Scherrer patterns of the heated samples showed that calcite lines disappear above 750°, that calcium silicate hydrate (I) is apparently stable to 900° although the X-ray pattern is weak, and that calcium silicate hydrate (I) converts to  $\beta$ -wollastonite between 900 and 1000° under these conditions.

**Products Formed Hydrothermally (170°). A. CaO:SiO<sub>2</sub>, 1:1.**—A series of hydrates (sample no. B-1, B-2, B-4, and B-18) were synthesized hydrothermally at 170° with reaction times of 1, 2, 4 and 18 days, respectively.

Debye-Scherrer patterns of the hydrates exhibited a pattern similar to that for calcium silicate hydrate (I). No changes in the patterns with time of reaction were noted.

The dehydration curves of the products were typical of calcium silicate hydrate (I). Very little calcium carbonate was found to be present in any of the samples. After 18 days of reaction, the curve of sample no. B-18 showed no breakdown of calcium carbonate. Apparently all the calcium carbonate had slowly reacted with the silica. The water contents of the samples, which are shown graphically in Fig. 3, decreased with time of reaction.

The surface areas of the sample, which may be noted in Fig. 3, were also found to decrease with

(11) H. F. W. Taylor, *Min. Mag.*, **30**, 155 (1953).

(12) G. F. Claringbull and M. H. Hey, *ibid.*, **29**, 960 (1952).

(13) ASTM X-ray Card Index, 1st Supplement, August 1945.

(14) V. A. Kind, S. D. Okorokov and E. P. Khodikel, *Tsment.* **6**, 32 (1939).

(15) R. M. Gruver, *J. Am. Cer. Soc.*, **33**, 96 (1950).

(16) G. L. Kalousek and M. Adams, *J. Am. Concrete Inst.*, **77** (1951).

(17) E. A. Hauser and D. S. le Beau, *This Journal*, **56**, 136 (1952).

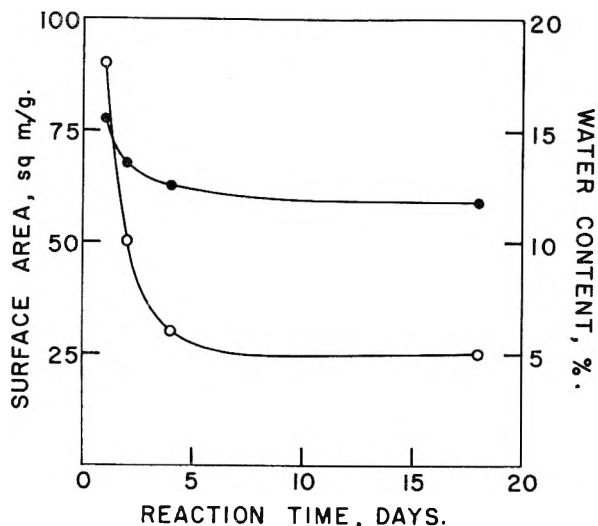


Fig. 3.—Variation with reaction time of water content, ● and surface area, ○.

time of reaction. It was also observed that the surface area of sample no. B-18 rose to 44 sq.m./g. from 25 sq.m./g. when the hydrate was degassed at 176° instead of at room temperature.

**Products Formed Hydrothermally (148 and 170°).** B. CaO:SiO<sub>2</sub>, 2:1 and 4:1.—Hydrates with CaO:SiO<sub>2</sub> ratios of 2:1 and 4:1 were prepared hydrothermally at 148° (sample no. C-1 and C-2) and 170° (sample no. C-3 and C-4) with reaction times of 18.5 and 24 hours.

Debye-Scherrer patterns of the products exhibited mainly strong calcium hydroxide patterns. However, very weak lines at 3.07 and 1.84 Å. were evidence of the presence of calcium silicate hydrate (I). Heller and Taylor<sup>4</sup> found similar products on hydrothermally (100 to 200°) treating reaction mixtures with CaO:SiO<sub>2</sub> ratios of 2:1 and 3:1.

The dehydration curves of the hydrates are presented in Fig. 4. In general, the curves have the shape characteristic of calcium silicate hydrate (I). Breaks in the curves may be noted in the decomposition ranges of calcium hydroxide and carbonate.

Sample no. C-3 and C-4 with calcium oxide to silica ratios of 2:1 and 4:1 hydrothermally treated at 170° were found to contain 11.7 and 29.2% unreacted calcium oxide (calcium hydroxide and carbonate). The unreacted calcium oxide contents of the corresponding samples (C-1 and C-2) prepared at 148° were 14.6 and 36.9%. It is interesting that the mole ratio of CaO (reacted):SiO<sub>2</sub> (total) in sample no. C-1, C-2 and C-3 was approximately 3:2 but that sample no. C-4 which had been prepared at 170° from a CaO:SiO<sub>2</sub>, 4:1 mole ratio of reagents showed a CaO (reacted):SiO<sub>2</sub> (total) of approximately 2:1.

**Products Formed Hydrothermally (148 and 170°).** C. CaO:SiO<sub>2</sub>, 1:2 and 1:4.—Hydrates with CaO:SiO<sub>2</sub> ratios of 1:2 and 1:4 were prepared hydrothermally at 148° (sample no. D-1 and D-2) and at 170° (sample no. D-3 and D-4).

Debye-Scherrer patterns of the samples prepared at 148° showed weak calcium silicate hydrate (I) patterns. However, the samples prepared at 170° showed patterns of calcium silicate hydrate (I) which were quite strong and weak calcite patterns.

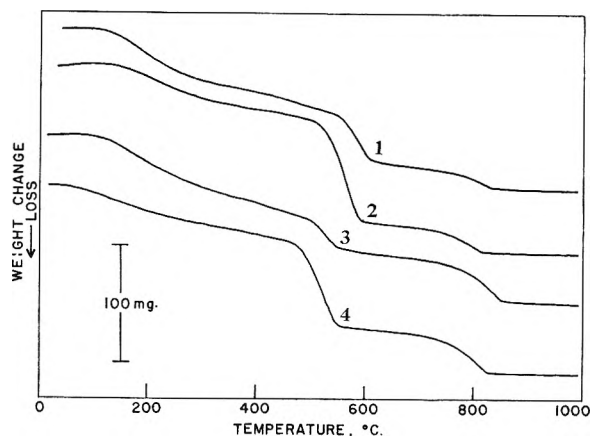


Fig. 4.—Thermal dehydration curves of hydrates formed from CaO:SiO<sub>2</sub> reaction mixtures of 2:1 and 4:1. Dehydration curves: 1, C-1 (2:1, 148°); 2, C-2 (4:1, 148°); 3, C-3 (2:1, 170°); 4, C-4 (4:1, 170°). (CaO:SiO<sub>2</sub> ratios and temperature of hydrothermal treatment are given in parentheses.)

The patterns include most of the spacings of natural crestmorite.<sup>5,11</sup> In addition, spacings at 8.2, 4.7, 4.2, 3.79 and 3.13 Å. appear. The 8.2 Å. spacing has been reported<sup>11</sup> in wilkeite.

The thermal stability of the synthetic crestmorite was traced by heating samples at 8°/min. to 200, 400, 600, 800, 900 and 1000°. Debye-Scherrer patterns of the heated samples were taken. It was found that the decomposition followed that of natural crestmorite described by Taylor<sup>5</sup> with only a few differences. The 11.3 and 14.5 Å. lines were stable to 400°, at 200° a 9.2 Å. spacing appeared, which was lost between 200 and 400°. By 600°, 11.3 and 14.5 Å. spacings were not present, but a new 12.3 Å. line (strong) appeared. By 800°, this spacing disappeared and a 11.5 Å. spacing (VS line) became evident. Between 800 and 900° the pattern of synthetic crestmorite had faded and the patterns of α- and β-wollastonite were found. An 8.2 Å. spacing (medium intensity line) was present to 800°.

The dehydration curves of the samples are typical for calcium silicate hydrate (I). Relatively small amounts of calcium carbonate impurities are present in the samples. The water contents of the samples prepared at 148° decreased from 17.1 to 13.8% with a rise in SiO<sub>2</sub>:CaO ratio from 2:1 to 4:1. Similarly, in the corresponding samples prepared at 170° the reduction was from 14.8 to 10.9%.

**Products Formed Hydrothermally at Atmospheric Pressure (93°).**—Equimolar mixtures of calcium oxide and hydroxide and hydrated silica (sample no. E-1 and E-2) were heated in dilute suspension at approximately 93° and atmospheric pressure.

A Debye-Scherrer pattern of sample no. E-1 obtained from a 20-hour exposure showed a strong calcium hydroxide pattern and a weak calcium silicate hydrate (I) pattern.

The thermobalance curve of sample no. E-1 shown in Fig. 5 exhibited a typical calcium silicate hydrate (I) curve with 1.0% unreacted calcium hydroxide, 3.8% calcium carbonate and 20.0% water present in the sample. The unreacted calcium hydroxide was thus sufficiently concentrated to give a pattern.<sup>4</sup>

The dehydration curve, given in Fig. 5, of sample no. E-2 serves to illustrate two interesting points. First, no unreacted calcium hydroxide is evident. Second, the sample was not vacuum dried and the weight loss may be noted to begin at a much lower temperature than that shown in the vacuum dried sample no. E-1. No unreacted calcium hydroxide, 4.6% calcium carbonate and 29.3% water were found in this sample.

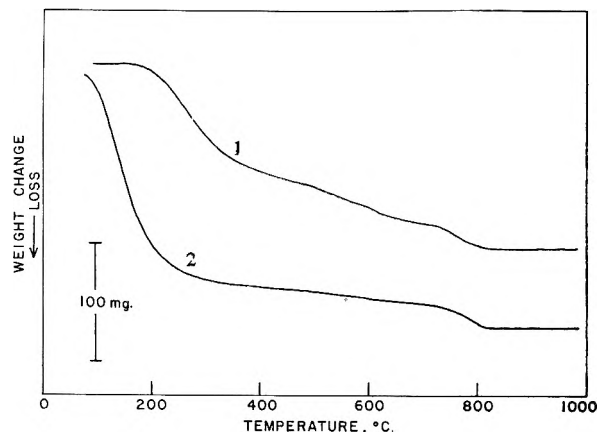


Fig. 5.—Thermal dehydration curves of calcium silicate hydrate formed at 93°: 1, sample no. E-1; 2, sample no. E-2.

### Conclusions

**Conditions for the Preparation of Calcium Silicate Hydrate (I).**—Taylor and Heller<sup>1-4</sup> have previously reported the preparation of calcium silicate hydrate (I) at room temperature and hydrothermally from CaO:SiO<sub>2</sub> mixtures of 1:1, 3:2, 2:1 and 3:1. In this study, calcium silicate hydrate (I) was prepared in dilute suspension at 93° after three hours of reaction and hydrothermally at 148, 170 and 186° from equimolar mixtures of calcium hydroxide and hydrated silica. In addition, various forms of calcium silicate hydrate (I) have been prepared from reaction mixtures with CaO:SiO<sub>2</sub> ratios of 1:2, 1:4, 2:1 and 4:1.

The products formed from 2:1 and 4:1 ratio mixtures contain unreacted calcium hydroxide. A maximum mole ratio of 3:2 of the reacted calcium hydroxide to total silica was found in these samples except the one prepared at 170° with a 4:1 CaO:SiO<sub>2</sub> ratio, which had a ratio of reacted calcium hydroxide to total silica greater than 3:2. With such an excess of calcium hydroxide present, it is reasonable to assume that all the silica had reacted. Taylor<sup>1</sup> found a maximum 3:2 ratio in calcium silicate hydrate (I) formed at room temperature.

When an excess of silica is present in the reaction mixture in the ratio of 2:1 and 4:1 SiO<sub>2</sub>:CaO, products are formed which contain strong lines for *c* spacings of 14.5 Å. and weak 11.3 Å. lines which are also present in natural crestmoroite.<sup>5,11</sup>

### Determination of Unreacted Calcium Hydroxide.

—It is apparent from the results of this investigation that products formed from CaO:SiO<sub>2</sub> mixtures of 1:1, 1:2 and 1:4 contain very little unreacted calcium hydroxide even after only three hours of reaction at 93° in dilute suspension. If calcium hydroxide is adsorbed<sup>5</sup> on the silica particles, that condition must be very unstable and chemical

reaction must immediately follow. In agreement with the work of Taylor<sup>5</sup> it was found that the quantitative determination of uncombined calcium hydroxide in the presence of hydrated calcium silicates was not possible by usual extraction procedures.<sup>18</sup> However, by use of the Chevenard Thermobalance it was possible to determine calcium hydroxide quantitatively.

**Stability of Calcium Silicate Hydrate (I) CaO<sub>2</sub>:SiO<sub>2</sub>, 1:1.**—When this compound is heated for prolonged periods it converts to β-wollastonite at 750 to 800°.<sup>5,7</sup> However, when the compound is heated rapidly at 8–12.5°/min. it has been shown in this work by X-ray and DTA that the structure converts to β-wollastonite between 900 and 1000°. These results agree with those of Kind, *et al.*<sup>14</sup> The differential thermal analysis of an unreacted equimolar mixture of calcium hydroxide and anhydrous silica offered no evidence that the materials react in the solid state below 1000°. Similarly, β-wollastonite was not shown to undergo any phase changes below 1000°.

The thermal stability of calcium silicate hydrate (I) does not seem to support the theory of Bernal<sup>19</sup> that hydrogen bonding occurs along the fiber axis. This author believes the 3.6 Å. periodicity along the fiber axis of many hydrated calcium silicates is possible because of hydrogen bonding.

**Stability of Synthetic Crestmoreite (14.5 Å. Spacing).**—The thermal stability of this variation of calcium silicate hydrate (I) is lower than that of the compound without the wider 14.5 Å. *c*-spacing. It was found to convert at 8°/min. to the wollastonite forms between 800 and 900° and the wide spacings were observed to decrease as the samples were heated. In general, the results agree with those found by Taylor<sup>5</sup> on the natural products.

**Constitutional Water in Calcium Silicate Hydrate (I).**—It has been reported<sup>14</sup> that theoretical silicic acid probably contains silicon tetrahedra coordinated by four hydroxyls. This compound Si(OH)<sub>4</sub> is very reactive and would then polymerize<sup>20</sup> to a hydrated silica particle with Si–OH groups on the surfaces and in the pores. This theory of the structure would thus indicate that water is chemically bound in the structure in SiOH groups.

Bernal<sup>19</sup> has stated that hydrated calcium silicates may be related to other hydrated silicates by having SiO<sub>4</sub><sup>-4</sup>, SiO<sub>3</sub>(OH)<sup>-3</sup>, SiO<sub>2</sub>(OH)<sub>2</sub><sup>-2</sup> and SiO(OH)<sub>3</sub><sup>-1</sup> groups. Evidence for the Si–OH linkage exists in afwillite SiO<sub>3</sub>(OH)<sup>-3</sup> groups,<sup>21</sup> which are also believed to be present in dicalcium silicate α-hydrate.<sup>22</sup>

The results reported here seem to substantiate the theory that calcium silicate hydrate (I) is built up of Ca<sup>+2</sup> and (H<sub>2</sub>SiO<sub>4</sub>)<sup>-2</sup> groups<sup>23,24</sup> rather than

(18) R. H. Bogue, "The Chemistry of Portland Cements," Reinhold Publ. Corp., New York, N. Y., 1943.

(19) J. D. Bernal, *Brit. J. Appl. Phys.*, **3**, 277 (1951).

(20) M. V. Tamele, in "Chemical Architecture," "Frontiers in Chemistry," Vol. V, Interscience Publishers, Inc., New York, N. Y., 1948.

(21) H. D. Megaw, *Acta Cryst.*, **2**, 419 (1949).

(22) L. Heller, *Brit. J. Appl. Phys.*, **3**, 277 (1951).

(23) P. S. Roller and G. Erwin, *J. Am. Chem. Soc.*, **62**, 461 (1940)

(24) E. Thilo, *Angew. Chem.*, **63**, 201 (1951).

$\text{Ca}^{+2}(\text{SiO}_3\text{H})(\text{OH})^{-2}$  groups.<sup>5</sup> This is based on the evidence that the dehydration curve of calcium silicate hydrate (I) is similar to that of hydrated silica which contains presumably only one species of hydroxyl groups. However, the possibility always exists that the decomposition of the other tetrahedra proposed may take place in the same temperature range as that of hydrated silica.<sup>25</sup>

The conclusions offered above are based on the assumption that vacuum drying removed sorbed water. This assumption is based on several pieces of evidence.

First, Shapiro and Weiss<sup>26</sup> have found that vacuum drying of hydrated silica removes free water. It is, therefore, reasonable to assume that free water is also removed by the same treatment from the hydrated silicate since the same attractive forces are probably active.

Second, the indication that water lost below 300° is not sorbed is shown by the lack of correlation between the water lost below 300° and the surface areas of the compounds (sample no. B-1, B-2, B-4, B-18) formed at 170° after 1, 2, 4 and 18 days of reaction. For example, the 1-day compound has a surface area of 90 sq. m./g. which is over three times that of the 18-day sample, yet the former sample loses 13% less water below 300° than the latter sample.

Third, the removal of water (presumably uncombined) from air dried calcium silicate hydrate (I) begins at a much lower temperature than that for the vacuum dried samples. This may be noted in the dehydration curves illustrated in Fig. 5.

**Hydration States of Calcium Silicate Hydrate (I): A.  $\text{CaO}:\text{SiO}_2$ , 1:1.**—The theoretical amount of water in a compound with the composition  $\text{CaO}:\text{SiO}_2\cdot\text{H}_2\text{O}$  is 13.4%. Compounds formed with this ratio of calcium hydroxide to silica were found to have water contents varying from 15% after 15 hours reaction at 186° (A-1) to 11.8% after 18 days of reaction at 170° (B-18). These results seem to indicate that the  $\text{CaO}:\text{SiO}_2\cdot\text{H}_2\text{O}$  composition is fairly closely approximated. In all of these compounds there were found 11–11.3 Å. spacings,

which are stable to 900° when the compound is heated at 8°/min.

**B.  $\text{CaO}:\text{SiO}_2$ , 1:2, 1:4.**—Compounds formed from this ratio of components were found to have water contents varying from 17.1 to 10.9%. According to Taylor<sup>5</sup> the 14.5 Å. spacing of these compounds should correspond to a compound with 2.5 moles of water. Therefore, if the calcium hydroxide reacts with the maximum amount of silica, then the compound should have the composition  $0.8\text{CaO}:\text{SiO}_2\cdot 2.5\text{H}_2\text{O}$ . This compound would contain 30% water. A comparison of the water contents in this series of compounds showed that the unreacted silica contains 2.2% water which leaves only 18.4% for the remainder of the hydrated calcium silicate. Thus, the evidence does not support the proposed layer structure<sup>5</sup> for calcium silicate hydrate (I).

**Interpretation of Surface Area Measurements.**—In Table I and Fig. 3 are given the surface areas of a series of compounds (B-1, B-2, B-4 and B-18) prepared at 170° after 1, 2, 4 and 18 days of reaction. It may be noted in Fig. 3 that the surface area decreases from 90 to 25 sq. m./g. in 17 days of reaction which indicates that the particle size is increasing with time of reaction. The increase of surface area of sample no. B-18 with the temperature (at which the sample is degassed for the surface area measurement) seems to present evidence that the porosity of the sample increases with loss of water.

It may be seen in Table I that sample no. E-2 which was prepared at 93° has a surface area of 26 sq. m./g. A comparison of this area with those of the hydrothermally treated samples indicates that these particles are larger and X-ray patterns show that they are not so well crystallized.

A comparison of the surface areas of samples no. B-1, C-1, D-1 and D-2 shows that with a large excess of calcium oxide or of silica, the compounds have lower surface areas than those of the equimolar or 1:2  $\text{CaO}:\text{SiO}_2$  ratio compounds. This would be expected in the samples with an excess of calcium hydroxide or hydrated silica in the reaction mixture. The unreacted material would, of course, have a much lower surface area than that of the calcium silicate hydrate (I).<sup>27</sup>

(25) T. Tamura and M. L. Jackson, *Science*, **117**, 381 (1953).

(26) I. Shapiro and H. G. Weiss, *THIS JOURNAL*, **57**, 219 (1953).

(27) Unpublished results.

# A METHOD FOR EVALUATING AND CORRELATING THERMODYNAMIC DATA

By C. HOWARD SHOMATE

*Chemistry Division, Research Department, U. S. Naval Ordnance Test Station, China Lake, California*

*Received December 12, 1953*

A useful thermodynamic function has been developed which permits (1) fitting of high-temperature heat content data with algebraic equations by a fast and accurate method; (2) accurate smoothing of high-temperature heat content data; (3) correlation of low-temperature heat capacity data with high-temperature heat content data; (4) accurate evaluation of heats of transition and fusion at high temperatures; (5) accurate calculation of heat capacities at high temperatures from heat content data.

Many laboratories are engaged in measurements of low temperature heat capacities, in which a measured amount of heat is added to a sample to raise its temperature by a relatively small amount. The heat capacity at the mean temperature is calculated from the energy supplied, divided by the temperature rise, the assumption being made that the heat capacity varies linearly with temperature over this small temperature interval. Precisions in the heat capacities measured by this method usually do not exceed a few tenths of one per cent.

Most attempts to use this method at moderately high temperatures have failed, however, so far as accuracy is concerned, because it was impossible to evaluate satisfactorily the corrections for heat interchange with the surroundings. In fact, the experimental plots of most low-temperature heat capacity data will have more scatter of the experimental points in the neighborhood of room temperature than at lower temperatures. Consequently, the experimental method most widely employed for extending thermodynamic data above room temperature has been the method of mixtures, or so-called "drop" method, in which a sample is heated in a furnace to a temperature  $T$ , allowed to drop into a calorimeter maintained at some convenient temperature near room temperature (e.g., 298.16°K.), and the amount of heat delivered to the calorimeter,  $H_T - H_{298.16}$ , measured.

The curves obtained by the usual plot of experimental  $H_T - H_{298.16}$  values vs.  $T$ , barring anomalies such as transitions and fusions, can be roughly approximated as straight lines, with  $H_T - H_{298.16} = 0$ , when  $T = 298.16^\circ\text{K}$ . Such a plot is not satisfactory for obtaining smoothed values of  $H_T - H_{298.16}$ , especially at the lower temperatures, where a certain vertical displacement becomes percentage-wise a much greater error. Some investigators plot the function  $(H_T - H_{298.16})/(T - 298.16)$  vs.  $T$ , which permits some magnification of the vertical scale, since the function is not equal to zero at 298.16°K., but becomes  $C_{p298.16}$  at this temperature.

High-temperature heat content data should not be considered entirely divorced from low-temperature heat capacity data for the same substance, and yet it is difficult to correlate the two sets of data. A few investigators attempt to differentiate graphically their high-temperature heat content curves<sup>1</sup> in order to evaluate the heat capacity at

high temperatures, but such a procedure is difficult and laborious, and its success depends a great deal on how well the heat content curves have been smoothed. There is no assurance that the heat capacities thus obtained will correlate smoothly with low-temperature heat capacities in the neighborhood of room temperature. Most low-temperature investigators graphically integrate their heat capacity curves to obtain low-temperature heat content values. This procedure is not too difficult, but, as mentioned above, the heat content plot is rather insensitive, and is a poor method for trying to correlate the two sets of data.

A few years ago the author<sup>2</sup> presented a graphical method for obtaining the best heat content equation of the form

$$H_T - H_{298.16} = aT + bT^2 + cT^{-1} + d \quad (1)$$

to fit a set of experimental high-temperature heat content data. In its differentiated form the equation becomes

$$C_p = a + 2bT - cT^{-2} \quad (2)$$

If the value of  $C_{p298.16}$  is known from heat capacity measurements at room temperature, one boundary condition is satisfied by setting  $C_p = C_{p298.16}$  in equation 2 when  $T = 298.16^\circ$ . The other boundary condition to be satisfied is that  $H_T - H_{298.16} = 0$  when  $T = 298.16^\circ$  in equation 1. This reduces the number of constants to be evaluated to two, and the following relationship can be derived

$$\frac{T[(H_T - H_{298.16}) - C_{p298.16}(T - 298.16)]}{(T - 298.16)^2} = bT + \frac{c}{(298.16)^2} \quad (3)$$

If the function on the left side of equation 3 is evaluated for each measured high-temperature heat content value, and the results are plotted against  $T$ , the resulting plot will be a straight line if the measured data are fitted exactly by equation 1, the slope of the line being  $b$ , and the "y"-intercept  $c/(298.16)^2$ . The constants  $a$  and  $d$  are evaluated from the boundary conditions at 298.16°K. The high-temperature heat content of most substances can be fitted over a wide temperature range by an equation of the form of equation 1 with a maximum error of only a few tenths of a per cent. For example, a straight line drawn in the high-temperature region of the function plot for aluminum oxide (Fig. 1) with a slope of 0.0117 and a "y"-intercept (value of the function at  $T = 0$ ) of 33.75 yields the following

(1) (a) D. C. Ginnings and R. J. Corruccini, *J. Research Natl. Bur. Standards*, **38**, 593 (1947); (b) G. Rutledge, *Phys. Rev.*, **40**, 262 (1932).

(2) C. H. Shomate, *J. Am. Chem. Soc.*, **66**, 928 (1944).

heat content equation, which fits the smoothed data within 0.5% in the range 298–1200°K.

$$H_T - H_{298.16}(\text{abs. j./mole}) = 105.78T + 0.0117T^2 + 3,000,000T^{-1} - 42,641$$

In addition to the utility of the function for fitting high-temperature heat content data with algebraic equations, it has several other practical applications, which will be described.

**Smoothing of High-Temperature Heat Content Data, and Correlating with Low-Temperature Heat Capacity Data.**—In order to apply the function to low temperature heat capacity data, the latter must first be graphically integrated to give heat contents below 298.16°K. In a paper on "Heat Capacity Standards" Ginnings and Furukawa<sup>3</sup> have presented a table of smoothed values of the heat capacity and heat content of aluminum oxide (synthetic sapphire) from 0 to 1200°K. The function curve for these heat content data is shown in Fig. 1. The curve bears a resemblance to the heat capacity curve of aluminum oxide, except that it does not have the pronounced S-shape in the neighborhood of 50–100°K. It should be noted that there is no discontinuity in the curve at 298.16°K.

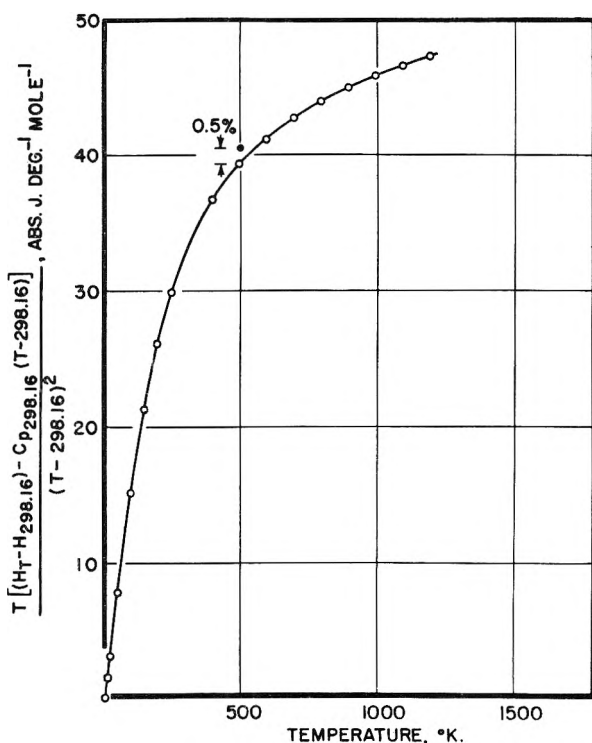


Fig. 1.—Thermodynamic data for  $\text{Al}_2\text{O}_3$  ( $C_{p298.16} = 79.01$  abs. j. deg.<sup>-1</sup> mole<sup>-1</sup>).

The extreme sensitivity of the function curve is indicated by a point above the curve at 500°K., in which the true  $H_{500} - H_{298.16}$  value has been increased by 0.5%. Errors of 0.1% in the heat content are easily detectable in this method of plotting, and since this is approximately the precision being achieved with some high-temperature heat content apparatuses, it is important not to

(3) D. C. Ginnings and G. T. Furukawa, *J. Am. Chem. Soc.*, **75**, 522 (1953).

sacrifice this precision in smoothing the data. Other graphical methods currently used do not have this sensitivity.

The question arises as to what effect an erroneous value of  $C_{p298.16}$  has on the application of the method. As far as smoothing the high-temperature heat content data is concerned, the value adopted for  $C_{p298.16}$  is immaterial, since in recalculating smoothed values of  $H_T - H_{298.16}$  from the function curve the erroneous value is eliminated. However, if a value close to the true value of  $C_{p298.16}$  is adopted, the function curve will have only slight curvature in the high-temperature region.

In applying the function to both high and low temperature data for the same compound, an erroneous value of  $C_{p298.16}$  is easily demonstrated by the function curve. Figure 2 shows a plot of the function for aluminum oxide, in which a value of  $C_{p298.16} = 79.17$  abs. j./deg./mole is used. This is only 0.2% higher than the true value of 79.01 abs. j./deg./mole used in Fig. 1, but the discontinuity at 298.16°K. is quite marked.

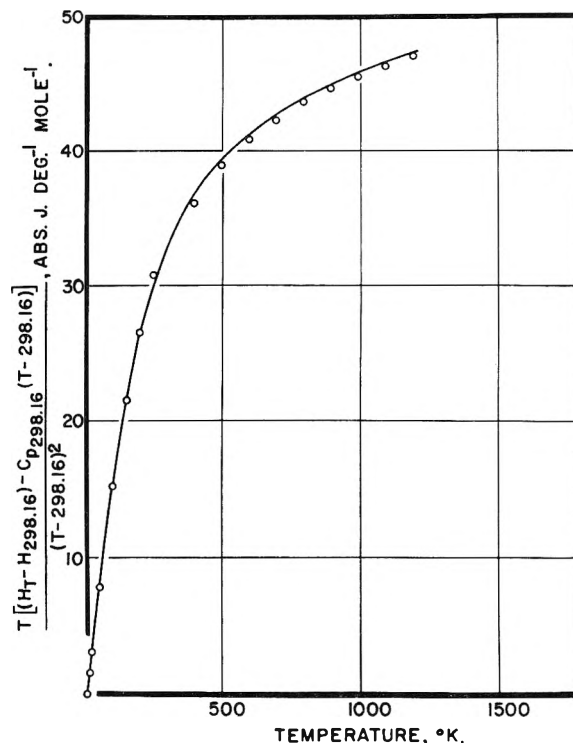


Fig. 2.—Thermodynamic data for  $\text{Al}_2\text{O}_3$  ( $C_{p298.16} = 79.17$  abs. j. deg.<sup>-1</sup> mole<sup>-1</sup>).

A more vivid example is shown in Fig. 3, in which the function is applied to the data for titanium metal taken from a Bureau of Standards compilation.<sup>4</sup> On a heat content plot the discontinuity is undiscernible. Most probably the error here is principally in the high-temperature heat content data, rather than in the value of  $C_{p298.16} = 6.01$  cal./deg./mole used to calculate the function curve.

Even in the absence of high-temperature data, the function is useful in determining how to draw

(4) National Bureau of Standards, "Selected Values of Chemical Thermodynamic Properties, Series III" (June 30, 1949).

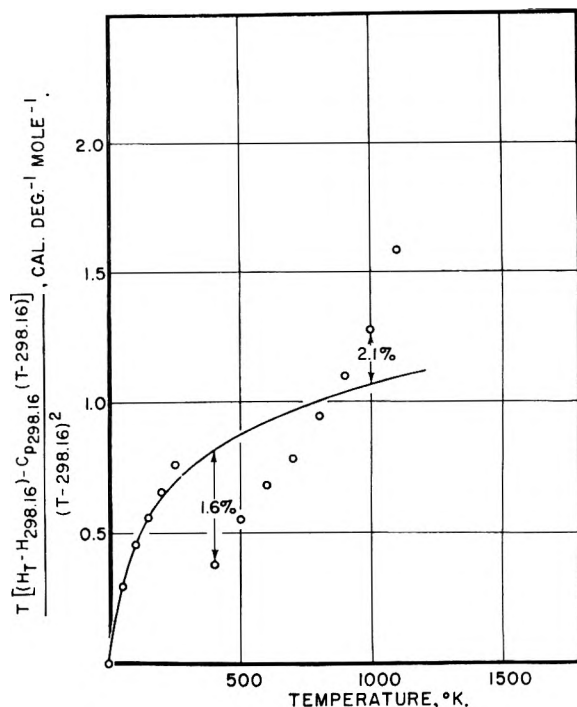


Fig. 3.—Thermodynamic data for Ti ( $C_{p298.16} = 6.01$  cal. deg.<sup>-1</sup> mole<sup>-1</sup>).

low-temperature heat capacity curves in the neighborhood of room temperature, where the data are least accurate. If the heat capacity curve, as drawn, yields a maximum in the function curve below 298.16°K., then the heat capacity curve should be raised slightly. On the other hand, if the function curve has an inflection point upward below 298.16°K., the heat capacity curve should be lowered slightly in the neighborhood of room temperature. These shifts in the heat capacity curve normally will not exceed a few tenths of a per cent., which is approximately the precision of the experimental data near room temperature.

**Evaluation of Heats of Fusion and Transition at High Temperatures.**—One of the disadvantages attributed to the high-temperature drop method is that it is not always adequate for obtaining heat effects at transition points, especially if the heat of transition is small. For example, Coughlin and Orr<sup>5</sup> reported measurements of the high-temperature heat content of barium metatitanate, and were unable to calculate the heat associated with a Curie-type transition occurring at 393°K. Figure 4 shows a heat content *vs.* temperature plot of their data, in which the transition is almost undiscernible.

Todd and Lorenson<sup>6</sup> made low-temperature heat capacity measurements on barium metatitanate which disclosed the existence of anomalies at 201.6 and 284.9°K., with heats of transition of 12 and 26 cal./mole, respectively. A recomputation of their data showed a heat of 33 cal./mole for the 284.9° transition, the difference being in the judgment on how to draw the "normal" heat capacity curve in that region. Todd and Lorenson also made low-temperature heat ca-

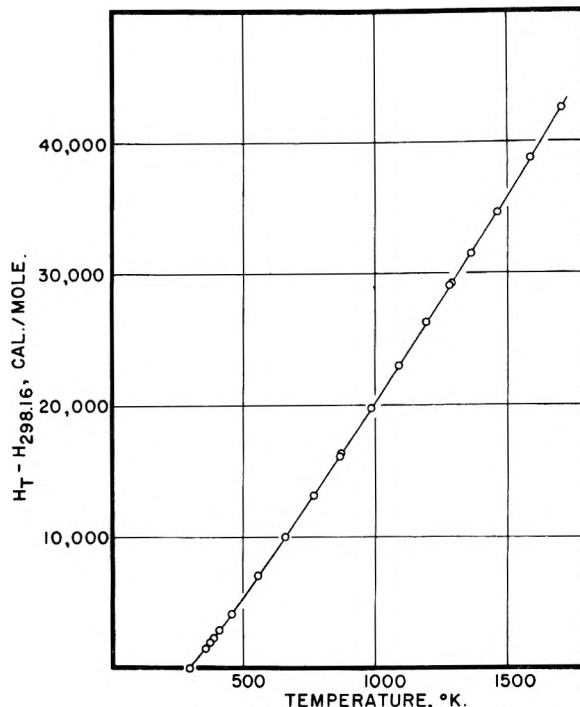


Fig. 4.—High-temperature heat content of BaTiO<sub>3</sub>.

capacity measurements on a crystalline solution of barium and strontium metatitanates (0.543 BaTiO<sub>3</sub>·0.457 SrTiO<sub>3</sub>) in the hope of lowering the 393° Curie point to a temperature within the range of their measurements (below 298°K.). The result, however, was the elimination of all transitions in the range 50–298°K.

The evaluation of the heat of the 393°K. transition is easily accomplished by the application of the function to Todd and Lorenson's "normal" curve for barium metatitanate, and to Coughlin and Orr's experimental data. The results are shown in Fig. 5. If 75, 85 and 95 cal./mole are successively subtracted from Coughlin and Orr's data above 393°K. before applying the function, the three upper curves in Fig. 5 are obtained. It should be noted that Coughlin and Orr rounded their heat content results to the nearest 10 cal./mole, allowing possible rounding errors of 5 cal./mole, which is about the precision to be attached to the heat of the 393°-transition of 85 cal./mole. This uncertainty compares favorably with the uncertainty of the heat of the transition at 284.9°K.

If the heat capacity curves below and above an anomaly (transition or fusion) are markedly different, so that it is difficult to draw a smooth "normal" heat capacity curve through the region of the anomaly, a similar difficulty will be encountered in drawing a continuous function curve in this region after the heat associated with the anomaly is subtracted. However, in the latter case, if the two function curves intersect at the temperature of the anomaly, then the correct heat has been subtracted to obtain the high-temperature curve.

Oftentimes it is difficult to ascertain on a heat content *vs.* temperature plot whether a particular point contains a small amount of premelting or

(5) J. P. Coughlin and R. L. Orr, *J. Am. Chem. Soc.*, **75**, 530 (1953).

(6) S. S. Todd and R. E. Lorenson, *ibid.*, **74**, 2043 (1952).

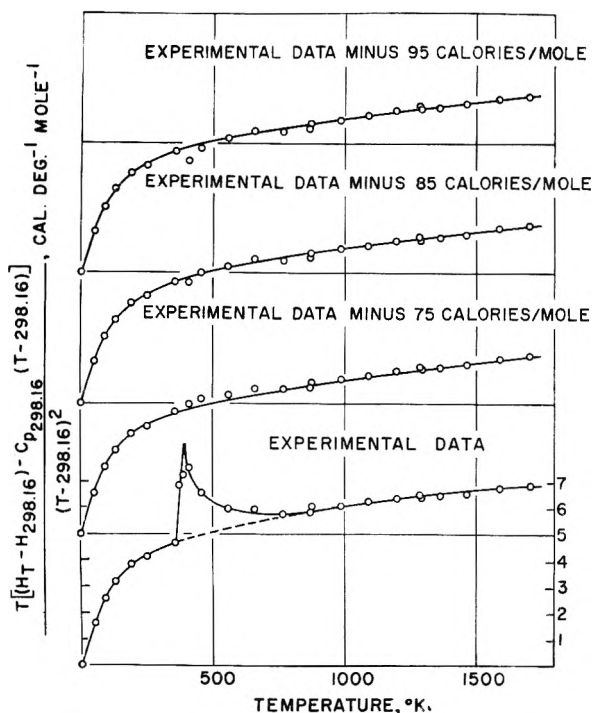


Fig. 5.—Thermodynamic data for BaTiO<sub>3</sub> ( $C_{p298.16} = 24.49$  cal. deg.<sup>-1</sup> mole<sup>-1</sup>).

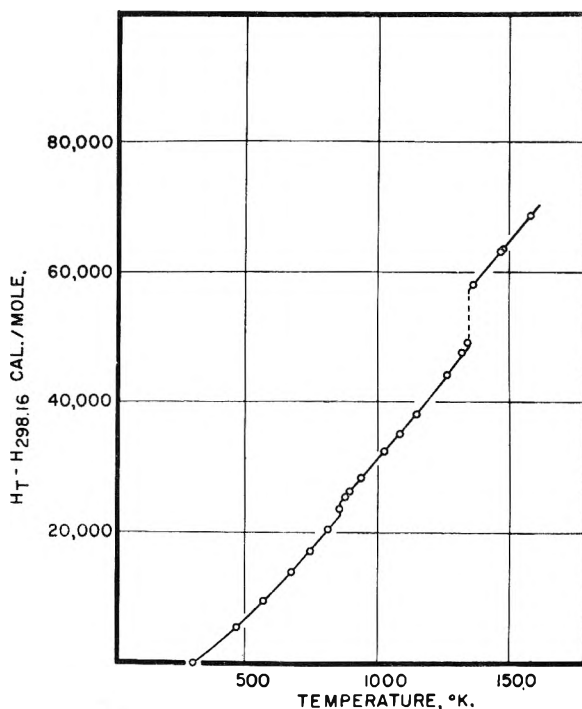


Fig. 6.—High-temperature heat content of K<sub>2</sub>SO<sub>4</sub>.

pretransition effect, but when the function is applied to the results, these effects are more easily identified. This observation is illustrated with data for potassium sulfate in Figs. 6 and 7. Both the low-temperature heat capacity data<sup>7</sup> and the high-temperature heat content data<sup>8</sup> for potassium sulfate are included in Fig. 7, in which the isothermal transition at 856°K. and the fusion at 1342°K. are greatly magnified.

**Calculation of High-Temperature Heat Capacities.**—Since the function plot is an effective method for smoothing high-temperature heat content data, it also permits accurate calculation of high-temperature heat capacities. For example, in the function plot for aluminum oxide (Fig. 1), the values of 39.09 and 39.51 are read from the curve at 490° and 510°K., respectively, from which are calculated  $H_{490} - H_{298.16} = 18,093$ , and  $H_{510} - H_{298.16} = 20,214$  abs. j./mole.  $C_{p500}$  is then calculated to be  $(20,214 - 18,093)/20$ , or 106.05 abs. j./deg./mole, the value reported by Ginnings and Furukawa.<sup>3</sup>

Since the value for  $H_{500} - H_{298.16}$  usually has been tabulated already, an easier method for calculating  $C_{p500}$  employs the following relationship derived by differentiating the function with respect to  $T$ :  $C_{pT} = (H_T - H_{298.16})(T + 298.16) / (T - 298.16)T - (298.16)(C_{p298.16}) / T + (b) / (T - 298.16)^2 / T$ , where  $b$  is the slope of the function curve at temperature  $T$ . The value of  $C_{pT}$  calculated from this expression is entirely independent of the value adopted for  $C_{p298.16}$ ; any change in  $C_{p298.16}$  is compensated by a corresponding change in  $b$ . At 500°K.  $b$  is calculated to be  $(39.51 - 39.09)/20$ , or 0.0210, and  $C_{p500} = 151.45 - 47.11 + 1.71$ , or 106.05 abs. j./deg./mole. An error

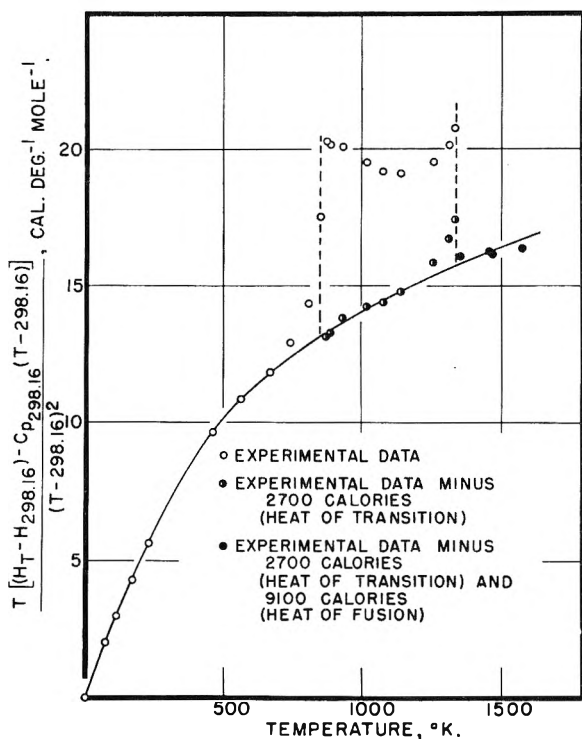


Fig. 7.—Thermodynamic data for K<sub>2</sub>SO<sub>4</sub> ( $C_{p298.16} = 31.27$  cal. deg.<sup>-1</sup> mole<sup>-1</sup>).

of 10% in the determination of the slope,  $b$ , of the function curve affects this heat capacity result by only 0.17 abs. j./deg./mole, or less than 0.2%, whereas an error of 10% in the slope of the heat content curve directly affects the value of  $C_p$  by 10%.

**Miscellaneous Applications.**—Johnston and Bauer<sup>9</sup> have used the function to derive general

(7) G. E. Moore and K. K. Kelley, *J. Am. Chem. Soc.*, **64**, 2949 (1942).

(8) C. H. Shonate and B. F. Naylor, *ibid.*, **67**, 72 (1945).

(9) H. L. Johnston and T. W. Bauer, *ibid.*, **73**, 1119 (1951).

expressions for  $\Delta H$ ,  $\Delta S$  and  $\Delta F$  as functions of temperature for a dissociation reaction from heat capacity and thermochemical data at 298.16°K. and dissociation pressure data at higher temperatures.

In some instances base temperatures other than 298.16°K. may be more convenient. For example, 273.16°K. may be a more convenient base for those employing an ice calorimeter in measuring high-temperature heat contents, where values of

$H_T - H_{273.16}$  are recorded. With lower base temperatures the sensitivity of the function plot is decreased. If a base of 0°K. is used, the function simplifies to  $(H_T - H_0)/T$ .

It is suggested that if the thermodynamic data for a substance have been determined with great accuracy up to a temperature  $T_1$ , the data can be extrapolated a few hundred degrees higher with greater certainty by using the function plot than by another graphical method.

## PHASES PRESENT AND PHASE EQUILIBRIUM IN THE SYSTEM $\text{In}_2\text{O}_3\text{-H}_2\text{O}$

BY RUSTUM ROY AND M. W. SHAFER

Contribution No. 53-39 from the College of Mineral Industries, The Pennsylvania State University, State College, Penna.

Received December 18, 1953

Phase equilibrium relations in the system  $\text{In}_2\text{O}_3\text{-H}_2\text{O}$  have been determined by a static hydrothermal method in the temperature range 25–800° at 500–20,000 p.s.i. A new phase  $\text{InOOH}$ , not isomorphous with any other trivalent oxyhydroxide, has been found and its properties described.

**Introduction.**—As part of a research program investigating equilibrium in systems involving metal oxides and water, our attention has been drawn to the  $\text{In}_2\text{O}_3\text{-H}_2\text{O}$  system. Earlier work in this Laboratory has resulted in new or revised data on compound formation and phase equilibrium in the systems  $\text{Al}_2\text{O}_3\text{-H}_2\text{O}$ ,<sup>1</sup>  $\text{Ga}_2\text{O}_3\text{-H}_2\text{O}$ ,<sup>2</sup>  $\text{Al}_2\text{O}_3\text{-Ga}_2\text{O}_3\text{-H}_2\text{O}$ ,<sup>3</sup>  $\text{Cr}_2\text{O}_3\text{-H}_2\text{O}$  and  $\text{Sc}_2\text{O}_3\text{-H}_2\text{O}$ ,<sup>4</sup> and the rare earth hydrates.<sup>5</sup> The literature contains less information regarding the hydrates of indium sesquioxide and the rare earth oxides than of any other oxide in this group of the periodic table. In addition since something is known of the structures of the compounds of both the smaller ions (Al-Sc) and the larger ones (Y-La) it was hoped that the indium compounds would fit into the structural picture.

It has been known for a long time (Milligan and Weiser<sup>6</sup>) that the precipitate which forms on the addition of alkali to indium(III) salts, after drying at 100°, has the composition  $\text{In}_2\text{O}_3 \cdot 3\text{H}_2\text{O}$ . This compound has been shown to be the trihydroxide  $\text{In}(\text{OH})_3$ , and attempts have been made to determine its structure by Milligan and Weiser,<sup>6</sup> Fricke and Seitz,<sup>7</sup> and Palm,<sup>8</sup> and Moeller and Schnizlein.<sup>9</sup> It is cubic, although the above authors report cell-edges of 7.95, 7.90, 7.92 Å., respectively, and the last named a value of 5.40 Å. based on an incorrect unit cell. Carnelley and Walker<sup>10</sup> reported a continuous loss of water from the fresh precipitate and no indication of the existence of a hydrate. Weiser and Milligan on the

other hand reported that the trihydroxide decomposed at 207° to yield directly the sesquioxide. No indication of another hydrate has been reported other than the rather early work of Renz.<sup>11</sup>

Most of the work on the stability of hydrates of the sesquioxides has been done by the dehydration isobar technique. The great disadvantage of such techniques is the fact that at the low partial pressures of water vapor used in most cases, the activation energy necessary for the formation of a new structure from the one that is decomposed on heating is very great. Hence in many cases so-called "amorphous" structures result, and in others metastable phases appear, and incorrect values for equilibrium decomposition temperatures are reached. In the present study, techniques designed for use in studying phase equilibrium in silicate and other systems, where reactions are notoriously sluggish, have been used.

**Experimental.**—The experimental techniques used in these studies have been more fully described in earlier papers<sup>1-5,12</sup> and will only be stated in outline here. The equipment used consists of an assembly of several (30) pressure vessels and furnaces, the former being attachable to a high pressure source of water pressure by a system of valves and fittings. Each vessel can be controlled independently with respect to both temperature and pressure: the temperature of the furnaces is automatically regulated. Two main types of vessels have been used: the vessels designed by Morey and Ingerson<sup>13</sup> and the "test-tube" bomb developed in this Laboratory. Details regarding equipment have been given by Roy and Osborn.<sup>14</sup> For examination of the products the petrographic microscope and X-ray diffraction patterns were used, the former being quite limited in application. The X-ray patterns were obtained on Geiger-counter diffractometers manufactured by G. E. Company (165° unit) or North American Phillips (90° units).  $\text{CuK}$  radiation was used filtered through nickel.

The starting material was prepared from C.P.  $\text{In}_2\text{O}_3$  by dissolving in nitric acid precipitating at room temperature with ammonium hydroxide and washing thoroughly. The  $\text{In}(\text{OH})_3$ ,  $\text{InOOH}$  and  $\text{In}_2\text{O}_3$  prepared from this material were also used as starting materials in various runs. These

- (1) G. Ervin and E. F. Osborn, *J. Geology*, **59**, 4 (1941).
- (2) R. Roy, V. G. Hill and E. F. Osborn, *J. Am. Chem. Soc.*, **74**, 197 (1952).
- (3) V. G. Hill, R. Roy and E. F. Osborn, *J. Am. Cer. Soc.*, **35**, 6 (1952).
- (4) M. W. Shafer and R. Roy, *Z. anorg. Chem.*, in press.
- (5) R. Roy and H. A. McKinstry, *Acta Cryst.*, **6**, Part 4, 365 (1953).
- (6) W. O. Milligan and H. B. Weiser, *J. Am. Chem. Soc.*, **59**, 1670 (1937).
- (7) R. Fricke and A. Seitz, *Z. anorg. Chem.*, **225**, 13 (1947).
- (8) A. Palm, *THIS JOURNAL*, **52**, 959 (1948).
- (9) T. Moeller and J. Schnizlein, *ibid.*, **51**, 771 (1947).
- (10) T. Carnelley and J. Walker, *J. Chem. Soc.*, **53**, 88 (1888).

- (11) C. Renz, *Ber.*, **35**, 1848, 2754 (1903).
- (12) R. Roy, D. M. Roy and E. F. Osborn, *J. Am. Cer. Soc.*, **33**, 1952 (1950).
- (13) G. W. Morey and E. Ingerson, *Am. Mineral.*, **22**, 1121 (1937).
- (14) R. Roy and E. F. Osborn, *Econ. Geol.*, **47**, 717 (1952).

mixtures are wrapped in gold or platinum envelopes introduced into the vessels and heated at the chosen temperature and pressure for a period of time varying from 24 hours to 200 hours. In this particular system equilibrium was attained rather rapidly usually 1-2 days. The products obtained on "quenching" the vessels were examined by microscopic and X-ray methods. Temperatures are probably no more accurate than  $\pm 5^\circ$  considering various sources of error, and pressure which is not as consequential a variable to  $\pm 10\%$  of the value.

In an attempt to compare a series of the hydroxides and oxyhydroxides of the third group both differential thermal analyses and infrared absorption spectra were run. Equipment used for the former has been described by DeVries and Roy.<sup>15</sup> For the infrared work a Perkin-Elmer Model 12A with NaCl prism was used, and since the particles were extremely fine a simple mulling-in-Nujol technique appeared to be adequate, although alcohol-evaporation and KBr-pellet methods were tried.

**Results.**—At least three compounds exist in the system. The trihydroxide  $\text{In}(\text{OH})_3$ , the oxyhydroxide  $\text{InOOH}$  and the sesquioxide  $\text{In}_2\text{O}_3$ : in addition the phase precipitated at room temperature is not quite amorphous to X-rays and may be considered as a crystalline hydrate of the hydroxide  $\text{In}(\text{OH})_3 \cdot x\text{H}_2\text{O}$ . Of the three the trihydroxide and the sesquioxide are both well known.

$\text{In}(\text{CH})_3$  occurs as the stable phase up to  $245 \pm 10^\circ$  at 10,000 p.s.i. and can easily be prepared in large quantities by boiling the precipitated hydroxide. When prepared in this manner and dried at  $110^\circ$  it is quite stoichiometric: it may adsorb some water in a damp atmosphere (as will any fine-grained powder) but the water does not enter the structure in any way. The compound was indeed cubic as reported, and we obtained a unit cell edge of  $7.958 \pm 0.005^\circ \text{ \AA}$ . comparing fairly well with other values (*vide supra*). Measurement of the refractive index by the immersion method on the very fine-grained material gave a value of  $1.716 \pm 0.01$ .  $\text{InOOH}$  is the oxyhydroxide hitherto unsuspected. It can be prepared by heating the gel or the trihydroxide in the range  $245\text{--}435^\circ$  at a water pressure of from 1000-25,000 p.s.i. A weight loss run on this phase shows that it loses 6.4% compared to 6.1% for the theoretical loss. Only very fine-grained crystals were obtained. The crystals were birefringent with an average refractive index of *ca.*  $1.85 \pm 0.02$ .

The X-ray diffraction pattern shown in Table I is the best means of characterization. The structure of the phase is unknown and comparisons were made with all the expected structures, but no analogies were found. Thus the diaspore structure can accommodate ions at least as large as  $\text{Sc}^{3+}$  but this phase did not have the diaspore structure: the next larger ion  $\text{Y}^{3+}$  has a compound  $\text{YOOH}$ , but  $\text{InOOH}$  showed no similarity to this either. On heating in air or hydrothermally  $\text{InOOH}$  dehydrates to  $\text{In}_2\text{O}_3$ , the equilibrium transformation temperature being  $435 \pm 10^\circ$  at 10,000 p.s.i.

$\text{In}_2\text{O}_3$ .—It was noticed that a distinct yellow color was directly correlatable to the presence of the anhydrous sesquioxide; it often grew as euhedral cubes of very high refractive index. Of all the sesquioxides those which can be prepared in only one polymorphic modification ( $\text{Y}^{3+}$ ,  $\text{Sc}^{3+}$ ,  $\text{In}^{3+}$ )

(15) R. C. DeVries and R. Roy, *J. Am. Chem. Soc.*, **75**, 2479 (1953).

TABLE I

| X-RAY POWDER DIFFRACTION DATA |         |                |         |
|-------------------------------|---------|----------------|---------|
| $\text{In}(\text{OH})_3$      |         | $\text{InOOH}$ |         |
| $d$                           | $I/I_0$ | $d$            | $I/I_0$ |
| 4.417                         | 40      | 3.365          | 90      |
| 3.990                         | 100     | 2.877          | 60      |
| 2.822                         | 90      | 2.666          | 70      |
| 2.521                         | 20      | 2.643          | 50      |
| 2.381                         | 10      | 2.377          | 20      |
| 2.303                         | 05      | 2.285          | 50      |
| 2.191                         | 10      | 1.874          | 80      |
| 2.146                         | 10      | 1.767          | 100     |
| 1.995                         | 10      | 1.727          | 50      |
| 1.784                         | 90      | 1.638          | 50      |
| 1.628                         | 75      | 1.548          | 40      |
| 1.367                         | 05      | 1.480          | 30      |
| 1.329                         | 40      | 1.462          | 30      |
| 1.260                         | 30      | 1.392          | 20      |
| 1.201                         | 30      | 1.383          | 20      |
| 1.149                         | 05      | 1.330          | 20      |
| 1.105                         | 15      | 1.257          | 10      |
| 1.065                         | 30      | 1.281          | 20      |
| 0.997                         | 05      | 1.223          | 20      |
| .967                          | 30      | 1.187          | 20      |
| .938                          | 30      | 1.181          | 10      |
| .915                          | 25      | 1.158          | 10      |
| .913                          | 10      | 1.150          | 10      |
| .907                          | 10      | 1.141          | 20      |
|                               |         | 1.091          | 10      |
|                               |         | 0.985          | 10      |
|                               |         | .966           | 10      |
|                               |         | .951           | 10      |
|                               |         | .937           | 10      |
|                               |         | .918           | 10      |

all have the C-type rare earth oxide structure. We obtained a unit cell edge of  $10.120 \pm 0.005 \text{ \AA}$ , in good agreement with earlier values.

**Phase Equilibrium.**—The phase relationships may best be expressed in the form of a  $p$ - $t$  diagram as is shown in Fig. 1. Here the areas of divariant equilibrium where the same phase assemblage (one solid and vapor) is stable over both a pressure and temperature range are separated from each other by lines of univariant equilibrium along which two solid phases are in equilibrium with vapor (or liquid). Alternatively, from the univariant lines one obtains the equilibrium temperature under any particular water vapor pressure for the reactions  $\text{In}(\text{OH})_3 \rightleftharpoons \text{InOOH} + \text{H}_2\text{O}$  and  $2\text{InOOH} \rightleftharpoons \text{In}_2\text{O}_3 + \text{H}_2\text{O}$ . The data for the construction of the diagram have been obtained from some 150 runs and selected data are shown in Table II. It will be seen that the diagram is very simple, areas of stability of the three phases being separated by univariant lines which have hardly any pressure slope from 2,000-20,000 p.s.i. Below this value there is a significant effect of pressure on the maximum temperature of stability of  $\text{In}(\text{OH})_3$  and  $\text{InOOH}$ . Two facts should be mentioned in connection with the equilibrium relationships. In no case either in the present study or in our numerous other investigations of both binary and ternary systems involving water has it been possible to approach equilibrium from the high temperature side. Thus one cannot convert  $\text{In}_2\text{O}_3$  to  $\text{InOOH}$ , nor will  $\text{InOOH}$  once formed revert to

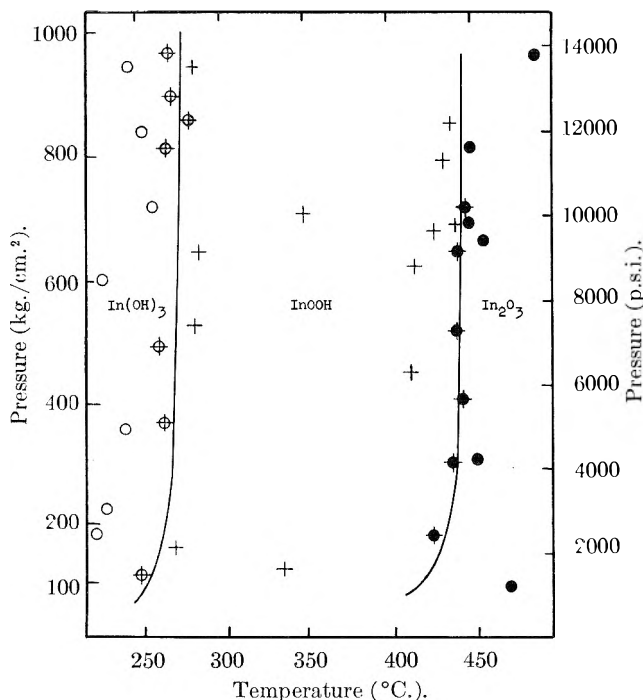


Fig. 1.—Phase equilibrium in the system  $\text{In}_2\text{O}_3\text{-H}_2\text{O}$ . Open circles show some runs in which only  $\text{In}(\text{OH})_3$  was detected, crosses indicate the detection of  $\text{InOOH}$ , and solid dots the presence of  $\text{In}_2\text{O}_3$ .

$\text{In}(\text{OH})_3$  even in a period of two months within the stability range of the latter. This question

has been treated in earlier work by Ervin and Osborn<sup>1</sup> on the system  $\text{Al}_2\text{O}_3\text{-H}_2\text{O}$ , where precisely the same phenomenon occurs. As a consequence of this situation, and further enhanced by the fact that conversions in this system are relatively rapid, is the occurrence of a relatively wide "band" in which two solid phases actually are found in equilibrium with vapor. This we ascribe to the fact that near the univariant line fluctuations of temperature or pressure for even a very short while (for example, during the initial overshoot of the automatic regulator) will give rise to the formation of some of the higher temperature phase: This phase will not reconvert under any conditions although the sample may be several degrees below the true equilibrium temperature for almost the entire length of time. Thus the univariant lines are generally drawn through the points of highest temperature persistence of the lower temperature phase.

**Further Characterization of Hydrates.**—Differential thermal analyses of the two hydrates were run at a heating rate of  $5^\circ/\text{min}$ . in apparatus described elsewhere.<sup>15</sup> The curves obtained are shown in Fig. 2. These may be used for the rapid characterization of the phases in the absence of X-ray equipment. It will be noted that the peak in the  $\text{In}(\text{OH})_3$  curve "begins" at approximately  $235^\circ$  which would be indicated as an "apparent" decomposition temperature under a partial pressure of a few mm. of water vapor. The equilibrium temperature would undoubtedly be much lower. Similarly the  $\text{InOOH}$  curve indicates an "ap-

TABLE II

TRANSITIONS FROM  $\text{In}(\text{OH})_3$  TO  $\text{InOOH}$  AND  $\text{InOOH}$  TO  $\text{In}_2\text{O}_3$  IN THE SYSTEM  $\text{In}_2\text{O}_3\text{-H}_2\text{O}$

| Max. temp., °C. | Pressure, p.s.i. | Time, hr. | Initial condition        | After run   |
|-----------------|------------------|-----------|--------------------------|---|
| 240             | 9,000            | 144       | $\text{In}(\text{OH})_3$ | $\text{In}(\text{OH})_3$ plus trace of $\text{InOOH}$ |
| 243             | 12,000           | 60        | $\text{In}(\text{OH})_3$ | $\text{In}(\text{OH})_3$ plus trace of $\text{InOOH}$ |
| 246             | 10,000           | 52        | $\text{In}(\text{OH})_3$ | $\text{In}(\text{OH})_3$ plus trace of $\text{InOOH}$ |
| 252             | 10,000           | 60        | $\text{In}(\text{OH})_3$ | Mostly $\text{In}(\text{OH})_3$ , some $\text{InOOH}$ |
| 258             | 10,000           | 45        | $\text{In}(\text{OH})_3$ | $\text{In}(\text{OH})_3 + \text{InOOH}$               |
| 258             | 14,000           | 56        | $\text{In}(\text{OH})_3$ | Mostly $\text{In}(\text{OH})_3$                       |
| 262             | 13,000           | 60        | $\text{In}(\text{OH})_3$ | Mostly $\text{In}(\text{OH})_3$                       |
| 268             | 10,000           | 38        | $\text{In}(\text{OH})_3$ | $\text{In}(\text{OH})_3 + \text{InOOH}$               |
| 267             | 2,000            | 36        | $\text{In}(\text{OH})_3$ | $\text{InOOH}$ plus trace of $\text{In}(\text{OH})_3$ |
| 252             | 1,000            | 96        | $\text{In}(\text{OH})_3$ | $\text{InOOH}$ plus trace of $\text{In}(\text{OH})_3$ |
| 284             | 13,000           | 96        | $\text{In}(\text{OH})_3$ | All $\text{InOOH}$                                    |
| 354             | 10,000           | 48        | $\text{In}(\text{OH})_3$ | All $\text{InOOH}$                                    |
| 411             | 10,000           | 60        | $\text{InOOH}$           | All $\text{InOOH}$                                    |
| 411             | 10,000           | 60        | $\text{In}(\text{OH})_3$ | All $\text{InOOH}$                                    |
| 427             | 10,000           | 30        | $\text{In}(\text{OH})_3$ | All $\text{InOOH}$                                    |
| 427             | 10,000           | 30        | $\text{InOOH}$           | All $\text{InOOH}$                                    |
| 431             | 10,000           | 27        | $\text{In}(\text{OH})_3$ | $\text{In}_2\text{O}_3 + \text{InOOH}$                |
| 431             | 10,000           | 27        | $\text{InOOH}$           | All $\text{InOOH}$                                    |
| 432             | 10,000           | 75        | $\text{In}(\text{OH})_3$ | All $\text{In}_2\text{O}_3$                           |
| 432             | 10,000           | 75        | $\text{InOOH}$           | All $\text{InOOH}$                                    |
| 432             | 10,000           | 48        | $\text{InOOH}$           | Practically all $\text{In}_2\text{O}_3$               |
| 432             | 10,000           | 60        | $\text{InOOH}$           | $\text{InOOH}$ and $\text{In}_2\text{O}_3$            |
| 432             | 10,000           | 60        | $\text{In}(\text{OH})_3$ | Mostly $\text{In}_2\text{O}_3$                        |
| 434             | 10,000           | 23        | $\text{In}(\text{OH})_3$ | $\text{InOOH} + \text{In}_2\text{O}_3$                |
| 434             | 10,000           | 23        | $\text{InOOH}$           | All $\text{InOOH}$                                    |
| 442             | 10,000           | 72        | $\text{InOOH}$           | $\text{InOOH} + \text{In}_2\text{O}_3$                |
| 441             | 10,000           | 60        | $\text{In}(\text{OH})_3$ | Mostly $\text{InOOH} + \text{In}_2\text{O}_3$         |
| 441             | 10,000           | 60        | $\text{InOOH}$           | Mostly $\text{InOOH} + \text{In}_2\text{O}_3$         |
| 442             | 12,000           | 14        | $\text{InOOH}$           | All $\text{InOOH}$                                    |
| 442             | 12,000           | 14        | $\text{In}(\text{OH})_3$ | Mostly $\text{In}_2\text{O}_3$                        |
| 446             | 12,000           | 2         | $\text{In}(\text{OH})_3$ | Mostly $\text{InOOH} + \text{In}_2\text{O}_3$         |
| 446             | 10,000           | 20        | $\text{In}(\text{OH})_3$ | Mostly $\text{InOOH} + \text{In}_2\text{O}_3$         |
| 448             | 10,000           | 50        | $\text{InOOH}$           | Mixture $\text{In}_2\text{O}_3$ and $\text{InOOH}$    |
| 448             | 10,000           | 50        | $\text{In}(\text{OH})_3$ | All $\text{In}_2\text{O}_3$                           |
| 449             | 10,000           | 96        | $\text{InOOH}$           | All $\text{In}_2\text{O}_3$                           |

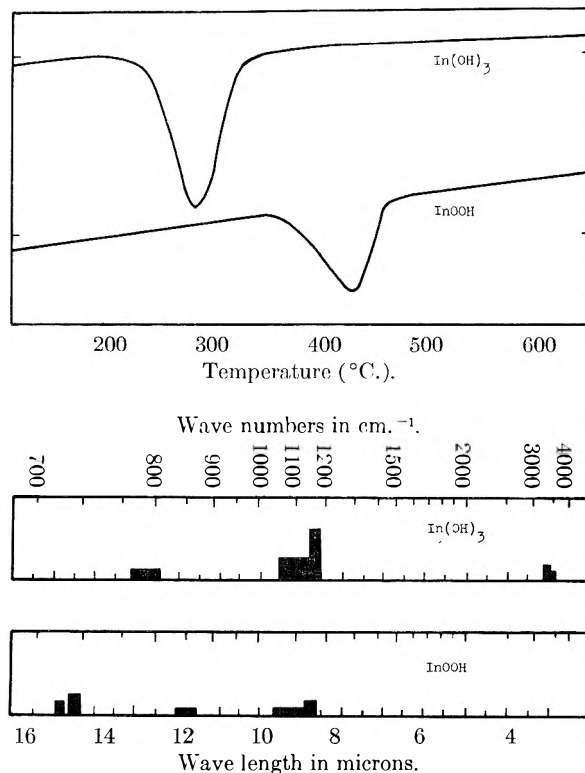


Fig. 2.—Characterization of indium oxide hydrates: upper diagram shows differential thermal analysis curves and the lower diagrams show in block diagram form the infrared absorption spectra of the trihydroxide and oxyhydroxide.

parent" decomposition temperature of about 375°. Further, it will be seen that in the  $\text{In}(\text{OH})_3$  curve there is no evidence for the formation and subsequent decomposition of  $\text{InOOH}$ , thus illustrating the danger in utilizing the data obtained from such methods for anything other than description of the original compound.

It has already been stated that no correspondence can be found between the  $\text{InOOH}$  structure and the other monohydrate structures. Similarly  $\text{In}(\text{OH})_3$  has a structure unique for hydroxides: It is essentially the perovskite structure with the large cations absent, and thus corresponds to  $\text{ReO}_3$ ,  $\text{ScF}_3$  and the high temperature form of  $\text{AlF}_3$ . It is significant to note that in all these structures the  $\text{F}^-$  and  $(\text{OH})^-$  although supposedly of nearly equal size, behave as though the former were distinctly smaller. The only other well-established tri-hydrate of a sesquioxide with a smaller ion is that of  $\text{Al}^{3+}$ , gibbsite: and it was considered worthwhile to compare the nature of the  $(\text{OH})^-$

ions in the two structures. Infrared absorption spectra were obtained as described earlier for  $\text{In}(\text{OH})_3$  and  $\text{InOOH}$  in the 2–15  $\mu$  region. A rather surprising similarity is found in the patterns for gibbsite and  $\text{In}(\text{OH})_3$  as can be seen from the block diagrams presented in Fig. 2. The absorption maximum at 3  $\mu$  and near 9.8–10.4  $\mu$  for gibbsite are also found in the  $\text{In}(\text{OH})_3$  with a slight hypsochromic shift in the latter. The monohydrate pattern is characterized by the absence of any pronounced absorption maxima, unlike the patterns for diasporite and boehmite. Electron microscopic examination of  $\text{In}(\text{OH})_3$  and  $\text{InOOH}$  failed to reveal any striking morphological characteristics in either.

**Acknowledgments.**—This work was performed as part of a research project on hydrothermal crystal studies, sponsored by the Frequency Control branch of the Signal Corps at the School of Mineral Industries, under the general supervision of Dean E. F. Osborn.

## THE EFFECT OF THE pH OF XANTHATE SOLUTIONS ON THE CONTACT ANGLE BETWEEN A BUBBLE OF AIR AND AN IRON DISULFIDE SURFACE NOT OF MINIMUM RUGOSITY

By P. F. WHELAN

Coal Preparation Department, National Coal Board, Central Research Establishment, Stoke Orchard, Cheltenham, Gloucestershire, England

Received December 19, 1953

The contact angles between air bubbles and pyrite, marcasite, and four specimens of massive iron disulfide from coal seams have been measured in solutions of xanthates at a concentration of 50 mg./liter. The results with all six forms of iron disulfide were similar. The existence of a critical pH, 10–11.5, above which bubbles do not adhere has been confirmed. With surfaces ground to only a comparatively poor polish, the contact angles are lower than those characteristic of the xanthates, and are related to the pH of the solution, being small at pH over 10, and rising as pH falls, until by pH 3 or thereabouts they approach the value of the characteristic angle. It is suggested that measurements of contact angles developed on surfaces not of minimum rugosity are of value, as the curves obtained as pH is varied appear to reflect the performance realized in practical mineral separations.

In an important industrial process, froth flotation, valuable minerals are separated from worthless associated ore constituents by virtue of their adhesion, as fine particles, to a swarm of air bubbles ascending through a water suspension. To facilitate the separation, the hydrophobicity of the wanted material is increased by treatment with certain chemical compounds; for non-metallic minerals a common reagent is oleic acid, and for metallic sulfides, a xanthate. That the fatty acid or long chain ionic hydrocarbon compound in the first case is irreversibly adsorbed onto the surface of the non-metallic mineral, so that the hydrocarbon-like ends of the amphipathic molecules are orientated toward the aqueous phase is now accepted. The application of trough technique and force-area measurements by Schulman and his associates have elucidated the structure of the films formed, which are usually monomolecular, but occasionally up to two molecules in thickness.<sup>1</sup> With regard to the mode of action of xanthates and similar "sulfhydryc collectors" the situation is less

clear, notwithstanding intensive study by Gaudin and others using radio-tracer technique<sup>2–6</sup> and by Hagihara and Sato using an electron diffraction procedure.<sup>7–9</sup> The take-up from solution of reagents of the xanthate type by metallic sulfides corresponds to multilayer formation,<sup>1–3,5,7–13</sup> but the deposit, far from being uniform in thickness, is probably so discontinuous that only perhaps 10% of the surface is covered.<sup>1–3</sup>

If a captive bubble, that is, one formed at the end of an upright tube dipping into the solution, is

- (2) A. M. Gaudin and F. W. Bloecher, Jr., *Mining Eng.*, **187**, 499 (1950).
- (3) G. L. Simard, J. Chupak and D. J. Salley, *ibid.*, **187**, 359 (1950).
- (4) G. L. Simard, M. Burke and D. J. Salley, *ibid.*, **190**, 39 (1951).
- (5) S. Ruby, Dissertation, Columbia University (1952).
- (6) A. M. Gaudin and C. S. Chang, *Mining Eng.*, **4**, 193 (1952).
- (7) H. Hagihara, Res. Rep. Mitsubishi, M & M Lab. No. 872 (1943) and Taihei No. 1203 (1950).
- (8) R. Sato, Res. Rep. Taihei, M & M Lab. No. 1257 (1951).
- (9) H. Hagihara, *THIS JOURNAL*, **56**, 637 (1952).
- (10) N. A. Held and Samochwalov, *Koll. Z.*, **72**, 13 (1935).
- (11) A. M. Gaudin and R. Schuhmann, *THIS JOURNAL*, **40**, 257 (1936).
- (12) A. F. Taggart and N. Arbiter, A.I.M.E. Tech. Pub. 1585 (1943).
- (13) J. Rogers, K. L. Sutherland, E. E. Wark and I. W. Wark, *Trans. A.I.M.E.*, **169**, 287 (1946).

(1) J. H. Schulman and T. D. Smith, Inst. Min. and Met. Symposium on Mineral Dressing, Paper 22 (1952).

brought into contact with a suitable smooth surface of a solid, it adheres, and the area of contact between air and solid rapidly extends until equilibrium is reached. Spreading is accompanied by energy reduction and by increase in the value of the contact angle  $\theta$ , the angle between the bubble wall and the solid surface, measured in the solution. The larger the contact angle the firmer the adhesion of the bubble and the more energy must be expended in its removal. When  $\theta$  is large, the tube often can be removed, leaving a free bubble adhering to the solid surface. When the contact angle is small this procedure is seldom possible and even if a small bubble should remain it is easily dislodged by slight mechanical shock.

The relation between contact angle and ease of flotation was early recognized. Following a classical paper by Taggart, Taylor and Ince,<sup>14</sup> many studies were made of the attachment of bubbles to polished mineral surfaces, particularly by Wark<sup>15,16</sup> and by Cox<sup>15</sup>; recent notable papers by Dzienisiewicz and Pryor on metallic sulfides<sup>17</sup> and by Horsley on coals<sup>18</sup> evidence the fertility of this field of research. From all this work two important generalizations have emerged. First, irrespective of the mineral surface, the contact angle of a fully developed adhering bubble is characteristic of the reagent, being, for example, 60° for the ethyl, 75° for the butyl, and 85° for the amyl homologs of the potassium salts of the xanthates. Second, for any mineral and concentration of reagent there exists a critical pH value below which bubble attachment occurs, and above which it is not possible; for instance, with potassium ethyl xanthate in 50 mg./liter solution, the critical pH for pyrite is 10.5, and for marcasite 11.

Galena, PbS, floats easily when treated with xanthates, and from some ores, even without such treatment. Sphalerite, ZnS, can also be floated by sulfhydryc collectors if its surface is first altered by reaction with copper sulfate in solution. Pyrite, FeS<sub>2</sub>, shows a variable tendency to float; from some ores it floats with great facility, in most cases addition of xanthate is necessary, while in a few even powerful sulfhydryc collectors are ineffective. In a general way, in all these instances there is a parallelism between floatability and the contact angles determined on polished surfaces in the laboratory, but in recent years it has become increasingly apparent that the connection is not as direct as was formerly believed. If the polished mineral shows a large contact angle in certain reagent conditions, then these conditions will almost certainly ensure good flotation on the large scale. The converse, however, is not invariably true. Often good flotation occurs in practice with conditions of reagent concentration and so on which fail to give large contact angles in laboratory tests with polished specimens.<sup>4,6,19</sup> In Arbiter's words "the assumption that a contact angle/no con-

tact angle or flotation/no flotation condition can be identified with a unique concentration of (anionic) collector in the surface phase has been shown . . . to be unwarranted."<sup>20</sup>

Only on highly polished surfaces are the large characteristic angles of xanthate type reagents fully developed. Several investigators have reported that on rough surfaces if contact is established, the angles are smaller.<sup>1,8,17,18</sup> In discussing Dzienisiewicz and Pryor's paper the present writer argued that in view of the importance of this factor, its quantitative measurement in contact angle researches was desirable. Unfortunately, a method for accurately determining the rugosity of a comparatively plane surface when immersed in a solution, without local alteration of its hydrophobicity, has proved difficult to find. In the experimental work now reported, visual observation and microscopical examination at low power have been relied on for assessment of rugosity.

In preparing mineral specimens for detailed microscopical examination, the major inequalities are first removed by grinding with coarse abrasive on iron wheels; the surface obtained, while substantially flat, is dull to the eye and rough to the touch. The specimen is then transferred to a dust-free environment and polished on steel, copper and lead laps in turn, using progressively finer grades of abrasive powder, its appearance gradually changing from matte to shiny, and its feel becoming more and more silky. Finally, treatment on cloth laps is often resorted to in order to obtain a mirror-like finish.

An essential preliminary operation in most practical separations of minerals from ores is comminution by wet grinding in a ball mill. Examination of the surfaces of grains produced in this way showed that the surface rugosity attained was intermediate between that of specimens coarsely flattened in the laboratory technique, and the specular surface finish considered necessary for microscopical study at high power. It corresponded to that reached by the specimen, if the order of treatment mentioned above were followed, on transfer to the copper lap or shortly after polishing on this metal began. Since at this stage the surface is intermediate between dull and shiny, the finish may be described as semi-matte. No gross inequalities are visible to the eye or under magnifications up to  $\times 30$ , but with powers  $\times 300$  or more uneven texture becomes apparent. The aim in the experiments now reported was to study the attachment of bubbles to surfaces of this degree of rugosity.

Galena, on which many contact angle studies have been made, is not convenient in this instance because the transition during polishing from dull to specular is too rapid. Sphalerite can be taken to the desired surface texture easily, but the need to alter its surface by treatment with copper sulfate as a preliminary to xanthate absorption introduces complications. Iron disulfide was therefore chosen as substrate for the reasons listed below: (a)

(14) A. F. Taggart, T. C. Taylor and C. R. Ince, *Trans. A. I. M. E.*, **87**, 285 (1930).

(15) I. W. Wark and A. B. Cox, *ibid.*, **112**, 189 (1934).

(16) I. W. Wark, *This Journal*, **37**, 623 (1933).

(17) J. Dzienisiewicz and E. J. Pryor, *Bull. Inst. Min. & Met.* April, 1950, June, 1950, and Nov., 1950.

(18) R. M. Horsley, *Fuel*, **30**, 54 (1951).

(19) G. A. Last and M. A. Cook, *This Journal*, **56**, 637 (1952).

(20) N. Arbiter, *Inst. Min. & Met. Symposium on Mineral Dressing*, Paper 21 (Sept. 1952).



Fig. 1.—Coal-pyrite from Plodder Seam, Lancashire; showing a vein of pyrite in a mosaic of marcasite, magnification 300 $\times$ .

It exists in two lattice forms, as pyrite and marcasite. (b) It is easily polished to a semi-matte finish. (c) Although in the laboratory bubbles attach themselves at the characteristic contact angle to highly polished xanthated surfaces provided the  $pH$  is below the critical value ( $pH$  10.5 or  $pH$  11), in practice there is a wide variability in the tendency of different pyrites to float at  $pH$  values well below 10.

### Experimental Work

**Selection and Preparation of Specimens.**—The natural iron disulfides used in the work are listed below: all come from sources in Great Britain and were samples specially selected for high purity.

1. Pyrite, from a vein in Cornwall
2. Marcasite, also from Cornwall
3. Coal-pyrite from Acomb seam, Northumberland
4. Coal-pyrite from Plodder seam, Lancashire
5. Coal-pyrite from Hutton seam, Co. Durham
6. Coal-pyrite from Hurlet seam, Scotland

As massive nodules or slabs up to 6 inches thick, iron disulfide occasionally occurs in the British coal seams quoted above. Specimens can be found of as high sulfur content as pyrite present in deposits of hydrothermal replacement or intrusive origin (up to 50% S). Although the term "coal-pyrite" is convenient and in universal use, X-ray examination shows that both marcasite and pyritic forms are present; as illustrated in Fig. 1, the former usually predominates.

After cutting by diamond wheel to a suitable size, about 1-inch square, specimens of each of the six samples were polished in grease-free conditions, the glass plate, Grade B Selvyt cloths and rubber gloves used being previously cleaned by at least 12 hours extraction with ether in Soxhlet apparatus. The semi-matt finish desired was achieved by

polishing on a steel lap with water, using successively 90, 220 and FF carborundum and 500-mesh alumina powders, degreasing with ether in a Soxhlet extractor, polishing on a glass plate under water with 600 mesh alumina, and desliming on a Selvyt cloth under water. In this and all other parts of the work the water used was doubly distilled. The test for absolute cleanliness of a surface was the absence of any contact angle and stickiness when an air bubble was pressed upon the surface in pure water. This was applied not only to each specimen after the repolishing step between tests, but also to all apparatus such as specimen-holders, which were made of glass and cleaned by sulfuric-chromic acid mixture treatment followed by prolonged washing with pure water.

**Purification of Xanthates.**—The xanthates studied are listed below with their commonly used abbreviated names, and analyses after purification.

|                                    |          |            |
|------------------------------------|----------|------------|
| Potassium ethyl xanthate           | K.Et.X   | 99.8% pure |
| Potassium isopropyl xanthate       | K.i-Pr.X | 93.7% pure |
| Potassium <i>n</i> -butyl xanthate | K.Bu.X   | 89.9% pure |
| Potassium <i>n</i> -amyl xanthate  | K.Am.X   | 86.0% pure |
| Potassium <i>n</i> -hexyl xanthate | K.He.X   | 87.0% pure |
| Potassium <i>n</i> -octyl xanthate | K.Oc.X   | 76.5% pure |

They were all purified immediately before use by the double precipitation method of DeWitt and Roper.<sup>21</sup> Some were analyzed argentometrically by the technique due to Makens<sup>22</sup>; the higher xanthates are very prone to oxidation and were difficult to obtain and preserve in high or even reasonable purity.

**$pH$  Determination.**—Decinormal solutions of hydrochloric acid and of potassium hydroxide served for altering  $pH$ , which was measured with a Cambridge meter and standardized glass electrodes.

**Optical System.**—This consisted of a half-plate camera with Compur shutter and Zeiss 10.5-cm. lens. Illumination

(21) C. E. DeWitt and E. E. Roper, *J. Am. Chem. Soc.*, **54**, 444 (1932).

(22) R. F. Makens, *ibid.*, **57**, 405 (1935).

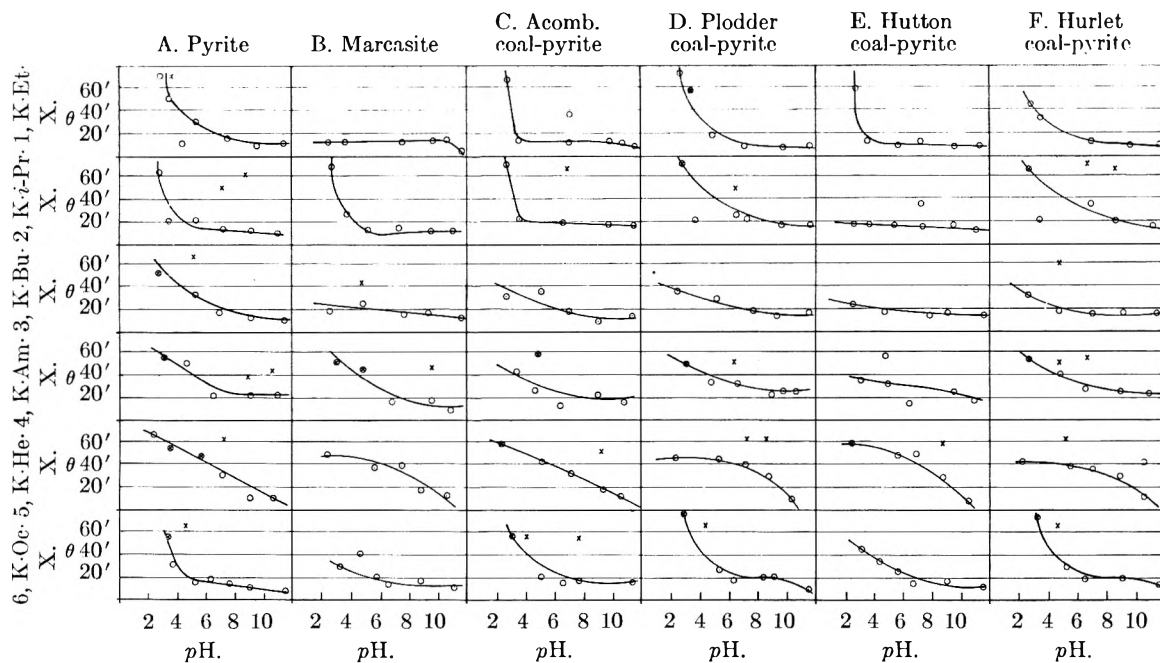


Fig. 2.—Contact angle determinations: X, self-anchored bubbles; O, captive bubbles;  $\otimes$ , self-anchored + captive bubbles.

was by a B.T.H. 250-watt mercury arc lamp, ON20 filter, iris diaphragm, convex lens and diffusing filter of ground glass. The illumination was slightly oblique as this made measurements easier since the reflection of the bubble in the polished surface could also be observed.<sup>15</sup>

**Cells and Bubble-holder.**—The cells for holding the xanthate solutions were constructed of 3.5 × 3.5 in. lantern slide cover glasses joined with "Araldite"; this cement proved very satisfactory, resisting all cleaning operations well. As bubble-holder, a ground glass tip of 1.75-mm. bore fixed to a hypodermic needle adaptor with Araldite, in turn attached to a 1-ml. all-glass syringe was employed. In practice, relative movement was found to be most conveniently arranged by mounting the cell and specimen holder on a microscope stage, and the bubble-holder on an independent lead screw.

**Test Procedure.**—With six types of iron disulfide and six xanthates, thirty-six combinations are possible; all were studied. The concentration of xanthate was fixed at a single value, 50 mg./liter, while pH was varied from about 2 to 11 in either five or six steps. Determination of mean contact angles therefore required in all about 200 experiments.

In each experiment the specimen was first stripped of its previous xanthate coating by dipping momentarily in nitric acid of medium strength and rinsing with water. It was then repolished to a semi-matte finish as already described, mounted in a specimen-holder and submerged in pure water in a cell which had previously been thoroughly cleaned. After confirming that the surface gave zero contact angle and that the bubble showed no tendency to stick, the water was replaced by a 50 mg./liter freshly prepared solution of the appropriate xanthate, adjusted to the desired pH value. A captive bubble, about 3 mm. in diameter, was pressed against a point on the surface for 5 minutes, and the contact angle measured after slightly withdrawing the bubble and tapping the bubble-holder to accelerate attainment of equilibrium. The bubble was then moved to a new spot and the procedure repeated. As a rule, twelve observations were made in each experiment, to obtain an accurate mean contact angle. The standard deviation of the twelve observations was about 2° for values below 20° and 5° for those over 50°, a coefficient of variation of the order of 10%; in view of the comparatively poor polish aimed at, the results were more consistent than might have been expected. Temperature in all tests was 22 ± 2°.

In certain circumstances, when the bubble-holder was withdrawn, an air bell remained adhering to the surface; in all such cases the contact angle of the self-anchored bubble was measured.

### Discussion of Results

The mean contact angles determined for captive bubbles, and the contact angles of the free air bells observed, are assembled in Fig. 2.

Confining attention first to the relatively few observations on self-anchored bubbles, it is at once noted that in no case was this phenomenon observed at pH in excess of 10.5–11; low hydrophobicity at pH above the critical value is thus once again demonstrated. Below pH 10 the occurrence of free bubbles on these semi-matte surfaces becomes more frequent, until at pH values below 4 it is common. The observed contact angles are almost without exception in the range 50 to 75°. It is well known that K.Et.X sometimes shows values in excess of the characteristic 60°, due to decomposition with formation of ethyl dixanthogen which has a contact angle in excess of 80°. If this effect is assumed to explain the surprisingly high angles noted in a few instances for the lower homologs in the present investigation, it may be concluded that on semi-matte pyrite the contact angles of self-anchored air bells are in general of the same order of magnitude as, but somewhat lower than, those formed on highly polished surfaces.

Turning to the curves of contact angle for captive bubbles on these semi-matte surfaces, an altogether different pattern is apparent, the angle being as a rule much smaller, and its value dependent in a regular way on pH level. With pH in excess of 10, the angle is usually 15° or lower. As pH falls to 9 and 8, with K.He.X the value rises rapidly. The rise only becomes evident for the other xanthates, K.Et.X, K.i-Pr.X, K.Bu.X, K.Am.X and K.Oc.X, at pH 7 or 6, and for the lower homologs K.Et.X. and K.i-Pr.X, may be delayed until pH 4 or 3.5. However, by pH 3 or 2.5 large contact angles, 40 or 60°, are shown with few exceptions, and high hydrophobicity is evidenced by a pronounced tendency of the bubble to cling to the surface

when lateral movement of the specimen is attempted.

No evidence that the angle of contact of a free bubble is regularly higher than that of a captive bubble on the same surface was obtained. The relatively few self anchored air-bells probably formed at places where the condition of the surface was anomalous, so that high contact angles were established.

The failure of pyrite to float at high concentrations of hydroxyl ion, over the critical  $pH$  10.5–11 for K.Et.X. 50 mg./liter solution for example, has been ascribed to the formation of anions of the form  $(Fe(OH)_x)^{-y}$ , with consequent unavailability of metallic ions to anchor the xanthate coating; surface closure by gelatinous hydroxide and mass-action effects due to ferrous and ferric ions at the pyrite surface have also been blamed.<sup>23</sup> In high concentration, iron sulfates are known to have a depressant action on some pyrites.<sup>18,23,24</sup> What is more difficult to explain is the wide variation in floatability of pyrites at  $pH$  values below the critical. Taggart<sup>25</sup> has summarized this general finding as follows—“ $pH$  is always held above 7, if possible, on account of high maintenance expense in acid pulps. The only sulfide that floats best in acid pulps is pyrite: where high recovery (of pyrite) is desired, as at the Boliden tin properties,  $pH$  is held at 4.5 to 7; otherwise pyrite flotation both in gold mills and in lead–zinc–iron differential mills is affected in the range from 8 to 9.” In this connection it is important to recall that the neutral-soap peak for iron lies on the acid side, and that of all common minerals, high contact angles with fatty acids persist to lower  $pH$  values with pyrite than any other,  $\theta$  being  $90^\circ$  at  $pH$  7, and  $90$ ,  $85$  and  $80^\circ$  at  $pH$ 's 4, 3 and 2, respectively.<sup>26</sup>

Whether the effect be due simply to the removal of an oxide film, the degree of ionization of the mineral surface, the concentration of xanthate ions in the solution, or the reaction rate and equilibrium attained in the surface phase, it is clear that in

many practical applications acidification of mill pulps to reduce the  $pH$  to well below the critical value indicated by laboratory contact angle studies is practiced in order to ensure rapid and complete flotation of iron disulfides. This is in agreement with the increase in contact angle for semi-matte surfaces as  $pH$  falls shown in many of the curves of Fig. 2, and argues that contact angles determined on surfaces not of minimum rugosity may be a more sensitive measure of flotation facility than the uniform values obtained over a wide  $pH$  range on highly polished surfaces.

The effect of surface rugosity on the contact angle of drops of liquid on solids in air has been investigated experimentally by Wenzell<sup>27</sup> and by Bartell and Shepard,<sup>28,29</sup> Shuttleworth and Bailey<sup>30</sup> have offered a mathematical treatment. It is predicted that where the contact angle on a smooth surface exceeds  $90^\circ$ , the apparent angle on a rough surface will be larger than on a smooth surface, whereas when the contact angle on a smooth surface is less than  $90^\circ$ , the reverse will be the case. Since for the systems of pyrite and lower xanthate solutions studied in the work now reported, the contact angles on highly polished surfaces are below  $90^\circ$ , roughening should reduce the value of the angle: this was the effect found.

At the end of the research several of the pyrite specimens used were polished to minimum rugosity and contact angles in xanthate solutions of  $pH$  from 6 to 8.5 were determined. Large contact angles, easily reproducible to within  $2^\circ$ , were obtained. The values were  $59^\circ$  for the ethyl,  $67^\circ$  for the isopropyl, and  $79^\circ$  for the butyl xanthate, in good agreement with those reported by other workers.<sup>31</sup>

The assistance of Mr. R. Bailey in the practical work involved in this research is acknowledged. The author wishes to express his thanks to the National Coal Board for permission to publish this paper. The views expressed in it are those of the author and not necessarily those of the Board.

(23) A. F. Yancey and J. A. Taylor, U.S.B.o.M., R.I. 3263 (1935).

(24) E. C. Plante and K. L. Sutherland, A.I.M.E. Tech. Pub. No. 2298 (1948).

(25) A. F. Taggart, "Handbook of Mineral Dressing," John Wiley & Sons, Inc., New York, N. Y., 1945, pp. 12–89.

(26) A. F. Taggart, *ibid.*, 1945, pp. 12–29, 39.

(27) R. N. Wenzell, *Ind. Eng. Chem.*, **28**, 988 (1936).

(28) F. E. Bartell and J. W. Shepard, *THIS JOURNAL*, **57**, 211 (1953).

(29) F. E. Bartell and J. W. Shepard, *ibid.*, **57**, 455 (1953).

(30) R. Shuttleworth and G. L. J. Bailey, *Discs. Faraday Soc.*, **3**, 16 (1948).

(31) B. K. Barnerji, *Min. Mag.*, **88**, 23 (1953).

## NOTES

### CRYSTALLINE TRIACETIN

By F. J. BAUR

*Chemical Division, The Procter and Gamble Company, Cincinnati 31, Ohio*

*Received November 13, 1953*

Most reference handbooks list  $-78^{\circ}$  as the melting point of triacetin.<sup>1</sup> This "melting point" in reality represents the temperature at which triacetin has transformed from a glass to a liquid.<sup>2</sup> Recently, the crystallization of triacetin under special conditions and a true melting point of  $3.2^{\circ}$  have been reported.<sup>3</sup>

pany, saponification value 764.9, acid value 0.9) at reduced pressures. The fraction used had a boiling point range of  $171-172^{\circ}$  (40 mm.),  $n_D^{26}$  1.4283, saponification value 769.4 (theory 769.9), and acid value 0 (theory 0).

An X-ray diffraction pattern characterizing the crystalline triacetin was obtained using a General Electric XRD-1 unit with 0.025" pinhole system. A flat-film pattern made with a sample-to-film distance of 10 cm. and a nickel strip to eliminate Cu  $K\beta$  radiation is shown in Fig. 1. The sample of crystalline triacetin was ground for five minutes in an agate mortar and the powder transferred to a

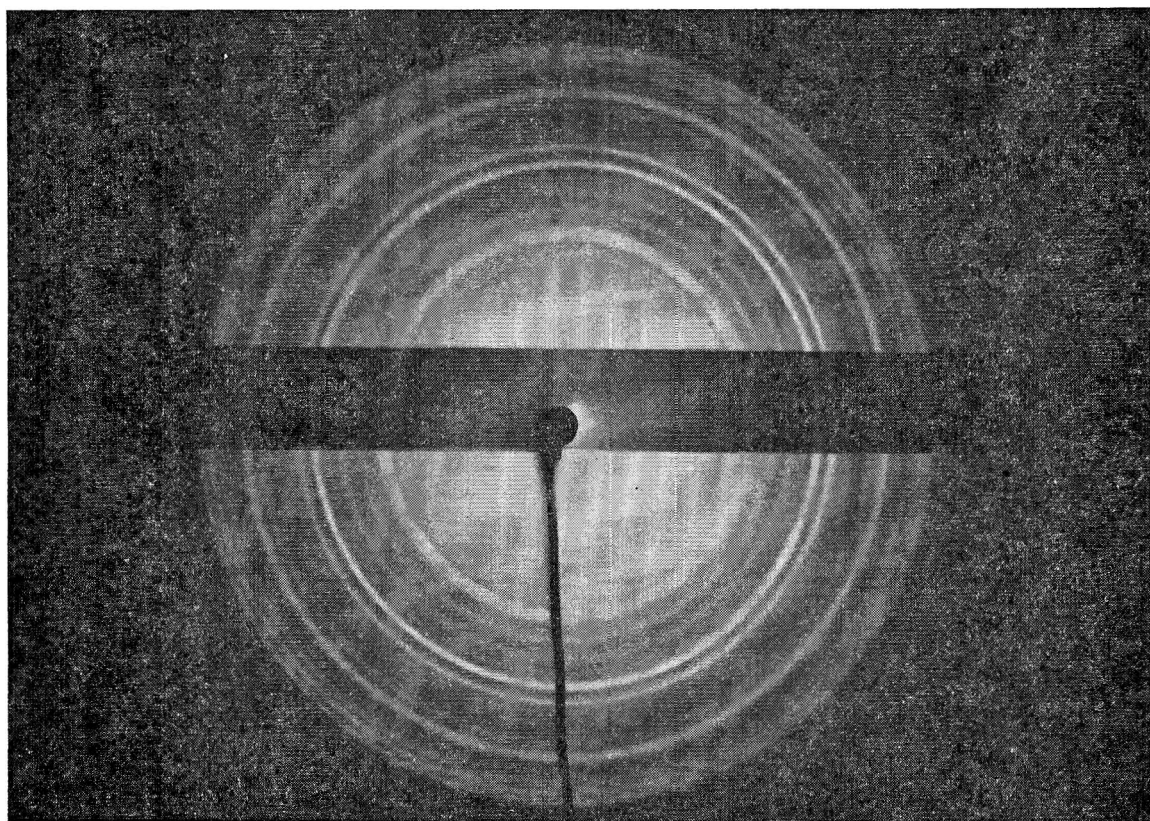


Fig. 1.—X-Ray diffraction pattern of triacetin.

It has now been found that triacetin can be crystallized quite readily. Crystallization was effected in a matter of days by storage of liquid triacetin or a 50% solution in 90% ethanol at  $-18^{\circ}$ . It was speeded up by the addition of Hengar granules, glass wool or similar materials. Commercial C.P. grade triacetin and material purified by fractional distillation were crystallized equally readily.

A melting point of  $4.1^{\circ}$  (cor.) was found for a preparation obtained by fractional distillation of a commercial product (Tennessee Eastman Com-

plastic (Plexiglas) capillary. The capillary was sealed at both ends and tempered 16 hours at  $-7^{\circ}$ . The X-ray diffraction pattern was taken at  $-7^{\circ}$ . The data obtained from the pattern are given in Table I.

TABLE I

CHARACTERISTIC X-RAY DATA ON TRIACETIN, SHORT SPACINGS, Å.

|        |        |         |          |
|--------|--------|---------|----------|
| 6.90 M | 4.60 W | 3.61 M  | 2.96 VVW |
| 6.63 M | 4.21 M | 3.43 W  | 2.55 W   |
| 6.06 M | 4.04 S | 3.33 W  | 2.47 W   |
| 5.04 S | 3.80 M | 3.17 W  | 2.36 VVW |
| 4.77 S | 3.69 M | 3.04 VW | 2.32 VVW |

In conformity with the size of the molecule no long spacings were observed.

(1) "Handbook of Chemistry and Physics," Chemical Rubber Publishing Co., 34th ed., 1952; "Handbook of Chemistry," N. A. Lange, Handbook Publishers, Inc., 8th ed., 1952.

(2) "Beilstein," Vol. II, First Supplement, p. 70.

(3) B. Hancock, D. M. Sylvester and S. E. Forman, *J. Am. Chem. Soc.*, **70**, 424 (1948).

### THREE ADDITIVE FUNCTIONS FOR THE $n$ -PARAFFINS

By S. S. MITRA AND Y. P. VARSHNI

Department of Physics, Allahabad University, Allahabad, India

Received December 8, 1953

In recent years several additive functions for the hydrocarbons depending on the physical properties like boiling point, critical temperature, etc., have been suggested.

The following symbols will be used.

$T_b$ , b. p. under 1 atm., in °K.  
 $T_c$ , critical temp. in °K.  
 $P_c$ , critical pressure in atm.  
 $M$ , mol. wt.  
 $n$ , no. of carbon atoms

It was shown by Burnop<sup>1</sup> that the quantity ( $M \log T_b + 8M^{1/2}$ ) is additive for several organic series.

Kinney<sup>2,3</sup> suggested the following formula for the boiling points

$$T_b = 230.14N^{1/3} - 543$$

where  $N$  is termed the boiling point numbers, which is additive.

The functions are

$$P = T_c/P_c^{3/4} \quad (1)$$

$$Q = \frac{10n}{\log T_c^2/P_c^{3/2}} \quad (2)$$

The 10 occurring in  $Q$  function is only to make it sizeable. As mentioned above, Grunberg and Nissan showed the additive character of  $T_c^3$ ; however, it was observed by Varshni<sup>4</sup> that there is a decrease in the additive value as we ascend the series. It is found that  $T_c^{1/2}$  gives somewhat better results.

$$R = T_c^{1/2}/10^9 \quad (3)$$

The observed values of the function are well fitted in the formulas.

$$P_n = 5.51n + 6.93 \quad (1a)$$

$$Q_n = 2.155n + 5.823 \quad (2a)$$

$$R_n = 7.62n - 16 \quad (3a)$$

In Table I, columns 3, 5 and 7 give the observed values of the  $P$ ,  $Q$  and  $R$  functions according to the relations 1, 2 and 3, the values of  $T_c$  and  $P_c$  being taken from "Landolt-Börnstein Tabellen" and Hodgman's "Handbook of Chemistry and Physics."

TABLE I

| $n$ | Paraffin    | $P$    |        | $Q$   |        | $R$    |          |
|-----|-------------|--------|--------|-------|--------|--------|----------|
|     |             | Obsd.  | Calcd. | Obsd. | Calcd. | Obsd.  | Calcd.   |
| 1   | Methane     | 10.83  | 12.44  | 4.83  | 7.98   | 0.958  | Negative |
| 2   | Ethane      | 16.54  | 17.95  | 8.21  | 10.13  | 4.97   | Negative |
| 3   | Propane     | 21.96  | 23.46  | 11.18 | 12.29  | 9.63   | 6.86     |
| 4   | Butane      | 29.00  | 28.97  | 13.70 | 14.44  | 15.98  | 14.48    |
| 5   | Pentane     | 34.14  | 34.48  | 16.30 | 16.60  | 22.58  | 22.10    |
| 6   | Hexane      | 40.00  | 39.99  | 18.73 | 18.75  | 29.55  | 29.72    |
| 7   | Heptane     | 45.73  | 45.50  | 21.08 | 20.91  | 36.59  | 37.34    |
| 8   | Octane      | 51.45  | 51.01  | 23.37 | 23.06  | 44.04  | 44.96    |
| 9   | Nonane      | 56.96  | 56.52  | 25.63 | 25.22  | 51.50  | 52.58    |
| 10  | Decane      | 62.61  | 62.03  | 27.83 | 27.37  | 59.11  | 60.20    |
| 11  | Undecane    | 68.13  | 67.54  | 29.99 | 29.53  | 67.24  | 67.82    |
| 12  | Dodecane    | 73.68  | 73.05  | 32.06 | 31.68  | 75.34  | 75.44    |
| 13  | Tridecane   | 79.50  | 78.56  | 34.20 | 33.84  | 83.32  | 83.06    |
| 14  | Tetradecane | 85.38  | 84.07  | 36.26 | 35.99  | 91.19  | 90.68    |
| 15  | Pentadecane | 90.77  | 89.58  | 38.31 | 38.15  | 99.01  | 98.30    |
| 16  | Hexadecane  | 95.86  | 95.09  | 40.37 | 40.30  | 107.25 | 105.92   |
| 17  | Heptadecane | 101.40 | 100.60 | 42.38 | 42.46  | 115.20 | 113.54   |
| 18  | Octadecane  | 106.40 | 106.11 | 44.41 | 44.61  | 122.70 | 121.16   |
| 19  | Nonadecane  | 110.60 | 111.62 | 46.49 | 46.77  | 130.20 | 128.78   |

Chen and Hu's<sup>4</sup> additive function is

$$M \log T_c + 6.4M^{1/2}$$

From critical viscosity considerations Grunberg and Nissan<sup>5</sup> showed that  $T_c^3$  is additive for the earlier members of the normal paraffins.

Varshni's<sup>6</sup>  $J$ -function is

$$J = T_c^2/100P_c^{1/2}$$

There are other relations due to Mitra<sup>7</sup> and others.

It is proposed to suggest three additive functions, depending on critical constants in this note.

(1) V. C. E. Burnop, *J. Chem. Soc.*, 826, 1614 (1938).

(2) C. R. Kinney, *J. Am. Chem. Soc.*, 60, 3032 (1938).

(3) C. R. Kinney, *ibid.*, 61, 3236 (1939).

(4) M. C. Chen and D. B. Hu, *J. Chinese Chem. Soc.*, 10, 208, 212 (1943).

(5) L. Grunberg and A. H. Nissan, *Nature*, 161, 170 (1948).

(6) Y. P. Varshni, *Curr. Sci.*, 22, 140 (1953).

(7) S. S. Mitra, *J. Chem. Phys.*, 21, in press (1953).

In columns 4, 6 and 8 are shown the values of the functions as calculated from the relations 1a, 2a and 3a.

It will be observed that, excepting the first few members, the agreement between the observed and calculated values is satisfactory for all the three functions. It is a well known fact that the lowest members of the organic series do not show the regular behavior of the higher homologs. While usually the observed value of  $P_c$  decreases with increasing  $n$ , in case of methane it is less than ethane. Further, the difference in  $P_c$  of consecutive members also decreases with increasing  $n$ , but the first few members do not conform to this behavior.

The authors are thankful to Dr. K. Majumdar and Dr. R. D. Tewari for their interest in the investigation.

(8) Y. P. Varshni, *ibid.*, 21, 1400 (1953); erratum, *ibid.*, 22, in press (1954).

## THE THERMAL DECOMPOSITION OF CYCLOTRIMETHYLENETRINITROSAMINE

By JOHN P. FOWLER AND MARVIN C. TOBIN<sup>1</sup>

*Arthur D. Little, Inc., Cambridge, Mass.*

Received January 14, 1954

As part of a program of study of the decomposition of nitrogen-oxygen compounds<sup>2</sup> the authors had occasion to examine cyclotrimethylenetrinitrosamine,  $(\text{CH}_2)_3(\text{NNO})_3$ , in the melt and in the solid state. It is hoped that this program will shed light on the little-investigated fields of the decomposition of solids and pure liquids.

### Experimental

The sample of cyclotrimethylenetrinitrosamine (CTT) was prepared by the method of Bachmann.<sup>3</sup> It was purified by twice recrystallizing from isopropyl alcohol, m.p. 105–106°. The purified material was powdered and dried under vacuum for one hour. The samples for the studies on the solid were taken from the same batch of powder, so as to standardize the particle size.

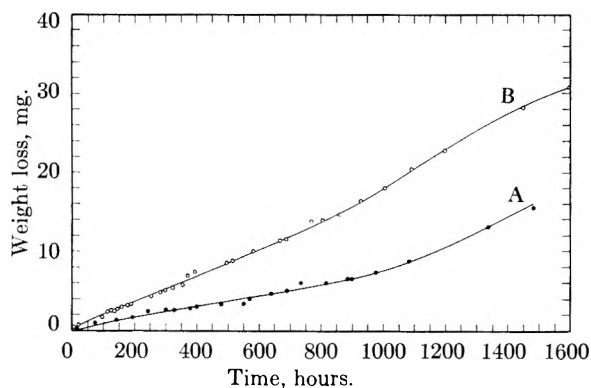


Fig. 1.—Weight loss vs. time for solid CTT, (A) ●, 80°, sample wt. 0.4060 g.; (B) ○, 90°, sample wt. 0.4135 g.

The decomposition of the solid and melt were in general followed by the weight loss method. The solid was heated in an oven in open sample tubes. The tubes were removed at intervals, cooled, weighed and returned. The times reported were corrected for time lost in weighing. No fusion was observed at any time in these samples. The data at 80 and 90° are shown in Fig. 1. Weight loss for the melt was followed by suspending the sample into an oven from

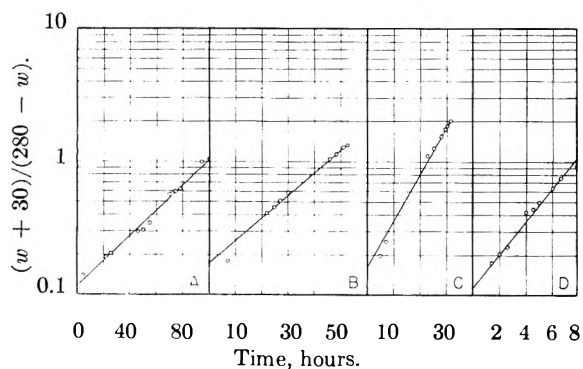


Fig. 2.— $\log \frac{(w + 30)}{(280 - w)}$  vs. time for CTT melt above 10% decomposition: A, 114°, sample wt. 0.5010 g.; B, 117°, sample wt. 0.5028 g.; C, 125°, sample wt. 0.4997 g.; D, 136°, sample wt. 0.5015 g.

(1) This work was done under Contract DAI-19-020-501-ORD (P) 33 with the Office of the Chief of Ordnance and has been released by the War Department for publication.

(2) For the first paper of this series, see M. C. Tobin, J. P. Fowler, H. A. Hoffman and C. W. Sauer, *J. Am. Chem. Soc.*, in press.

(3) W. Bachmann and N. Deno, *ibid.*, **73**, 2777 (1951).

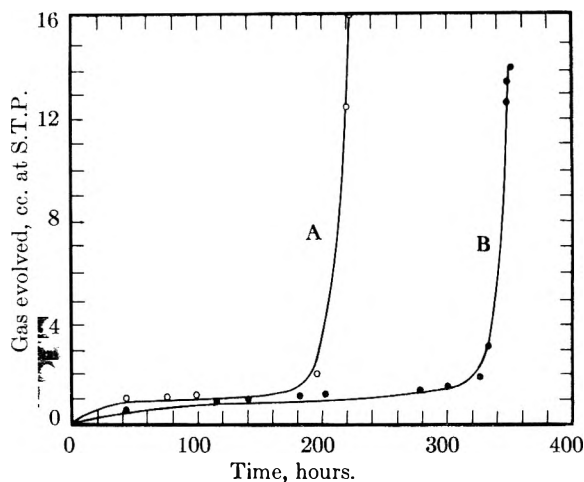


Fig. 3.—Cc. gas at S.T.P. evolved for CTT solid at 90°. (A) ○, sample wt. 0.5390 g.; (B) ●, sample wt. 0.1150 g.

a Roller-Smith torsion balance on which weight loss could be measured as a function of time. Measurements were made at 114, 117, 125, 136 and 146° (see Fig. 2).

Other experiments on the solid were made by heating the solid at 90° in an evacuated sample tube leading to a mercury manometer. The tube was removed from the oven at frequent intervals, cooled to room temperature and the volume change read. Data were recorded in terms of cc. of gas evolved at S.T.P. versus time. The data are shown in Fig. 3.

All temperatures were followed on a Brown multi-channel recording thermocouple, and are estimated accurate to at least  $\pm 1^\circ$ . The weighing on the solid is estimated to be accurate to  $\pm 0.0001$  g., that on the melt to 0.002 g. The volumes recorded for gas evolution are estimated to be accurate to  $\pm 0.1$  cc.

### Results for Melt

It was found that the melt of CTT, originally a pale yellow, darkened to blood red on heating. Decomposition was complete at 114, 117, 125 and 136° at some 55% weight loss, leaving a red, glassy residue. cursory examination of this residue showed it to consist of at least two fractions, one water-soluble. At 146°, the sample fumed off at 2 hours, leaving a dark porous mass at the top of the sample tube. This is ascribed to self-heating. The plots of weight loss vs. time are of the sigmoid type, with one possible odd feature, a suggestion of a plateau observable at the beginning of the decomposition. The curves are reminiscent of the decomposition of nitroglycerin, which also shows this initial plateau.<sup>4</sup> It was found possible to fit the experimental curves above 10% decomposition to the equation

$$\log \frac{(w + 30)}{(280 - w)} = kt + c \quad (1)$$

at all four temperatures. Here  $w$  is the weight loss in mg. to time  $t$  (hours), 280 is the mean final weight loss in mg. (all samples were very nearly the same weight),  $k$  and  $c$  are constants, " $k$  having the dimensions of a rate constant." A plot of  $\log k$  vs.  $1/T$  gives a straight line, leading to an activation energy of 36.2 kcal./mole. The values for  $k$  and  $c$  at each temperature are given in Table I. Equation 1 does not match the experimental curves below 10% decomposition, in particular predicting

(4) N. Semenov, "Chemical Kinetics and Chain Reactions," Oxford University Press, New York, N. Y., 1935, p. 426.

a small weight loss at zero time. However, in view of the peculiar nature of the initial stages of the decomposition, it was not thought worthwhile to try to match the early stages of the curves.

TABLE I

| T, °C.               | 114    | 117    | 125    | 136    |
|----------------------|--------|--------|--------|--------|
| k, hr. <sup>-1</sup> | 0.0094 | 0.0172 | 0.0360 | 0.128  |
| c                    | -0.920 | -0.772 | -0.800 | -0.923 |

### Discussion

The results of the weight loss measurements on the solid show no unusual characteristics. They show the qualitative features indicated by Tobin, Fowler, Hoffman and Sauer,<sup>2</sup> and these are ascribed to the same general phenomena. The gas evolution curves are quite interesting. The decomposition evidently remains in an induction period for an extended period, the induction period ending suddenly in a very sharp increase in reaction rate. This indicates violent autocatalysis of solid CTT by its gaseous reaction products, since no such phenomenon appears in the weight loss experiments, where the gaseous products are allowed to escape. It is not clear why the rate of gas evolution is the same for the 0.1150-g. sample as for the 0.5390-g. sample during the induction period or why the induction period for the smaller sample is only twice that for the larger sample. The larger sample showed no sign of fusion at any time, but the smaller sample started to fuse during the sharp rise in pressure. The experiments were stopped when the pressure in the tube reached one atmosphere.

When the sample tubes were opened to the atmosphere, brown fumes formed, showing that one of the gaseous products is nitric oxide.

Sigmoid curves of the type obtained here for the melt may arise as the result of an equilibrium reaction, a sequence of consecutive reactions, or an autocatalytic reaction. The first possibility may be disregarded, due to the continuous removal of reaction product from the system. Other than this, little may be said about the mechanism. It is of interest to note that equation 1 has the same algebraic form as the equation representing the loss of reactant or evolution of non-catalytic product for several types of autocatalytic reactions.

There is no doubt that the reaction is a complex one, so that the activation energy calculated from *k* in equation 1 must be regarded as a composite quantity.

**The Infrared Spectrum of Cyclotrimethylenetrinitrosamine.**—In the course of this work, occasion arose to obtain the infrared spectrum of cyclotrimethylenetrinitrosamine. The spectrum was obtained in Nujol mull on a Perkin-Elmer automatic recording spectrophotometer at Arthur D. Little, Inc. The region 650–1400 cm.<sup>-1</sup> was covered with a NaCl prism, the region 1400–3500 cm.<sup>-1</sup> with a CaF<sub>2</sub> prism.

The observed bands, in cm.<sup>-1</sup> are

3050 (m), 2960 (s), 2890 (s)\*, 1485 (s, v. br.)  
 1442 (br)\*, 1370 (br)\*, 1345 (s, br), 1300 (s), 1255 (s)  
 1150 (m), 1075 (s, br), 995 (m), 952 (s, br), 875 (s),  
 860 (m, shoulder to 875), 840 (m), 765 (s), 700 (s)

The asterisks represent regions of Nujol absorp-

tion. These data are not sufficient to make possible a classification of frequencies, but it does seem reasonable to assign 1345 cm.<sup>-1</sup> to the nitroso N–O stretching frequency.<sup>5</sup>

(5) E. Lieber, D. Levering and L. Patterson, *Anal. Chem.*, **23**, 1504 (1951).

## THE LIQUIDUS CURVE OF THE BINARY SYSTEM CADMIUM ACETATE–POTASSIUM ACETATE

BY ALEXANDER LEHRMAN AND DONALD SCHWEITZER

*Department of Chemistry, The City College of New York, New York 31, N. Y.*

Received December 29, 1953

The binary system cadmium acetate–potassium acetate was explored as part of a program<sup>1</sup> of investigating the double salts of acetates.

### Experimental

**Materials.**—Analytical Reagent potassium acetate was dried in an oven at 140° for one week before weighing. Cadmium acetate of C.P. grade to which 5–10 drops of glacial acetic acid had been added to prevent decomposition of the cadmium acetate was dried in an oven at 140° before weighing.

**Apparatus.**—The initial crystallization temperatures were measured with a copper–constantan thermocouple of No. 24 wire in conjunction with a potentiometer (16-millivolt range), the cold junction being cracked ice. The e.m.f. could be read to ±0.02 mv. The couple was encased in a narrow guard tube that was made by drawing out Pyrex tubing and sealing one end. It was standardized by determining the e.m.f.'s at the boiling points of water and of benzophenone, the melting points of U. S. Bureau of Standards tin and of purified potassium nitrate, and then plotting the deviations from the standard table of Adams.<sup>2</sup> A molten salt-bath was used to heat the mixtures. It consisted of a eutectic mixture of lithium, potassium and calcium nitrates<sup>3</sup> contained in a tall Pyrex beaker.

**Method.**—Definite mixtures of the salts (total weight between 25 and 35 g.) were made by weighing the components to the nearest centigram, and in some cases to ±3 milligrams. The mixed salts were finely ground together and placed in 2.5 × 20 cm. Pyrex test-tubes. In order to prevent decomposition of cadmium acetate on heating, 5 drops of glacial acetic acid were added to each tube before immersing it in the hot salt-bath. The acetic acid distilled out of the mixtures during melting since the temperatures were raised to about 200°. However, the mixtures rich in cadmium acetate began to decompose at the temperatures needed for fusion, and determinations on mixtures above 0.7 mole fraction of cadmium acetate could not be made.

The tube containing the mixture of acetates and the couple in its guard tube was suspended in the molten nitrate-bath until the mixture was liquefied, and then the tube was allowed to cool slowly while stirring constantly. A beam of light was passed through the mixture, and the initial crystallization temperature was observed. Crossed Polaroid filters, one on each side of the tube, made the detection of the initial crystal easier. Supercooling was prevented by repeated insertions and withdrawals of a capillary glass rod into the mixture when the initial crystallization temperature was approached. When the capillary was withdrawn from the mixture the few drops clinging to it immediately solidified, and the insertion served to inoculate the melt. At least three determinations of the initial crystallization temperature of each mixture were made, or until agreement to within 1° was achieved.

To make sure that no breaks in the curve were overlooked, and to fix the eutectic temperatures, simultaneous cooling and differential cooling curves of mixtures over the range

(1) For previous work see A. Lehrman and E. Leifer, *J. Am. Chem. Soc.*, **60**, 142 (1938); A. Lehrman and P. Skell, *ibid.*, **61**, 3340 (1939).

(2) Pyrometric Practice, U. S. Bureau of Standards Technological Paper No. 170, p. 309.

(3) A. Lehrman, *et al.*, *J. Am. Chem. Soc.*, **59**, 179 (1937).

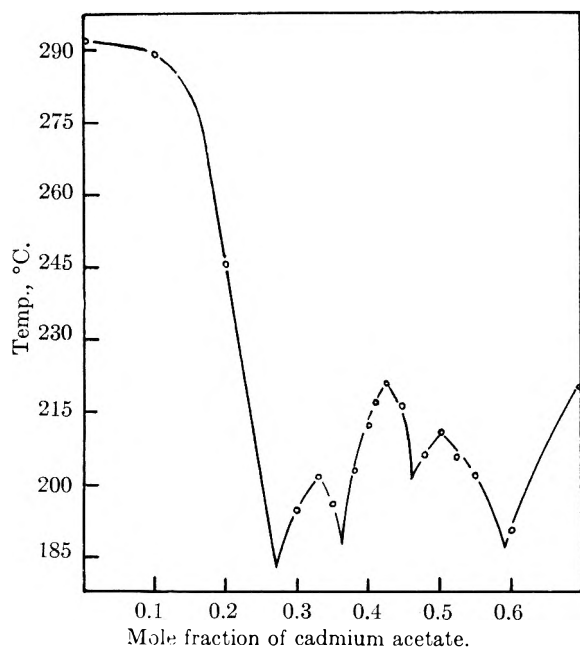


Fig. 1.—The liquidus curve of the binary system cadmium acetate-potassium acetate.

0.0 to 0.7 mole fraction of cadmium acetate were taken with separate copper-constantan thermocouples, each in conjunction with a potentiometer. The differential cooling curves were taken between tubes containing mixed acetates and a tube containing potassium acetate, each in a hole in a single copper block that had been heated by a small resistance furnace. Potassium acetate was used as the inert

substance because it undergoes no transition in the temperature range used, and it has approximately the same heat capacity as the mixtures.

**Experimental Results.**—Temperatures of the initial crystallization and eutectic temperatures are given in Table I and are plotted in Fig. 1.

TABLE I

| THE SYSTEM CADMIUM ACETATE-POTASSIUM ACETATE |                                    |                     |                                    |                                    |                     |
|--|------------------------------------|---------------------|------------------------------------|------------------------------------|---------------------|
| Cd(AcO) <sub>2</sub> mole fraction           | Initial crystallization temp., °C. | Eutectic temp., °C. | Cd(AcO) <sub>2</sub> mole fraction | Initial crystallization temp., °C. | Eutectic temp., °C. |
| 0.000  | 292                                |                     | 0.4286                             | 221                                |                     |
| .100   | 289                                |                     | .4444                              | 216                                | 201                 |
| .200   | 246                                | 183                 | .480                               | 206                                |                     |
| .300   | 195                                |                     | .500                               | 210                                |                     |
| .333   | 202                                |                     | .520                               | 205                                |                     |
| .350   | 196                                | 188                 | .550                               | 202                                | 187                 |
| .380   | 203                                |                     | .600                               | 190                                |                     |
| .400   | 213                                |                     | .700                               | 220                                |                     |
| .410   | 217                                |                     |                                    |                                    |                     |

**Discussion.**—The data show the existence of the double salts  $2\text{KC}_2\text{H}_3\text{O}_2 \cdot \text{Cd}(\text{C}_2\text{H}_3\text{O}_2)_2$ ,  $\text{KC}_2\text{H}_3\text{O}_2 \cdot \text{Cd}(\text{C}_2\text{H}_3\text{O}_2)_2$  and  $4\text{KC}_2\text{H}_3\text{O}_2 \cdot 3\text{Cd}(\text{C}_2\text{H}_3\text{O}_2)_2$ .

It might be well to investigate these solid substances by crystallographic methods to see if complex ions containing cadmium and acetate groups exist. There is also a possibility of polynuclear complexes of tetra-coordinated cadmium involving acetate bridges.<sup>4</sup>

(4) In connection with this, see I. Leden, *Svensk. Kem. Tid.*, **58**, 129 (1946); W. C. Cagle and W. C. Vosburgh, *J. Am. Chem. Soc.*, **57**, 414 (1935).

# COLLECTIVE NUMERICAL PATENT INDEX to Volumes 31-40 of CHEMICAL ABSTRACTS

- Contains more than 143,000 entries, classified by countries in numerical order.
- Classification by patent number is an enormous timesaver.
- Index references give volume, page and location of patent abstract in CHEMICAL ABSTRACTS.
- Cloth bound, 182 pages, 7½" x 10" overall, 8 columns of listings per page covering all patents abstracted in CHEMICAL ABSTRACTS from 1937-46, inclusive.

PRICE \$6.50 POSTPAID

Send orders and inquiries to:  
Special Publications Dept.

**American Chemical Society**  
1155 Sixteenth St., N.W., Washington 6, D. C.

## BOOKS FROM CHICAGO



### *The Physical Chemistry of the Silicates*

By **WILHELM EITEL**. A monumental, systematic treatise on the physical-chemical facts of the constitution and reaction of silicate systems, *The Physical Chemistry of the Silicates* will prove invaluable to academic and industrial libraries as well as to theoretical and practical research workers in geology, glass, ceramics, cement, and related fields.  
*1,575 pages, illustrated, \$30.00*

### *Structure and Properties of Solid Surfaces*

Edited by **ROBERT GOMER & CYRIL S. SMITH**. Fourteen papers from the 1952 National Research Council meeting discuss thermodynamics of surfaces, atomic theory of surface forces and energy, epitaxy, adhesion, physical and chemical adsorption of gases, electron diffraction and catalytic investigations.  
*\$8.50*

At your bookstore, or from

**THE UNIVERSITY OF CHICAGO PRESS**  
5750 Ellis Ave., Chicago 37, Ill.

## CHEMICAL NOMENCLATURE

Number eight of the Advances in Chemistry Series  
Edited by the staff of Industrial and Engineering Chemistry

A collection of papers comprising the Symposium on Chemical Nomenclature, presented before the Division of Chemical Literature at the 120th meeting—Diamond Jubilee—of the American Chemical Society, New York, N. Y., September 1951

Paper bound . . . . \$2.50

Published August 15, 1953, by  
**AMERICAN CHEMICAL SOCIETY**  
1155 Sixteenth Street, N.W.  
Washington, D. C.

### CONTENTS

|   |     |
|---|-----|
| Introduction . . . . .  | 1   |
| Letter of Greeting . . . . .  | 3   |
| Some General Principles of Inorganic Chemical Nomenclature . . . . .                                | 8   |
| Nomenclature of Coordination Compounds and Its Relation to General Inorganic Nomenclature . . . . . | 9   |
| Problems of an International Chemical Nomenclature . . . . .  | 38  |
| Chemical Nomenclature in Britain Today . . . . .  | 49  |
| Chemical Nomenclature in the United States . . . . .  | 55  |
| Basic Features of Nomenclature in Organic Chemistry . . . . .                                       | 45  |
| Organic Chemical Nomenclature, Past, Present, and Future . . . . .                                  | 76  |
| Work of Commission on Nomenclature of Biological Chemistry . . . . .                                | 83  |
| Nomenclature in Industry . . . . .  | 95  |
| Development of Chemical Symbols and Their Relation to Nomenclature . . . . .                        | 99  |
| The Role of Terminology in Indexing, Classifying, and Coding . . . . .                              | 106 |



## INSTRUMENTAL ANALYSIS

By JOHN H. HARLEY, *U. S. Atomic Energy Commission*  
and STEPHEN E. WIBERLEY, *Rensselaer Polytechnic Institute.*

*Instrumental Analysis* is no mere catalog of instrumental methods, but a book of key principles and practical applications. Emphasis is on the instruments themselves, rather than on the systems being measured. Theory is strictly limited to what the analyst needs in his day-to-day work.

The usefulness of this book is increased by its systematic organization. First, there is a discussion of the theory involved; second, an examination of the components of each instrument; third, the consideration of various commercial instruments; and fourth, typical procedures and applications. Limitations as well as advantages of the various methods are discussed.

*Instrumental Analysis* contains far more detailed and advanced coverage of such topics as absorption spectroscopy than is currently available in any other book. Among its many topics it includes a treatment of echelle spectroscopy and entire chapters devoted to flame photometry and to high frequency titration methods.

1954

440 pages

\$6.50

## ORGANIC COATING TECHNOLOGY, Volume I

By HENRY FLEMING PAYNE, *Technical Editor, American Cyanamid Co.*  
*Adjunct Professor, Polytechnic Institute of Brooklyn.*

Here is a book which fills the need for a comprehensive but concise survey of the chemistry, manufacture, and applications of the oils, resins, varnishes, high polymeric materials, plasticizers, and driers used for clear coatings, and as the vehicle or liquid portion of pigmented coatings. The first book of its kind to be written by a single author, it presents ideas in an orderly and logical manner, with emphasis on practical aspects.

1954

674 pages

\$10.00

## NUCLEAR MOMENTS

By NORMAN F. RAMSEY, *Harvard University.*

This is the only book since World War II to cover the field of nuclear moments for stable nuclei, and for radioactive nuclei whose lifetimes are sufficiently long to be measured by techniques similar to those used for stable nuclei. It originated from the author's section on "Nuclear Moments and Statistics" in Volume I of *Experimental Nuclear Physics*, edited by Emilio Segrè. Dr. Ramsey defines the quantities concerned in moment measurement, describes the interaction between nuclear moments and atomic and molecular fields, and discusses the experimental methods used in measuring nuclear moments and their derived molecular quantities.

1953

169 pages

\$5.00

Send today for your examination copies

**JOHN WILEY & SONS, Inc., 440-4th Ave., New York 16, N. Y.**